DISSERTATION

Titel der Dissertation

„Impact of pungent aroma compounds on mechanisms regulating satiety and energy metabolism"

verfasst von

Dipl.-Ernährungswiss. Barbara Rohm

angestrebter akademischer Grad

Doktorin der Naturwissenschaften (Dr. rer.nat.)

Wien, 2014

Studienkennzahl lt. Studienblatt:	A 791 419
Dissertationsgebiet lt. Studienblatt:	Chemie
Betreuerin / Betreuer:	Univ.-Prof. Mag. Dr. Veronika Somoza

Für meinen Vater

Success is not final,
failure is not fatal:
it is the courage to continue that counts.

-Sir Winston Churchill (1874-1965)

Danksagung

Table of content

III.   PART II

Impact of the pungent aroma compounds capsaicin, nonivamide and *trans*-pellitorine on mechanisms regulating satiety and energy metabolism 80

List of abbreviations

5–HT	serotonin
Acsl	long chain acyl Coenzyme A synthetase
AgRP	agouti-related protein
α-MSH	α-melanozyte stimulating hormone
ARC	arcuate nucleus
AUC	Area under the curve
cAMP	Cyclic adenosine monophosphate
CART	Cocaine and amphetamine-regulated transcript
CCK	cholecystokinin
C/EBP	Ccaat-enhancer-binding proteins
CNS	Central nervous system
CoA	Coenzyme A
CREB	cAMP response element-binding protein
DA	Dopamine
FFA	Free fatty acid
FABP	Fatty acid binding protein
FATP	Fatty acid transporter
GLP-1	Glucagon-like peptide 1
LCFA	Long-chain fatty acid
miRNA	microRNA
NPY	Neuropeptide Y
POMC	Pro-opiomelanocortin
PYY	Peptide YY
PPAR	peroxisome proliferator-activated receptor
TRPV1	transient receptor potential cation channel subfamily V member 1

I. Introduction

1.1 Strategies in the treatment of obesity

Overweight and obesity count as the major health threat of the 21st century, with progressively growing prevalence worldwide. In Europe, obesity has reached the dimension of an epidemic (1), with higher prevalences for Central and Eastern Europe than for Italy, France and some Scandinavian countries (2). Obesity, especially during childhood, is associated with a higher morbidity for certain diseases. According to estimates, 85% of all cases of diabetes mellitus type II, 45% of the hypertonia cases, 35% of the coronary heart diseases and 18% of the hypercholesterolemia cases could be avoided by maintaining a healthy body weight (3). In addition, adiposity is associated with osteoarthritis, certain types of cancer, impaired mental health and increased mortality (4-9).

Weight gain is the result of a long-term positive energy balance (caloric intake – energy expenditure). Strategies to shift energy balance into negative range in order to lose weight include, but are not limited to 1) reduction of food intake via increasing satiety and satiation, 2) regulation of intestinal nutrient, especially fat, uptake, and 3) modulation of fat storage, for instance via an inhibition of adipogenesis (10).

1.2 Regulation of food intake

Food intake by omnivores is displayed in episodic patterns of discrete size and duration. The frequently used terms 'satiety' and 'satiation' are descriptors of eating behavior, at which 'satiation' describes modulation of meal size, whereas 'satiety' refers to inter-meal intervals. However, both terms are used to describe the biological process that causes people to begin and terminate eating and suppress eating for a given passage of time (11).

Food intake is driven by different factors, which can be divided into metabolic needs (homeostatic factors) and non-homeostatic factors. The latter include experience, habits, opportunity, stress and biological rhythm. Homeostatic factors are a complex network of neural, hormonal and metabolic signals from the periphery, which are mediated to the central nervous system (CNS), where the sense of hunger and satiety originates. The following section will provide a summary of important aspects of relevant central and peripheral signals (see also **Figure 1**), without aiming for completeness.

1.2.1. CNS control of food intake

Formerly, it was thought that two discrete hypothalamic centers, an appetite center located in the lateral hypothalamic area, and a satiety center in the ventromedial area, control the regulation of food intake (12). However, more recent work demonstrated that instead of discrete centers, eating behavior is organized in a diffuse network. This network is distributed across the spinal cord, brainstem and the hypothalamus (13). Within the brainstem, primarily the nucleus tractus solitaries controls incoming gastrointestinal signals, whereas the hypothalamus can be described as the master controller of ingestive behavior (14). Especially the hypothalamic arcuate nucleus (ARC) holds a special role concerning the inflow of incoming signals from the periperhy. The ARC contains two functionally opposed populations of neurons which control food intake. The first population comprises the anorexigenic peptides proopiomelanocortin (POMC) and cocaine and amphetamine-regulated transcript (CART) (15). The polypeptide POMC is the precursor of α-melanozyte stimulating hormone (α-MSH) (16), which binds to melanocortin receptors MC3-R and MC4-R located in the hypothalamus, thereby inhibiting food intake (17). In addition, about 30% of the POMC containing neurons are sensitive to the adipose signal leptin due to the expression of leptin receptors (18). Functional studies confirmed that in addition to POMC, also CART inhibits food intake (19), although the exact mechanism of action is not fully elucidated yet.

A second hypothalamic population of neurons contains neuropeptide Y (NPY), co-localized with agouti-related protein (AgRP), which have both orexigenic effects (15). NPY is the most powerful stimulator of food intake known so far (20). NPY acts on at least five identified receptors (Y1, Y2, Y4, Y5 and Y6 receptor) (21). However, the stimulation of food intake is thought to be mediated via Y1R and Y5R (22), or a synergistic interaction of both (23). Activation of Y1R decreases the firing rate of POMC containing neurons in the ARC (24) and ventromedial hypothalamic neurons (25). In addition, evidence for a cross-talk between melaoncortin/NPY and the dopaminergic system points to a role for NPY in food reward as well (26). However, in NPY-containing neurons, NPY is co-localized with the anorexigenic peptide AgRP, which unfolds its effects mainly via antagonizing the effects of α-MSH on its receptor MC4R (27). In addition, AgRP may directly inhibit POMC perikarya, which allows an inhibition of melanocortin cells when NPY/AgRP neurons are active (28).

Effect of central and peripheral signals on food intake
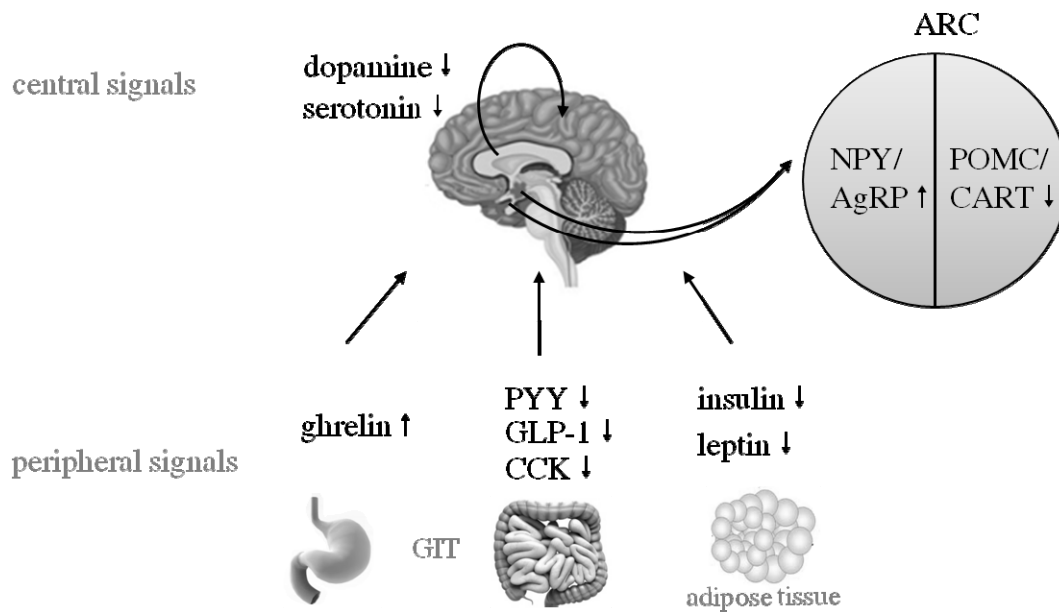
Figure 1. Schematic overview of the most important central and peripheral signals in the control of food intake. Peripheral signals from the gastrointestinal tract (GIT) and adiposity signals interact with central signals from the brain, influencing two populations of neurons (orexigenic NPY and AgRP neurons *versus* anorexigenic POMC/CART containing neurons) in the hypothalamic arcuate nucleus (ARC), where the senses of hunger and satiety originates. Enhanced release or activation of central and peripheral signal molecules increase (↑) or decrease (↓) food intake.

The hypothalamic neurotransmitters dopamine and serotonin have been also demonstrated to be relevant brain-messengers in the regulation of food intake (29). The neurotransmitter dopamine modulates the activity of target neurons via a post-synaptic activation of several dopamine receptors. In contrast to the inhibiting dopamine receptors D2, D3 and D4, dopamine receptors D1 and D5 stimulate adenylyl cyclase activity. Hypothalamic neurons express both types of dopamine receptors, thus dopamine can, depending on the function of the subtype and the expression rate, promote or inhibit the activity of target neurons (29). A satiety-mediating effect of dopamine is proposed by various studies that show a decreased D2 receptor availability in addicted subjects, including overeating and obesity (30-33). Furthermore, administration of D1 agonists reduce duration in feeding, whereas D2 agonists reduce the local rate of eating in rats (34). In addition, dopaminergic neurons are targets for peripherial appetite-regulating peptides like leptin, galanin and cholecystokinin and, are an important part of the natural reward system (35).

Hypothalamic serotonin is associated with decreased food intake and reflects carbohydrate intake (29). So far, more than fifteen serotonin receptors are known, but only 5-HT$_{1A,\ 1B,\ 2A}$ and $_{2C}$ are thought to be directly involved in the regulation of food intake (36). More recently, inhibition of 5-HT$_6$ receptor signaling has been associated with reduced food

intake and decreased body weight, suggesting an involvement of 5-HT$_6$ in the regulation of hunger and satiety as well (37). The exact mechanisms underlying the satiety-stimulating effect of serotonin are not yet fully understood. However, a close interaction with other neuropeptides is likely. For example, the serotonin receptor agonist fenfluramine inhibits NPY-induced food intake (38). In addition, 5-HT$_{2c}$ activation stimulates POMC containing neurons (39-40), whereas 5-HT$_{1B}$ receptor activation inhibits AgRP containing neurons. This leads to a decreased release of orexigenic AgRP and stimulates α-MSH release (41). However, mediation of the satiety effects of peripheral signals as cholecystokinin is a mechanism discussed for serotonin action as well (42).

1.2.2. Peripheral control of food intake

Expression and release of the central orexigenic substances NPY and AgRP is stimulated or suppressed by numerous peripheral signals. So far, the stomach-derived ghrelin is the only known orexigenic gastrointestinal polypeptide (14). The central and peripheral administration of ghrelin has been shown to stimulate food intake in animal models (43-44) and humans (45). Ghrelin acts as a meal initiator, with the consequence that ghrelin enhances food intake by increasing satiety, the number of meals, without affecting satiation, the meal size (46). Ghrelin unfolds its effects not only via the ARC, but also via vagal efferent loops, counteracting the effects of leptin and stimulating AgRP and NPY (47).

Opposed to ghrelin, the intestinal polypeptides cholecystokinin (CCK), glucagon-like peptide 1 (GLP-1) and polypeptide Y (PYY) unfold anorexigenic effects.

Numerous studies in various species including humans, give strong evidence for the satiety-mediating effect of CCK (48), which is released by intestinal L-cells in response to nutrients like protein and lipids (49). Its peripheral administration has been shown not only to increase the release of serotonin and to activate POMC neurons as well as CART neurons (50-51), but also to increase expression of CART and NPY Y2 receptors (52-53). An interplay has also been described for CCK with ghrelin, demonstrating that ghrelin inhibits CCK (54), whereas administration of CCK prior to ghrelin leads to an inhibition of ghrelin-mediated effects (55). Two known receptors are thought to mediate satiety effects of CCK: CCK1R and CCK2R. It has been shown that knockout mice lacking CCK1R ingest larger and longer meals due to impaired short-term satiation (56-57). Furthermore, CCK1R knockout mice were shown to have an increased ghrelin-dependent drive to eat, which could be associated with increased expression of CART in vagal afferent neurons (58).

As implied by its name, glucagon-like peptide-1 (GLP-1), stimulates insulin production while inhibiting glucagon (59). Released by illeal L-cells in response to fat and carbohydrate intake (49), GLP-1 reduces ad libitum food intake in lean and obese humans (60-61). The mechanism of GLP-1 action is not fully understood yet, since data regarding a vagal pathway are inconsistent (62-63). However, since GLP-1 was shown to cross the blood-brain barrier, a direct central pathway seems more convincing (63).

The polypeptide Y (PYY) is mainly secreted from endocrine L cells in its truncated form $PYY_{(3-36)}$ (64). Inhibition of food intake has been demonstrated in fasted mice (65), but also in obese humans (66). As a member of the NPY family, PYY is a ligand for the NPY autoreceptor Y2 of NPY neurons in the ARC, thus mediating satiating effects (62,67). A study with Y2R knockout mice, which are not sensitive to the anorectic effects of PYY, provided further evidence for a Y2R-involvement in PYY signaling (64). Recent studies indicate a common final pathway of GLP-1 and PYY, which also involves food reward (68).

Besides the short-term signals here discussed (nutrients, neural signal, hormones), long-term (adiposity) signals also play a pivotal role in the regulation of food intake by providing information about energy stores and induce adaptive responses for the maintenance of energy homeostasis. Leptin and insulin are well-investigated adiposity signals that regulate energy homeostasis, body weight and body composition (69). Leptin also suppresses appetite by targeting NPY (70) and POMC neurons in the ARC, which also involves modulation of glucose metabolism (71-72) .

1.2.3. Regulation of food intake for body weight reduction

Improved understanding during the past years of the mechanisms regulating food intake provided the basis for new therapeutic measures, which target central and peripheral signals. For example, serotonin receptors have been widely-studied as a centrally target for anti-obesity therapeutics. Especially $5-HT_{2C}$ has been used as a target for anti-obesity drugs and, the selective 5-HT2c agonist lorcaserin is a currently used anti-obesity drug in the US (73). Also, positive effects on weight loss of a 12-week treatment with the NPY_5 antagonist S-2367 in a PhaseIIa proof of concept study have been reported, without significant adverse events (74). In addition, a clinical trial concerning the usage of leptin as a therapeutic drug have been carried out and demonstrated a promising dose-related weight loss (75). Leptin can cross the blood-brain barrier (76) and thus unfold effects on central NPY and POMC containing neurons, making leptin an important connection between peripheral and central treatments. To

target peripheral control of food intake, peptide analogues of CCK have been tested, but none of them made it to a clinical phase, probably due to major side effects (10). Several groups also have focused on selective agonist for the α-MSH MCR4 receptor, however, with only limited clinical development following (77). More promising results were obtained from a two-year intervention with diabetic subjects, which showed significant weight loss after administration of GLP-1 or the GLP-1 receptor agonist exenatide (78).

Nevertheless, investigation of potential novel targets remains an area of great interest and are focused for instance on monoamine reuptake inhibition and 5-HT$_6$ antagonists (74). However, these approaches are still at an early stage and data from clinical studies are crucial to evaluate cost-benefit relation of potential drugs in the treatment of obesity.

1.3. Regulation of intestinal nutrient (especially fat) uptake

Beside the control of food intake, the regulation of macronutrient uptake is a potential target for significant weight loss. Energy-rich foods, especially high fat diets, contribute to the development of overweight and obesity. That inhibition of dietary fat absorption can be useful in anti-obesity therapy has been proven by the successful introduction of the drug Xenical (Roche), with its active pharmaceutical ingredient Orlistat, to the US and European market (10). Thus, in the treatment of obesity, especially a blockage of fatty acid uptake by enterocytes might be a promising strategy.

1.3.1. Intestinal fatty acid uptake

In the small intestine, composed of the duodenum, jejunum and ileum, major parts of nutrient absorption occurs. The mucosa of the small intestine consists of a simple columnar epithelium, which harbors, beside the actual absorptive cells (enterocytes), also mucosa secreting goblet cells and enteroendocrine cells. The latter secrete hormones like GLP-1, CCK and PPY for the peripheral regulation of food intake. However, enterocytes are the predominant cell type lining the lumen of the small intestine and exhibit a dense array of microvilli at the apical surface. Actual nutrient uptake occurs predominantly at the tip of each microvilli. The microvilli are microscopically visible as the brush border membrane and increase the absorptive surface of each cell by a factor of 600 (79).

Dietary fat is taken up mostly in the form of triacylglycerides, consisting of a glycerol backbone, which is esterified with three fatty acids. Pancreatic lipases within the intestinal

lumen hydrolyse triacylglycerides to two fatty acids and monoacylglycerides, which can be absorbed by the enterocytes. However, the exact molecular mechanisms of fatty acid uptake are not completely understood and protein-mediated mechanisms are likely to coexist with diffusion (80). Diffusion of long-chain fatty acids (LCFA) along a favorable concentration gradient is realized by a so called "flip-flop" mechanism, at which uncharged fatty acids can flip between the two membrane sites while still remaining membrane-bound (81). This process is much slower for fatty acids anions (81). Within the enterocyte, LCFAs are trapped by binding to an intracellular fatty acid binding protein (82) or via metabolic conversion to acyl-coenzyme A derivates (83). However, a protein involvement in this process is most likely for 1) the delivery of fatty acids to the membrane, 2) transmembrane movement and 3) removal of fatty acids from the membrane (84). To date, four membrane-associated proteins have been identified that participate in one or more of the above described steps: Fatty acid translocase (CD36/FAT), fatty acid binding proteins (FABPs), fatty acid transport proteins (FATP) and long chain acyl Coenzyme A synthetase (Acsl).

CD36 is located on the brush-border membranes of duodenal and jejunal villi (85). The transport function of CD36 involves directing the absorbed fatty acids proximally to chylomicron formation (86). In addition, CD36 provides oleic acid for the formation of satiety-mediating oleoylethanolamide, which may play a major role in the satiety response after lipid ingestion (87). However, CD36 also contributes to a small extent to fatty acid uptake (88) and binding of fatty acids by CD36 on taste buds may also contribute to fat perception and preference (89).

Fatty acid binding proteins (FABP) comprise an abundant class of cytosolic proteins which bind long chain fatty acids. Their major functions have been described as modulation of specific enzymes, regulation of fatty acid responsive genes, maintenance of cellular membrane fatty acid levels and, most-likely, also a transport function (90).

The family of fatty acid transport proteins (FATPs) have an architecture similar to acyl-coenzyme A synthetases (Acsl), which includes an ATP and a fatty acid binding domain (91). Fatty acid transport through the membrane via vectorial acylation requires a FATP alone or in combination with an Acsl, resulting in acyl coenzyme A. This activation is also necessary for further metabolic transformation, and can be mediated by specific FATPs from the endoplasmatic reticulum (84). In the intestine, predominantly FATP4 and FATP2 are expressed (84), which both unfold Acsl activity (92).

Although the molecular mechanism of intestinal fatty acid uptake has not been completely investigated yet, the increasing knowledge over the past years provided the basis for screening of compounds that effectively block fatty acid uptake as a strategy in the treatment of obesity.

1.3.2. Regulation of intestinal fatty acid uptake for body weight reduction

Blocking fat absorption in the small intestine for weight loss has been proven to be a successful strategy. For example, the drug 'Orlistat', which is sold under the trade name Xenical by Roche in most countries, inhibits pancreatic lipase activity, thus decreasing the digestion of dietary triglycerides (93). However, major side effects of a treatment with Orlistat are fecal fat loss and a reduced absorption of fat-soluble vitamins. Thus, current research focuses on the blockage of fatty acid uptake by enterocytes. This would allow the digestion of triglycerides, avoiding side effects, without allocating fatty acids for further metabolization (10). Some selective inhibitors of human intestinal FATP2 have already been identified (94). However, data for the usage *in vivo* and the efficacy in reducing plasma lipid levels are lacking.

1.4. Modulation of fat storage

Intensive research during the past decades revealed that adipose tissue is not only storing and releasing lipids, but also a complex (endocrine) organ. It was shown that, via the release of adipokines (e.g. leptin and adiponectin), adipose tissue also plays a major role in energy homeostasis and interacts with numerous central and peripheral satiety signals. Thus, adipose tissue also plays a pivotal role in lipid and carbohydrate metabolism, regulation of food intake, energy expenditure, blood pressure, blood coagulation and inflammation (95). However, excessive caloric intake with decreased energy expenditure leads to pathophysiological overgrowth of adipose tissue, which is associated with overweight and obesity (96). Hyperplasia, an increase in adipocyte number, is triggered by different signals which mediate the conversion of mesenchymal stemcells to preadipocytes, differentiating to mature adipocytes (97). Since adults are also capable of adipogenesis (98), the regulation of adipogenesis to avoid overgrowth of adipose tissue is an interesting target for the treatment of obesity (10).

1.4.1. Regulation of adipogenesis

Adipocytes originate from pluripotent mesenchymal stem cells (MSC), which can develop into several cell types, like myocytes, osteocytes, chondrocytes and adipocytes (99).

Several factors have been identified that regulate the conversion of pluripotent MSCs to one or another cell type. For example, the signaling glycoprotein Wnt10b promotes osteogenesis and myogenesis, while inhibiting adipogenesis (100-101). Whereas BMP4, a member of the bone morphogenetic protein family, inhibits myogenesis but promotes adipogenesis (102). Also, the transcription factor peroxisome proliferator-activated receptor (PPAR) gamma stimulates adipogenesis, but inhibits chondrogenesis at the same time (103). In summary, upon appropriate stimulation, the progenitor cells are restricted to the adipocytes linage, which gives rise to preadipocytes.

The final differentiation of preadipocytes to mature adipocytes has been widely investigated. However, most of the present knowledge has been gained via studying of cell model systems, like 3T3-L1 cells, since the diffuse nature of adipocyte differentiation *in vivo* makes *in vivo* or *ex vivo* studies difficult (97).

The process of differentiation of preadipocytes to mature adipocytes starts with growth cycle arrest, e.g. in G1 phase of the cell cycle. In cultured cells, at that point, differentiation can be initiated with a hormone cocktail, which includes high levels of insulin and a glucocorticoid (e.g. dexamethasone) and a substance that increases cellular cAMP levels (e.g. a cAMP analog). The hormone cocktail induces the IGF1-, glucocorticoid-, and cAMP signaling pathways and induces the differentiation program (104). The cAMP response starts immediately after initiation of differentiation by phosphorylation of CREB (cyclic AMP response element binding protein), which activates the expression of C/EBPβ (CCAAT enhancer binding protein beta) (105). About 16-20 hours after initiation of differentiation, C/EBPβ acquires DNA-binding activity through phosphorylation by MAP kinase and GSK-3β (106), and preadipocytes synchronously reenter the cell cycle for about two additional rounds of mitosis. This process is referred to as mitotic clonal expansion and is a crucial step for adipogenesis (107). The following morphologic changes include cytoplasmatic accumulation of triglycerides with an increased rate of de novo lipogenesis and expression of enzymes regulating triacylglycerol biosynthesis. In addition, C/EBPβ activates the expression of PPARγ and C/EBPα, which cross activate each other through C/EBP regulatory elements, leading, finally, to the transcription of a large group of genes that produce the adipocytes phenotype (108). The fully mature adipocyte contains one single large fat droplet, which is surrounded by cytoplasm. To release fatty acids to the blood, hormone-sensitive lipase (109) and adipocyte-triglycerid lipase (110) translocase to the surface of the fat droplet and catalyze lipolysis of triglycerides.

More recent research also identified a regulatory role for certain microRNAs (miRNA) in adipogenesis. Some miRNAs like miR-27 and miR-210 have been shown to promote adipogenesis, whereas others, e.g. members of the let-7 group seem to play an inhibitory role (111). Mechanisms of actions for the miRNAs have not been fully investigated; however, for example miR-27b has been shown to directly target the key transcription factor PPARγ (112).

1.4.2. Targeting adipogenesis for the treatment of obesity

The regulation of adipogenesis involves a complex signaling cascade with different crucial steps. Hence, there are many potential targets to reduce adipogenesis. For example, adipogenesis can be inhibited by blocking the progression of the cell cycle and, thereby blocking clonal expression and adipogenesis (107). But also a regulation of transcription factors, possibly via regulation of miRNAs, is conceivable. However, data demonstrating the efficacy of any adipogenesis-inhibiting compound *in vivo* are lacking. In addition, it is important to consider that the reduced fat mass would have to be recognized by the body. Otherwise, serious side effects from the inability to store excessive calories in fat depots could occur (10). Thus, drugs that reduce adipogenesis, without completely inhibiting it, could be used as a supporting measure in addition to an energy adapted diet and increased exercise.

1.5. Red pepper and capsaicin as anti-obesity compounds

Aroma compounds do not only contribute to the taste and flavor of our foods, but may also have medicinal properties and thus, beneficial effects on body weight maintenance (113). A compound that has been widely studied for its anti-obesity effects is capsaicin, the major pungent principle from red pepper. Red peppers are members of the *Capsicum* genus, with more than 200 varieties of different pungency (114). The pungency of a compound depends on their potency to activate the transient receptor potential vanilloid subtype 1 (TRPV1), a non-specific cation channel (115). However, also non-pungent structural analogues, so called capsinoids, have been shown to activate the TRPV1 receptor (116) and unfold anti-obesity effects (117). As a mechanism, it is suggested that capsiate and other capsinoids are not able to
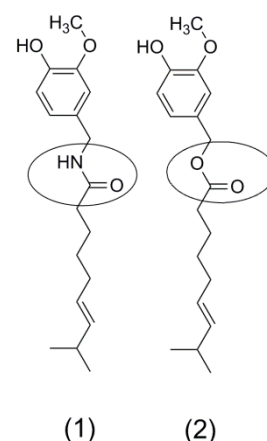
Figure 2. Chemical structures of capsaicin (1) and capsiate (2)

activate the TRPV1 receptor in the oral cavity, but still induce a TRPV1-mediated activation of intestinal extrinsic nerves in the gut of mice. This proposes gastrointestinal TRPV1 as a critical target for capsinoids (118).

In the following, the major effects of red pepper and its ingredients capsaicin and the caspinoid capsiate on different aspects of body weight maintenance will be discussed (**Figure 2**).

1.5.1. Capsaicin and capsiate in the regulation of food intake

Satiating properties of TRPV1-agonists have been focused on capsaicin with ten human intervention studies (119-126), whereas only two studies investigated the effects of capsiate on food intake (126-127).

In these studies, intake of capsaicin has been associated with suppressed feelings of hunger in general (122), especially with a reduced drive to eat hot (126), fatty, sweet and salty (123) foods. Several studies demonstrated that intake of capsaicin did not only reduce the self-reported desire to eat, but also the actual energy intake. In a first study, a reduced self-reported desire to eat and a reduced energy intake during lunch was shown in 13 Japanese women after a breakfast containing 10 g of red pepper (30 mg capsaicin) (122). A follow-up study with ten Caucasians demonstrated that also the application of an appetizer containing 6 g red pepper, corresponding to ~18 mg capsaicin, decreased total energy and carbohydrate intake in the following meal (122). A more recent study from the same group also showed a dose-response effect of red pepper on energy intake (121). Application of 0.9 g red pepper, containing 2.25 mg capsaicin, during a 2-day treatment was associated with reduced fat and total energy intake accompanied with a decreased energy density of the food (125). A very recent study found a small, but significant decrease in self-reported desire to eat over a period of 36 h after consuming a dinner balancing energy demand containing 2.56 mg capsaicin. However, decrease in desire to eat did not reach level of significance after dinner with a negative energy balance (75% of energy demand). The corresponding food intake of the standardized dinner tended to be lower (p=0.07) when dinner contained capsaicin at balanced energy demand as well as at negative energy balance (128). This underlines that capsaicin may have satiety and satiation effects in humans, prolonging inter-meal intervals and reducing meal size. In agreement with these findings for capsaicin, also the non-pungent capsiate was shown to decrease total energy intake during a positive energy balance (126).

However, not all studies are consistent with these findings. Lower amounts of 0.375 mg capsaicin did not demonstrate an effect on total energy intake (126), and, application of 1.09 g red pepper, containing about 2.6 mg capsaicin did not change self-reported satiety, although there was an increase in GLP-1 plasma levels (120). However, also the application of higher amounts of 33 mg capsaicin per day in a 4-week cross-over trial did not lead to significant changes in energy intake (119). In addition, no effect on total energy intake was reported from the second study adminsitering 6 mg capsinoids in a capsule per day for 12 weeks (127).

The inconsistency in the data could be due to the differences in the subject characteristics and their adaption to hot food due to cultural differences. Especially the definition of 'frequent users' versus 'naive users' is not consistent over the studies (129). An impact of eating habits regarding capsaicinoids and/or capsinoid-containing food intake is supported by a randomized crossover trial that showed a significant decrease in energy intake in non-users, but not in users. In this study, users were defined as subjects consuming spicy food more than 3 times a week (123).

Since the study designs and subject characteristics are quite variable throughout the different studies, an appropriate meta-analysis regarding regulation of food intake could not be conceived for neither for capsaicin nor for capsiate (129).

1.5.2. Capsaicin and capsiate in the regulation of thermogenesis and body composition

Several studies reported a stimulation of thermogenesis via an increase in energy expenditure after ingestion of capsaicin (123-124,130-133). This effect was also shown for an ingestion of different capsinoids (127,134-136). However, data are still conflicting, since other studies with comparable amounts of capsaicin and capsinoids did not report an effect on energy expenditure (117,119,137). A potential explanation for the inconsistent results may be found in the differences in body composition of the test subjects throughout the different studies, which may have an impact on the thermogenic effects (129). Whereas the majority of the studies that report increased energy expenditure have been conducted with lean individuals (123,130-131,133), data reading energy expenditure from overweight subjects are inconsistent (119,124,130). In addition, a certain tolerance over time is thought to play a major role. Inoue et al. (127) reported a declining effect of capsinoid treatment after four weeks compared to two weeks. And, similar to the studies that assessed an effect of capsaicin

on appetite, there might also be effects of an adaption to hot food due to cultural differences (129). A meta-analysis revealed an overall effect on energy expenditure for capsiate treatments, but not for that of capsaicin. However, when subdivided by dose, capsaicin led to an increased energy expenditure at high amounts above 135 mg, but not below. Although these data point to a dose-dependent effect, the result should be treated with caution, since the data originate from studies of different length and in different environments (129).

The question whether an increased thermogenesis, combined with reduced appetite may also lead to changes in body weight composition can only be answered to a limited extent, since most studies were designed as short-term interventions. A total of four studies assessed long term effects (>3 weeks), but only two of them included changes in body composition (119,124). However, both studies did not show an effect of capsaicin treatment, however, at least one study (124) reported compliance issues due to pungency of capsaicin. Beside low compliance of the test subjects, a desensitization to capsaicin over time as well as limited study duration could be responsible for the lack of effect (129).

In contrast to capsaicin, several studies investigating the effect of capsinoids have been carried out for more than two weeks (117,127,136-138). Three reported a decrease in body weight (117,127,138), which is inconsistent with the findings of the other two studies (134,136). The discrepancies may be due to large differences in study design, since the two-week study carried out by Kawabata et al. (138) was conducted in a very controlled environment, especially regarding diet. In addition, different capsinoids, capsiate, dihydrocapsiate, nordihydrocapsiate or a mixture thereof, with or without encapsulation were used in the studies and the studies all differed in duration.

1.5.3. Hypolipidemic and hypocholesterolemic properties of capsaicin

Consumption of red pepper and/or capsaicin is not only associated with decreased food intake and increased energy metabolism, but also with hypolipidemic and hypocholesteremic activities. A whole series of animal studies from the 1980s investigated the serum-cholesterol-lowering effect of red pepper and capsaicin. First, Sambaiah and Satyanarayana reported that addition of 5% red pepper resulted in a hypocholesterolemic effect in rats fed a 1% cholesterol diet (139). This serum-cholesterol lowering effect was confirmed by another study, in which rats were fed equivalent amounts of pure capsaicin of 1.5, 3 and 15mg% in a 10% fat diet for eight weeks (140). But also significantly lower levels of 0.2mg% of synthetic and natural capsaicin lowered serum cholesterol levels in rats fed a 10 % and a

30% fat diet for eight or 13 wekks (141). In addition, a more recent study by Kempaiah and colleagues from 2006 demonstrated that 0.015% capsaicin in the diet also acts as a hypotriglyceridemic agent in rats fed a 30% fat diet for eight weeks (142). However, the underlying mechanisms are not fully elucidated yet. Negulesco et al. argued that decreased cholesterol absorption combined with increased excretion of bile acids and cholesterol in the feces lead to an enhanced expression of hepatic LDL receptors, and hence to decreased plasma cholesterol concentrations (143). Also a stimulation of cholesterol-7α-hydroxylase activity, an important pathway for elimination of cholesterol from the body, has been considered, but seems unlikely since a simultaneous increase in of HMG-CoA reductase stimulates cholesterol synthesis as wells (144). In addition, another study demonstrating a hypocholsterolemic effect of 0.014% capsaicin in a 30 w/w-% lard diet over ten days showed an increase in adipose lipoprotein lipase, but no effect on hormone sensitive lipase or lipid absorption (145).

However, data from human interventions or *in vitro* mechanistic studies concerning the effect of capsaicin or related compounds on lipid or fatty acid metabolism, especially regarding (intestinal) fatty acid uptake, are lacking so far.

1.5.4. *In vitro* mechanistic approaches to identify anti-obesity effects of capsaicin

None of the presented *in vivo* studies explained the underlying mechanism of the capsaicin-induced effects. However, several *in vitro* studies may be consulted to illuminate capsaicin effects from a mechanistic point of view.

Reduced appetite after oral administration of capsaicin could be partly the result of an enhanced catecholamine secretion. It was shown that TRPV1 activation by 50 µM capsaicin and the subsequent calcium influx into the cell have a stimulating effect on the firing rate of dopaminergic neurons in rat brain slices (146). In addition, microdialysis in rats revealed a three-fold increase in extracellular serotonin levels in the ventromedial medulla after application of 0.1 mg capsaicin in 50 µL, corresponding to 6.5 mM capsaicin (147). The neurotransmitter-stimulating effect of capsaicin is supported by increased expression of the 5-HT_{2A} serotonin receptor and D_1-dopamine receptor in rat brain slices following subcutaneous application of a dose of 50 mg/kg body weight capsaicin (148). However, catecholamine secretion could also account for increased thermogenesis, mainly via activation of the central nervous system. Since the capsaicin-induced thermogenesis could be prevented by the

addition of beta blockers, an enhanced thermogenesis is probably based on a β-adrenergic stimulation (149).

The effects of capsaicin on 3T3-L1 adipocytes may help explain capsaicin-derived changes in body composition. Application of 0.1-10 µM capsaicin for 24 h revealed a dose-dependent decrease in intracellular lipids and triglycerides, accompanied with increased gene expression of hormone-sensitive lipase (HSL), carnitine palmitoyltransferase-1α (CPT1α) and uncoupling protein 2 (UCP2). Whereas HSL and CPT1α are markers of lipid catabolism, UCP2 is associated with thermogenesis (150). In addition, application of capsaicin in the lower µM range was shown to inhibit adipogenesis via TRPV1 receptor activation (151). As a mechanism for TRPV1-mediated anti-adipogenic effects, activation of calcineurin by increased intracellular calcium levels, leading to decreased PPARγ and C/EBPα levels, is proposed (152).

These findings from *in vitro* studies shed light on possible mechanistic pathways of capsaicin-mediated anti-obesity effects, however, complete signaling pathways, especially for the hypocholesteremic and hypolipidemic effects of capsaicin, are not available yet.

In summary, the TRPV1-agonists capsaicin and capsiate, especially at high doses, have been shown to target different mechanisms of body weight maintenance, like regulation of food intake, thermogenesis, body composition, and blood lipids under certain conditions. However, inter alia, variable study designs and subjects with different adaption to hot food, accompanied with varying compliance to pungency, led to conflicting findings *in vivo*. The pungency of a compound is directly correlated with the kinetics of TRPV1 receptor activation (153). For capsaicin, EC_{50} values between 0.1 and 0.7 µM for TRPV1 activation are described in the literature (116,154). For capsiate, an EC_{50} value in the same range, 0.3 µM, has been calculated (116). Therefore, it seems reasonable that experiments with the non-pungent capsaicin-analog capsiate and other capsinoids were not able to overcome all compliance problems, since activation of the TRPV1 receptor in the gut led sometimes to stomach irritations comparable to those after consumption of capsaicin (117), although there is no pungent sensation after intake of capsiate in the oral cavity.

In summary, this underlines the need for more 1) additional long-term interventions with capsaicinoids and 2) less pungent alternatives with lower TRPV1 binding affinity, but similar efficacy compared to capsaicin and capsiate. In addition, the mechanisms of action underlying the effects of TRPV1-agonists regarding body weight management have not been fully elucidated yet and require further mechanistic (*in vitro*) approaches.

The main objectives of this work were to establish suitable screening systems to investigate mechanisms regulating satiety (refer to PART I) and to assess the impact of the pungent aroma compounds capsaicin, nonivamide and *trans*-pellitorine on mechanisms regulating satiety and energy metabolism (refer to PART II).

1.6. References

1. Swinburn, B. A., Sacks, G., Hall, K. D., McPherson, K., Finegood, D. T., Moodie, M. L., and Gortmaker, S. L. (2011) The global obesity pandemic: shaped by global drivers and local environments. *Lancet* **378**, 804-814

2. Berghofer, A., Pischon, T., Reinhold, T., Apovian, C. M., Sharma, A. M., and Willich, S. N. (2008) Obesity prevalence from a European perspective: a systematic review. *BMC Public Health* **8**, 200

3. Oster, G., Edelsberg, J., O'Sullivan, A. K., and Thompson, D. (2000) The clinical and economic burden of obesity in a managed care setting. *Am J Manag Care* **6**, 681-689

4. Canoy, D., Boekholdt, S. M., Wareham, N., Luben, R., Welch, A., Bingham, S., Buchan, I., et al. (2007) Body fat distribution and risk of coronary heart disease in men and women in the European Prospective Investigation Into Cancer and Nutrition in Norfolk cohort: a population-based prospective study. *Circulation* **116**, 2933-2943

5. Mokdad, A. H., Bowman, B. A., Ford, E. S., Vinicor, F., Marks, J. S., and Koplan, J. P. (2001) The continuing epidemics of obesity and diabetes in the United States. *JAMA* **286**, 1195-1200

6. Pischon, T., Boeing, H., Hoffmann, K., Bergmann, M., Schulze, M. B., Overvad, K., van der Schouw, Y. T., et al. (2008) General and abdominal adiposity and risk of death in Europe. *N Engl J Med* **359**, 2105-2120

7. Pischon, T., Nothlings, U., and Boeing, H. (2008) Obesity and cancer. *Proc Nutr Soc* **67**, 128-145

8. Whitlock, G., Lewington, S., Sherliker, P., Clarke, R., Emberson, J., Halsey, J., Qizilbash, N., et al. (2009) Body-mass index and cause-specific mortality in 900 000 adults: collaborative analyses of 57 prospective studies. *Lancet* **373**, 1083-1096

9. Bijlsma, J. W., Berenbaum, F., and Lafeber, F. P. (2011) Osteoarthritis: an update with relevance for clinical practice. *Lancet* **377**, 2115-2126

10. Bray, G. A., and Tartaglia, L. A. (2000) Medicinal strategies in the treatment of obesity. *Nature* **404**, 672-677

11. Bellisle, F., and Blundell, J. (2013) Satiation, satiety: concepts and organisation of behaviour. *Satiation, satiety and the control of food intake: theory and practice*, 3-11

12. Konturek, S. J., Konturek, J. W., Pawlik, T., and Brzozowski, T. (2004) Brain-gut axis and its role in the control of food intake. *J Physiol Pharmacol* **55**, 137-154

13. Grill, H. J., and Kaplan, J. M. (2002) The neuroanatomical axis for control of energy balance. *Front Neuroendocrinol* **23**, 2-40

14. Naslund, E., and Hellstrom, P. M. (2007) Appetite signaling: from gut peptides and enteric nerves to brain. *Physiol Behav* **92**, 256-262

15. Harrold, J. A., Dovey, T. M., Blundell, J. E., and Halford, J. C. (2012) CNS regulation of appetite. *Neuropharmacology* **63**, 3-17

16. Cowley, M. A., Smart, J. L., Rubinstein, M., Cerdan, M. G., Diano, S., Horvath, T. L., Cone, R. D., et al. (2001) Leptin activates anorexigenic POMC neurons through a neural network in the arcuate nucleus. *Nature* **411**, 480-484

17. Wikberg, J. E., Mutulis, F., Mutule, I., Veiksina, S., Lapinsh, M., Petrovska, R., and Prusis, P. (2003) Melanocortin receptors: ligands and proteochemometrics modeling. *Ann N Y Acad Sci* **994**, 21-26

18. Cheung, C. C., Clifton, D. K., and Steiner, R. A. (1997) Proopiomelanocortin neurons are direct targets for leptin in the hypothalamus. *Endocrinology* **138**, 4489-4492

19. Lambert, P. D., Couceyro, P. R., McGirr, K. M., Dall Vechia, S. E., Smith, Y., and Kuhar, M. J. (1998) CART peptides in the central control of feeding and interactions with neuropeptide Y. *Synapse* **29**, 293-298

20.   Stanley, B. G., Chin, A. S., and Leibowitz, S. F. (1985) Feeding and drinking elicited by central injection of neuropeptide Y: evidence for a hypothalamic site(s) of action. *Brain Res Bull* **14**, 521-524

21.   Michel, M. C., Beck-Sickinger, A., Cox, H., Doods, H. N., Herzog, H., Larhammar, D., Quirion, R., et al. (1998) XVI. International Union of Pharmacology recommendations for the nomenclature of neuropeptide Y, peptide YY, and pancreatic polypeptide receptors. *Pharmacol Rev* **50**, 143-150

22.   Gerald, C., Walker, M. W., Criscione, L., Gustafson, E. L., Batzl-Hartmann, C., Smith, K. E., Vaysse, P., et al. (1996) A receptor subtype involved in neuropeptide-Y-induced food intake. *Nature* **382**, 168-171

23.   Mashiko, S., Moriya, R., Ishihara, A., Gomori, A., Matsushita, H., Egashira, S., Iwaasa, H., et al. (2009) Synergistic interaction between neuropeptide Y1 and Y5 receptor pathways in regulation of energy homeostasis. *Eur J Pharmacol* **615**, 113-117

24.   Acuna-Goycolea, C., and van den Pol, A. N. (2005) Peptide YY(3-36) inhibits both anorexigenic proopiomelanocortin and orexigenic neuropeptide Y neurons: implications for hypothalamic regulation of energy homeostasis. *J Neurosci* **25**, 10510-10519

25.   Chee, M. J., Myers, M. G., Jr., Price, C. J., and Colmers, W. F. (2010) Neuropeptide Y suppresses anorexigenic output from the ventromedial nucleus of the hypothalamus. *J Neurosci* **30**, 3380-3390

26.   Pandit, R., la Fleur, S. E., and Adan, R. A. (2013) The role of melanocortins and Neuropeptide Y in food reward. *Eur J Pharmacol*

27.   Ollmann, M. M., Wilson, B. D., Yang, Y. K., Kerns, J. A., Chen, Y., Gantz, I., and Barsh, G. S. (1997) Antagonism of central melanocortin receptors in vitro and in vivo by agouti-related protein. *Science* **278**, 135-138

28.   Dietrich, M. O., and Horvath, T. L. (2013) Hypothalamic control of energy balance: insights into the role of synaptic plasticity. *Trends Neurosci* **36**, 65-73

29.   Meguid, M. M., Fetissov, S. O., Varma, M., Sato, T., Zhang, L., Laviano, A., and Rossi-Fanelli, F. (2000) Hypothalamic dopamine and serotonin in the regulation of food intake. *Nutrition* **16**, 843-857

30.   Volkow, N. D., Wang, G. J., Telang, F., Fowler, J. S., Thanos, P. K., Logan, J., Alexoff, D., et al. (2008) Low dopamine striatal D2 receptors are associated with prefrontal metabolism in obese subjects: possible contributing factors. *NeuroImage* **42**, 1537-1543

31.   Wang, G. J., Volkow, N. D., Logan, J., Pappas, N. R., Wong, C. T., Zhu, W., Netusil, N., et al. (2001) Brain dopamine and obesity. *Lancet* **357**, 354-357

32.   Wang, J., Yuan, Z., Dong, J., Zhang, D., Usami, T., Murata, T., Narita, K., et al. (2013) Neuropeptide Y loses its orexigenic effect in rats with lesions of the hypothalamic paraventricular nucleus. *Endocr Res* **38**, 8-14

33.   Volkow, N. D., and Wise, R. A. (2005) How can drug addiction help us understand obesity? *Nat Neurosci* **8**, 555-560

34.   Terry, P., Gilbert, D. B., and Cooper, S. J. (1995) Dopamine receptor subtype agonists and feeding behavior. *Obes Res* **3 Suppl 4**, 515S-523S

35.   Erlanson-Albertsson, C. (2005) How palatable food disrupts appetite regulation. *Basic Clin Pharmacol* **97**, 61-73

36.   Halford, J. C., Harrold, J. A., Boyland, E. J., Lawton, C. L., and Blundell, J. E. (2007) Serotonergic drugs : effects on appetite expression and use for the treatment of obesity. *Drugs* **67**, 27-55

37.   Woolley, M. L., Marsden, C. A., and Fone, K. C. (2004) 5-ht6 receptors. *Curr Drug Targets CNS Neurol Disord* **3**, 59-79

38. Rogers, P., McKibbin, P. E., and Williams, G. (1991) Acute fenfluramine administration reduces neuropeptide Y concentrations in specific hypothalamic regions of the rat: possible implications for the anorectic effect of fenfluramine. *Peptides* **12**, 251-255

39. Heisler, L. K., Cowley, M. A., Tecott, L. H., Fan, W., Low, M. J., Smart, J. L., Rubinstein, M., et al. (2002) Activation of central melanocortin pathways by fenfluramine. *Science* **297**, 609-611

40. Heisler, L. K., Jobst, E. E., Sutton, G. M., Zhou, L., Borok, E., Thornton-Jones, Z., Liu, H. Y., et al. (2006) Serotonin reciprocally regulates melanocortin neurons to modulate food intake. *Neuron* **51**, 239-249

41. Heisler, L. K., Cowley, M. A., Kishi, T., Tecott, L. H., Fan, W., Low, M. J., Smart, J. L., et al. (2003) Central serotonin and melanocortin pathways regulating energy homeostasis. *Ann N Y Acad Sci* **994**, 169-174

42. Halford, J. C., and Blundell, J. E. (2000) Separate systems for serotonin and leptin in appetite control. *Ann Med* **32**, 222-232

43. Tschop, M., Smiley, D. L., and Heiman, M. L. (2000) Ghrelin induces adiposity in rodents. *Nature* **407**, 908-913

44. Wren, A. M., Small, C. J., Abbott, C. R., Dhillo, W. S., Seal, L. J., Cohen, M. A., Batterham, R. L., et al. (2001) Ghrelin causes hyperphagia and obesity in rats. *Diabetes* **50**, 2540-2547

45. Wren, A. M., Seal, L. J., Cohen, M. A., Brynes, A. E., Frost, G. S., Murphy, K. G., Dhillo, W. S., et al. (2001) Ghrelin enhances appetite and increases food intake in humans. *J Clin Endocrinol Metab* **86**, 5992

46. Faulconbridge, L. F., Cummings, D. E., Kaplan, J. M., and Grill, H. J. (2003) Hyperphagic effects of brainstem ghrelin administration. *Diabetes* **52**, 2260-2265

47. Nakazato, M., Murakami, N., Date, Y., Kojima, M., Matsuo, H., Kangawa, K., and Matsukura, S. (2001) A role for ghrelin in the central regulation of feeding. *Nature* **409**, 194-198

48. Pi-Sunyer, X., Kissileff, H. R., Thornton, J., and Smith, G. P. (1982) C-terminal octapeptide of cholecystokinin decreases food intake in obese men. *Physiol Behav* **29**, 627-630

49. Cummings, D. E., and Overduin, J. (2007) Gastrointestinal regulation of food intake. *J Clin Invest* **117**, 13-23

50. Fan, W., Ellacott, K. L., Halatchev, I. G., Takahashi, K., Yu, P., and Cone, R. D. (2004) Cholecystokinin-mediated suppression of feeding involves the brainstem melanocortin system. *Nat Neurosci* **7**, 335-336

51. Peter, L., Stengel, A., Noetzel, S., Inhoff, T., Goebel, M., Tache, Y., Veh, R. W., et al. (2010) Peripherally injected CCK-8S activates CART positive neurons of the paraventricular nucleus in rats. *Peptides* **31**, 1118-1123

52. Burdyga, G., de Lartigue, G., Raybould, H. E., Morris, R., Dimaline, R., Varro, A., Thompson, D. G., et al. (2008) Cholecystokinin regulates expression of Y2 receptors in vagal afferent neurons serving the stomach. *J Neurosci* **28**, 11583-11592

53. de Lartigue, G., Dimaline, R., Varro, A., and Dockray, G. J. (2007) Cocaine- and amphetamine-regulated transcript: stimulation of expression in rat vagal afferent neurons by cholecystokinin and suppression by ghrelin. *J Neurosci* **27**, 2876-2882

54. Date, Y., Toshinai, K., Koda, S., Miyazato, M., Shimbara, T., Tsuruta, T., Niijima, A., et al. (2005) Peripheral interaction of ghrelin with cholecystokinin on feeding regulation. *Endocrinology* **146**, 3518-3525

55. Kobelt, P., Tebbe, J. J., Tjandra, I., Stengel, A., Bae, H. G., Andresen, V., van der Voort, I. R., et al. (2005) CCK inhibits the orexigenic effect of peripheral ghrelin. *Am J Physiol Regul Integr Comp Physiol* **288**, R751-758

56.   Bi, S., Scott, K. A., Kopin, A. S., and Moran, T. H. (2004) Differential roles for cholecystokinin a receptors in energy balance in rats and mice. *Endocrinology* **145**, 3873-3880

57.   Donovan, M. J., Paulino, G., and Raybould, H. E. (2007) CCK(1) receptor is essential for normal meal patterning in mice fed high fat diet. *Physiol Behav* **92**, 969-974

58.   Lee, J., Martin, E., Paulino, G., de Lartigue, G., and Raybould, H. E. (2011) Effect of ghrelin receptor antagonist on meal patterns in cholecystokinin type 1 receptor null mice. *Physiol Behav* **103**, 181-187

59.   Naslund, E., Bogefors, J., Skogar, S., Gryback, P., Jacobsson, H., Holst, J. J., and Hellstrom, P. M. (1999) GLP-1 slows solid gastric emptying and inhibits insulin, glucagon, and PYY release in humans. *Am J Physiol* **277**, R910-916

60.   Gutzwiller, J. P., Goke, B., Drewe, J., Hildebrand, P., Ketterer, S., Handschin, D., Winterhalder, R., et al. (1999) Glucagon-like peptide-1: a potent regulator of food intake in humans. *Gut* **44**, 81-86

61.   Naslund, E., Barkeling, B., King, N., Gutniak, M., Blundell, J. E., Holst, J. J., Rossner, S., et al. (1999) Energy intake and appetite are suppressed by glucagon-like peptide-1 (GLP-1) in obese men. *Int J Obes Relat Metab Disord* **23**, 304-311

62.   Abbott, C. R., Monteiro, M., Small, C. J., Sajedi, A., Smith, K. L., Parkinson, J. R., Ghatei, M. A., et al. (2005) The inhibitory effects of peripheral administration of peptide YY(3-36) and glucagon-like peptide-1 on food intake are attenuated by ablation of the vagal-brainstem-hypothalamic pathway. *Brain Res* **1044**, 127-131

63.   Zhang, J., and Ritter, R. C. (2012) Circulating GLP-1 and CCK-8 reduce food intake by capsaicin-insensitive, nonvagal mechanisms. *Am J Physiol Regul Integr Comp Physiol* **302**, R264-273

64.   Batterham, R. L., Cowley, M. A., Small, C. J., Herzog, H., Cohen, M. A., Dakin, C. L., Wren, A. M., et al. (2002) Gut hormone PYY(3-36) physiologically inhibits food intake. *Nature* **418**, 650-654

65.   Challis, B. G., Pinnock, S. B., Coll, A. P., Carter, R. N., Dickson, S. L., and O'Rahilly, S. (2003) Acute effects of PYY3-36 on food intake and hypothalamic neuropeptide expression in the mouse. *Biochem Biophys Res Commun* **311**, 915-919

66.   Batterham, R. L., Cohen, M. A., Ellis, S. M., Le Roux, C. W., Withers, D. J., Frost, G. S., Ghatei, M. A., et al. (2003) Inhibition of food intake in obese subjects by peptide YY3-36. *N Engl J Med* **349**, 941-948

67.   Balasubramaniam, A., Joshi, R., Su, C., Friend, L. A., and James, J. H. (2007) Neuropeptide Y (NPY) Y2 receptor-selective agonist inhibits food intake and promotes fat metabolism in mice: combined anorectic effects of Y2 and Y4 receptor-selective agonists. *Peptides* **28**, 235-240

68.   De Silva, A., Salem, V., Long, C. J., Makwana, A., Newbould, R. D., Rabiner, E. A., Ghatei, M. A., et al. (2011) The gut hormones PYY 3-36 and GLP-1 7-36 amide reduce food intake and modulate brain activity in appetite centers in humans. *Cell Metab* **14**, 700-706

69.   Rodríguez, A., Catalán, V., Frühbeck, G., Blundell, J., and Bellisle, F. (2013) Metabolism and satiety. in *Satiation, satiety and the control of food intake: theory and practice*, Woodhead Publishing Ltd

70.   Mercer, J. G., Moar, K. M., Rayner, D. V., Trayhurn, P., and Hoggard, N. (1997) Regulation of leptin receptor and NPY gene expression in hypothalamus of leptin-treated obese (ob/ob) and cold-exposed lean mice. *FEBS Lett* **402**, 185-188

71.   Berglund, E. D., Vianna, C. R., Donato, J., Jr., Kim, M. H., Chuang, J. C., Lee, C. E., Lauzon, D. A., et al. (2012) Direct leptin action on POMC neurons regulates glucose homeostasis and hepatic insulin sensitivity in mice. *J Clin Invest* **122**, 1000-1009

72.   Hill, J. W., Elias, C. F., Fukuda, M., Williams, K. W., Berglund, E. D., Holland, W. L., Cho, Y. R., et al. (2010) Direct insulin and leptin action on pro-opiomelanocortin neurons is required for normal glucose homeostasis and fertility. *Cell Metab* **11**, 286-297

73.   Meltzer, H. Y., and Roth, B. L. (2013) Lorcaserin and pimavanserin: emerging selectivity of serotonin receptor subtype-targeted drugs. *J Clin Invest* **123**, 4986-4991

74.   Sargent, B. J., and Moore, N. A. (2009) New central targets for the treatment of obesity. *Br J Clin Pharmacol* **68**, 852-860

75.   Heymsfield, S. B., Greenberg, A. S., Fujioka, K., Dixon, R. M., Kushner, R., Hunt, T., Lubina, J. A., et al. (1999) Recombinant leptin for weight loss in obese and lean adults: a randomized, controlled, dose-escalation trial. *JAMA* **282**, 1568-1575

76.   Banks, W. A., Kastin, A. J., Huang, W., Jaspan, J. B., and Maness, L. M. (1996) Leptin enters the brain by a saturable system independent of insulin. *Peptides* **17**, 305-311

77.   Wikberg, J. E., and Mutulis, F. (2008) Targeting melanocortin receptors: an approach to treat weight disorders and sexual dysfunction. *Nat Rev Drug Discov* **7**, 307-323

78.   Henry, R. e. a. (2006) Exenatide maintained glycemic control with associated weight reduction over 2 years in patients with type 2 diabetes [abstract]. in *66th Scientific Sessions of the American Diabetes Association*, Washingtion DC, USA

79.   Thews, G., Mutschler, E., and Vaupel, P. (1999) *Anatomie, Physiologie und Pathophysiologie des Menschen:135 Tabellen*, 5 ed., Wissenschaftliche Verlagsgesellschaft mbH, Stuttgart

80.   Pownall, H. J., and Hamilton, J. A. (2003) Energy translocation across cell membranes and membrane models. *Acta Physiol Scand* **178**, 357-365

81.   Hamilton, J. A. (1999) Transport of fatty acids across membranes by the diffusion mechanism. *Prostaglandins Leukot Essent Fatty Acids* **60**, 291-297

82.   Storch, J., and Thumser, A. E. (2010) Tissue-specific functions in the fatty acid-binding protein family. *J Biol Chem* **285**, 32679-32683

83.   Mashek, D. G., and Coleman, R. A. (2006) Cellular fatty acid uptake: the contribution of metabolism. *Curr Opin Lipidol* **17**, 274-278

84.   Black, P. N., Sandoval, A., Arias-Barrau, E., and DiRusso, C. C. (2009) Targeting the Fatty Acid Transport Proteins (FATP) to Understand the Mechanisms Linking Fatty Acid Transport to Metabolism. *mmunol Endocr Metab Agents Med Chem* **9**, 11-17

85.   Lobo, M. V., Huerta, L., Ruiz-Velasco, N., Teixeiro, E., de la Cueva, P., Celdran, A., Martin-Hidalgo, A., et al. (2001) Localization of the lipid receptors CD36 and CLA-1/SR-BI in the human gastrointestinal tract: towards the identification of receptors mediating the intestinal absorption of dietary lipids. *J Histochem Cytochem* **49**, 1253-1260

86.   Nauli, A. M., Nassir, F., Zheng, S., Yang, Q., Lo, C. M., Vonlehmden, S. B., Lee, D., et al. (2006) CD36 is important for chylomicron formation and secretion and may mediate cholesterol uptake in the proximal intestine. *Gastroenterology* **131**, 1197-1207

87.   Schwartz, G. J., Fu, J., Astarita, G., Li, X., Gaetani, S., Campolongo, P., Cuomo, V., et al. (2008) The lipid messenger OEA links dietary fat intake to satiety. *Cell Metab* **8**, 281-288

88.   Abumrad, N. A., and Davidson, N. O. (2012) Role of the gut in lipid homeostasis. *Physiol Rev* **92**, 1061-1085

89.   Laugerette, F., Passilly-Degrace, P., Patris, B., Niot, I., Febbraio, M., Montmayeur, J. P., and Besnard, P. (2005) CD36 involvement in orosensory detection of dietary lipids, spontaneous fat preference, and digestive secretions. *J Clin Invest* **115**, 3177-3184

90.   Storch, J., and Thumser, A. E. (2000) The fatty acid transport function of fatty acid-binding proteins. *Biochim Biophys Acta* **1486**, 28-44

91.   Coe, N. R., Smith, A. J., Frohnert, B. I., Watkins, P. A., and Bernlohr, D. A. (1999) The fatty acid transport protein (FATP1) is a very long chain acyl-CoA synthetase. *J Biol Chem* **274**, 36300-36304

92.   Sandoval, A., Fraisl, P., Arias-Barrau, E., Dirusso, C. C., Singer, D., Sealls, W., and Black, P. N. (2008) Fatty acid transport and activation and the expression patterns of genes involved in fatty acid trafficking. *Arch Biochem Biophys* **477**, 363-371

93.   Guerciolini, R. (1997) Mode of action of orlistat. *Int J Obes Relat Metab Disord* **21 Suppl 3**, S12-23

94.   Sandoval, A., Chokshi, A., Jesch, E. D., Black, P. N., and DiRusso, C. C. (2010) Identification and characterization of small compound inhibitors of human FATP2. *Biochem. Pharm.* **79**, 990-999

95.   Harwood, H. J., Jr. (2012) The adipocyte as an endocrine organ in the regulation of metabolic homeostasis. *Neuropharmacol.* **63**, 57-75

96.   Wahlqvist, M. L. (2005) Dietary fat and the prevention of chronic disease. *Asia Pac J Clin Nutr* **14**, 313-318

97.   Tang, Q. Q., and Lane, M. D. (2012) Adipogenesis: from stem cell to adipocyte. *Annu Rev Biochem* **81**, 715-736

98.   Hausman, D. B., DiGirolamo, M., Bartness, T. J., Hausman, G. J., and Martin, R. J. (2001) The biology of white adipocyte proliferation. *Obes. Rev.* **2**, 239-254

99.   Tang, Q. Q., Otto, T. C., and Lane, M. D. (2004) Commitment of C3H10T1/2 pluripotent stem cells to the adipocyte lineage. *Proc Natl Acad Sci U S A* **101**, 9607-9611

100.   Ross, S. E., Hemati, N., Longo, K. A., Bennett, C. N., Lucas, P. C., Erickson, R. L., and MacDougald, O. A. (2000) Inhibition of adipogenesis by Wnt signaling. *Science* **289**, 950-953

101.   Bennett, C. N., Longo, K. A., Wright, W. S., Suva, L. J., Lane, T. F., Hankenson, K. D., and MacDougald, O. A. (2005) Regulation of osteoblastogenesis and bone mass by Wnt10b. *Proc Natl Acad Sci U S A* **102**, 3324-3329

102.   Kang, S., Bennett, C. N., Gerin, I., Rapp, L. A., Hankenson, K. D., and Macdougald, O. A. (2007) Wnt signaling stimulates osteoblastogenesis of mesenchymal precursors by suppressing CCAAT/enhancer-binding protein alpha and peroxisome proliferator-activated receptor gamma. *J Biol Chem* **282**, 14515-14524

103.   Isenmann, S., Arthur, A., Zannettino, A. C., Turner, J. L., Shi, S., Glackin, C. A., and Gronthos, S. (2009) TWIST family of basic helix-loop-helix transcription factors mediate human mesenchymal stem cell growth and commitment. *Stem Cells* **27**, 2457-2468

104.   Student, A. K., Hsu, R. Y., and Lane, M. D. (1980) Induction of fatty acid synthetase synthesis in differentiating 3T3-L1 preadipocytes. *J Biol Chem* **255**, 4745-4750

105.   Zhang, J. W., Klemm, D. J., Vinson, C., and Lane, M. D. (2004) Role of CREB in transcriptional regulation of CCAAT/enhancer-binding protein beta gene during adipogenesis. *J Biol Chem* **279**, 4471-4478

106.   Tang, Q. Q., Gronborg, M., Huang, H., Kim, J. W., Otto, T. C., Pandey, A., and Lane, M. D. (2005) Sequential phosphorylation of CCAAT enhancer-binding protein beta by MAPK and glycogen synthase kinase 3beta is required for adipogenesis. *Proc Natl Acad Sci U S A* **102**, 9766-9771

107.   Patel, Y. M., and Lane, M. D. (2000) Mitotic clonal expansion during preadipocyte differentiation: calpain-mediated turnover of p27. *J Biol Chem* **275**, 17653-17660

108. Clarke, S. L., Robinson, C. E., and Gimble, J. M. (1997) CAAT/enhancer binding proteins directly modulate transcription from the peroxisome proliferator-activated receptor gamma 2 promoter. *Biochem Biophys Res Commun* **240**, 99-103

109. Egan, J. J., Greenberg, A. S., Chang, M. K., Wek, S. A., Moos, M. C., Jr., and Londos, C. (1992) Mechanism of hormone-stimulated lipolysis in adipocytes: translocation of hormone-sensitive lipase to the lipid storage droplet. *Proc Natl Acad Sci U S A* **89**, 8537-8541

110. Ahmadian, M., Wang, Y., and Sul, H. S. (2010) Lipolysis in adipocytes. *Int J Biochem Cell Biol* **42**, 555-559

111. McGregor, R. A., and Choi, M. S. (2011) microRNAs in the regulation of adipogenesis and obesity. *Curr. Mol. Med.* **11**, 304-316

112. Karbiener, M., Fischer, C., Nowitsch, S., Opriessnig, P., Papak, C., Ailhaud, G., Dani, C., et al. (2009) microRNA miR-27b impairs human adipocyte differentiation and targets PPARgamma. *Biochem Biophys Res Commun* **390**, 247-251

113. Yun, J. W. (2010) Possible anti-obesity therapeutics from nature - A review. *Phytochemistry* **71**, 1625-1641

114. Iwai, K., Yazawa, A., and Watanabe, T. (2003) Roles as metabolic regulators of the non-nutrients, capsaicin and capsiate, supplemented to diets. *Proc Jpn Acad, B* **79**, 207-212

115. Ursu, D., Knopp, K., Beattie, R. E., Liu, B., and Sher, E. (2010) Pungency of TRPV1 agonists is directly correlated with kinetics of receptor activation and lipophilicity. *Eur J Pharmacol* **641**, 114-122

116. Iida, T., Moriyama, T., Kobata, K., Morita, A., Murayama, N., Hashizume, S., Fushiki, T., et al. (2003) TRPV1 activation and induction of nociceptive response by a non-pungent capsaicin-like compound, capsiate. *Neuropharmacology* **44**, 958-967

117. Snitker, S., Fujishima, Y., Shen, H., Ott, S., Pi-Sunyer, X., Furuhata, Y., Sato, H., et al. (2009) Effects of novel capsinoid treatment on fatness and energy metabolism in humans: possible pharmacogenetic implications. *Am J Clin Nutr* **89**, 45-50

118. Kawabata, F., Inoue, N., Masamoto, Y., Matsumura, S., Kimura, W., Kadowaki, M., Higashi, T., et al. (2009) Non-pungent capsaicin analogs (capsinoids) increase metabolic rate and enhance thermogenesis via gastrointestinal TRPV1 in mice. *Biosci Biotechnol Biochem* **73**, 2690-2697

119. Ahuja, K. D. K., Robertson, I. K., Geraghty, D. P., and Ball, M. J. (2007) The effect of 4-week chilli supplementation on metabolic and arterial function in humans. *Eur J Clin Nutr* **61**, 326-333

120. Smeets, A. J., and Westerterp-Plantenga, M. S. (2009) The acute effects of a lunch containing capsaicin on energy and substrate utilisation, hormones, and satiety. *Eur J Nutr* **48**, 229-234

121. Yoshioka, M., Imanaga, M., Ueyama, H., Yamane, M., Kubo, Y., Boivin, A., St-Amand, J., et al. (2004) Maximum tolerable dose of red pepper decreases fat intake independently of spicy sensation in the mouth. *Br J Nutr* **91**, 991-995

122. Yoshioka, M., St-Pierre, S., Drapeau, V., Dionne, I., Doucet, E., Suzuki, M., and Tremblay, A. (1999) Effects of red pepper on appetite and energy intake. *Br. J. Nutr.* **82**, 115-123

123. Ludy, M. J., and Mattes, R. D. (2011) The effects of hedonically acceptable red pepper doses on thermogenesis and appetite. *Physiol Behav* **102**, 251-258

124. Lejeune, M. P., Kovacs, E. M., and Westerterp-Plantenga, M. S. (2003) Effect of capsaicin on substrate oxidation and weight maintenance after modest body-weight loss in human subjects. *Br J Nutr* **90**, 651-659

125. Westerterp-Plantenga, M. S., Smeets, A., and Lejeune, M. P. G. (2005) Sensory and gastrointestinal satiety effects of capsaicin on food intake. *Int J Obesity* **29**, 682-688

126.   Reinbach, H. C., Martinussen, T., and Moller, P. (2010) Effects of hot spices on energy intake, appetite and sensory specific desires in humans. *Food Qual Prefer* **21**, 655-661

127.   Inoue, N., Matsunaga, Y., Satoh, H., and Takahashi, M. (2007) Enhanced energy expenditure and fat oxidation in humans with high BMI scores by the ingestion of novel and non-pungent capsaicin analogues (capsinoids). *Biosci Biotechnol Biochem* **71**, 380-389

128.   Janssens, P. L., Hursel, R., and Westerterp-Plantenga, M. S. (2014) Capsaicin increases sensation of fullness in energy balance, and decreases desire to eat after dinner in negative energy balance. *Appetite* **77C**, 46-51

129.   Ludy, M. J., Moore, G. E., and Mattes, R. D. (2012) The effects of capsaicin and capsiate on energy balance: critical review and meta-analyses of studies in humans. *Chem Senses* **37**, 103-121

130.   Matsumoto, T., Miyawaki, C., Ue, H., Yuasa, T., Miyatsuji, A., and Moritani, T. (2000) Effects of capsaicin-containing yellow curry sauce on sympathetic nervous system activity and diet-induced thermogenesis in lean and obese young women. *J Nutr Sci Vitaminol (Tokyo)* **46**, 309-315

131.   Yoshioka, M., St-Pierre, S., Suzuki, M., and Tremblay, A. (1998) Effects of red pepper added to high-fat and high-carbohydrate meals on energy metabolism and substrate utilization in Japanese women. *Br J Nutr* **80**, 503-510

132.   Chaiyata, P., Puttadechakum, S., and Komindr, S. (2003) Effect of chili pepper (Capsicum frutescens) ingestion on plasma glucose response and metabolic rate in Thai women. *J Med Assoc Thai* **86**, 854-860

133.   Yoshioka, M., Lim, K., Kikuzato, S., Kiyonaga, A., Tanaka, H., Shindo, M., and Suzuki, M. (1995) Effects of red-pepper diet on the energy metabolism in men. *J Nutr Sci Vitaminol (Tokyo)* **41**, 647-656

134.   Galgani, J. E., and Ravussin, E. (2010) Effect of dihydrocapsiate on resting metabolic rate in humans. *Am J Clin Nutr* **92**, 1089-1093

135.   Josse, A. R., Sherriffs, S. S., Holwerda, A. M., Andrews, R., Staples, A. W., and Phillips, S. M. (2010) Effects of capsinoid ingestion on energy expenditure and lipid oxidation at rest and during exercise. *Nutr Metab (Lond)* **7**, 65

136.   Lee, T. A., Li, Z., Zerlin, A., and Heber, D. (2010) Effects of dihydrocapsiate on adaptive and diet-induced thermogenesis with a high protein very low calorie diet: a randomized control trial. *Nutr Metab (Lond)* **7**, 78

137.   Galgani, J. E., Ryan, D. H., and Ravussin, E. (2010) Effect of capsinoids on energy metabolism in human subjects. *Br J Nutr* **103**, 38-42

138.   Kawabata, F., Inoue, N., Yazawa, S., Kawada, T., Inoue, K., and Fushiki, T. (2006) Effects of CH-19 sweet, a non-pungent cultivar of red pepper, in decreasing the body weight and suppressing body fat accumulation by sympathetic nerve activation in humans. *Biosci Biotechnol Biochem* **70**, 2824-2835

139.   Sambaiah, K., and Satyanarayana, M. N. (1980) Hypocholesterolemic effect of red pepper & capsaicin. *Indian J. Exp. Biol.* **18**, 898-899

140.   Srinivasan, M. R., Sambaiah, K., Satyanarayana, M. N., and Rao, M. V. L. (1980) Influence of Red Pepper and Capsaicin on Growth, Blood-Constituents and Nitrogen-Balance in Rats. *Nutr. Rep. Int.* **21**, 455-467

141.   Srinivasan, M. R., and Satyanarayana, M. N. (1987) Influence of Capsaicin, Curcumin and Ferulic Acid in Rats Fed High-Fat Diets. *J. Bioscience* **12**, 143-152

142.   Kempaiah, R. K., and Srinivasan, K. (2006) Beneficial influence of dietary curcumin, capsaicin and garlic on erythrocyte integrity in high-fat fed rats. *J. Nutr. Biochem.* **17**, 471-478

143. Negulesco, J. A., Noel, S. A., Newman, H. A., Naber, E. C., Bhat, H. B., and Witiak, D. T. (1987) Effects of pure capsaicinoids (capsaicin and dihydrocapsaicin) on plasma lipid and lipoprotein concentrations of turkey poults. *Atherosclerosis* **64**, 85-90

144. Srinivasan, K., and Sambaiah, K. (1991) The effect of spices on cholesterol 7 alpha-hydroxylase activity and on serum and hepatic cholesterol levels in the rat. *Int J Vitam Nutr Res* **61**, 364-369

145. Iwai, K., Kawada, T., and Watanabe, T. (1986) Effects of Capsaicin on Lipid-Metabolism in Rats Fed a High-Fat Diet. *Appetite* **7**, 268-268

146. Marinelli, S., Pascucci, T., Bernardi, G., Puglisi-Allegra, S., and Mercuri, N. B. (2005) Activation of TRPV1 in the VTA excites dopaminergic neurons and increases chemical- and noxious-induced dopamine release in the nucleus accumbens. *Neuropsychopharmacol* **30**, 864-870

147. Smith, V. A., Beyer, C. E., and Brandt, M. R. (2006) Neurochemical changes in the RVM associated with peripheral inflammatory pain stimuli. *Brain Res* **1095**, 65-72

148. Zavitsanou, K., Dalton, V. S., Wang, H., Newson, P., and Chahl, L. A. (2010) Receptor changes in brain tissue of rats treated as neonates with capsaicin. *J Chem Neuroanat* **39**, 248-255

149. Watanabe, T., Kawada, T., Yamamoto, M., and Iwai, K. (1987) Capsaicin, a pungent principle of hot red pepper, evokes catecholamine secretion from the adrenal medulla of anesthetized rats. *Biochem Biophys Res Commun* **142**, 259-264

150. Lee, M. S., Kim, C. T., Kim, I. H., and Kim, Y. (2011) Effects of capsaicin on lipid catabolism in 3T3-L1 adipocytes. *Phytother Res* **25**, 935-939

151. Zhang, L. L., Yan Liu, D., Ma, L. Q., Luo, Z. D., Cao, T. B., Zhong, J., Yan, Z. C., et al. (2007) Activation of transient receptor potential vanilloid type-1 channel prevents adipogenesis and obesity. *Circ. Res.* **100**, 1063-1070

152. Cioffi, D. L. (2007) The skinny on TRPV1. *Circ. Res.* **100**, 934-936

153. Ursu, D., Knopp, K., Beattie, R. E., Liu, B., and Sher, E. (2010) Pungency of TRPV1 agonists is directly correlated with kinetics of receptor activation and lipophilicity. *Eur J Pharmacol* **641**, 114-122

154. Caterina, M. J., Schumacher, M. A., Tominaga, M., Rosen, T. A., Levine, J. D., and Julius, D. (1997) The capsaicin receptor: a heat-activated ion channel in the pain pathway. *Nature* **389**, 816-824

II. PART I

Establishment of screening systems to investigate mechanisms regulating satiety and energy metabolism

1. Objectives

The first part of the present work was focused on the establishment of screening systems to investigate mechanisms regulating satiety and energy metabolism. The aim of this establishment was to find suitable models and assays to (1) identify potential satiety-mediating aroma compounds and (2) validate the effects of the most promising candidates in different target tissues regarding their ability to modulate mechanisms regulating satiety and/ or energy.

2. Results

The first part of this cumulative thesis is based on the following research articles:

(1) Identification of coffee components that stimulate dopamine release from pheochromocytoma cells (PC-12)

Walker, J., **Rohm, B**., Lang, R., Pariza, M. W., Hofmann, T., and Somoza, V.

Food and Chemical Toxicology (2012) 50, 390-398.

The impact of coffee and selected, quantified coffee components on dopamine release and intracellular Ca^{2+}-mobilization in the pheochromocytoma cell line PC-12 was investigated by means of luminescence and fluorescence assays and ELISA.

Within this study, I set up and performed luminescence assays and ELISAs for the determination of dopamine release from PC-12 cells and evaluated the data statistically.

(2) N(epsilon)-Carboxymethyllysine (CML), a Maillard reaction product, stimulates serotonin release and activates the receptor for advanced glycation end products (RAGE) in SH-SY5Y cells

Holik, A. K*., **Rohm, B**.*, Somoza, M. M., and Somoza, V.

* The authors A.K. Holik and B.Rohm contributed equally to this work.

Food and Function (2013) 4, 1111-1120

This study investigated the effect of CML on the serotonin system of SH-SY5Y cells using a combined approach of a customized cDNA microarray, qPCR and functional serotonin release in SH-SY5Y cells.

I participated in design, synthesis and analysis of the microarrays, and developed the measuring system to quantify serotonin release from human neural SH-SY5Y cells. In addition, I wrote parts of the manuscript.

(3) Simultaneous light-directed synthesis of mirror-image microarrays in a photochemical reaction cell with flare suppression

Sack, M., Kretschy, N., **Rohm, B**., Somoza, V., Somoza, M. M.

Analytical Chemistry (2013) 85, 8513-7.

The study presents a novel photochemical reaction cell, which allows the simultaneous synthesis of two identical microarrays on two separate glass substrates.
Within the study, I provided biological test material for evaluation of the synthesized microarrays.

(4) Structure-dependent effects of pyridine derivatives on mechanisms of intestinal fatty acid uptake: Regulation of nicotinic acid receptor and fatty acid transporter expression
Riedel, A., Lang, R., **Rohm, B**., Rubach, M., Hofmann, T., Somoza,V.

The Journal of Nutritional Biochemistry (2014), accepted

The impact of different pyridine derivates on intestinal fatty acid uptake was assessed in order to identify their structural determinants. Further mechanistic studies were carried with the most actives compounds, nicotinic acid and N-methyl-4-phenylpyridinium.

Within the study, I largely participated in the development of the measuring systems to assess glucose uptake, gene expression, intracellular calcium mobilization and trans-epithelial electrical resistance in the human intestinal cell line Caco-2.

(5) Caffeine dose-dependently induces thermogenesis but restores ATP in HepG2 cells in culture

Riedel, A., Pignitter, M., Hochkogler, C. M., **Rohm, B**., Walker, J., Bytof, G., Lantz, I., and Somoza, V.

Food and Function (2012), 3955-964.

This study analyzed the effect of caffeine on mechanisms of energy metabolism in the liver carcinoma cell line HepG2 and in mouse 3T3-L1 adipocytes.

I established analysis of lipid accumulation via oil red O staining in 3T3-L1 adipocytes in the present form.

2.1 "Identification of coffee components that stimulate dopamine release from pheochromocytoma cells (PC-12) "

Walker, J. [a,b], **Rohm, B** [. a], Lang, R [. c], Pariza, M. W. [b], Hofmann, T. [c], and Somoza, V. [a,b,]

[a] Department of Nutritional and Physiological Chemistry, University of Vienna, Althanstrasse 14, A-1090 Vienna, Austria

[b] Department of Food Science, Food Research Institute, University of Wisconsin-Madison, 1550 Linden Drive, Madison, WI 53706-1521, USA

[c] Bioanalytics Unit of the Nutrition and Food Research Center of the Technical University of Munich, Technical University of Munich, Lise-Meitner-Str. 34, D-85354 Freising, Germany

Identification of coffee components that stimulate dopamine release from pheochromocytoma cells (PC-12)

J. Walker [a,b], B. Rohm [a], R. Lang [c], M.W. Pariza [b], T. Hofmann [c], V. Somoza [a,b,*]

[a] Department of Nutritional and Physiological Chemistry, University of Vienna, Althanstrasse 14, A-1090 Vienna, Austria
[b] Department of Food Science, Food Research Institute, University of Wisconsin-Madison, 1550 Linden Drive, Madison, WI 53706-1521, USA
[c] Bioanalytics Unit of the Nutrition and Food Research Center of the Technical University of Munich, Technical University of Munich, Lise-Meitner-Str. 34, D-85354 Freising, Germany

ARTICLE INFO

ABSTRACT

Coffee and caffeine are known to affect the limbic system, but data on the influence of coffee and coffee constituents on neurotransmitter release is limited. We investigated dopamine release and Ca^{2+}-mobilization in pheochromocytoma cells (PC-12 cells) after stimulation with two lyophilized coffee beverages prepared from either *Coffea arabica* (AR) or *Coffea canephora var. robusta* (RB) beans and constituents thereof. Both coffee lyophilizates showed effects in dilutions between 1:100 and 1:10,000. To identify the active coffee compound, coffee constituents were tested in beverage and plasma representative concentrations. Caffeine, trigonelline, *N*-methylpyridinium, chlorogenic acid, catechol, pyrogallol and 5-hydroxytryptamides increased calcium signaling and dopamine release, although with different efficacies. While *N*-methylpyridinium stimulated the Ca^{2+}-mobilization most potently (EC_{200}: $0.14 \pm 0.29\ \mu M$), treatment of the cells with pyrogallol (EC_{200}: $48 \pm 14\ nM$) or 5-hydroxytryptamides (EC_{200}: $10 \pm 3\ nM$) lead to the most pronounced effect on dopamine release. In contrast, no effect was seen for the reconstituted biomimetic mixture.

We therefore conclude that each of the coffee constituents tested stimulated the dopamine release in PC-12 cells. Since no effect was found for their biomimetic mixture, we hypothesize other coffee constituents being responsible for the dopamine release demonstrated for AR and RB coffee brews.

© 2011 Elsevier Ltd. All rights reserved.

1. Introduction

Coffee is one of the most consumed beverages worldwide, with an overall consumption of more than 5 million tons per year. Consumers prefer coffee because of its taste and its excitatory effects (Fernstrom, 2000; Geel et al., 2005). In previous studies of our group, coffee was investigated for its antioxidant and chemopreventive activity, and its effects on gastric acid secretion (Boettler et al., 2011; Lang et al., 2010a; Rubach et al., 2008; Somoza et al., 2003). In these studies, the coffee constituent *N*-methylpyridinium (NMP) has been identified as an *in vivo* antioxidant and as a potent inhibitor of gastric acid secretion when added to the coffee brew (Somoza et al., 2003), whereas 5-hydroxytryptamides (C5HTs) and caffeine (CAF) were demonstrated to effectively stimulate

gastric acid secretion (Lang et al., 2010a). In the study presented here, we focus on the neurotransmitter excitatory effect of coffee.

It is well-known that coffee, CAF and other coffee components influence brain function (Fernstrom, 2000). CAF is the most frequently consumed dietary stimulant of the central nervous system (CNS) and has been demonstrated to improve mental performance at a bolus dose of 3.3 mg/kg (Battig and Welzl, 1993). As mechanism of action, CAF and other methylxanthines were shown to be nonselective competitive adenosine receptor antagonists (Michaelis et al., 1979; Wood et al., 1989). Also, results from *in vivo* studies in rats indicate that CAF induces dopamine release after 30 min at i.p. doses of 1.3–2.6 mg/kg or after 60 min at doses of 10 and 30 mg/kg (Morgan, 1998; Solinas et al., 2002). Another well-studied coffee component is trigonelline (TRI). TRI is known to influence neuronal functions like neurite outgrowth in human neuroblastoma cells (Tohda et al., 1999). However, the effect of TRI on neurotransmitter release has not been investigated yet.

Psychostimulants such as cocaine and amphetamine display their impact on the CNS via an increase of the extracellular dopamine concentration in the *nucleus accumbens* (Pontieri et al., 1995). Dopamine exocytosis is regulated by neuronal electrical activity, where the calcium (Ca^{2+}) signal evoked is modulated by protein kinase C (PKC) (Jaffe, 1998; Westerink et al., 2002). Dopamine fluctuation in the *nucleus accumbens* is involved in the

rewarding effects of psychomotor stimulants and correlated with drug and food reward (Di Chiara and Imperato, 1988; Ikemoto et al., 1997). These fluctuations of the dopamine concentration can underlie different mechanisms, for example blocking dopamine reuptake, releasing it from stores, inhibiting autoreceptor-mediated feedback inhibition or directly increasing the phasic activity of dopaminergic neurons (Dayan, 2009). Cocaine, for example, binds to monoamine receptors and blocks the inward transport of dopamine via the neuronal dopamine transporter (DAT) which results in increasing dopamine concentrations in the synaptic cleft (Farnsworth et al., 2009). An additional function of the DAT is the outward transport of dopamine, which can be enhanced by drugs like amphetamines (Eshleman et al., 1994). This reverse transport is regulated by PKCβ_{II} (Johnson et al., 2005) and can be promoted by the interaction of the DAT by proteins, like syntaxin 1A (Binda et al., 2008).

However, with the exception of CAF, little is known about the effects of different coffee compounds on the neurotransmitter release and their contribution to the CNS-stimulating effect of coffee. This raised the question whether coffee or coffee constituents have a direct influence on neurotransmitter release from neural cells. Although, coffee, as a beverage does not reach the neurons, it has been shown for coffee constituents to contribute to the excitatory effect of this beverage (Ferre, 2010). In the work presented here, the time and concentration dependent effects of two lyophilized coffee beverages and multiple compounds thereof (Fig. 1) on dopamine release and Ca^{2+}-mobilization were studied in pheochromocytoma-12 cells (PC-12). The lyophilized coffee beverages were prepared from two commercial coffee roasts, one brewed from arabica (AR), the other one brewed from robusta (RB) beans. PC-12 cells originate from rat adrenal pheochromocytoma cells and display an established *in vitro* model for catecholamine neurotransmitter release such as dopamine and noradrenaline (Greene and Tischler, 1976). In fact, this cell line has already been used to determine the effects of food ingredients such as glucose (Avidor et al., 1994) and CAF (Koshimura et al., 2003) on dopamine release.

2. Materials and methods

2.1. Materials

Commercial Arabica Brazil (AR) and Robusta (RB) ground roast coffees were obtained from Tchibo GmbH (Hamburg, Germany). Of each coffee, a total amount of 54 g was weighed into a paper filter commonly used for home preparation of coffee beverage (Melitta Gold, Nr. 4, Aldi, Germany) to prepare 1 L of coffee beverage. Portions of freshly boiled tap water ($T \sim 90$–$95\ ^\circ$C, approximately 100 mL each) were poured over the powder and the hot filtrate was collected in a volumetric flask of 1000 mL. Exactly 500 mL of the coffee solution was transferred to crystallizing dishes, frozen ($-20\ ^\circ$C) immediately, and finally dried by lyophilization (48 h, 0.77 mbar, 25 $^\circ$C) yielding a fluffy brown lyophilizate. The yields for 500 mL of the AR and RB coffees used in this study were 12.74 and 15.80 g, respectively. For the cell culture experiments, both samples were reconstituted in accordant buffer dilutions of up to 1/10,000 (w/v) freshly for every experiment. All purified compounds tested were dissolved in respective concentrations in buffer prior to every experiment.

CAF, PYR, CAT and TRI were purchased from Sigma Aldrich, USA. NMP iodide was synthesized as reported previously (Stadler et al., 2002). Briefly, methyliodide (60 mmol) was added dropwise to a solution of pyridine (60 mmol) in acetonitrile (15 mL). This mixture was stirred for 20 min at room temperature and then heated for 6 h at 50 $^\circ$C. The oily mixture was then chilled on ice (200 g), the precipitate obtained was washed with ice-cooled acetonitrile and filtered. After recrystallization from acetonitrile, the target compound was obtained as colorless crystals (Stadler et al., 2002).

Unless stated otherwise, all further chemicals were purchased from Sigma Aldrich, USA. PC-12 cells were obtained from ATCC, as well as the cell culture media. All reagents, solutions and buffers were prepared with ultra-pure water.

2.2. Methods

2.2.1. Cell culture

The PC-12 cells were cultivated in Ham's F12-K nutrient mixture containing 15% DHS, 2.5% FBS and 1% P/S at 37 $^\circ$C, 5% CO$_2$ and 95% humidity in 75 cm^2 flasks (Sarstedt, Greiner). The cells were tested for mycoplasm contamination on a regular basis.

2.2.2. Dopamine ELISA

For the ELISA, 500,000 PC-12 cells were seeded in a 35 mm culture dish and allowed to settle for 48 h. After a wash with 1 mL PBS, the cells were stimulated with the compound of interest for 3.5 min at 37 $^\circ$C in Krebs Ringer solution (128 mM NaCl, 1.9 mM KCl, 1.2 mM KH$_2$PO$_4$, 2.4 mM CaCl$_2$, 1.3 mM MgSO$_4$, 26 mM NaHCO$_3$, 10 mM glucose, 10 mM HEPES, pH 5). Of the supernatant, 300 μL were immediately diluted with 30 μL 1 N HCl and the ELISA was performed according to the manufacturer's protocol (dopamine ELISA, DLD Diagnostika, Hamburg, Germany).

2.2.3. Luminescence assay for dopamine release

For the dopamine release assays, 25,000 cells per well were seeded in a white 96-well plate (Nunc, Rochester, NY, USA) and allowed to attach for at least 24 h. The incubation media was discarded and the cells were washed with Locke's buffer (154 mM NaCl, 5.6 mM KCl, 2.3 mM CaCl$_2$, 3.6 mM NaHCO$_3$, 5.6 mM glucose, 4.6 mM HEPES) twice. Thereafter, the measurement solution (200 μL Locke's buffer, 0.46 U/mL MAO A, 6.4 U/mL horseradish peroxidase, 30 μM luminol, with a total volume of 290 μL) was added to each well.

The assay was performed as described by Shinohara et al. (2008) with slight modifications (Shinohara et al., 2008). After 10 min of incubation at 37 $^\circ$C, 5% CO$_2$ and 95% humidity, the plate was stimulated with the compound of interest by injection with a plate reader (infinite M200, Tecan, USA) and the luminescence signal was measured immediately. The following compounds have been tested using this assay: CAF (3 nM to 3 mM), TRI (4.977 nM to 497.7 μM), NMP (14.7 pM to 291 μM), C5HTs (40.5 pM to 4.05 μM) and PYR (3.2 pM to 32 nM). The dopamine standard curve (data not shown) demonstrated a dose-dependent signal for dopamine in the test system.

Protein concentrations of each well were determined using the BCA protein assay kit from Pierce. For this test, cells were washed with PBS three times and lysed in PBS at $-20\ ^\circ$C.

2.2.4. Determination of compound efficacy on dopamine release

To compare the different compounds and their efficacy to stimulate the dopamine release from PC-12 cells, the concentrations of the substances at which the neurotransmitter release was doubled compared to non-treated control cells (100%) were calculated (EC$_{200}$-values). Linear regression for the T/C-values vs. the concentration was used to determine the y-intercept (b) and the slope (m). Afterwards, the EC$_{200}$-value was assessed with the following formula: EC$_{200}$ = $(200 - b)/m$.

2.2.5. Fluorescence assay for determination of intra-cellular calcium levels

In a 96-well plate, 100,000 PC-12 cells were seeded per well. After 24 h, the growth media was exchanged by 50 μL/well serum-free media to achieve a synchronization of the cells. After another 24 h, the cells were loaded with 50 μL of the fluo-4 direct dye and incubated for 30 min at 37 $^\circ$C, followed by a 5 min incubation step at room temperature. Reference compounds, diluted coffee lyophilizates or purified compounds thereof were added by injection using a multimode plate reader (infinite M200, Tecan, Austria). Fluorescence at 490 nm excitation and 520 nm emission was measured immediately after addition of the compound, every 2 s for a total of 1 min. The obtained relative fluorescence units (RFU) were normalized against the DNA concentration of the samples.

DNA content was determined after washing and lysis of the cells using the Nanoquant plate for the infinite M200 plate reader by absorbance measurements at 260 and 280 nm.

To compare the effects of the coffees and coffee constituents in different concentrations, the area under the curve (AUC) of the individual experiments was calculated and normalized against the DNA content of each well. Data displayed are expressed as mean AUC values ± SD.

2.2.6. Statistics

All experiments were done in multiple replicates ($n \geqslant 3$). The average of the AUC values was determined and displayed after performing a Nalimov outlier test. Significant differences were determined using the student's t-test, when testing against the non-treated control and using a one-way ANOVA with a Holm–Sidak post hoc test to measure concentration dependent effects.

3. Results

3.1. Chemical characterization of Arabica Brazil (AR) and Robusta (RB) coffees

The two coffees, AR and RB, were previously studied for their effects on gastric acid secretion (Rubach et al., 2010). In these studies, both coffees were characterized and their major constituents were quantified (Table 1). Briefly, CAF and CA (Fig. 1) were identified as the two major coffee constituents, and while the CA concentration was comparable between the two coffees, the AR coffee contained only half of the amount of CAF compared to the RB

coffee. Further constituents that were quantified in the two coffees were NMP, PYR, CAT and C5HTs (Fig. 1) (Rubach et al., 2010). The RB coffee exceeded a higher extraction yield than the AR coffee and contained higher concentrations of the two phenolic compounds CAT and PYR, but lower concentrations of NMP and C5HTs.

3.2. Influence of freeze-dried coffee beverages on PC-12 cells' intra-cellular calcium levels and dopamine release

After dietary intake, a coffee beverage gets diluted upon absorption and only 1:100 to 1:1000 of the amounts of the original coffee constituents can be detected in the plasma. For CAF and CA, e.g., concentrations in regular coffee beverages range between 3 and 7 mM, whereas plasma concentrations after coffee intake of 2–10 μM have been reported for these compounds (Monteiro et al., 2007; Newton et al., 1981). Concentrations of TRI and NMP in coffee beverages range from 1500 to 2300 and 25 to 500 μM (Rubach et al., 2010), respectively, whereas plasma concentrations of up to about 6 and 0.8 μM (Lang et al., 2010b) have been analyzed for these two compounds.

To prove that freeze-dried coffee beverages and dilutions thereof stimulate the neurotransmitter release from PC-12 cells by increasing the second messenger Ca^{2+} in the cells, we measured the intracellular Ca^{2+} levels using a Ca^{2+}-sensitive fluorescent dye. Peak signals were detected within the first 30 s after injection and varied depending on the stimulant. Fig. 2A shows the results of four independent experiments for buffer-treated cells (buffer control) and those stimulated with either the diluted freeze-dried coffee beverages or bradykinin (1 μM) as a well-known stimulant of Ca^{2+}-fluctuation. Lyophilized RB coffee had a more pronounced effect than the AR coffee. However, in these experiments, cells were treated only with 1:1000 diluted freeze-dried coffee beverages. Therefore, coffee beverage dilutions of 1:100 up to 1:10,000 were tested in the following experiments. As can be seen in Fig. 2B, treatment of the cells with both coffee lyophilizates increased the Ca^{2+}-mobilization in a dose-dependent manner ($p < 0.05$) up to 620 ± 189% (RB). At dilutions of 1:1000, 1:5000 and 1:10,000 the RB coffee showed a significantly stronger effect on the Ca^{2+}-mobilization than the AR coffee (Fig. 2B).

To test whether this Ca^{2+}-signal leads to dopamine exocytosis, an ELISA for dopamine release was performed (Fig. 2C). Both freeze-dried coffee beverages evoked a dopamine release from PC-12 cells compared to the buffer control up to a maximum of 229 ± 65.5% and 269 ± 110% after stimulation with a 1:10,000 dilution of the AR and the RB coffee, respectively. This result raised the question which coffee constituent is responsible for the effect or whether the dopamine release stimulated by reconstituted freeze-dried coffee beverages is based on a synergistic effect of multiple compounds.

3.3. Intra-cellular calcium levels in PC-12 cells after stimulation with coffee constituents

CAF and TRI have already been described in the literature to have an effect on the neuroregulation (Fernstrom, 2000; Hossain

Table 1
Composition of the tested coffee beverages (Reprinted with permission from Rubach et al. (2010), Copyright 2010, American Chemical Society).

| Substances	AR coffee [mg/L]	RB coffee [mg/L]
Chlorogenic acid	1038	975
Caffeine	618	1389
NMP	32.2	22.4
Pyrogallol	4.05	5.63
Catechol	5.73	9.29
C5HTs	0.21	0.12
Of which C22-5HT	0.14	0.06
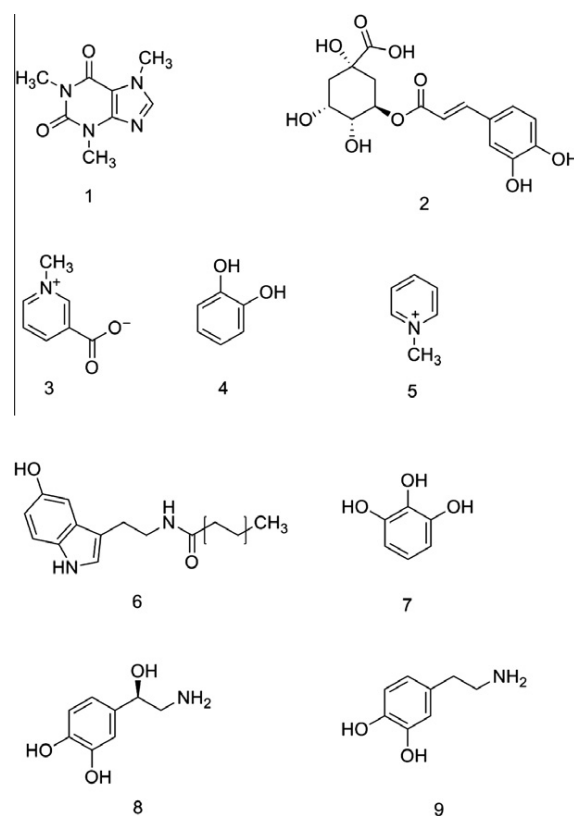
Fig. 1. Chemical structures of the tested coffee compounds (1) caffeine (CAF), (2) chlorogenic acid (CA), (3) trigonelline (TRI), (4) catechol (CAT), (5) N-methylpyridinium (NMP), (6) 5-hydroxytryptamides (C5HTs), (7) pyrogallol (PYR), and the neurotransmitters (8) norepinephrine and (9) dopamine.

et al., 2003; Tohda et al., 1999). C5HTs are also likely candidates to affect neurotransmitter release since these compounds are structural serotonin analogs. We further tested other compounds quantified in coffee beverages in earlier studies (Rubach et al., 2010): TRI and its degradation product formed upon roasting, NMP, as well as the phenolic compounds CA, CAT and PYR.

The effective concentrations to mobilize twice as much Ca^{2+} compared to non-treated control cells (EC_{200}-value) are given in Table 2. The eight tested compounds were analyzed in concentrations found in coffee and plasma representative dilutions thereof. Fig. 3A–D shows the effect measured for these substances in AR representative concentrations and dilutions thereof on Ca^{2+}-mobilization. In contrast to the six other tested compounds ($p < 0.05$), for CAF (Fig. 3A) and CAT (Fig. 3C), no dose-dependent increase in the calcium mobilization was measured. The effect of CAF peaked already at a coffee dilution of 1:300,000 (265 ± 47.7%, data not shown) and varied between 67.4 ± 29.6% and 175 ± 59.0% at dilutions between 1:10 and 1:100 (Fig. 3A). The highest effect of CAT (Fig. 3C) was measured at a dilution of 1:100 (305 ± 81.5%). However, the results presented in Fig. 3 clearly demonstrate that all substances mobilized the intracellular calcium and could, therefore, lead to a signal for a dopamine exocytosis. Based on the concentrations of the individual compounds in the test system, the most effective compounds were determined by the EC_{200}-values as TRI < CA < C22-5HT < PYR < NMP.

3.4. Dopamine release from PC-12 cells after stimulation with coffee constituents

All tested compounds showed a dopamine release excitatory effect (Fig. 4A–D). For bradykinin, a well-studied compound that
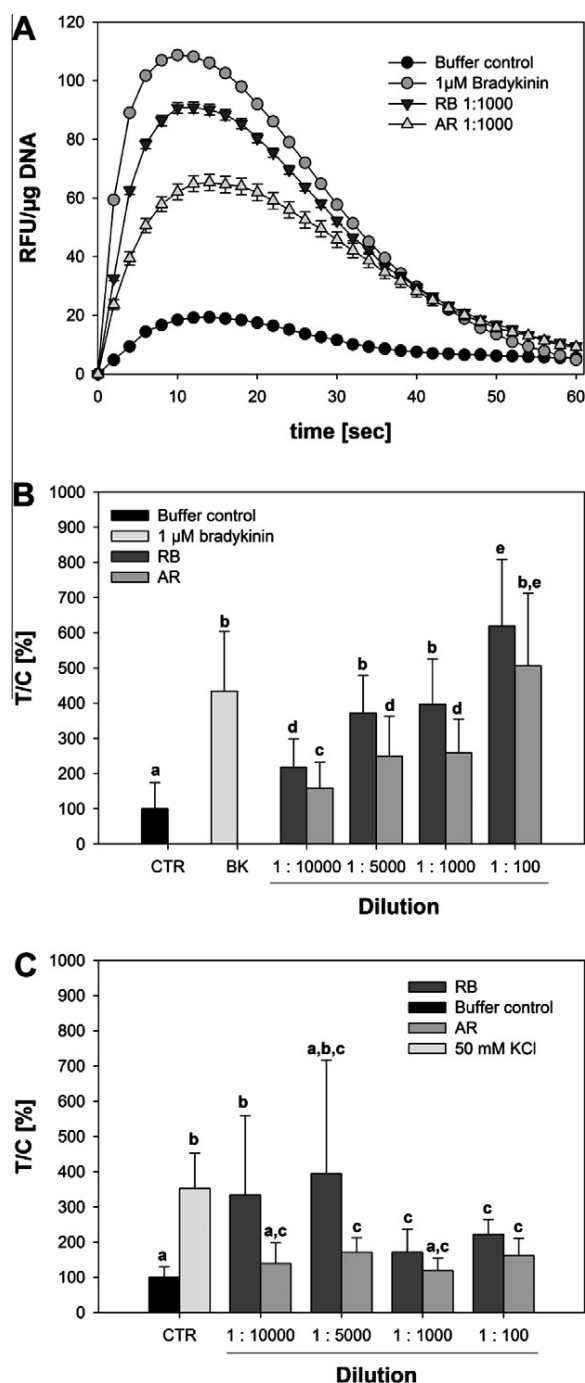
Fig. 2. Effects of the two coffee beverages, AR and RB, on the Ca^{2+}-mobilization and the dopamine release by PC-12 cells. (A) Example of a Ca^{2+}-curve with 1:1000 dilutions of the two tested coffees compared to the buffer control and the positive control bradykinin, $n = 4$. (B) Ca^{2+}-mobilization by different dilutions of the tested coffees. Results represent mean AUC of the substance vs. mean AUC of the control (%) ± SD normalized to the DNA content of the sample, $n = 4$. (C) Dopamine release by PC-12 cells after stimulation with the two test coffees in different dilutions compared to the buffer control (=100%). Significances were tested according to unpaired student's t-test and the differences are indicated with the letters a to e.

Table 2
EC_{200}-values of the tested coffee compounds of the Ca^{2+}-mobilization in PC-12 cells. EC, effective concentration.

Compounds	EC_{200}-value [µM]
NMP	0.14 ± 0.29
PYR	1.34 ± 0.59
C22-5HT	1.51 ± 0.27
CA	204 ± 108
TRI	439 ± 475

Interestingly, for some compounds, CAF, TRI, NMP and CA, a hormesis effect was observed, with highest effects at low concentrations and that decreased again in a dose-dependent manner at higher concentrations. CAF, e.g., significantly increased the neurotransmitter release in concentrations of 3 µM (1:1000 dilution) and 30 µM (1:100 dilution), although the peak stimulation was analyzed for 100 nM CAF (1:3333 dilution; 158 ± 15.5%, data not shown). Similar effects were found for the induction of neurotransmitter release after stimulation with TRI and NMP. Compared to the buffer control, TRI induced the neurotransmitter release from PC-12 cells significantly to an extent of 136 ± 31.0% at a concentration of 4.977 µM (1:100 dilution). The peak effect (134 ± 3.99%) for NMP, the decarboxylation product of TRI formed upon roasting, was detected at a concentration of 145.7 nM (1:100 dilution). At a concentration of 145.7 µM, neither an induction nor a suppression of the neurotransmitter release was determined.

The results obtained for PYR, C5HTs and CAT were used to calculate EC_{200}-values (Table 3). To exclude an over-estimated or artificial effect due to the fact that the serotonin derivatives C5HTs are substrates for the monoamine oxidase A (MAO A), a cell-free assay with the C5HTs was performed and the signal derived was subtracted as background (Fig. 4D). After background correction, the most effective compounds were the C5HTs with an EC_{200}-value of 10 ± 3 nM. Also, the roasting product PYR showed a strong dopamine excitatory effect at concentrations in the nanomolar range. The order of efficacy from the least to the most effective compound based on the EC_{200}-values was determined thereby as followed: CAT < PYR < C5HTs.

3.5. Calcium mobilization and dopamine release from PC-12 cells after stimulation with coffee constituents in high dilutions

At concentrations representative of a 1:100 dilution of the freeze-dried coffee beverage AR, the most effective compounds were CAT and NMP (Fig. 5A). Treatment of the cells with 450 nM (1:100 dilution) CAT evoked an elevated Ca^{2+}-mobilization of 305 ± 81%. The respective result for NMP was 384 ± 108% (900 nM; 1:100 dilution).

In contrast, at a dilution of 1:100, PYR elevated the dopamine release most effectively (Fig. 5B). PYR increased the dopamine release to 658 ± 266% at a concentration of 320 nM (Fig. 5B). Furthermore, CAT and CA showed a strong tendency to induce dopamine release from PC-12 cells in concentrations of 450 nM and 30 µM, respectively.

3.6. Calcium mobilization and neurotransmitter release from PC-12 cells after stimulation with AR and RB coffee reconstitutes

To test the effect of CAF, CA, PYR, CAT, C5HTs, TRI and NMP on Ca^{2+}-mobilization and dopamine release in a coffee representative biomimetic mixture, the individual compounds were mixed in amounts representative for the AR and the RB coffee. Each mixture was reconstituted in a 1:100 dilution of the respective coffee with HBSS buffer containing 20 mM HEPES to test the effect on calcium

induces dopamine fluctuation (Koizumi et al., 2002), a 100% increase of the dopamine release compared to buffer-treated control cells was demonstrated (Fig. 4A–D).
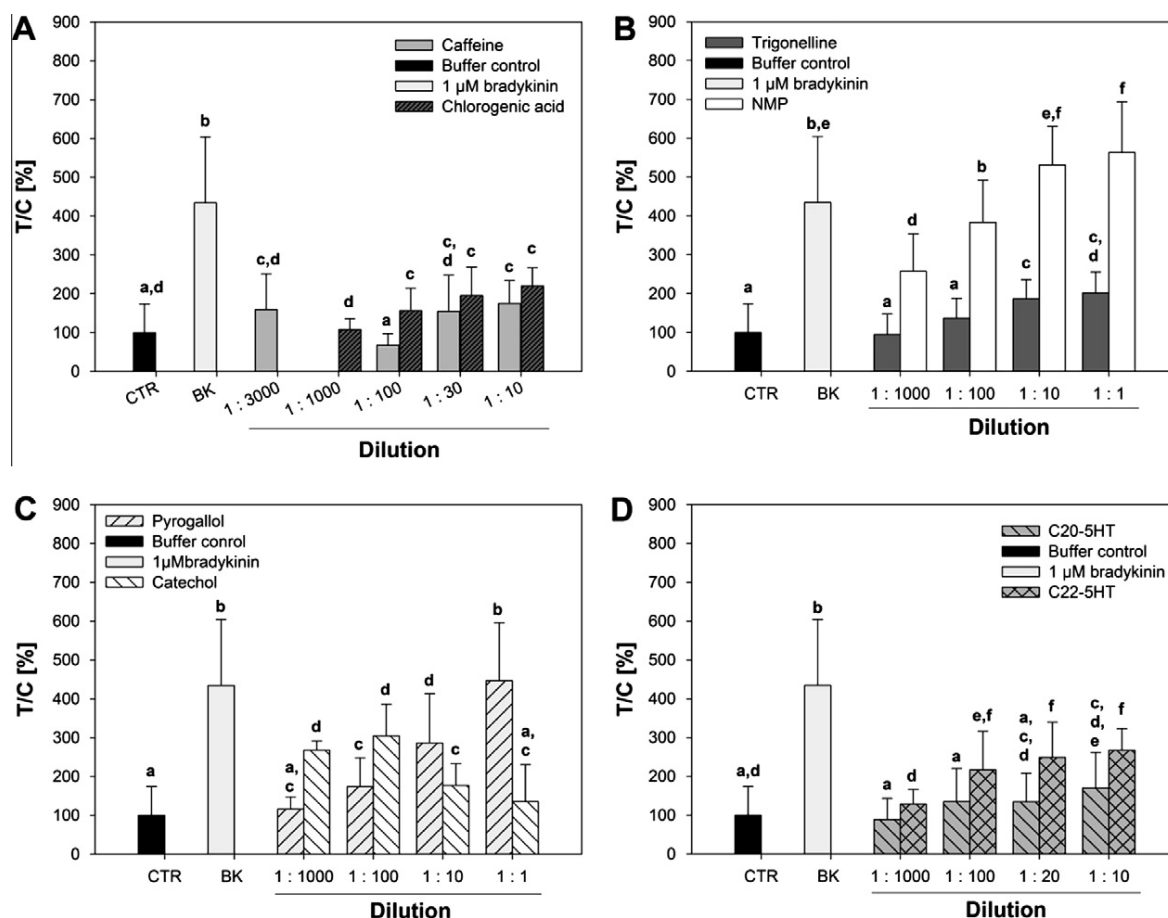
Fig. 3. Ca^{2+}-mobilization by the different coffee constituents shown as AR representative concentration (1:1) and dilutions thereof. Results represent mean AUC of the substance vs. mean AUC of the control (%) ± SD normalized to the DNA content of the sample, n = 3–6. (A) CAF and CA, (B) TRI and NMP, (C) PYR and CAT, (D) C5HTs. Significances were tested according to the unpaired student's t-test and the differences are indicated with the letters a to f.

mobilization and with KRS to test the effect on dopamine release. As a result, none of the reconstitutes induced intracellular calcium mobilization (Fig. 6A) nor dopamine release in PC-12 cells (Fig. 6B). The reconstituted coffees did not stimulate the dopamine release from PC-12 cells.

4. Discussion

We hypothesized that coffee and coffee constituents could excite dopamine release from neuronal cells via calcium signaling. To investigate this hypothesis, we tested two different coffees and seven previously quantified coffee constituents (Rubach et al., 2010) for their potential to induce intra-cellular calcium mobilization and dopamine exocytosis in PC-12 cells. In a first set of experiments, we were able to demonstrate that coffee and components thereof in coffee representative concentrations stimulate mechanisms of neurotransmitter release from PC-12 cells with different efficacies.

Chu et al. (2009) showed that the neuroprotective activity of coffee depends on the roasting process and that a roasted coffee, rich in lipophilic antioxidants and CA lactones, has better neuroprotective properties than a green coffee. Although these results were primarily based on antioxidant effects, Chu et al. (2009) demonstrated that the impact of coffee lyophilizates on intracellular signal transduction pathways in primary neuronal cells depends

on the chemical composition of the coffee. The two coffees chosen in this study, AR and RB, were roasted to a commercial roast and did not differ in their roasting degree, but varied in their extraction yields (Rubach et al., 2010). We could show that the RB coffee, bearing a higher extraction yield than the AR coffee, had a stronger effect on Ca^{2+}-mobilization and the dopamine release from PC-12 cells than the AR coffee.

To determine the contribution of individual coffee compounds to the neurotransmitter-stimulating effect of the tested coffees, mobilization of intra-cellular calcium was analyzed. Comparing the mean AUC-values, NMP was identified as the most potent compound, followed by the efficacies of PYR > C22-5HT > CA > TRI. Dopamine release, however, was stimulated most effectively by C5HTs, followed by PYR and CAT. This means that, although NMP leads to the strongest effect regarding the Ca^{2+}-mobilization, PYR and C5HTs elicit the strongest effect on the dopamine release in nanomolar concentrations and are thereby the most potent coffee compounds tested to stimulate neurotransmitter release from PC-12 cells. Thus, both C5HTs and PYR, although found in coffee only in micromolar concentrations, may contribute to the effect of coffee.

The most prominent coffee compound CAF is also known to influence the neurological system (Kaasinen et al., 2004; Nehlig et al., 1992). However, for most of the tested compounds, only limited data is available on their influence on the neurotransmitter release. The
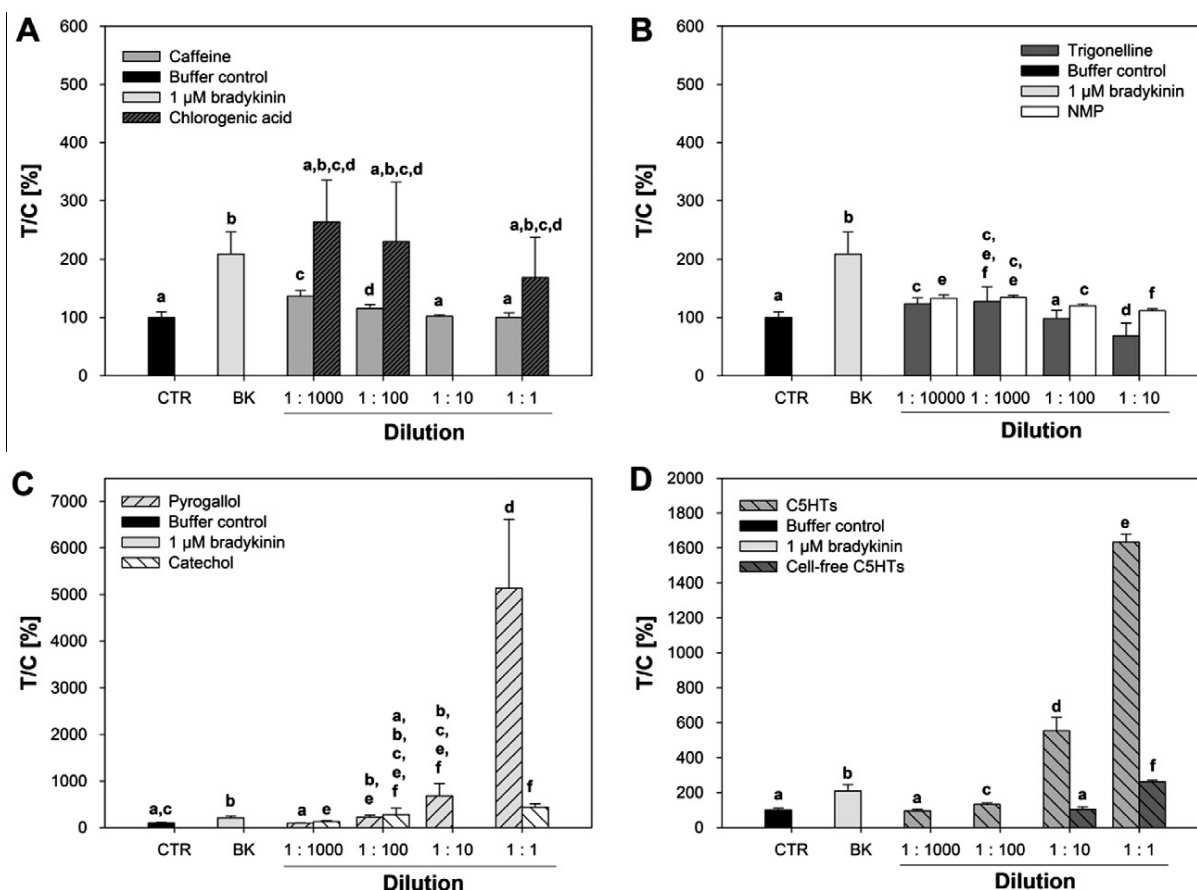
Fig. 4. Dopamine release by PC-12 cells after stimulation with the different coffee constituents compared to the buffer control (=100%). The results represent mean ± SD, normalized to the protein content of the sample, n = 3–4. (A) CAF and CA, (B) TRI and NMP, (C) PYR and CAT, (D) C5HTs significances were tested according to the unpaired student's t-test and the differences are indicated with the letters a to f.

Table 3
EC$_{200}$-values of the tested coffee compounds on the dopamine release from PC-12 cells.

| Compounds	EC$_{200}$ [µM]
C5HTs	0.01 ± 0.003
Pyrogallol	0.048 ± 0.014
Catechol	5.32 ± 9.46

results of the present study show that there are coffee constituents that may have a stronger neurotransmitter excitatory effect than CAF.

To transfer these results from an *in vitro* model to *in vivo* conditions, the bioavailability of the compounds has to be considered. In addition, to stimulate the neurotransmitter release in the human brain, the coffee compounds have to cross the blood–brain barrier. Substances can pass this barrier via transmembrane diffusion or via a substrate-specific, saturable transport (Banks, 2009). To diffuse through the membrane, a molecule needs to have a low molecular weight and a high degree of lipophilicity.

Very limited data can be found on the bioavailability and passage of the blood–brain barrier of most compounds tested in this study. CAF is well described to be highly bioavailable in humans (Blanchard and Sawers, 1983). Also, the transport of CAF and TRI through the blood–brain barrier is well characterized (Banks, 2009; Cornford et al., 1992; McCall et al., 1982; Pop et al., 1989). Our results indicate that TRI did not significantly contribute to the effect of the coffee

beverages, whereas CA, CAT, PYR and C5HTs were more active, although data on the bioavailability of these compounds and their ability to cross the blood–brain barrier are limited. After the consumption of CA-rich foods like coffee, CA is absorbed and rapidly metabolized, with caffeic acid being reported as the major metabolite found in the plasma (Lafay et al., 2006; Monteiro et al., 2007). In addition, CAT and PYR are also described to be highly bioavailable and metabolized by biotransformation enzymes (Balant et al., 1979; Goldberg et al., 2003; Holt et al., 2002; Lautala et al., 2001; Zhu et al., 1995). No data is available yet whether phenolic compounds, such as CAT, PYR or CA can cross the blood–brain barrier in humans. However, the tea polyphenol (−)-epigallocatechin gallate has been described to be bioavailable and to be able to cross the blood–brain barrier (Lin et al., 2007). This compound has a higher molecular weight than the tested compounds and is comparably lipophilic, so that it is likely that also CAT, PYR and CA might be able to cross the blood–brain barrier and have an influence on the neurotransmitter release in the human brain. In rat brain slices, significant effects of CAT and PYR on neurotransmitter uptake were found (Minchin and Pearson, 1981). For PYR, our data indicate that this compound might be a potent drug targeting the neurotransmitter signaling, leading to an increased neurotransmitter release and inhibiting the degradation of the signal molecules.

To investigate the overall effects of the tested compounds, experiments with biomimetic mixtures were performed. These reconstituted mixtures, containing the compounds tested in coffee representative concentrations, did not bear an effect on neither the
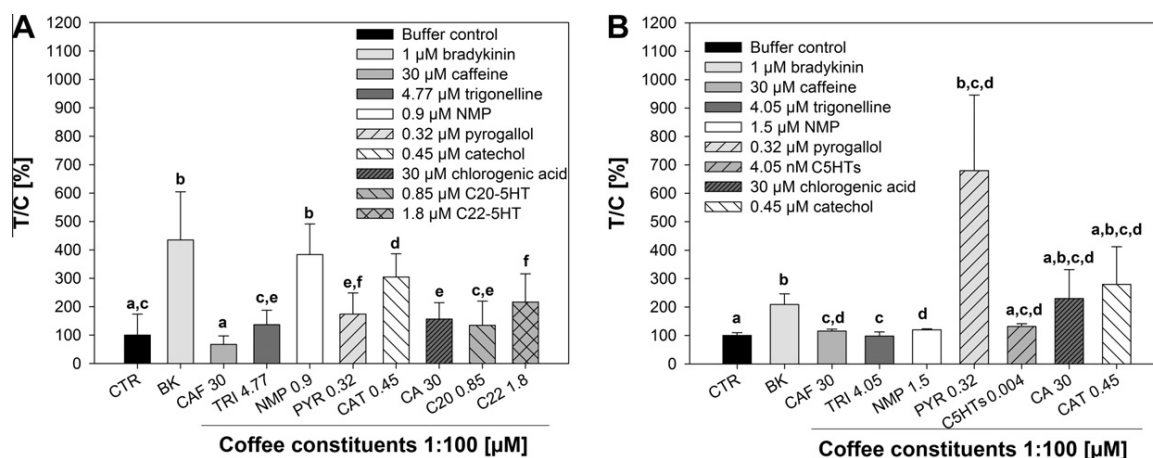
Fig. 5. Effects of the coffee compounds in concentrations corresponding a 1:100 of AR on (A) the Ca^{2+}-mobilization, results represent mean AUC of the substance vs. mean AUC of the control (%) ± SD normalized to the DNA content of the sample, $n = 4$, and (B) the dopamine release by PC-12 cells. The results represent mean ± SD. Significances were tested according to the unpaired student's t-test and the differences are indicated with the letters a to f.
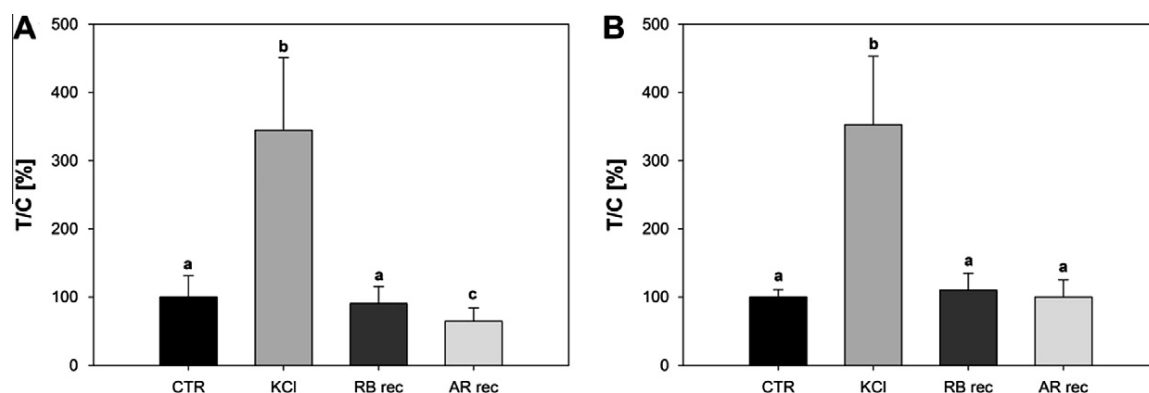
Fig. 6. Effects of the two reconstituted coffees, AR_{rec} and RB_{rec} on (A) the Ca^{2+}-mobilization, results represent mean AUC of the substance vs. mean AUC of the control (%) ± SD normalized to the DNA content of the sample, $n = 4$, and (B) the dopamine release by PC-12 cells. The results represent mean ± SD. Significances were tested according to the unpaired student's t-test and the differences are indicated with the letters a, b and c.

Ca^{2+}-mobilization nor the dopamine release from PC-12 cells, showing that the effect of the individual compounds was abolished. This could be due to cross-reactivity of the compounds with each other or through different receptor binding affinities. It has been shown for CAF, CAT and (−)-catechins that these compounds possess different binding affinities to the GABA (A) receptor, a brain receptor that is targeted by mood defining drugs (Hossain et al., 2003). In contrast to the biomimetic mixtures, the here tested AR and RB coffee possessed an effect tested at a 1:100 dilution, raising the question why the coffee reconstitutes did not. Compared to the reconstitutes, the coffees contained a large variety of other compounds, like melanoidins, lactones or volatiles. Chemical characterization of melanoidins revealed that low molecular weight melanoidins incorporate CA, leading to a lower concentration of free CA (Bekedam et al., 2008). In addition, CA serves as precursor for different lactones, formed upon roasting of the beans and present as bitter flavor compounds in the coffee beverage (Bruhl et al., 2007; Frank et al., 2007). Thus, other compounds than those investigated in this study, might have contributed to the effect demonstrated for the lyophilized AB and RB coffee. On the other hand, the lack of effect shown for the biomimetic mixture might also be due to antagonistic effects from the here tested compounds. Since their mode of action might be different when they

are absorbed from a complex coffee beverage matrix, further investigations need to identify the most relevant compounds in coffee which stimulate mechanisms of neurotransmitter release in the human brain.

5. Conclusion

We were able to prove that coffee and coffee constituents mobilize intracellular calcium, leading to dopamine release from PC-12 cells. Most of the active compounds tested are bioavailable and our results show that these compounds stimulated the neurotransmitter release already in nanomolar concentrations and could therefore be bioactive in humans. Furthermore, one of the most potent compounds tested, PYR, has been shown to stimulate the release of neurotransmitters in the human brain and could therefore contribute to the excitatory effect of coffee. The mechanism of action of PYR as well as of another potent class of compounds, e.g., C5HTs, have to be identified in future studies. In contrast to the lyophilized and then reconstituted beverages, the biomimetic mixtures of CA, CAF, TRI, NMP, PYR, CAT and C5HTs were not effective. Here, we hypothesize (1) antagonistic effects of these compounds and (2) that there are other compounds in coffee that induce the

dopamine release from PC-12 cells and contribute to the effect demonstrated for a coffee beverage.

Conflict of Interest

The authors declare that there are no conflicts of interest.

Acknowledgment

References

Avidor, T., Clementi, E., Schwartz, L., Atlas, D., 1994. Caffeine-induced transmitter release is mediated via ryanodine-sensitive channel. Neurosci. Lett. 165, 133–136.

Balant, L., Burki, B., Wermeille, M., Golden, G., 1979. Comparison of some pharmacokinetic parameters of (+)-cyanidanol-3 obtained with specific and nonspecific analytical methods. Arzneimittel-Forschung 29–2, 1758–1762.

Banks, W.A., 2009. Characteristics of compounds that cross the blood–brain barrier. BMC Neurol. 9 (Suppl. 1), S3.

Battig, K., Welzl, H., 1993. Psychopharmacological profile of caffeine. In: Garattini, S. (Ed.), Monographs of the Mario Negri Institute for Pharmacological Research Milan; Caffeine, coffee, and health. RavenPress, New York, pp. 213–253.

Bekedam, E.K., Roos, E., Schols, H.A., Van Boekel, M.A., Smit, G., 2008. Low molecular weight melanoidins in coffee brew. J. Agric. Food Chem. 56, 4060–4067.

Binda, F., Dipace, C., Bowton, E., Robertson, S.D., Lute, B.J., Fog, J.U., Zhang, M., Sen, N., Colbran, R.J., Gnegy, M.E., Gether, U., Javitch, J.A., Erreger, K., Galli, A., 2008. Syntaxin 1A interaction with the dopamine transporter promotes amphetamine-induced dopamine efflux. Mol. Pharmacol. 74, 1101–1108.

Blanchard, J., Sawers, S.J., 1983. The absolute bioavailability of caffeine in man. Eur. J. Clin. Pharmacol. 24, 93–98.

Boettler, U., Sommerfeld, K., Volz, N., Pahlke, G., Teller, N., Somoza, V., Lang, R., Hofmann, T., Marko, D., 2011. Coffee constituents as modulators of Nrf2 nuclear translocation and ARE (EpRE)-dependent gene expression. J. Nutr. Biochem. 22, 426–440.

Bruhl, L., Matthaus, B., Fehling, E., Wiege, B., Lehmann, B., Luftmann, H., Bergander, K., Quiroga, K., Scheipers, A., Frank, O., Hofmann, T., 2007. Identification of bitter off-taste compounds in the stored cold pressed linseed oil. J. Agric. Food Chem. 55, 7864–7868.

Chu, Y.F., Brown, P.H., Lyle, B.J., Chen, Y., Black, R.M., Williams, C.E., Lin, Y.C., Hsu, C.W., Cheng, I.H., 2009. Roasted coffees high in lipophilic antioxidants and chlorogenic acid lactones are more neuroprotective than green coffees. J. Agric. Food Chem. 57, 9801–9808.

Cornford, E.M., Young, D., Paxton, J.W., 1992. Comparison of the blood–brain barrier and liver penetration of acridine antitumor drugs. Cancer Chemother. Pharmacol. 29, 439–444.

Dayan, P., 2009. Dopamine, reinforcement learning, and addiction. Pharmacopsychiatry 42, S56–S65.

Di Chiara, G., Imperato, A., 1988. Drugs abused by humans preferentially increase synaptic dopamine concentrations in the mesolimbic system of freely moving rats. Proc. Natl. Acad. Sci. USA 85, 5274–5278.

Eshleman, A.J., Henningsen, R.A., Neve, K.A., Janowsky, A., 1994. Release of dopamine via the human transporter. Mol. Pharmacol. 45, 312–316.

Farnsworth, S.J., Volz, T.J., Hanson, G.R., Fleckenstein, A.E., 2009. Cocaine alters vesicular dopamine sequestration and potassium-stimulated dopamine release: the role of D2 receptor activation. J. Pharmacol. Exp. Ther. 328, 807–812.

Fernstrom, J.D., 2000. Can nutrient supplements modify brain function? Am. J. Clin. Nutr. 71, 1669–1673.

Ferre, S., 2010. Role of the central ascending neurotransmitter systems in the psychostimulant effects of caffeine. J. Alzheimers Dis. 20 (Suppl. 1), S35–S49.

Frank, O., Blumberg, S., Kunert, C., Zehentbauer, G., Hofmann, T., 2007. Structure determination and sensory analysis of bitter-tasting 4-vinylcatechol oligomers and their identification in roasted coffee by means of LC–MS/MS. J. Agric. Food Chem. 55, 1945–1954.

Geel, L., Kinnear, M., de Kock, H.L., 2005. Relating consumer preferences to sensory attributes of instant coffee. Food Qual. Prefer. 16, 237–244.

Goldberg, D.A., Yan, J., Soleas, G.J., 2003. Absorption of three wine-related polyphenols in three different matrices by healthy subjects. Clin. Biochem. 36, 79–87.

Greene, L.A., Tischler, A.S., 1976. Establishment of noradrenogenic clonal line of rat adrenal pheocytochroma cells which respond to nerve growth factor. Proc. Natl. Acad. Sci. USA 73, 2424–2428.

Holt, R.R., Lazarus, S.A., Sullards, M.C., Zhu, Q.Y., Schramm, D.D., Hammerstone, J.F., Fraga, C.G., Schmitz, H.H., Keen, C.L., 2002. Procyanidin dimer B2 [epicatechin-(4 beta-8)-epicatechin] in human plasma after the consumption of a flavanol-rich cocoa. Am. J. Clin. Nutr. 76, 798–804.

Hossain, S.J., Aoshima, H., Koda, H., Kiso, Y., 2003. Effects of coffee components on the response of GABA$_A$ receptors expressed in *Xenopus* oocytes. J. Agric. Food Chem. 51, 7568–7575.

Ikemoto, S.G.B.S., Murphy, J.M., McBride, W.J., 1997. Role of dopamine D$_1$ and D$_2$ receptors in the nucleus accumbens in mediating reward. J. Neurosci. 17, 8580–8587.

Jaffe, L.F., 1998. Free calcium signals. Science 279, 1833.

Johnson, L.A., Guptaroy, B., Lund, D., Shamban, S., Gnegy, M.E., 2005. Regulation of amphetamine-stimulated dopamine efflux by protein kinase C beta. J. Biol. Chem. 280, 10914–10919.

Kaasinen, V., Aalto, S., Nagren, K., Rinne, J.O., 2004. Expectation of caffeine induces dopaminergic responses in humans. Eur. J. Neurosci. 19, 2352–2356.

Koizumi, S., Rosa, P., Willars, G.B., Challiss, R.A., Taverna, E., Francolini, M., Bootman, M.D., Lipp, P., Inoue, K., Roder, J., Jeromin, A., 2002. Mechanisms underlying the neuronal calcium sensor-1-evoked enhancement of exocytosis in PC12 cells. J. Biol. Chem. 277, 30315–30324.

Koshimura, K., Tanaka, J., Murakami, Y., Kato, Y., 2003. Effect of high concentration of glucose on dopamine release from pheochromocytoma-12 cells. Metabolism 52, 922–926.

Lafay, S., Morand, C., Manach, C., Besson, C., Scalbert, A., 2006. Absorption and metabolism of caffeic acid and chlorogenic acid in the small intestine of rats. Br. J. Nutr. 96, 39–46.

Lang, R., Bardelmeier, I., Weiss, C., Rubach, M., Somoza, V., Hofmann, T., 2010a. Quantitation of (beta)N-Alkanoyl-5-hydroxytryptamides in coffee by means of LC–MS/MS-SIDA and assessment of their gastric acid secretion potential using the HGT-1 cell assay. J. Agric. Food Chem. 58, 1593–1602.

Lang, R., Wahl, A., Skurk, T., Yagar, E.F., Schmiech, L., Eggers, R., Hauner, H., Hofmann, T., 2010b. Development of a hydrophilic liquid interaction chromatography-high-performance liquid chromatography–tandem mass spectrometry based stable isotope dilution analysis and pharmacokinetic studies on bioactive pyridines in human plasma and urine after coffee consumption. Anal. Chem. 82, 1486–1497.

Lautala, P., Ulmanen, I., Taskinen, J., 2001. Molecular mechanisms controlling the rate and specificity of catechol O-methylation by human soluble catechol O-methyltransferase. Mol. Pharmacol. 59, 393–402.

Lin, L.C., Wang, M.N., Tseng, T.Y., Sung, J.S., Tsai, T.H., 2007. Pharmacokinetics of (−)-epigallocatechin-3-gallate in conscious and freely moving rats and its brain regional distribution. J. Agric. Food Chem. 55, 1517–1524.

McCall, A.L., Millington, W.R., Wurtman, R.J., 1982. Blood–brain barrier transport of caffeine: dose-related restriction of adenine transport. Life Sci. 31, 2709–2715.

Michaelis, M.L., Michaelis, E.K., Myers, S.L., 1979. Adenosine modulation of synaptosomal dopamine release. Life Sci. 24, 2083–2092.

Minchin, M.C., Pearson, G., 1981. The effect of the convulsant agent, catechol, on neurotransmitter uptake and release in rat brain slices. Br. J. Pharmacol. 74, 715–721.

Monteiro, M., Farah, A., Perrone, D., Trugo, L.C., Donangelo, C., 2007. Chlorogenic acid compounds from coffee are differentially absorbed and metabolized in humans. J. Nutr. 137, 2196–2201.

Morgan, M.E.V.R.E., 1998. Methylxanthine effects on caudate dopamine release as measured by *in vivo* electrochemistry. Life Sci. 45, 2025–2039.

Nehlig, A., Daval, J.L., Debry, G., 1992. Caffeine and the central nervous system: mechanisms of action, biochemical, metabolic and psychostimulant effects. Brain Res. Rev. 17, 139–170.

Newton, R., Broughton, L.J., Lind, M.J., Morrison, P.J., Rogers, H.J., Bradbrook, I.D., 1981. Plasma and salivary pharmacokinetics of caffeine in man. Eur. J. Clin. Pharmacol. 21, 45–52.

Pontieri, F.E., Tanda, G., Di Chiara, G., 1995. Intravenous cocaine, morphine, and amphetamine preferentially increase extracellular dopamine in the "shell" as compared with the "core" of rat nucleus accumbens. Proc. Natl. Acad. Sci. USA 92, 12304–12308.

Pop, E., Shek, E., Murakami, T., Bodor, N.S., 1989. Improved anticonvulsant activity of phenytoin by a redox brain delivery system I: Synthesis and some properties of the dihydropyridine derivatives. J. Pharm. Sci. 78, 609–616.

Rubach, M., Lang, R., Hofmann, T., Somoza, V., 2008. Time-dependent component-specific regulation of gastric acid secretion-related proteins by roasted coffee constituents. Ann. NY. Acad. Sci. 1126, 310–314.

Rubach, M., Lang, R., Skupin, C., Hofmann, T., Somoza, V., 2010. Activity-guided fractionation to characterize a coffee beverage that effectively down-regulates mechanisms of gastric acid secretion as compared to regular coffee. J. Agric. Food Chem. 58, 4153–4161.

Shinohara, H., Wang, F., Hossain, S.M., 2008. A convenient, high-throughput method for enzyme-luminescence detection of dopamine released from PC12 cells. Nat. Protoc. 3, 1639–1644.

Solinas, M., Ferre, S., You, Z.-B., Karcz-Kubicha, M., Popoli, P., Goldberg, S.R., 2002. Caffeine induces dopamine and glutamate release in the shell of the nucleus accumbens. J. Neurosci. 22, 6321–6324.

Somoza, V., Lindenmeier, M., Wenzel, E., Frank, O., Erbersdobler, H.F., Hofmann, T., 2003. Activity-guided identification of a chemopreventive compound in coffee beverage using in vitro and in vivo techniques. J. Agric. Food Chem. 51, 6861–6869.

Stadler, R.H., Varga, N., Hau, J., Vera, F.A., Welti, D.H., 2002. Alkylpyridiniums. 1. Formation in model systems via thermal degradation of trigonelline. J. Agric. Food Chem. 50, 1192–1199.

Tohda, C., Nakamura, N., Komatsu, K., Hattori, M., 1999. Trigonelline-induced neurite outgrowth in human neuroblastoma SK-N-SH cells. Biol. Pharm. Bull. 22, 679–682.

Westerink, R.H., Klompmakers, A.A., Westenberg, H.G., Vijverberg, H.P., 2002. Signaling pathways involved in Ca^{2+}- and Pb^{2+}-induced vesicular catecholamine release from rat PC12 cells. Brain Res. 957, 25–36.

Wood, P.L., Kim, H.S., Boyar, W.C., Hutchison, A., 1989. Inhibition of nigro-stratial release of dopamine in the rat by adenosine receptor agonists: A1 receptor mediation. Neuropharmacology 28, 21–25.

Zhu, J., Filippich, L.J., Ng, J., 1995. Rumen involvement in sheep tannic acid metabolism. Vet. Hum. Toxicol. 37, 436–440.

2.2 "N(epsilon)-Carboxymethyllysine (CML), a Maillard reaction product, stimulates serotonin release and activates the receptor for advanced glycation end products (RAGE) in SH-SY5Y cells"

Holik, A. K.*[b], **Rohm, B**.*[a], Somoza, M. M.[c], and Somoza, V. [ab]

The authors A.K. Holik and Barbara Rohm contributed equally to this work.

a Christian Doppler Laboratory for Bioactive Aroma Compounds, University of Vienna, Althanstraße 14, 1090 Vienna, Austria. E-mail: Veronika.Somoza@univie.ac.at; Fax:+43 1 4277 9706; Tel: +43 1 4227 70601

b Department of Nutritional and Physiological Chemistry, University of Vienna, Althanstraße 14, Vienna, Austria

c Department of Inorganic Chemistry, University of Vienna, Währinger Straße 42, Vienna, Austria

N^{ε}-Carboxymethyllysine (CML), a Maillard reaction product, stimulates serotonin release and activates the receptor for advanced glycation end products (RAGE) in SH-SY5Y cells

Ann-Katrin Holik,†[b] Barbara Rohm,†[a] Mark M. Somoza[c] and Veronika Somoza*[ab]

Maillard reaction products, which are formed in highly thermally treated foods, are commonly consumed in a Western diet. In this study, we investigated the impact of N^{ε}-carboxymethyllysine (CML), a well-characterized product of the Maillard reaction, on the gene regulation of the human neuroblastoma cell line SH-SY5Y. Pathway analysis of data generated from customized DNA microarrays revealed 3 h incubation with 50 μM and 500 μM CML to affect serotonin receptor expression. Further experiments employing qRT-PCR showed an up-regulation of serotonin receptors 2A, 1A and 1B after 0.25 h and 3 h. In addition, 500 μM CML increased serotonin release, thus showing effects of CML not only at a genetic, but also at a functional level. Intracellular calcium mobilization, which mediates serotonin release, was increased by CML at concentrations of 0.05–500 μM. Since calcium mobilization has been linked to the activation of the receptor for advanced glycation end products (RAGE), we further investigated the effects of CML on RAGE expression. RAGE was found to be up-regulated after incubation with 500 μM CML for 0.25 h. Co-incubation with the calcium blocker neomycin for 0.25 h blocked the up-regulation of RAGE and the serotonin receptors 2A, 1A and 1B. These results indicate a possible link between a CML-induced calcium-mediated serotonin release and RAGE.

Introduction

Heat treatment of food results in the generation of Maillard reaction products, which make the food more palatable due to the formation of aroma compounds.[1,2] The interactions of Maillard reaction products with biological systems are diverse and regular consumption of highly thermally processed food has been linked to increased cardiovascular risk factors in healthy subjects[3] and to the progression of cardiovascular complications in compromised individuals, *e.g.* type II diabetes mellitus patients.[4] However, Maillard reaction products may exert potentially health beneficial effects as well. Bread crust extract, a source of dietary Maillard reaction products, has been shown to improve the antioxidant defense in mouse cardiac fibroblasts *in vitro* and also to positively influence the antioxidant status of the heart of mice fed with a diet containing bread crust.[5]

Foods high in Maillard reaction products are commonly consumed in a typical Western diet and may add significantly to the body's endogenous advanced glycation endproduct (AGE) load due to partial absorption into circulation.[6–9] Furthermore, dietary intake of heat-treated foods has been shown to be associated with an increase in energy intake. One major reason for this effect is the higher nutrient density of heat-treated foods.[3] Another hypothesis is that heat-treated foods contain high amounts of aroma compounds that affect the regulation of hunger and satiety and thereby alter food and energy intake. Retro-nasal aroma release, for instance, has been shown to influence perceived satiation.[10] Previous studies on Maillard reaction products demonstrated that a Maillard reaction product-rich diet containing 25% (w/w) bread crust increased insulin and leptin receptor mRNA levels and decreased NPY mRNA levels in the olfactory bulb of male Wistar rats.[11] Higher insulin levels in the brain are associated with reduced food intake and increased energy expenditure mediated by anabolic (*e.g.* neuropeptide Y, NPY) and catabolic (*e.g.* proopiomelanocortin) neuropeptides.[12]

However, insulin is only one factor in the regulation of food intake. The regulation of hunger and satiety is a complex interaction of neural and hormonal signals derived from different tissues in the central nervous system (CNS).[13] Another important satiety signal is the hypothalamic release of the neurotransmitter

ªChristian Doppler Laboratory for Bioactive Aroma Compounds, University of Vienna, Althanstraße 14, 1090 Vienna, Austria. E-mail: Veronika.Somoza@univie.ac.at; Fax: +43 1 4277 9706; Tel: +43 1 4227 70601

ᵇDepartment of Nutritional and Physiological Chemistry, University of Vienna, Althanstraße 14, Vienna, Austria

ᶜDepartment of Inorganic Chemistry, University of Vienna, Währinger Straße 42, Vienna, Austria

† A.K. Holik and B. Rohm contributed equally to this work.
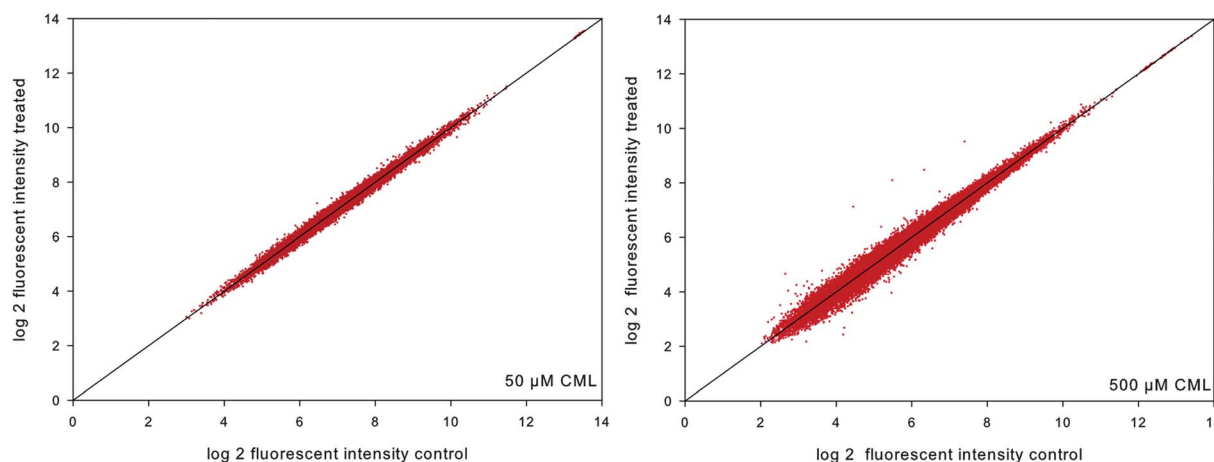
Fig. 1 Scatterplots of log 2 fluorescence intensity after incubation of SH-SY5Y cells with 50 μM or 500 μM CML. Bisector represents equal regulation in control and treated samples ($n = 3$).

serotonin.[14] Increased serotonin release, which is mediated by mobilization of Ca^{2+} from intracellular calcium stores, is associated with decreased appetite *via* inhibition of the orexigenic NPY, whereas low levels or disturbed receptor signalling leads to an increased craving for carbohydrates.[15] So far, four out of the currently known 14 serotonin receptors have been demonstrated to be involved in the regulation of food intake. The serotonin auto-receptor 5-HT$_{1A}$ controls serotonin release. Activation of this receptor subtype consequently leads to enhanced food intake.[16,17] In contrast, activation of the serotonin receptors 5-HT$_{1B}$, 5-HT$_{2C}$ and 5-HT$_{2A}$ will lower food intake.[18–20]

The present study aimed to investigate effects of the Receptor for Advanced Glycation End products (RAGE) ligand N^ε-carboxymethyllysine (CML), a stable and well-investigated Maillard reaction product,[21–23] on serotonin release in SH-SY5Y cells as a mechanism involved in satiety regulation. In order to cover the broad field of satiety signalling, a genome-wide gene expression analysis in neural SH-SY5Y cells by means of a customized microarray was performed after application of CML. Pathway analysis of regulated genes revealed an influence on the serotonin system, which was verified by qRT-PCR and functional assays.

SH-SY5Y cells were chosen since this cell line has been shown to express the serotonin receptor subtype 5-HT$_{1A}$,[24] whose activation has been linked to enhanced food intake.[16,17] Additionally, our own studies demonstrate that also the two

satiety-mediating serotonin receptors 5-HT$_{2A}$ and 5-HT$_{1B}$ are endogenously expressed in SH-SY5Y cells. We therefore consider this cell line suitable for investigations into the effect of CML on satiety.

Furthermore, the cell line has been used in studies using AGEs. Specifically, the identification of AGE-modified proteins and the effects of AGEs on glucose utilization and ATP levels have been studied in SH-SY5Y cells.[25,26]

Results

Effect of CML on gene expression in SH-SY5Y cells

The impact of 50 μM and 500 μM CML on the gene expression in SH-SY5Y cells was investigated using customized DNA microarrays. After incubation with 50 μM CML, a scatter plot of treated *vs.* control (Fig. 1) revealed little changes in gene expression, while incubation with 500 μM CML showed a more pronounced effect (Fig. 1). In total, 143 probes with fold-changes of at least 1.2 up/down were observed for 50 μM CML. This corresponds to 0.3% of all probes. Treatment of SH-SY5Y cells with 500 μM CML revealed 413 probes, corresponding to 0.9% of the total number of probes, to be differentially expressed.

In order to identify genes whose expression may be altered by incubation with 500 μM CML, probes with a fold-change above 1.2 up/down were entered into the functional annotation

Table 1 Annotation cluster with the highest enrichment score found by DAVID using input data of microarray probes with fold-changes below 0.8 or above 1.2 after treatment with 500 μM CML for 3 h

Annotation cluster	Enrichment score: 3.86	Count	P value	Benjamini
GOTERM_MF_FAT	Serotonin receptor activity	8	5.5×10^{-09}	3.3×10^{-06}
GOTERM_MF_FAT	Amine receptor activity	11	2.5×10^{-08}	7.5×10^{-06}
SP_PIR_KEYWORDS	Neurotransmitter receptor	9	2.6×10^{-05}	1.1×10^{-02}
GOTERM_BP_FAT	Serotonin receptor signaling pathway	4	1.2×10^{-04}	6.2×10^{-02}
GOTERM_BP_FAT	Cell–cell signaling	27	1.6×10^{-03}	3.0×10^{-01}
GOTERM_BP_FAT	Transmission of nerve impulse	18	3.3×10^{-03}	3.3×10^{-01}
GOTERM_MF_FAT	Amine binding	9	4.3×10^{-03}	4.7×10^{-01}
GOTERM_BP_FAT	Synaptic transmission	15	9.7×10^{-03}	4.4×10^{-01}
GOTERM_BP_FAT	Neurological system process	34	1.8×10^{-01}	9.1×10^{-01}

clustering software DAVID.[27] Of the 413 input DAVID IDs, 152 clusters were created. The cluster with the highest enrichment score of 3.86 was found to involve genes associated with serotonin receptor activity (Table 1).

Fig. 2 shows a heat map of a selection of genes, including probes corresponding to serotonin receptors. The heat map allows for a direct comparison between the three biological replicates for each concentration and the response of the multiple probes for one target gene. This shows that some of the customized probes for a single target may not respond uniformly.

Consequently, probes relating to the serotonin receptors 1A, 2A and 1B were analyzed more closely. As shown in Fig. 3, seven

out of the eleven probes for HTR1A were up-regulated after 3 h incubation with 500 μM CML. Out of the seven up-regulated probes, two reached a fold-change of 1.2, and thus the majority of the probes for HTR1A remained between 1.0 and 1.2 up or down. The sequences of the probes shown in the heat map are shown in Table 2.

Experiments using the more sensitive qRT-PCR method (Fig. 4) revealed that incubation with 500 μM CML alters the gene expression of HTR1A, HTR2A and HTR1B in a time-dependent manner. After incubation for 3 h, serotonin auto-receptor 5-HT_{1A} and satiety-mediating receptor 5-HT_{2A} were significantly up-regulated with fold-changes of 4.12 ± 0.53
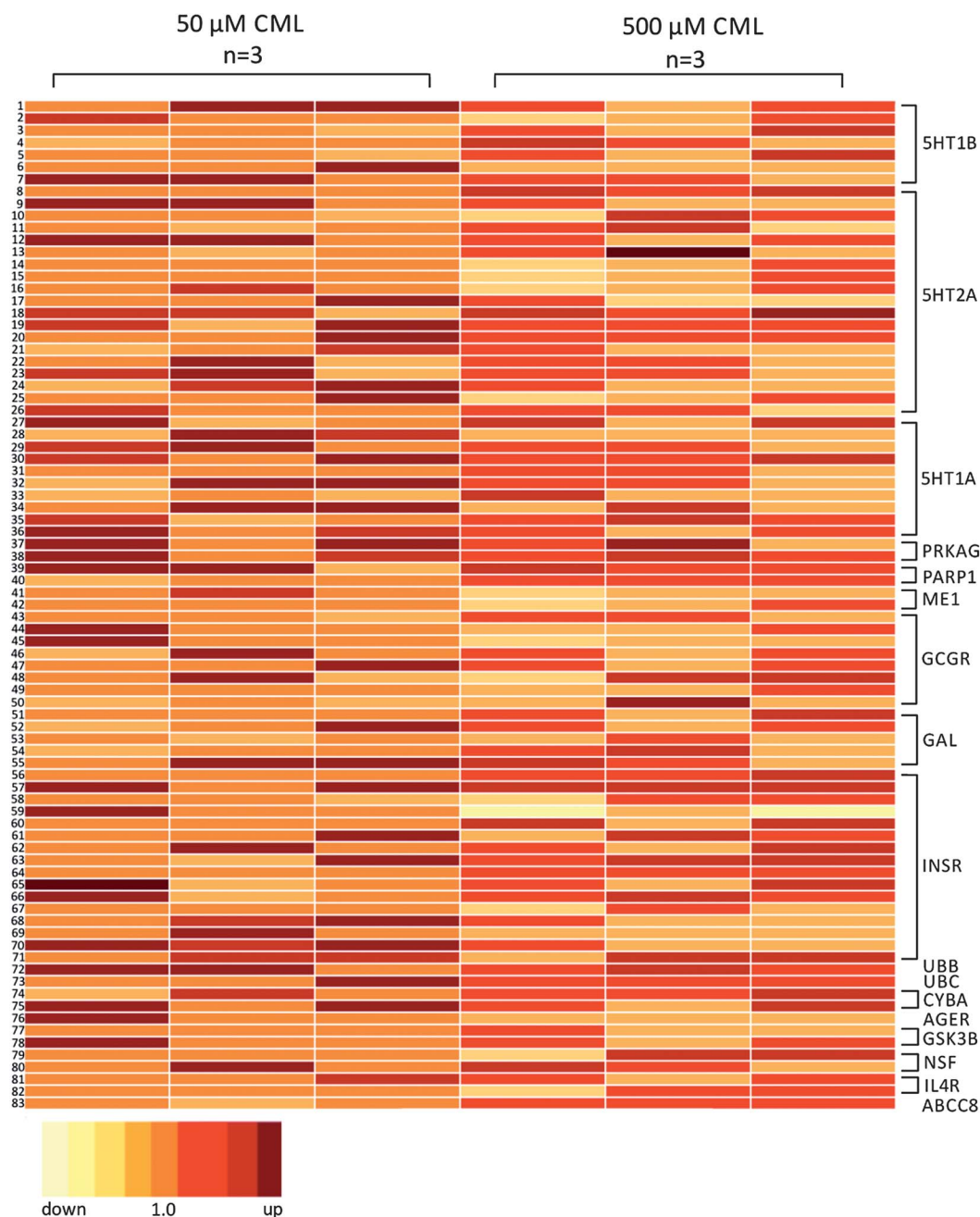
Fig. 2 Heat map illustrating effects of 50 μM or 500 μM CML on gene expression in SH–SY5Y cells (n = 3). For clarification purposes only a small number of genes tested on the microarray are shown. Numbers next to the heat map refer to the corresponding probe. Sequence can be found in Table 2.
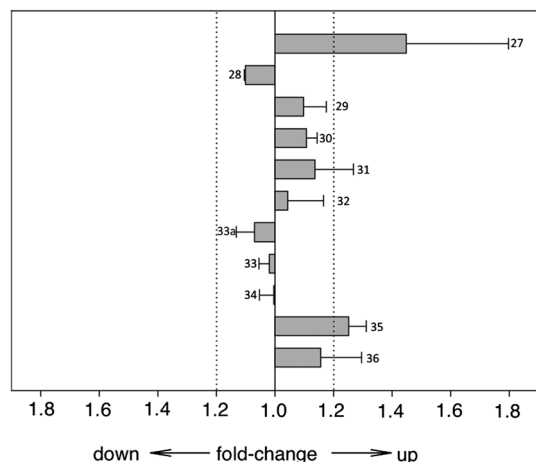
Fig. 3 Graphical representation of the response of the 11 microarray probes for HTR1A after treatment with 500 µM CML for 3 h. Results are displayed as mean fold-change ± SEM (*n* = 2–3). Numbers refer to the corresponding probe. Sequence can be found in Table 2.

($p < 0.001$ *vs.* control) and 3.58 ± 0.53 ($p < 0.001$ *vs.* control). Similarly, serotonin receptor 5-HT$_{1B}$ reached a maximum expression after 3 h incubation at a fold-change of 4.82 ± 1.07 ($p < 0.001$ *vs.* control) (Fig. 4). In addition, the gene expression of HTR1A, HTR2A and HTR1B was up-regulated after 0.25 h incubation with fold-changes of 2.75 ± 1.17 ($p < 0.001$ *vs.* control), 3.45 ± 2.51 ($p < 0.001$ *vs.* control) and 3.08 ± 1.91 ($p < 0.001$ *vs.* control), respectively. Expression of all three receptors was at a minimum after 6 h incubation.

Effect of CML on serotonin release and Ca^{2+} mobilization in SH-SY5Y cells

As CML was found to influence the expression of serotonin receptors 1A, 2A and 1B, the effect on serotonin release was determined. SH-SY5Y cells were incubated with CML in a concentration range from 0.05 to 500 µM. The highest concentration tested, 500 µM, significantly increased serotonin release ($144 \pm 38.5\%$, $p = 0.040$) in comparison to non-treated control cells (Fig. 5).

In addition, intracellular Ca^{2+} mobilization was measured, as intracellular Ca^{2+} is a known mediator in neurotransmitter release. Similar to the serotonin release experiment, SH-SY5Y cells were treated with CML in a concentration range of 0.05 to 500 µM. Intracellular Ca^{2+} mobilization was found to be increased in all tested concentrations (Fig. 6). CML, at a concentration of 500 µM, led to an increase in intracellular Ca^{2+} of $156 \pm 13.6\%$ ($p = 0.005$ *vs.* control). Lower concentrations of CML showed similar effects as 50 µM, 5 µM and 0.5 µM CML increased intracellular Ca^{2+} levels by $172 \pm 32.6\%$ ($p < 0.001$ *vs.* control), $150 \pm 21.4\%$ ($p = 0.006$ *vs.* control) and $167 \pm 42.6\%$ ($p < 0.001$ *vs.* control), respectively.

Effect of CML on gene expression of RAGE

The effect of the RAGE ligand CML on the expression of RAGE in SH-SY5Y cells was determined in a time-course qRT-PCR experiment.

RAGE expression was significantly up-regulated after incubation with 500 µM CML for 0.25 h and 0.5 h, with fold-changes of 1.34 ± 0.09 ($p < 0.001$ *vs.* control) and 1.13 ± 0.15 ($p = 0.004$ *vs.* control), respectively. After incubation for 1 h (0.61 ± 0.07, $p < 0.001$ *vs.* control) and 6 h (0.86 ± 0.12, $p = 0.001$ *vs.* control), RAGE expression was down-regulated (Fig. 7).

Effect of neomycin on CML-induced expression changes of RAGE and serotonin receptors 5-HT$_{1A}$, 5-HT$_{2A}$ and 5-HT$_{1B}$

In order to investigate the influence of calcium signaling on the CML-induced expression changes of RAGE and serotonin receptors 5-HT$_{1A}$, 5-HT$_{2A}$ and 5-HT$_{1B}$, SH-SY5Y cells were pre-incubated with 100 µM of the calcium blocker neomycin or media only for 0.25 h prior to incubation with 500 µM CML for further 0.25 h. The 15 min incubation time was chosen, as it is the only time point tested where both the serotonin receptor expression and RAGE were significantly up-regulated. Here, we hypothesized that neomycin blocks the up-regulation of these receptors. While incubation with 500 µM CML for 0.25 h led to a significant increase in RAGE expression (1.34 ± 0.09, $p < 0.001$ *vs.* control), the expression did not increase after pre-incubation with 100 µM neomycin (0.88 ± 0.07, $p = 0.005$ *vs.* control). A similar pattern was observed for serotonin receptors 5-HT$_{1A}$, 5-HT$_{2A}$ and 5-HT$_{1B}$ (Table 3). Their expression increased after incubation with 500 µM CML for 0.25 h by 2.75 ± 1.17 ($p < 0.001$ *vs.* control), 3.45 ± 2.51 ($p < 0.001$ *vs.* control) and 3.08 ± 1.91 ($p < 0.001$ *vs.* control), respectively. When pre-incubated with 100 µM neomycin the expression did not increase significantly, reaching only fold-changes of 1.41 ± 0.10 ($p > 0.05$ *vs.* control), 1.16 ± 0.09 ($p > 0.05$ *vs.* control) and 1.17 ± 0.15 ($p > 0.05$ *vs.* control) for HTR1A, HTR2A and HTR1B, respectively.

Discussion

In order to examine the effects of CML on mechanisms regulating food intake in neural cells, a genome-wide gene expression analysis was performed. For this purpose, human neural SH-SY5Y cells were treated with 50 or 500 µM CML as indicator of Maillard reaction products, for 3 h and gene expression was analyzed using customized DNA microarrays.

Recent studies show CML plasma levels of healthy humans to centre around 2.6 µM.[28,29] However, elevated CML plasma levels up to 12 µM[30] have been found in several conditions such as diabetes.[28] Also, CML has been demonstrated to accumulate with age in diverse tissues including hippocampal neurons.[31] No conclusive quantitative data on the maximum concentration of CML in different tissues at times are currently available, as experiments investigating CML accumulation employ qualitative immunostaining methods.[31] Based on an accumulation of CML in the human body, concentrations of 50 and 500 µM were chosen for the initial experiments. A concentration of 500 µM of CML regulated more genes than a concentration of 50 µM of CML (413 *vs.* 143) (Fig. 1) and was, therefore, chosen for further experiments.

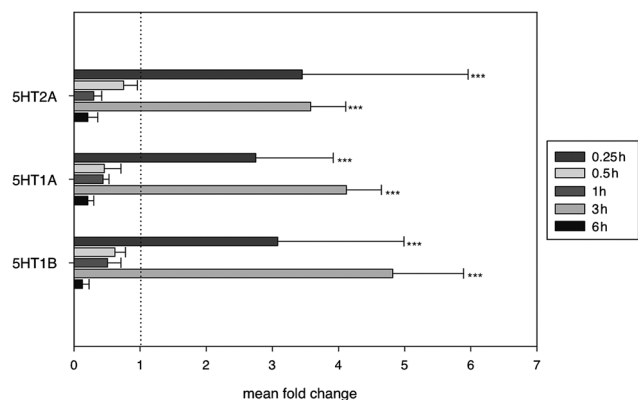Regulated probes (fold-change higher than 1.2 or lower than 0.8) after treatment with 500 µM CML were used for pathway

Table 2 Sequences of probes shown in the heat map. Highlighted sequences are included on commercially available arrays

Gene	Sequence	ID
HTR1B	TGTGTGTTGGCTACCCTTCTTCATCATCTCCCTAGTGATGCCTATCTGCAAAGATGCCTG	1
	TTCTTCATCATCTCCCTAGTGATGCCTATCTGCAAAGATGCCTGGTTCCACCTAGCC	2
	ACTGCTGGTTATGCTATTGGCGCTCATCCACTTGGCCACCACGCTCTCCAATGCCTTTGT	3
	GTCACCGACCTGCTTGTGTCCATCCTGGTGATGCCCATCAGCACCATGTACACTGTCACC	4
	CTACCCTGGAAAGTACTGCTGGTTATGCTATTGGCGGCTCATCACCTTGGCCACCACGCTC	5
	TGGGTTCCTCAAGCCAACTTATCCTCGTCCTCCCAAAACTGCAGCGCCAAGGACTAC	6
	ACTGCTGGTTATGCTATTGGCGCTCATCACCTTGGCCACCACGCTCTCCAATGCCTTTGT	7
	TGACAGTGGTAGAGTCCTAGGACATCTCTGTAAAAGCAGGTGACTTTCCTATGACACTC	8
	TGGAAACCTTGCTGCTATGCTGTTCATTGATGACATGGGATTGAGTTGGTTACCTATTGC	9
	TCAGGTTTCCGGCTACTGACAGTGGTAGAGTCCTAGGACATCTCTGTAAAAGCAGGTGA	10
HTR2A	ATTATCTGATCCTTGTGGCCACACACTGTGGTCCCAGCTACAGGGGAGGCTGAGACGCAA	11
	TCCTAGCACTTTGGGAGGCTGAGATGGGAGGGATCACTTGAGGCCAAGAGTTTGAGACCAA	12
	ATAATTAAAACAAAATCCTTGCCTTCAAACGAAAATGGCTCGGCCAGGCACGGAGGCTCGT	13
	CGACGGAGTGAATGAAAAGGTGAGCTGTGTGTATAGGCTAGTTGCCGTGGCAACTGTGG	14
	GAGTCCTGCAATGAGGATGTCATTGGGCGCCCTGCTCAATGTGTTTGTTTGGATCGGTTAT	15
	TGCTGGGCATCGTCTCTTCTGTTTGTTGGTGATGTGTGCCCTTTCTTCATCACAAAACA	16
	CCCTCAGAGTTCTTTGTCTTCAGAAAAGCTCTTCCAGCGGTGATCCATAGGGAGGCCAGG	17
	GCCATCCAGAATCCCATCCACCACAGCCGCTTCAACCTCAGAACTAAGGCATTTCTGAAA	18
	CCTTGTCATGCCCGTGTCCATGTTAACCATCCTGTATGGGTACCGGTGGCCTCTGCCGAG	19
	CTGGAAACATACTCGTCATCATGGCAGTGTCCTAGAGAAAAGCTGCAGAAAAGCCACCA	20
	GGACAGTGCGACTCGAAAATGCAACCAACCTTTCTGTGAAGGGTGCCTCTCACCGTCGT	21
	CAAAAATCCAGCCCGGAGAACAAGCATGTACACCAGCCTCAGTGTTACAGAGTGTGGGT	22
	GTGGACCCTGAAGACAAAATGACATTTATCTTCCCGAGCCGTCAAAAAAAAACCTGCAACC	23
	CAACAGGATCCTAGCAGTGCGGGAGCTGGCTCAGCTCTTTGTTGCATGCAGTTTTGAAGTCAG	24
	GGTGCAGACAGCTCTTCCCATGCAGTTCTTTGTGCGACTTTGAGGGGCTCG	25
	TCAGGTTTCCGGCTACTGACAGTGGTAGAGTCCTAGGACATCTCTGTAAAAGCAGGTGA	26
HTR1A	ACATGCCCACCCTGTGGGCGCCATAATCAATCAATTGGCTGGGCTTCCCAACTCTGCTTA	27
	TGGTTCTTCTATGGGCGCATATTCCGAGCTGCGCGCTTCCGATCCGCAAGACGGTCAAAA	28
	ACACTGGGCCAGGTAACCTGACCGACCTGTTCATCGCCCTGCGACGTGTGTGCACCTCA	29

Gene	Sequence	ID
GCGR	CTCAGGTGATGGACTTCCTGTTTGAGAAGTGGAAGCTCACGGTGACCAGTGTCACCACA	48
	AGTTTGCACCGACCCCGATCTGGCACGGCCGCCGAAGACGAGGCGGTCACCGGCGCCGACC	49
	GGCTGTGCCGTGAACTGCGTGGCCGGTGTTCATCAATATGGCATCGTGGCCAACTACTGCTGGCT	50
	CCAAGCTGCGGGCACGGCAGATGCACCACACAGACTACAAGTTCCGGCGTGGCCAAGTCCA	
	TGGATAATCTTCGGCCAATTTATGCAGAGTCAGCCATTCCTGTTCTCTTTGCCTTGATGT	51
	GCAGCCTCCAGAAGACATCGAGCGGTCTCGAGAGCCTCCTGAGGCGTGTTTGTCTGTGT	52
	TTTCTGTCTTTCTTGCATCTCAAAGAGGCCGGTGCCCTGACCGCCTCTGGATCTCCCC	53
GAL	ACATGAAACCAGGAAGCTTGACAGGTCCATACCTGAAAACAATATCATGCGCACAATCA	54
	GTGTGCTGTAACCTGAAGTCAAACCTTAAGATAATGATAATCTTCGGCCAATTTATGCA	55
	GGAAGCTTTGACAGGTCCATACCTGAAAACAATATCATGCGCACAATCATTGAGTTTCTG	
	TTTCTTGCATCTCAAAGAGGCCGGTGCCCTGACCGCCTCTGGATCTCCCCGCCAGC	56
	ATCAACATTCGAGGAGGCAACAATCTGCAGTGAGCTAGAAGCAACCTCGGCCTCATT	57
	ACAACAAGTGCATCCCTGAGTGTCCCTCGGGTACAGATGAATTCCAGCAACTTGCTGT	58
INSR	CCGTCATCAACGGCAGTTTGTCGAACGATGTTGGACTCATAGTCACTGCCAGAAAGTTT	59
	GGCCACTATCGACTGGTCCCGTATCCTGGATTCCGTGGAGGATAATTACATCGTTGTTGAA	60
	TACAACCTGATGAAACATCACCCGGGGTTCTGTCCGCATCGAGAAGAACAATGAGCTCTGT	61
	CCGGGGATCACGACTGTTCTTTAACTACGCGCTGGTCATCTTCGAGATGGTTCACCTCAA	62
	TGATTACTTGCTGCTCTTCCCGGGTCTATGGGCTCGAGAGCCTGAAGGACCTGTTCCCCAA	63
	ACTTGCAGATACTTCTTGATGTTCAAAAGCGAGGCCCGAAGATTTCCGAGACCTCAGTTTCC	64
	CAAGAGTGACATCATTTATGTCCAGACAGATGCCACCAACCCCTGTGCCCCTGGATCC	65
	CAGTATGCCATCTTTGTGAAGACCTGGCTCACCTTTTCGGATGAACGCCGGACCTATGGG	66
	TCTACAAAGAGGGCCCTTATCAGAATTGTACGGAGTTCGACGGGCCAGGATGTGGTGGTT	67
	AATCCACAAGATGGAAGAAGTTTCAGGAACCCAAGGGGCCCAGGAGGAGAAACGACATTGC	68
	AACCTAAGGCAGCTCTGGGACTGGAGCAAACACAACCTCACCATCACTCAGGGGAAACTC	69
	CCGCCGATCCTACGCTCGTGGTGTCACTTTCCTTCCTCCGGAAGTTACGTCGATTCGAGG	70
	GGCATGGGATATCCGGAACAACCTCACTAGGTTGCATGAGCGTGGAGAATTGCTCGTCATC	71
	TTTGTGCATCGGGGACCTGGCAGGGAGGAGAAACTCATGGTCGCCCATGATTTACTGTCAAA	
	TGACATGGTGTCCTTTGGCCTGTGCTCTTTGGGAAATCACCAGCTTGGCAGAACAGCCTTA	
UBB	AGAGACCCCGGTGGCGGTGAAGACGTCAAGGAGTCCGAGAGCGGATTGA	72
	TTGCAGGCAAGCAGCTGGAAGATGGCGAAGATGCCCGCACTCTTTCTGACTACAAACATCCAGAAAGAGT	

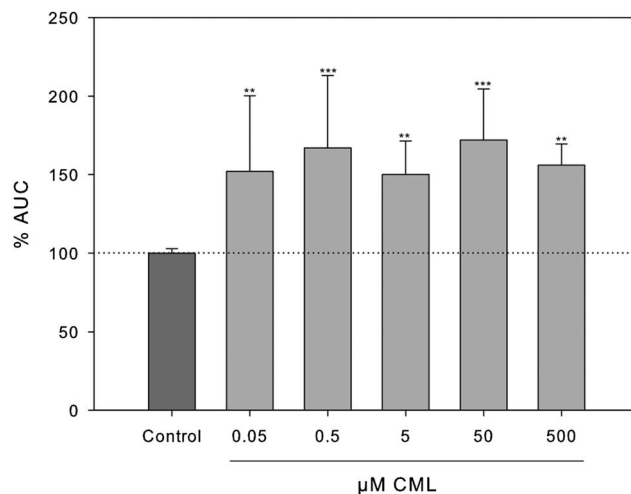| Gene	No.	Primer sequence	Gene	No.	Primer sequence	Ref.
PRKAG2		AAGAAGAGTGTGAATGGAGAGTCGGGGAGGCAGGAACTGGAGGCGTGGGCGTGGAGAGCAAG		30	CCTGACTGGTAAGACACTCACTCTCGAAGTGGAGCCGAGTGACACCATTGAGAATGTCAA	73
		CTTTGGAGCTTTCTACATCCGCTGCTCATGCTGGTTCTCTATGGGCGCATATTCCG	UBC	31	ACCTGGTGTCCGTCTCAGAGGTGGGATGCAAATCTTCGTGAAGACCCTGACTGGTAAGA	
		GACCGCTGGACCCGACGCATGCACCATTAGCAAGGATCCATGGCTACACTATCTATTCC		32	AGCAGAGGTTGATCTTTGCCGGAAAACAGCTGGAAGATGGTCGTACCGTGTCTGACTACA	
		CTGTATCAGGTGCTCAACAAGTGGACACTGGGCCAGTAACCTGCGACCTGTTCATCGCC		33	TTCCTGCTGGCCACCATCCTTGGGACCGGCTGCCTGGCCATTGCGAGCGGGCATCTACCTA	74
		CTCATCCGCTCACTTGGCTTATTGGCTCTCCTCATCTCTATCCGCCCATGCTGGGCTGG		33a	GCTTCACCCAGTGGTACTTGGTGCCTACTCCATTGTGGCGGGGCGTGTTTGTGTGCCTGC	
		AGAACGGTGGCCAATTATCTTATTGGCTCTTTGGCGGTCACCGACCTCATGGTGTCGGTGT		34	AGCCCAAGCCCGGGAGCGGGCCGCAGATCGGAGGCACCATCAAGCAGCCGCCCAGCAACC	75
		AACAACACCATCACCACCGGCTCCCTTTGAGACCGGCGGCCAACACTACTTGGTATCC	CYBA	35	GGAATTACTATGTTCGGGCCGTCCTGCATCTCCGGTGCCCGGCTTCCTG	
		TGGTTCTCTATGGGGGCCATATTCCGAGCTGCGCGTTCCGCATCCGCAAGACGGTCAAAA		36	TTCCTGCTGGCCACCATCCTTGGGACCGCCTGCCTGGCCATTGCGAGCGGGCATCTACCTA	
		ACATGCCCACCCTGTTGGGCGCCATAATCAATTGCGGCTACTCCAACTCTCTGCTTA			GCTTCACCCAGTGGTACTTGGTGCCTACTCCATTGTGGCGGGGCGTGTTTGTGTGCCTGC	
		ACACTGGGCCAGGTAACCTGCGACCTGTTCATCGCCCTCGACGTGCTGTGCTGCACCTCA			AAGGAAGCAGGATGGCAGCCGGAACAGCAGTTGGAGCCTGGTGGCCACTGGTGTGCGTGGTGGTCCTCAGTCTGT	
RAGE		GTTTCCCTGGAATCCTATAAGCACGAGCCTGAACGGTTAGAGAATCGCATCTATGCCTC	RAGE	37	AGTAGTAGGTGCTCAAAACATCACAGCCCGGATTGGCGAGCCACTGGTGTGCGAAGTGTAA	76
		TGGAATCCTATAAGCACGAGCCTGAACGGTTAGAGAATCGCATCTATGCTGTCTTCCC			AGACACCCTGAGACAGGGGCTCTTCACACTGCAGTCGCAGTCGGAGCTAATGGTGACCCAGCCCGG	
		TGCTGAGAAAAACATACAATAACCTAGATATCACGGTGACCCAGGCCCTTCAGCACCGTTC			ACAGCCAGCGTCAGATGCTAATACTGGAGACCGTGACAGCAACCAATAATGCTGCTTCTGCA	77
		GTGCACGGTATGTTCAGATCACAGTGCCTTATGTCCGAATACACAGCAATATGTCACCGCCG			GCACATCCTTGGACTAAGGATTCGTCAGGAACAGCATTTCACCTCAGGAGTGCGGGTC	
		ATGTGGCATAAGGTGAGTGCACGGTATGTTCAGATCACAGTGCCTTATGTCCGAATACAG		38	CAAGTAATCACCTCTGGCTACCATCCTTATTCCTCCTCATGCTCGGATTCAAGCAGCTG	
		GGCATAAGGTGAGTGCACGGTATGTTCAGATCACAGTGCCTTATGTTGTCCGAATACAGCAAT	GSK3B		TGGAAGTGCAAAGCAGCTGGTCCGAGGAGAACCCAATGTTTCGTATATCGTTTCTCGGTA	78
		CTGAAGCGCCGTGACAGGGCTACATGTTTGGTAAAGGGATCTATTTCGTGACATGGTCT			CAAGTAATCACCTCTGGCTACCATCCTTATTCCTCCTCATGCTCGGATTCAAGCAGCTG	
		GTGAAGGCGAATGCCAGCGTTACAGAGCCCCTTTAAGCAGTTCTCATAAACCGAAGGATTGTGT		39	CCCAAATGTCAAACTACCAAATGGGCGGACACCGACCTCACTCTTCAACTTCACCACTCA	
PARP1		TTAAGCAGCTTCATAACCGAAGATTGCTGTGGCACGGGTCCAGGACCAACAACTTTGCTG			AAGAAGTGGATTGTATTGTGAGATCCTGTGTGATTCCTGGTGCCCAGTATCCTGGATTCCTC	79
		CTCAGGGCAGCAGCGACTCTCAGATCCTGATCTCTCAAATCGCTTTACACCCTGATCC		40	GTGGGAACCATCCAGTACTTGTGGACACTACACGTTTCAACCTCTCTACTAGCACCATCA	
		TTAAGCAGCTTCATAACCGAAGATTGCTGTGGCACGGGTCCAGGACCACCAACTTTGCTG	NSF		TAAAATGCAAGGACAAAGCAATTAGAAGCAATTGGAGTTGCCTTACCTCCACACGCCACCCA	
		GGGAGGGTCTGATGATAGCAGCAAGGATCCCATCGATGTCAACTATGAGAAGTCAAAAC			GCAGGAATTTAATTAGGTCATATTTGGTGATGAGACTTATGGAGTGTGCCTCTCTCCC	
ME1		CAGTCCTTTTGATCCAGTCACTCTTCCAAATGGACAGACCCTATATCTGGCCAAGGCAA			TGTTGGTTGGACTTCCCCTTAAGTATAACTAATTTGCTCTGTGGTAAGAGATATGCTCA	80
		GGCATCCCTGGGTAAATTGGCTCTATATACAGCTTGCGGAGGGATGAATCCTCAAGAA		41	AAGCAATTAGAAAGCCATCCTCTATATACAGCTGCTTACCTCACGCACGCCCCATGAGGCTTGTGGCC	
		TAAAGATCCACTCTACATTGGACTACAGGAGAAGAGTTCTGAATATGATGA	IL4R		CTGTCGACCTGGAGCAACCCGTATCCCCCTGACAATTACCTGTATAATCATCTCACCTAT	
		TAAAGATCCACTCTACATTGGACTACGGCAGGAGGAAGAGTTCTGAATATGATGA		42	GTATAATCATCTCACCTATGCAGTCAACATTTGGAGTGAAAAACGACCCGGCAGATTTCAG	81
		GCCAATGTGAATGCCATTTCGTCTCCGAACAAGTAATCGAAACCAGTATTGCACATTCAAT			GTGTGCCACCTGCTCATGGATGACGTGGTCAGTGCGGATAACTATACACTGGACCTGTGG	
		CAGTCCTTTTGATCCAGTCACTCTTCCAAATGGACAGACCCTATATCTGGCCAAGGCAA			CCTCTGTCCACTGAACTAGAAGCCGAGCCTAGAAAACTAACAACAGCCATCAAGGGAATGA	
GCGR		GGCACGCACCCCATGTGCATGGAAAATGTCTCCAACATAAAGAGCTCAAGGTGTCACCGTG		43	CACAGCCATCAAGGGAATGAACGACTTGGGCGGCCTTGGGAAATGATGAGAAATTGAACTTCA	82
		TTCGACCTTCTCCTGCATGCTCCTCCTCCAGGGCTGCTGGGCTGTCGTCTCCTACTGCTTCTC		44	GGGAGGGGTGGTCATTGCCTAGAGGTGCTCATTCATTTAACAGAGCTTCCTTAGGTTGATG	
		GATGCACCACAGACTACAAGTTCCGGCTGCTGGCCCAAGTCCACGCTGACCCTCATCCCTCT		45	ATCCTGAACAGATTTTCATCTGACTGTAACACCATCGACCAGCACATCCCATCCCCTG	
		CTGCGGGTTCCCCGTCTTCCTGGCCATCCTGATCAACTTCTTCATCTGTCCGCCATCGTT	ABCC8	46	TGCGCTACGACAGCTCCCTGGAAGCCGGTGCTCAATGCGTCAAGCACGTCAATGCCCTCCCTG	83
		CAGATGGGATGGCGAGGAGATTGAGGTCAGCTTCCAGAAGAGGAGGAGGAGGCACGCAGCTTC		47	TCTCTTGCCTTCTTCCCGCATGGTGGACACGTTCGAAGGGCACATCATTGATGGCATT	

46

Fig. 4 Serotonin receptor expression after treatment with 500 μM CML at indicated time points. Results are displayed as mean fold-change in comparison to control ($n = 3$, tr = 2–3). Significance was tested with two-way ANOVA followed by the Holm-Sidak post hoc test and marked with *($p < 0.05$), **($p < 0.01$) or ***($p < 0.001$).
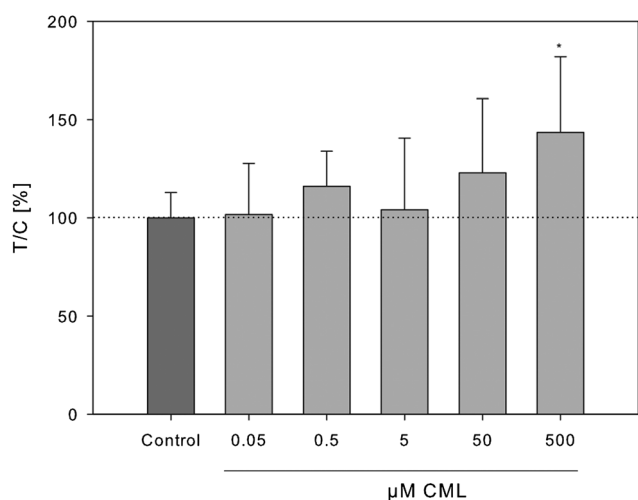

Fig. 5 Serotonin release after stimulation with different concentrations of CML (0.05–500 μM). Results are displayed as T/C (%) in comparison to control cells treated with buffer only ($n = 3$, tr = 2). Significant differences between treatment and control were tested with Student's t-test and marked with *($p < 0.05$), **($p < 0.01$) or ***($p < 0.001$).

Fig. 6 Intracellular Ca^{2+}-mobilization after stimulation with different concentrations of CML (0.05–500 μM). Results are displayed as area under the curve (%) in comparison to control cells treated with buffer ($n = 3$, tr = 2–6). Significant differences were tested with one-way ANOVA *vs.* control followed by the Holm-Sidak post hoc test and marked with *($p < 0.05$), **($p < 0.01$) or ***($p < 0.001$).
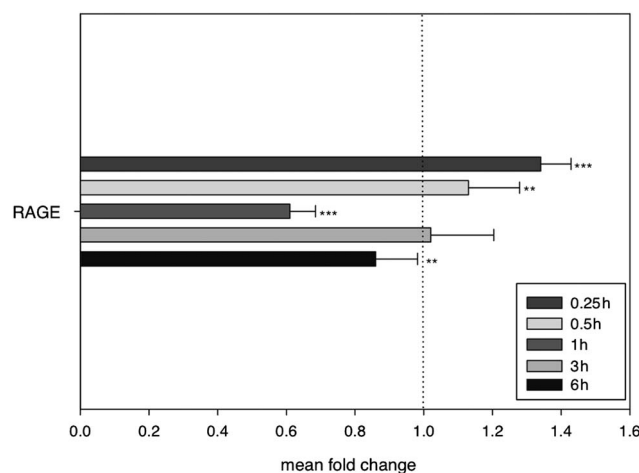
Fig. 7 RAGE expression after treatment with 500 μM CML at indicated time points. Results are displayed as mean fold-change in comparison to control ($n = 3$–4, tr = 2–4). Significance was tested with two-way ANOVA followed by the Holm-Sidak post hoc test and marked with *($p < 0.05$), **($p < 0.01$) or ***($p < 0.001$).

analysis using the database for annotation, visualization and integrated discovery (DAVID). Functional annotation clustering identified 152 annotation clusters.

The cluster "neurotransmitters and serotonin receptors" (Table 1), which showed the lowest p-value annotation, pointed to an effect of CML on the neural serotonin system. To validate this effect, the gene expression of HTR1A, HTR1B, HTR2A was analysed after treatment of SH-SY5Y cells with 500 μM of CML for 0.25, 0.5, 1, 3 and 6 h using the more sensitive qRT-PCR method.[32,33] The qRT-PCR results confirm a regulation for those serotonin receptors, which have been shown to be involved in the regulation of hunger and satiety.[16–20] The serotonin receptor 5-HT$_{2C}$, which is known for its satiating effect and target for several appetite-reducing drugs, could not be detected in SH-SY5Y cells. However, probes for HTR1A, HTR1B, HTR2A showed an up-regulation after

3 h treatment with 500 μM CML on the DNA microarray. qRT-PCR analysis of those genes confirmed this up-regulation after 3 h. Statistical analysis also revealed time-dependent effects of the treatment. Expression of HTR1A, HTR1B and HTR2A was significantly up-regulated after incubation for 0.25 and 3 h.

Furthermore, CML stimulated serotonin release from SH-SY5Y cells at a concentration of 500 μM. This reveals an effect of CML on the serotonin system not only at the genetic level, but at the functional level as well. Serotonin release is mediated by an increase in intracellular calcium levels.[34] The calcium ion is a common second messenger and its involvement in neurotransmitter release has been demonstrated in various studies.[34,35] To investigate the participation of calcium ions in CML-triggered

47

Table 3 Expression of RAGE, HTR2A, HTR1A and HTR1B after 15 min incubation with CML, neomycin or combination of both. Results are displayed as mean fold-change in comparison to control ($n = 1$–4, tr $= 2$–4). Significant differences were tested by one-way ANOVA *vs.* control followed by the Holm-Sidak post hoc test and marked with *($p < 0.05$), **($p < 0.01$) or ***($p < 0.001$)

Treatment	RAGE	HTR2A	HTR1A	HTR1B
Control	1.00 ± 0.03	1.00 ± 0.07	1.00 ± 0.09	1.00 ± 0.09
Neomycin (100 μM)	1.00 ± 0.01	1.28 ± 0.18	1.56 ± 0.10	1.20 ± 0.06
CML (500 μM)	1.34 ± 0.09***	3.45 ± 2.51***	2.75 ± 1.17***	3.08 ± 1.91***
Neomycin CML co-incubation	0.88 ± 0.07**	1.16 ± 0.09	1.41 ± 0.10	1.17 ± 0.15

serotonin release, intracellular Ca^{2+} mobilization was determined after stimulation with CML. Exposure of SH-SY5Y cells to CML in concentrations ranging from 0.05 to 500 μM CML stimulated intracellular Ca^{2+} mobilization, indicating an involvement of calcium ions in the pathway of CML-evoked serotonin release.

CML is a known target of the RAGE receptor. Our qRT-PCR results show a time-dependent effect of 500 μM CML on the mRNA levels of the RAGE receptor. After incubation with CML for 0.25 and 0.5 h, RAGE expression was significantly up-regulated. Similar to HTR1A, HTR1B and HTR2A, RAGE expression was down-regulated after 1 h. The up- and down-regulation of the gene expression of serotonin receptors and RAGE might be explained by a counter-regulation. This is a phenomenon that has previously been described in the context of time-dependent gene expression experiments.[36,37]

Since results reported by Collison *et al.*[38] indicated a connection between activation of the RAGE receptor and Ca^{2+} mobilization, we hypothesized that an activation of the RAGE receptor by CML is mediated by intracellular calcium mobilization as well. In order to investigate the dependency of RAGE activation and calcium signalling, RAGE receptor expression after 15 min incubation with 500 μM CML was analyzed by means of qRT-PCR with or without a 15 min pre-incubation with 100 μM neomycin. Pre-incubation with 100 μM neomycin, which is known to inhibit Ca^{2+} release from IP3 and ryanodine-sensitive intracellular calcium stores,[39,40] blocked the up-regulation in comparison to an incubation with CML only. This indicates that RAGE receptor activation depends on intracellular calcium levels, confirming our hypothesis. In addition to blocking RAGE expression, incubation with neomycin blocked the expression of serotonin receptors 5-HT$_{1A}$, 5-HT$_{2A}$ and 5-HT$_{1B}$, thus pointing to involvement of intracellular calcium not only in CML induced changes in RAGE expression, but also in serotonin receptor expression.

In conclusion, the present study demonstrates for the first time, that CML, a Maillard reaction product, affects the serotonin system at a genetic and functional level. Furthermore, this study shows a calcium dependent regulation of the RAGE receptor mRNA levels by CML, pointing to a possible link between the RAGE receptor and the calcium-triggered serotonin release.

Materials and methods

Materials

The human neuroblastoma cell line SH-SY5Y was obtained from the American Type Culture Collection (Manassas, VA, USA). Unless indicated otherwise, reagents and chemicals were purchased from Sigma-Aldrich, Austria. Protein-free, chemically synthesized CML was supplied by Iris Biotech, Marktredwitz, Germany.

Cell culture

SH-SY5Y cells were cultured in a 1 : 1 mixture of Ham's F-12 Nutrient Mixture and Minimum Essential Medium Eagle. Medium was supplemented with 10% FBS (Life Technology Corporation, Carlsbad, CA, USA), 2% L-glutamine, 1% pyruvate and 1% penicillin/streptomycin. Incubations were carried out using serum-free media. Cells were maintained at 37 °C and 5% CO_2 in a humidified incubator.

Custom-made DNA microarrays

Maskless microarray synthesis was employed to synthesize customized DNA microarrays on glass slides.[41] A detailed procedure of the microarray synthesis has been published by Agbavwe *et al.*[42] The customized microarray probes were designed using OligoWiz v2.2. Four to fifteen 60mer oligonucleotide probes of 145 genes relating to satiety were included.

For gene expression experiments, 2.5×10^6 SH-SY5Y cells were seeded into 35 mm dishes 24 h prior to the experiment. After incubation with 50 μM or 500 μM CML for 3 h RNA was isolated using the RNeasy Mini Kit (Qiagen, Hilden, Germany). The RNA quality was analyzed photometrically using a NanoQuant plate on an infinite plate reader (Tecan, Menningen, Switzerland) in addition to agarose gel electrophoresis. The corresponding cDNA was synthesized using Cy3-labeled random nonamer primers (Tebu Bio, Offenbach, Germany) in the reverse transcription as described by Ouellet *et al.*[43] The microarrays were hybridized with the labeled cDNA at 42 °C for 24 h prior to scanning with an Axon GenePix 4100A microarray scanner (Molecular Devices, Sunnyvale, CA, USA). The scanned images were analyzed using NimbleScan 2.1 (NimbleGen, Madison, USA). For normalization purposes, robust multichip analysis (RMA) was employed. Additionally, differences in labeling efficiency and input cDNA concentration were accounted for by normalizing intensity data to the intensities of five non-regulated genes (HPRT, MRPL, NSE, TBP and UBC). Fold-changes (T/C) were calculated using Microsoft Excel 2011. Probes with a fold-change below 0.8 or above 1.2 were selected and subjected to a pathway analysis using the database for annotation, visualization and integrated discovery (DAVID; http://david.abcc.ncifcrf.gov). The created annotation clusters were sorted by enrichment score and clusters reaching a score

Table 4   Sequence of the primers used in qRT-PCR experiments

Target	Forward primer	Reverse primer	Product length (bp)
HTR1A	TCATCGTGGCTCTTGTTCTG	CGGGGGTTAAGCAGAGAGTTG	108
HTR1B	CTGGTGTGGGTCTTCTCCAT	AGAGGATGTGGTCGGTGTTC	109
HTR2A	GTTGCTTACTCGCCGATGATA	TGCCAAGATCACTTACACACAAA	144
TBP	CCCGAAACGCCGAATATAATCC	GACTGTTCTTCACTCTTGGCTC	130
RAGE	ACTACCGAGTCCGTGTCTACC	GGAACACCAGCCGTGAGTT	79

≥1.3 were considered as potential candidates for further investigation.[27] Additionally, a heat map was created using R and RColorBrewer.

Quantitative real-time-PCR

A total of 2.5×10^6 SH-SY5Y cells were incubated with 500 μM CML for 0.25, 0.5, 1, 3 and 6 h prior to mRNA isolation using the MasterPure Complete DNA and RNA isolation kit (Epicentre, Madison, WI, USA). For incubations with the calcium blocker, cells were pre-incubated with 100 μM neomycin for 15 minutes prior to co-incubation with 500 μM CML for another 15 minutes. Isolated mRNA was reverse transcribed with the high capacity cDNA Kit (Life Technology, Carlsbad, CA, USA). All qRT-PCR experiments were carried out in triplicate using SYBR Green MasterMix (Life Technology, Carlsbad, CA, USA) on a StepOnePlus device. Serotonin receptor primers used in the experiment were designed using Primer3Plus software and synthesized by VBC Biotech, Vienna, Austria (Table 4). The primer pair used for the detection of RAGE was taken from a primer database (PrimerBank, http://pga.mgh.harvard.edu/cgi-bin/primerbank) and synthesized by Sigma-Aldrich, Austria. Data analysis was carried out using LinRegPCR v.2012.2.[44,45] The calculated mRNA quantity of target genes was normalized to the reference gene TBP.[46,47]

Serotonin release

SH-SY5Y cells at a density of 1.25×10^6 were seeded in 35 mm dishes 48 h prior to the experiment. Cells were then washed with PBS and stimulated with CML (0.05–500 μM) or Krebs Ringer HEPES buffer (pH 6.2) for five minutes. The serotonin concentration in the supernatant was determined using a serotonin-sensitive ELISA kit (DLD Diagnostika, Hamburg, Germany) following the manufacturer's protocol. The cells were lysed with 0.1% sodium lauryl sarcosinate in PBS and the DNA concentration was measured using a NanoQuant plate on an infinite plate reader (Tecan, Menningen, Switzerland). The serotonin release values were normalized to the respective DNA concentration.

Intracellular Ca²⁺ mobilization

As described previously, intracellular Ca^{2+} mobilization was determined using the Fluo-4 Direct Calcium Assay Kit (Invitrogen, Life Technology, Carlsbad, USA).[48] SH-SY5Y cells were seeded into a 96-well plate at a density of 75 000 cells per well and allowed to settle for 48 h. Cells were incubated with fluo-4 at 37 °C for 30 min followed by incubation at room temperature for further 30 min prior to stimulation with Hank's balanced salt solution (HBSS) or CML (0.05–500 μM). Immediately after

addition of the corresponding sample, the dye was excited at 490 nm and the emission measured at 520 nm every two seconds for 1.5 min using a Tecan infinite reader (Tecan, Menningen, Switzerland). The areas under the curve were calculated using SigmaPlot 11.0.

Statistical analysis

All experiments were done in multiple replicates as indicated in the legends of the corresponding figures. Data are presented as fold-change $(T/C) \pm$ standard deviation (SD) unless stated otherwise. Outliers were determined using the Nalimov outlier test. Statistical significance between treatment and non-treated control was assessed by one-way ANOVA. Two-way ANOVA was used for assessing significance of dose- and time-dependent effects. Statistical analysis was carried out using SigmaPlot 11.0.

Conflict of interest

The authors declare no conflict of interest.

Abbreviations

5HT	serotonin
AGE	advanced glycation endproduct
AUC	area under curve
CML	N^ε-carboxymethyllysine
CNS	central nervous system
HTR	gene name of the serotonin receptor
qRT-PCR	quantitative Real-Time PCR
NPY	neuropeptide Y
RAGE	receptor for advanced glycation end products
SD	standard deviation.

Acknowledgements

References

1 F. Jousse, T. Jongen, W. Agterof, S. Russell and P. Braat, *J. Food Sci.*, 2002, **67**, 2534–2542.

2 M. A. van Boekel, *Biotechnol. Adv.*, 2006, **24**, 230–233.

3 I. Birlouez-Aragon, G. Saavedra, F. J. Tessier, A. Galinier, L. Ait-Ameur, F. Lacoste, C. N. Niamba, N. Alt, V. Somoza and J. M. Lecerf, *Am. J. Clin. Nutr.*, 2010, **91**, 1220–1226.

4 H. Vlassara, W. Cai, J. Crandall, T. Goldberg, R. Oberstein, V. Dardaine, M. Peppa and E. J. Rayfield, *Proc. Natl. Acad. Sci. U. S. A.*, 2002, **99**, 15596–15601.

5 S. Ruhs, N. Nass, B. Bartling, H. J. Bromme, B. Leuner, V. Somoza, U. Friess, R. E. Silber and A. Simm, *Exp. Gerontol.*, 2010, **45**, 752–762.

6 K. Sebekova, G. Saavedra, C. Zumpe, V. Somoza, K. Klenovicsova and I. Birlouez-Aragon, *Ann. N. Y. Acad. Sci.*, 2008, **1126**, 177–180.

7 V. Somoza, E. Wenzel, C. Weiss, I. Clawin-Radecker, N. Grubel and H. F. Erbersdobler, *Mol. Nutr. Food Res.*, 2006, **50**, 833–841.

8 J. Uribarri, W. J. Cai, O. Sandu, M. Peppa, T. Goldberg and H. Vlassara, *Ann. N. Y. Acad. Sci.*, 2005, **1043**, 461–466.

9 E. Wenzel, S. Tasto, H. F. Erbersdobler and V. Faist, *Ann. Nutr. Metab.*, 2002, **46**, 9–16.

10 R. M. Ruijschop, A. E. Boelrijk, J. A. de Ru, C. de Graaf and M. S. Westerterp-Plantenga, *Br. J. Nutr.*, 2008, **99**, 1140–1148.

11 K. Sebekova, K. S. Klenovics, P. Boor, P. Celec, M. Behuliak, P. Schieberle, A. Heidland, M. Palkovits and V. Somoza, *Physiol. Behav.*, 2012, **105**, 693–701.

12 D. P. Begg and S. C. Woods, *Handbook of Experimental Pharmacology: Appetite Control*, ed. H.-G. Joost, Springer, Berlin Heidelberg, 2012, vol. 209, pp. 111–129.

13 S. C. Woods and D. A. D'Alessio, *J. Clin. Endocrinol. Metab.*, 2008, **93**, S37–S50.

14 M. M. Meguid, S. O. Fetissov, M. Varma, T. Sato, L. Zhang, A. Laviano and F. Rossi-Fanelli, *Nutrition*, 2000, **16**, 843–857.

15 C. Erlanson-Albertsson, *Basic Clin. Pharmacol. Toxicol.*, 2005, **97**, 61–73.

16 C. T. Dourish, P. H. Hutson and G. Curzon, *Psychopharmacology*, 1985, **86**, 197–204.

17 L. F. Mohammad-Zadeh, L. Moses and S. M. Gwaltney-Brant, *J. Vet. Pharmacol. Ther.*, 2008, **31**, 187–199.

18 M. Feijo Fde, M. C. Bertoluci and C. Reis, *Rev. Assoc. Med. Bras.*, 2011, **57**, 74–77.

19 R. Rosmond, C. Bouchard and P. Bjorntorp, *Obes. Res.*, 2002, **10**, 585–589.

20 C. Jonnakuty and C. Gragnoli, *J. Cell. Physiol.*, 2008, **217**, 301–306.

21 M. U. Ahmed, S. R. Thorpe and J. W. Baynes, *J. Biol. Chem.*, 1986, **261**, 4889–4894.

22 T. Kislinger, C. Fu, B. Huber, W. Qu, A. Taguchi, S. Du Yan, M. Hofmann, S. F. Yan, M. Pischetsrieder, D. Stern and A. M. Schmidt, *J. Biol. Chem.*, 1999, **274**, 31740–31749.

23 J. Uribarri, S. Woodruff, S. Goodman, W. Cai, X. Chen, R. Pyzik, A. Yong, G. E. Striker and H. Vlassara, *J. Am. Diet. Assoc.*, 2010, **110**, 911–916 e912.

24 J. S. Kruk, M. S. Vasefi, H. Liu, J. J. Heikkila and M. A. Beazely, *Cell. Signalling*, 2013, **25**, 133–143.

25 B. Kuhla, C. Loske, S. Garcia De Arriba, R. Schinzel, J. Huber and G. Munch, *J. Neural Transm.*, 2004, **111**, 427–439.

26 A. K. Langer, H. F. Poon, G. Munch, B. C. Lynn, T. Arendt and D. A. Butterfield, *Neurotoxic. Res.*, 2006, **9**, 255–268.

27 W. Huang da, B. T. Sherman and R. A. Lempicki, *Nat. Protoc.*, 2009, **4**, 44–57.

28 B. O. Boehm, S. Schilling, S. Rosinger, G. E. Lang, G. K. Lang, R. Kientsch-Engel and P. Stahl, *Diabetologia*, 2004, **47**, 1376–1379.

29 T. Teerlink, R. Barto, H. J. Ten Brink and C. G. Schalkwijk, *Clin. Chem.*, 2004, **50**, 1222–1228.

30 M. L. Lieuw-A-Fa, V. W. van Hinsbergh, T. Teerlink, R. Barto, J. Twisk, C. D. Stehouwer and C. G. Schalkwijk, *Nephrol., Dial., Transplant.*, 2004, **19**, 631–636.

31 T. Kimura, J. Takamatsu, K. Ikeda, A. Kondo, T. Miyakawa and S. Horiuchi, *Neurosci. Lett.*, 1996, **208**, 53–56.

32 E. D. Bruder, J. J. Lee, E. P. Widmaier and H. Raff, *Physiol. Genomics*, 2007, **29**, 193–200.

33 M. S. Rajeevan, S. D. Vernon, N. Taysavang and E. R. Unger, *J. Mol. Diagn.*, 2001, **3**, 26–31.

34 G. J. Augustine, *Curr. Opin. Neurobiol.*, 2001, **11**, 320–326.

35 T. I. Nishiki and G. J. Augustine, *J. Comp. Neurol.*, 2001, **436**, 1–3.

36 M. Rubach, R. Lang, E. Seebach, M. M. Somoza, T. Hofmann and V. Somoza, *Mol. Nutr. Food Res.*, 2012, **56**, 325–335.

37 A. C. Zambon, E. L. McDearmon, N. Salomonis, K. M. Vranizan, K. L. Johansen, D. Adey, J. S. Takahashi, M. Schambelan and B. R. Conklin, *Genome Biol.*, 2003, **4**, R61.

38 K. S. Collison, R. S. Parhar, S. S. Saleh, B. F. Meyer, A. A. Kwaasi, M. M. Hammami, A. M. Schmidt, D. M. Stern and F. A. Al-Mohanna, *J. Leukocyte Biol.*, 2002, **71**, 433–444.

39 S. Y. Eun, S. J. Jung, Y. K. Park, J. Kwak, S. J. Kim and J. Kim, *Biochem. Biophys. Res. Commun.*, 2001, **285**, 1114–1120.

40 D. R. Laver, T. Hamada, J. D. Fessenden and N. Ikemoto, *J. Membr. Biol.*, 2007, **220**, 11–20.

41 S. Singh-Gasson, R. D. Green, Y. J. Yue, C. Nelson, F. Blattner, M. R. Sussman and F. Cerrina, *Nat. Biotechnol.*, 1999, **17**, 974–978.

42 C. Agbavwe, C. Kim, D. Hong, K. Heinrich, T. Wang and M. M. Somoza, *J. Nanobiotechnol.*, 2011, **9**, 57.

43 M. Ouellet, P. D. Adams, J. D. Keasling and A. Mukhopadhyay, *BMC Biotechnol.*, 2009, **9**, 97.

44 J. M. Ruijter, C. Ramakers, W. M. H. Hoogaars, Y. Karlen, O. Bakker, M. J. B. van den Hoff and A. F. M. Moorman, *Nucleic Acids Res.*, 2009, **37**, 45.

45 J. M. Tuomi, F. Voorbraak, D. L. Jones and J. M. Ruijter, *Methods*, 2010, **50**, 313–322.

46 V. Valente, S. A. Teixeira, L. Neder, O. K. Okamoto, S. M. Oba-Shinjo, S. K. N. Marie, C. A. Scrideli, M. L. Paco-Larson and C. G. Carlotti, *BMC Mol. Biol.*, 2009, **10**, 17.

47 S. Wierschke, S. Gigout, P. Horn, T. N. Lehmann, C. Dehnicke, A. U. Brauer and R. A. Deisz, *Biochem. Biophys. Res. Commun.*, 2010, **403**, 385–390.

48 J. Walker, B. Rohm, R. Lang, M. W. Pariza, T. Hofmann and V. Somoza, *Food Chem. Toxicol.*, 2012, **50**, 390–398.

50

2.3 "Simultaneous light-directed synthesis of mirror-image microarrays in a photochemical reaction cell with flare suppression"

Sack, M.[a], Kretschy, N.[a], **Rohm, B**.[b,c], Somoza, V.[b,c], Somoza, M. M.[a]

[a] Institute of Inorganic Chemistry, University of Vienna, Währinger Strasse 42, A-1090 Vienna, Austria

[b] Department of Nutritional and Physiological Chemistry, University of Vienna, Althanstraße 14 (UZA II), A-1090 Vienna, Austria

[c] Christian Doppler Laboratory for Bioactive Aroma Compounds, University of Vienna, Althanstraße 14, A-1090 Vienna, Austria

Simultaneous Light-Directed Synthesis of Mirror-Image Microarrays in a Photochemical Reaction Cell with Flare Suppression

Matej Sack,[†] Nicole Kretschy,[†] Barbara Rohm,[‡,§] Veronika Somoza,[‡,§] and Mark M. Somoza*,[†]

[†]Institute of Inorganic Chemistry, University of Vienna, Währinger Strasse 42, A-1090 Vienna, Austria
[‡]Department of Nutritional and Physiological Chemistry, University of Vienna, Althanstraße 14 (UZA II), A-1090 Vienna, Austria
[§]Christian Doppler Laboratory for Bioactive Aroma Compounds, University of Vienna, Althanstraße 14, A-1090 Vienna, Austria

ABSTRACT: The use of photolabile protecting groups is a versatile and well-established means of synthesizing high complexity microarrays of biopolymers, such as nucleic acids and peptides, for high-throughput analysis. The synthesis takes place in a photochemical reaction cell which positions the microarray substrate at the focus of the optical system delivering the light and which can be connected to a fluidics system which delivers appropriate reagents to the surface in synchrony with the light exposure. Here we describe a novel photochemical reaction cell which allows for the simultaneous synthesis of microarrays on two substrates. The reaction cell positions both substrates within the limited depth-of-focus of the optical system while maintaining the necessary reagent flow conditions. The resulting microarrays are mirror images of each other but otherwise essentially identical. The new reaction cell doubles the throughput of microarray synthesis without increasing the consumption of reagents. In addition, a secondary flow chamber behind the reaction cell can be filled with an absorbent and index-matching fluid to eliminate reflections from light exiting the reaction cell assembly, greatly reducing unintended light exposure that reduces the sequence fidelity of the microarray probes.
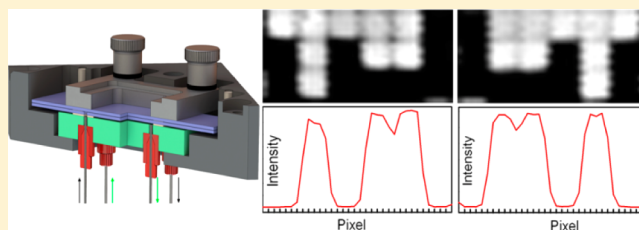
Microarrays are versatile and widely used analytical tools with the capacity to simultaneously detect several hundred thousand to millions of different biomolecules simultaneously. Microarrays can be made by presynthesizing the probe molecule and spotting it on a surface using appropriate tethering chemistry, but modern microarrays are made with *in situ* methods in which the biomolecules are synthesized directly on the substrate from their monomer components, which allows for high probe densities, high uniformity, and high reproducibility.

Light-directed *in situ* synthesis of microarrays derives from the photolithographic technology used in the semiconductor industry in combination with combinatorial chemistry based on the selective removal of photolabile protecting groups. The technology was first commercialized by Affymetrix, which used the photolabile MeNPOC group on the 5′ end of DNA phosphoramidites to synthesize high-density DNA microarrays for genomics applications.[1] The synthesis technology was improved with the use of optical systems incorporating digital micromirror devices (DMD) to replace physical masks in the patterning of light on the microarray substrate, as well as by the use of the NPPOC photolabile group, which has significantly improved photodeprotection yield.[2−7] This maskless array synthesis (MAS) technology, originally used for DNA microarray synthesis has also been extended for the synthesis of RNA, aptamer,[8] and peptide microarrays.[9−13]

In situ microarray synthesis is robust and efficient in comparison with spotted synthesis; however, the total synthesis time and the consumption of solvents and reagents are still a significant economic constraint. In addition, the light-directed chemistry is sensitive to stray light in the system, which leads to unintended photodeprotection which degrades the sequence fidelity of the microarray probes.[7,14] Here we present an improved microfluidic photochemical reaction cell for use in light-directed synthesis that addresses both of these concerns. This reaction cell places two microarray substrates within the depth-of-focus plane of the optical system, so that two microarrays are synthesized simultaneously using the same reagents. The microarrays thus synthesized are mirror images of each other but otherwise essentially identical. The microarrays can be used independently but may have additional utility as matched pairs for experiments that would benefit from very close data comparisons; the quality of *in situ* synthesized microarrays, however, is very high and in most common applications, variations in quality between microarrays synthesized at different times are not experimentally relevant. In addition, the reaction cell assembly has a secondary chamber that can be filled with a light-absorbing and index-matching fluid to eliminate reflections that are a primary source of sequence error in light-directed synthesis.

MATERIALS AND METHODS

Photochemical Reaction Cell Concept and Assembly.
The reaction cell needs to position the two microarray substrates at the focal plane of the optical system. There is some tolerance to this positioning: the depth of focus of the imaging optics. The imaging optics are a 1:1 Offner relay system,[15,16] an off-axis conjugate system composed of two spherical concentric mirrors, primary and secondary. The system was designed with a numerical aperture (NA) of 0.08 to result in a resolving power of 2.7 μm. This resolving power is sufficient since it is significantly smaller than the size of individual mirrors of the digital micromirror device (DMD), 13 μm × 13 μm, separated by a 0.7 μm gap and is similar or better than those of most available microarray scanners. A low value of numerical aperture lowers the cost of the primary mirror but, more importantly, reduces the amount of scattered light originating from dust and imperfections in the optical system, which is proportional to NA^2. Unintended photodeprotection, from scattering, diffraction, and local flare, is the largest source of sequence error in light-directed microarray synthesis.[7] The depth of focus is intrinsically limited by diffraction to $< \sim \lambda/$NA^2, $\sim$60 μm, but in practice, the positioning of the microarray substrates in the focal plane is somewhat less restricted due to limited resolution of microarray scanners. Therefore, the primary optical constraint in the simultaneous light-directed synthesis of microarray pairs is that the two substrates must be within $\sim$60−100 μm of each other, depending on the scanner resolution.

A secondary constraint is imposed by reagent delivery. A larger reaction cell volume requires larger flow rates of solvents and reagents, the consumption of which scales with cell volume. Since our original reaction cell (for synthesizing microarrays on a single surface) had a depth of 70 μm and worked well with a standard oligonucleotide synthesizer (Expedite 8909), we took this value as a starting point. Thus, the reaction cell should consist of two standard microarray substrates (75 mm × 25 mm × 1 mm) separated by a uniform gap of $\sim$70 μm. The microarray substrates form the entrance and exit windows for the ultraviolet light used in the synthesis. Reagents need to be introduced into this gap and to uniformly flow across the surface before exiting. We used these criteria to design and built the reaction cell shown in Figure 1. The reaction cell assembly consists of a black anodized aluminum support block, a quartz block, the two microarray substrates, two gaskets, and a clamping frame and screws to hold the parts together. Reagent delivery tubes attach to the underside of the quartz block and connect to the oligonucleotide synthesizer.

The support block forms the rigid structure for the assembly of the reaction cell and allows for the reaction cell to be precisely positioned in the focal plane. Three alignment points make contact with ball-tipped, high-precision adjustment screws (Newport AJS127-0.5H) in the optical system. After initial adjustment of the screws, the reaction cell assembly can be quickly and reproducibly positioned. The support blocks hold a quartz block. The quartz block has four 0.8 mm through-holes (two inlets, two outlets) that are countersunk on the back side to accommodate microfluidics ports. The microfluidics ports (IDEX 6-32 Coned NanoPort Assemblies) were turned on a lathe to reduce their diameter to 6.4 mm and attached within each countersunk hole with common cyanoacrylate adhesive. The front and back surfaces of the quartz block were machined to a surface parallelism error of <30 arc sec and
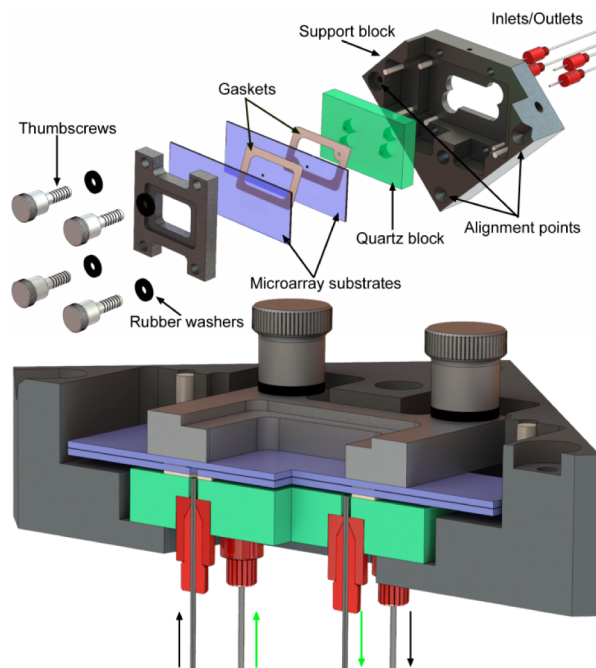
Figure 1. Exploded and section view of reaction cell assembly. The reaction cell is formed by two microarray substrates (75 mm × 25 mm × 1 mm) separated by a 50 μm PTFE gasket. Reagents enter and exit the cell via two 0.9 mm holes through the lower substrate. These holes are coupled to the inlets/outlets via an additional 250 μm thick FFKM gasket separating the lower substrate from the quartz block. The lower gasket forms a chamber that can be independently filled with a light-absorbing and index-matching fluid to reduce reflections from both quartz surfaces and from the back surface of the lower substrate. The thickness of the upper and lower gaskets in the section view have been exaggerated by a factor of 2 for visual clarity.

polished to an optical flatness of $\lambda/4$ (Mindrum Precision). During reaction cell assembly, the lower gasket is placed on the quartz surface. This gasket forms the lower chamber, which can be filled via two of the fluidics ports. Prior to microarray synthesis, this chamber can be filled with an index-matching and light absorbing fluid to prevent light reflections from light exiting the reaction chamber. In the legacy reaction cell design, an antireflective coating on the back surface of the quartz block can reduce the back reflection to a minimum of about 0.25% when new, but this value is typically larger, $\sim$1%, due to the presence of dust, chemical films, and scratches. This 0.25−1% value is sufficient to make this unintended light exposure the largest source of error after diffraction, but unlike diffraction, the error is not confined primarily to the gaps between microarray features.[7] An alternative strategy to reduce back reflections is to fill the lower chamber with an index-matching fluid with dissolved chromophores which absorb the light exiting the reaction chamber and which either convert the light to heat or Stokes shift it beyond the absorption band of the light-labile group.

The lower gasket has two holes that align with two of holes in the quartz block. These holes couple the corresponding fluidics ports to the microarray synthesis cell. This gasket is made from 250 μm thick Chemraz 584 perfluoroelastomer (FFKM), cut to shape with a laser cutter (Spirit GX). The microarray synthesis cell is a chamber consisting of two glass substrates separated by a very thin gasket. This chamber is

accessed via two 1 mm holes, in the lower substrates, which align with the holes in the lower gasket.

The thickness of the upper gasket determines the depth of the photochemical reaction cell and therefore needs to be ~70 μm thick, chemically resistant and sufficiently elastic to form a seal for the duration of the synthesis, up to ~12 h for an array of 70mers. These requirements are quite exceptional and we were unable to find any references to such thin gaskets in the scientific or engineering literature. A perfluoroelastomer, such as Chemraz, would likely work, but the manufacturer is unable to make them thinner than 250 μm. We tried expanded polytetrafluoroethylene (ePTFE), which is commonly used in gasket applications due to its chemical resistance and ability to compress to form a seal, but found seepage through the gasket, presumably due to its porous nature. In the end we found that the common PTFE tape used for plumbing applications works well. This tape is made from unsintered PTFE and is therefore sufficiently compressible to form a seal but not porous. PTFE tape is made in many thicknesses and densities, which allowed for some experimentation. We initially used ~100 μm (120 μm uncompressed) PTFE with a density of ~1.4 g/cm^3 (Gasoila yellow tape), sintered PTFE has a density of about 2 g/cm^3, but found some loss of focus when microarrays were scanned at a resolution of 2.5 μm. Another problem with the 100 μm gap were indications that reagents were flowing in a channel through the center of the reaction cell rather than sweeping the whole surface. This was particularly apparent with the helium drying step, which was not capable of fully removing solvent from the corners of the reaction cell. Switching to thinner and lower density PTFE tape (Gasoila Industrial Strength SD, ~0.7 g/cm^3) gave a thickness of ~50 μm under compression. With this thickness, both of the paired arrays produce sharp scans with resolution limited only by the 2.5 μm pixel size of the scanner and both reagent and helium flow sweep uniformly across the entire surface of both substrates. The 50 μm PTFE gaskets are also formed with a laser cutter. Because of their thinness, they are too delicate to be reusable but can be made quickly and inexpensively.

Microarray Synthesis and Hybridization. Schott Nexterion Glass D slides functionalized with *N*-(3-triethoxysilylprop-yl)-4-hydroxybutryamide (Gelest SIT8189.5). The arrays with holes were drilled with a 0.9 mm diamond bit and washed and rinsed in an ultrasonic bath prior to functionalization. The slides were loaded in a metal staining rack and completely covered with a 500 mL of a solution of 10 g of the silane in 95:5 (v/v) ethanol–water and 1 mL of acetic acid. The slides were gently agitated for 4 h and then rinsed twice for 20 min with gentle agitation in the same solution but without the silane. The slides were then drained and cured overnight in a preheated vacuum oven (120 °C). After cooling to room temperature, the slides were stored in a desiccator cabinet until use. Microarrays were synthesized directly on the slides using a maskless array synthesizer, which consists of an optical imaging system that used a digital micromirror device to deliver patterned ultraviolet light near 365 nm to the synthesis surface. Microarray layout and oligonucleotide sequences are determined by selective removal of the NPPOC photocleavable 5′-OH protecting group. Reagent delivery and light exposures are synchronized and controlled by a computer. The chemistry is similar to that used in conventional solid-phase oligonucleotide synthesis. The primary modification is the use of NPPOC phosphoramidites. Upon absorption of a UV photon, and in the presence of a weak organic base, e.g., 1% (m/v) imidazole in DMSO, the

NPPOC group comes off, leaving a 5′-terminal hydroxyl which is able to react with an activated phosphoramidite in the next cycle. The DNA sequences on the microarrays in this project were synthesized with a light exposure dose of 4.5 J/cm^2, with coupling time of 40 s at monomer concentrations of 30 mM. After synthesis, the microarrays were deprotected in 1:1 (v/v) ethylenediamine in ethanol for 2 h at room temperature, washed twice with distilled water, dried with argon, and stored in a desiccator until hybridization.

Microarrays were hybridized in an adhesive chamber (SecureSeal SA200, Grace Biolabs) with a solution consisting of 0.3 pmol of 5′-Cy5-labeled probe and 200 μg of acetylated BSA in 400 μL of MES buffer (100 mM MES, 1 M NaCl, 20 mM EDTA, 0.01% Tween-20). After 2 h of rotation at 42 °C, the chamber was removed and the microarrays were vigorously washed in a 50 mL centrifuge tube with 30 mL of nonstringent wash buffer (SSPE; 0.9 M NaCl, 0.06 M phosphate, 6 mM EDTA, 0.01% Tween-20) for 2 min and then with stringent wash buffer (100 mM MES, 0.1 M NaCl, 0.01% Tween-20) for 1 min. The microarrays were then dipped for a few seconds in a final wash buffer (0.1× SSC) and then dried with a microarray centrifuge. Arrays were scanned with a Molecular Devices GenePix 4400A at a resolution of 2.5 μm.

Detection and Suppression of Reflected Light. To test the possibility of eliminating reflected light reaching the synthesis area, a small piece of radiochromic film (Far West Technology, FWT-60-20f), with a 2 mm punched hole, was placed in the reaction cell. A 9.5 mm metal disk with a 1 mm pinhole (Edmund Optics, 39730) was aligned over the hole in the film to serve as a physical mask. The entire reaction cell assembly was tilted by ~7° to move the reflection spot away from the mask hole. The lower chamber was filled with either DMSO (control) or UV absorbers dissolved in DMSO or dichloromethane. The UV absorbers (beta carotene, 9-methylanthracene, and riboflavin) were chosen for high extinction coefficients near 365 nm, high Stokes shift, low fluorescence quantum yield, and solubility in DMSO. The synthesis cell was exposed using all mirrors, with an exposure of 60 J/cm^2 (80 mW/cm^2 for 750 s).

■ RESULTS AND DISCUSSION

Synthesis of Mirror-Image Microarrays. Simultaneous synthesis of mirror-image microarrays in this microfluidic photochemical reaction chamber produces high-quality microarrays with little additional cost or effort beyond those of the single microarray synthesis of the legacy method. The primary concern with this method is that both arrays are in focus. To test the image quality of paired microarrays, we initially synthesized simple microarrays of 30mers (GTC ATC ATC ATG AAC CAC CCT GGT CTT TTT), hybridized them with labeled complementary oligonucleotides and scanned them at high resolution. The results of one such experiment is shown in Figure 2. The top row shows pixel-level close-ups from both of the arrays. Each white square corresponds to a microarray feature synthesized with a single DMD mirror. In both close-ups, the features are individually resolved, and the 0.7 μm gap between features are also clearly visible. The middle row shows plots of the scan image intensity along a horizontal line through the center of each of the pixel-level close-ups. The intensity drops by ~1000-fold between the center of hybridized pixels and unhybridized pixels, which is a typical signal/background for this type of microarray. The gap between immediately adjacent hybridized pixels is visible as a drop in intensity of
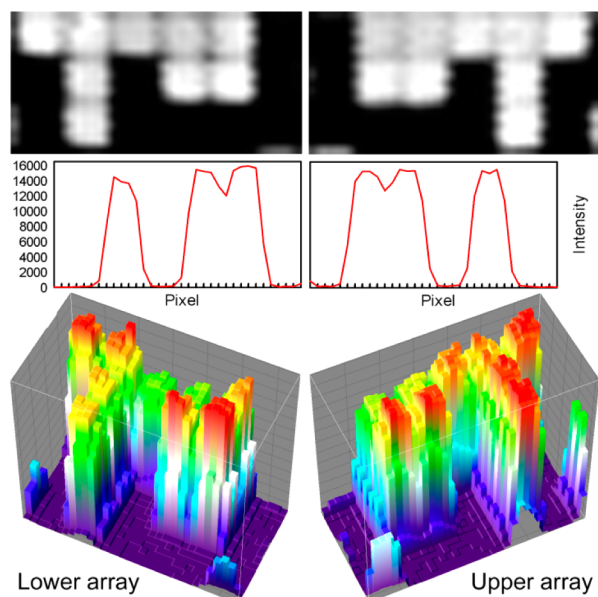
Figure 2. Scanned images and pixel intensities from two mirror-image microarrays synthesized simultaneously. Figures on the left are from the lower substrate (closest to quartz block in Figure 1), and those on the right are from the upper substrate. Top row: 3 × 6 array of features from the center of a 1024 × 768 array, scanned at 2.5 μm. Each features measures 13 μm × 13 μm and are separated by a 0.7 μm gap. Middle row: Intensity profiles of lines drawn horizontally through the close-ups above. Lower row: 3D surface intensity plots of the same close-ups.

about 20%. This interstitial intensity is due to the limited resolution of the scanner (2.5 μm), which leads to image pixels that derive most of their intensity from the adjacent bright microarray features. Diffraction also contributes significantly to intensity in gaps between microarray features, about 40% of the intensity of adjacent features when both features are exposed, and about 20% of the intensity of an adjacent feature when only one of the features is exposed.[7] The vertical sawtooth pattern probably originates from signal latency during rastering by the scanner. The microarrays are fully resolved within the constraints of scanner resolution and diffraction. The bottom row of Figure 2 shows 3-D surface intensity plots of the same close-ups. From the perspective of common microarray use, the each of the mirror image microarrays from the pair can be used as an individual microarray, but in some experimental contexts requiring close comparisons, matched pairs might be used to increase confidence in the comparison.

Blocking Reflections. The use of a light-absorbing fluid in the lower chamber resulted in the complete blockage of reflected light. Initial trials with 9-methylanthracence and riboflavin in DMSO were only partially successful due to incomplete absorption of violet light from the mercury lamp. Most of the photodeprotection of NPPOC results from the 365 nm line, but the mercury lines at 405 and 436 nm are also transmitted through the optical system and result in measurable deprotection. Beta carotene was able to completely absorb the incident light and prevent any reflection. Beta carotene is insufficiently soluble in DMSO but is highly soluble in dichloromethane,[17] which also has an index of refraction similar to that of glass. Figure 3 shows the effect of 5.5 mM beta carotene in dichloromethane. The control experiment (left film) has DMSO in the lower chamber and clearly shows the
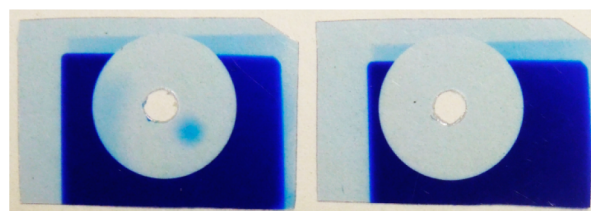
Figure 3. Visualization of light reflected into the synthesis chamber from the back surface of the quartz block and the complete suppression thereof using a light-absorbing fluid in the lower chamber. A 9.5 mm metal disk with a 1 mm diameter pinhole was used to mask radiochromic film in the synthesis chamber. The pinhole was aligned with a 2 mm hole in the film to allow the passage of light (60 J/cm^2), and the reaction cell assembly was tilted 7° to direct the reflection away from the hole. With the secondary chamber filled with a nonabsorbent fluid (left), there is a clear reflection to the lower right of the hole. When the secondary chamber is filled with a light-absorbing fluid, the reflection is completely suppressed (right).

reflection from the light transmitted through the 1 mm pinhole as a round exposed spot on the lower right-hand side. Another reflection is also apparent on the left side of the circle; this originates from transmission outside the pinhole disk that is not entirely absorbed by the radiochromic film. The film on the right shows that the beta carotene solution completely suppresses the reflections.

There are four principle sources of unintended photo-deprotection: (1) global scattering, (2) edge scattering, (3) local flare (which includes reflections), and (4) diffraction.[7] Global scattering from imperfections and dust in the optical system is relatively small and results in a contrast ratio of better than 1/2500. Edge scattering originates primarily from the edges of the micromirrors and has a similar magnitude as global scattering. Diffraction is an intrinsic limitation of all imaging systems and results in partial exposure (~20%) of the area of the synthesis surface corresponding to the gaps between mirrors. Local scattering is primarily due to reflections of light exiting the reaction block but also includes scattering from bubbles in the exposure solvent. Bubbles can be eliminated by using appropriate fluidics protocols, primarily the use of helium as the blanket gas and adequate flushing of the reaction cell with exposure solvent before exposure. Reflection and diffraction remain alone as the largest sources of unintended exposure, each contributing approximately 1−2% of incident light. The use of an effective light absorber in the lower chamber, as demonstrated here, therefore reduces unintended exposure by approximately 50%. Diffraction remains as a large source of unintended exposure, but because the intensity is mostly confined to the gaps between microarray features ("spots"), it does not strongly affect the sequence fidelity within the features.

CONCLUSIONS

We have presented a method for doubling the efficiency of *in situ*, light directed microarray synthesis by assembling a reaction cell from two very closely spaced substrates. The method is straightforward, and we have adopted the method for routine synthesis of both DNA and RNA microarrays and for applications including gene expression and miRNA expression studies.[18,19] For microarray applications requiring high sequence fidelity, the reaction cell assembly provides a chamber that can be used to completely suppress reflections.

■ AUTHOR INFORMATION

Corresponding Author

*E-mail: mark.somoza@univie.ac.at.

Notes

The authors declare no competing financial interest.

■ REFERENCES

(1) Fodor, S. P.; Read, J. L.; Pirrung, M. C.; Stryer, L.; Lu, A. T.; Solas, D. *Science* **1991**, *251*, 767−773.

(2) Singh-Gasson, S.; Green, R.; Yue, Y.; Nelson, C.; Blattner, F.; Sussman, M.; Cerrina, F. *Nat. Biotechnol.* **1999**, *17*, 974−978.

(3) Beier, M.; Hoheisel, J. D. *Nucleic Acids Res.* **2000**, *28*, e11.

(4) Hasan, A.; Stengele, K.; Giegrich, H.; Cornwell, P.; Isham, K.; Sachleben, R.; Pfleiderer, W.; Foote, R. *Tetrahedron* **1997**, *53*, 4247−4264.

(5) Pirrung, M. C.; Wang, L.; Montague-Smith, M. P. *Org. Lett.* **2001**, *3*, 1105−1108.

(6) Agbavwe, C.; Somoza, M. M. *PLoS ONE* **2011**, *6*, e22177.

(7) Agbavwe, C.; Kim, C.; Hong, D. G.; Heinrich, K.; Wang, T.; Somoza, M. M. *J. Nanobiotechnol.* **2011**, *9*, 57.

(8) Franssen-van Hal, N. L. W.; van der Putte, P.; Hellmuth, K.; Matysiak, S.; Kretschy, N.; Somoza, M. M. *Anal. Chem.* **2013**, *85*, 5950−5957.

(9) Bhushan, K. R. *Org. Biomol. Chem.* **2006**, *4*, 1857−1859.

(10) Shin, D.-S.; Lee, K.-N.; Yoo, B.-W.; Kim, J.; Kim, M.; Kim, Y.-K.; Lee, Y.-S. *J. Comb. Chem.* **2010**, *12*, 463−471.

(11) Lackey, J. G.; Mitra, D.; Somoza, M. M.; Cerrina, F.; Damha, M. J. *J. Am. Chem. Soc.* **2009**, *131*, 8496−8502.

(12) Wang, T.; Oehrlein, S.; Somoza, M. M.; Perez, J. R. S.; Kershner, R.; Cerrina, F. *Lab Chip* **2011**, *11*, 1629−1637.

(13) Lackey, J. G.; Somoza, M. M.; Mitra, D.; Cerrina, F.; Damha, M. J. *Chim. Oggi* **2009**, *27*, 30−33.

(14) Garland, P. B.; Serafinowski, P. J. *Nucleic Acids Res.* **2002**, *30*, e99.

(15) Offner, A. *Opt. Eng.* **1975**, *14*, 130−132.

(16) Offner, A. *Photogr. Sci. Eng.* **1979**, *23*, 374.

(17) Craft, N. E.; Soares, J. H. *J. Agric. Food Chem.* **1992**, *40*, 431−434.

(18) Holik, A.-K.; Rohm, B.; Somoza, M. M.; Somoza, V. *Food Funct.* **2013**, *4*, 1111−1120.

(19) Rohm, B.; Holik, A.-K.; Somoza, M. M.; Pignitter, M.; Zaunschirm, M.; Ley, J. P.; Krammer, G. E.; Somoza, V. *Mol. Nutr. Food Res.* **2013**, DOI: 10.1002/mnfr.201200846.

8517

dx.doi.org/10.1021/ac4024318 | *Anal. Chem.* 2013, 85, 8513−8517

56

2.4 "Structure-dependent effects of pyridine derivatives on mechanisms of intestinal fatty acid uptake: Regulation of nicotinic acid receptor and fatty acid transporter expression"

Riedel, A.[a], Lang, R.[b], **Rohm, B**.[a,c], Rubach, M.[d], Hofmann, T.[b], Somoza,V.[a,c]

[a] Department of Nutritional and Physiological Chemistry, University of Vienna, Vienna, Austria

[b] Chair of Food Chemistry and Molecular Sensory Science, Technische Universität München, Freising, Germany

[c] Christian Doppler Laboratory for Bioactive Aroma Compounds, University of Vienna, Vienna, Austria

[d] Deutsche Forschungsanstalt für Lebensmittelchemie, Freising, Germany

Structure-dependent effects of pyridine derivatives on mechanisms of intestinal fatty acid uptake: regulation of nicotinic acid receptor and fatty acid transporter expression☆

Annett Riedel[a], Roman Lang[b], Barbara Rohm[a, c], Malte Rubach[d], Thomas Hofmann[b], Veronika Somoza[a, c,*]

[a]*Department of Nutritional and Physiological Chemistry, University of Vienna, Vienna, Austria*
[b]*Chair of Food Chemistry and Molecular Sensory Science, Technische Universität München, Freising, Germany*
[c]*Christian Doppler Laboratory for Bioactive Aroma Compounds, University of Vienna, Vienna, Austria*
[d]*Deutsche Forschungsanstalt für Lebensmittelchemie, Freising, Germany*

Abstract

Pyridines are widely distributed in foods. Nicotinic acid (NA), a carboxylated pyridine derivative, inhibits lipolysis in adipocytes by activation o fth e orphan NA receptor (HM74A) and is applied to treat hyperlipidemia. However, knowledge on the impact of pyridine derivatives on intestinal lipid metabolism is scarce. This study was performed to identify the structural determinants of pyridines for their effects on fatty acid uptake in enterocyte-like Caco-2 cells and to elucidate the mechanisms of action. The impact of 17 pyridine derivatives on fatty acid uptake was tested. Multiple regression analysis revealed the presence of a methyl group to be the structural determinant at 0.1 mM, whereas at 1 mM, the presence of a carboxylic group and the *N*-methylation presented further structural characteristics to affect the fatty acid uptake. NA, showing a stimulating effect on FA uptake, and *N*-methyl-4-phenylpyridinium (MPP), inhibiting FA uptake, were selected for mechanistic studies. Gene expression of the fatty acid transporters *CD36*, *FATP2* and *FATP4*, and the lipid metabolism regulating transcription factors peroxisome proliferator-activated receptor (PPAR) α and *PPARγ* was up-regulated upon NA treatment. Caco-2 cells were demonstrated to express the low-affinity NA receptor *HM74* of which the gene expression was up-regulated upon NA treatment. We hypothesize that the NA-induced fatty acid uptake might result from NA receptor activation and related intracellular signaling cascades. In contrast, MPP increased transepithelial electrical resistance. We therefore conclude that NA and MPP, both sharing the pyridine motif core, exhibit t h e i r   contrary effects on intestinal FA uptake by activation of different mechanisms.
© 2014 Published by Elsevier Inc.

Keywords: Pyridines; Fatty acid uptake; Caco-2; Nicotinic acid; Nicotinic acid receptor; *N*-methyl-4-phenylpyridinium

1. Introduction

Pyridines are widely distributed in plants and foods. Coffee beverages, in particular, are rich in pyridine derivatives such as trigonelline, *N*-methylpyridinium, nicotinamide and nicotinic acid

(NA) [1,2]. *N*-methylpyridinium has recently been shown to possess bioactive properties [3–6]. NA, also known as niacin or vitamin B₃, is an essential, pellagra-preventing nutrient whose physiological effects have been extensively described [7]. In gram amounts, NA is used to treat hyperlipidemia because it lowers plasma cholesterol [8] and reduces plasma free fatty acids by inhibiting lipolysis in adipocytes [9]. However, side effects of high-dose intake of NA, such as intense flushing due to increased prostaglandin D2 release, accompany its beneficial effects as plasma lipid-lowering drug [10].

The mode of action of NA was not elucidated until the deorphanization of the NA receptor, a G-protein-coupled receptor that appears in the two subtypes HM74A (GRP109A) and HM74 (GPR109B). HM74A is the high-affinity receptor, and HM74, homologous with HM74A, but with 24 additional C-terminus amino acids, is the low-affinity receptor [11–13]. These receptors have also been classified as hydroxy-carboxylic acid receptors since ligand receptor studies have shown that the carboxylic acid group determines the affinity of potential ligands [14]. β-Hydroxybutyrate has been identified as the endogenous ligand for these receptors [15]. In

contrast, nicotinamide, possessing a carboxamide group instead of a carboxylic group, was inactive in G-protein activation and showed an EC_{50} >1000 μM, whereas NA showed an EC_{50} of 1.42 μM in rat adipocytes [16].

Although evidence for the lipolysis inhibiting effect of NA exists, the role of pyridine derivatives in fatty acid absorption at the intestinal level is poorly understood.

Therefore, we aimed to elucidate the structural features of pyridine derivatives for their effects on intestinal fatty acid uptake and intended to verify the potential role of the NA receptors as mediators for pyridine-induced changes *in vitro*. We selected 17 test compounds, either by synthesis or from commercial sources, sharing the pyridine core motif, and tested their potential to alter fatty acid uptake in differentiated Caco-2 cells. Upon differentiation, the colon carcinoma cell line Caco-2 undergoes profound morphological changes resulting in enterocyte-like cells. As Caco-2 cells are characterized by polarization and the development of a brush border membrane as well as intercellular tight junctions, they present a suitable cellular model for intestinal uptake studies [17].

The absorption of long-chain fatty acids is facilitated by passive diffusion or active transport mediated by fatty acid transporters such as fatty acid translocase CD36 or fatty acid transport proteins (FATPs) [18]. Therefore, we assessed gene expression of *CD36*, *FATP2*, *FATP4*, intestinal fatty acid binding protein (*IFABP*), peroxisome proliferator-activated receptor *(PPAR) α* and *PPARγ*, as genes representative of those regulating fatty acid metabolism. We further analyzed NA receptor gene expression. Transepithelial electrical resistance (TEER) was assessed to estimate cellular integrity.

2. Material and methods

2.1. Chemicals

Pyridine (**1**), nicotinic acid (**2**), 4-carboxypyridine (iso-nicotinic acid; **3**), picolinic acid (**4**), trigonelline hydrochloride (**9**), nicotinamide (**11**), *N*-methylnicotinamide iodide (**12**), nicotinamide-*N*-oxide (**16**) and *N*-methyl-4-phenylpyridinium (MPP) (**17**) were purchased from Sigma-Aldrich (Steinheim, Germany). *N*-methylpyridinium iodide (**5**), *N*-methyl-2-picolinium iodide (**6**), *N*-methyl-3-picolinium iodide (**7**), *N*-methyl-4-picolinium iodide (**8**), *N*-methyl-2-pyridone-5-carboxylic acid (**10**), *N*-methyl-2-pyridone-5-carboxamide (**13**), *N*-methyl-2-pyridone-3-carboxamide (**14**) and *N*-methyl-4-pyridone-5-carboxamide (**15**) were synthesized and purified by recrystallization or preparative high-performance liquid chromatography, respectively, as reported [2,19]. All other materials, chemicals and reagents were obtained from Sigma-Aldrich (Austria) unless stated otherwise.

2.2. Cell culture

The human colon cancer cell line Caco-2 cells was cultured in Dulbecco's modified Eagle medium (DMEM) supplemented with 10% fetal bovine serum, 2 mM L-glutamine and 1% penicillin/streptomycin at 37°C and 5% CO₂ in a humidified incubator. To avoid undesired initiation of differentiation, cells were passaged at a maximum of 90% confluency. For experiments, cells were seeded into 96-well plates, 6-well plates or transwell plates reaching confluency after 2 days. Cell differentiation was obtained by subsequent culture for further 18 days including medium changes every second to third day. Then, enterocyte-like differentiated Caco-2 cells were used for further studies.

2.3. Fatty acid uptake

The fatty acid uptake was assessed in differentiated Caco-2 cells by the QBT Fatty Acid Uptake Assay Kit (Molecular Devices Corporation, Germany) that applies a BODIPY-dodecanoic acid fluorescent fatty acid analog. Differentiated Caco-2 cells were starved with serum-free medium for 1 h under standard cell culture conditions prior to the addition of pyridine derivates (1–17) at 0.1 and 1 mM diluted in Hank's balanced salt solution (HBSS)/HEPES buffer. Controls were treated with HBSS/HEPES only. After a 30-min preincubation at 37°C, the fluorescent fatty acid analog diluted in HBSS/HEPES (supplemented with 0.2% essential fatty acid free bovine serum albumin) was added. Fluorescence signals were recorded at an emission wavelength of 515 nm after excitation at 485 nm with a microplate reader (infinite M200; Tecan, Austria) for 60 min. A time–signal intensity curve was plotted, and thereof, the area under curve (AUC) was calculated to determine treatment-dependent cellular fatty acid uptake. Results are described as percentage of controls.

2.4. Cell viability

Cytotoxic effects of test compounds were excluded by performance of the MTT assay that is based on the ability of viable cells to reduce the yellow tetrazole MTT (3-(4,5-dimethylthiazol-2-yl)-2,5-diphenyltetrazolium bromide) reagent to a purple formazan. Differentiated Caco-2 cells were starved with serum-free medium 1 h prior to the addition of NA and MPP diluted in HBSS/HEPES in a concentration range of 0.001–1 mM. Test substances were removed after a 90-min exposure to cells. The MTT stock solution (5 mg/ml) was diluted (1:6) in serum-free DMEM and led to incubate for about 13 min. After removal of the MTT solution, the resulting formazan was diluted in dimethyl sulfoxide, and absorbance was measured at 550 nm with a multiwell plate reader (Tecan infinite M200; Tecan). Results were further corrected for unspecific interferences recorded at a reference wavelength of 690 nm, and viability was determined relative to untreated control cells (100%).

2.5. Glucose uptake

Glucose uptake was assessed using the 2-(N-(7-nitrobenz-2-oxa-1,3-diazol-4-yl) amino)-2-deoxyglucose (2-NBDG) fluorescence glucose analog (Life Technologies, Austria). Differentiated Caco-2 cells were starved with glucose-free DMEM (without L-glutamine and fetal bovine serum) for 1 h at 37°C and 5% CO₂ in a humidified incubator. Then, cells were preincubated with NA and MPP, respectively, diluted in HBSS/HEPES buffer in concentrations ranging from 0.001 to 1 mM for 30 min prior to the addition of 2-NBDG (diluted in HBSS/HEPES) to a final concentration of 200 μM. After another 30-min incubation in which cellular absorption of the fluorescent glucose analog occurs, cells were washed three times with ice-cold phosphate-buffered saline (PBS) to remove excess dye, and fluorescence emission was measured at 550 nm after excitation at 485 nm with a multiwell plate reader (Tecan infinite M200; Tecan). Results are expressed relative to untreated controls (100%).

2.6. Quantitative reverse transcriptase polymerase chain reaction

Gene expression patterns of differentiated Caco-2 cells after treatment with NA and MPP were analyzed by quantitative real-time reverse transcription polymerase chain reaction (qPCR). Differentiated Caco-2 cells were exposed to 1 mM NA and 1 mM MPP for 30, 60 and 90 min. After a brief washing step with ice-cold PBS, cells were lysed and total RNA was extracted applying the peqGOLD Total RNA Kit (Peqlab, Germany). RNA content and purity were analyzed with the NanoQuant Plate specified for the infinite M200 plate reader (Tecan), and a total of 2 μg RNA was used for cDNA transcription applying the High Capacity cDNA Reverse Transcription Kit (Life Technologies, Austria). Real-time qPCR was conducted with 100 ng cDNA that were amplified with the Fast SYBR Green Master Mix (Life technologies Austria). Analyses were performed in triplicates by means of a StepOnePlus Realtime PCR System (Life technologies). Specific primers were designed using NCBI/Primer-BLAST or extracted from PrimerBank and purchased from Sigma-Aldrich (Austria). Primer sequences for the target genes FATP2, FATP4, IFABP, fatty acid translocase (CD36), PPARα and PPARγ and NA receptor (HM74 and HM74A) are given in Table 1 and applied at a concentration of 100 nM each. Results were analyzed using the LinRegPCR software. Hypoxanthine guanine phosphoribosyl transferase (HPRT-1) was used as reference gene, and gene expression of target genes was calculated as a ratio to HPRT-1 expression [20]. Results are given as expression relative to HPRT-1 for comparison of gene expression patterns in undifferentiated and differentiated Caco-2 cells or fold changes when comparing alteration in gene expression after treatment with NA or MPP to untreated controls.

Table 1
qPCR primer pairs

| Gene	Primer	Sequence (5′–3′)	Product length (bp)
FATP2	FW	TGGAACCACAGGTGCTACTC	116
	RV	ACCGAAGCAGTTCACCGATA	
FATP4	FW	GGCTGCCCTGGTGTACTATG	93
	RV	CCCACGATGTTTCCTGCTGA	
IFABP	FW	AACTGAACTCAGGGGGACCT	78
	RV	TCGTTTCCATTGTCTGTCCGT	
CD36	FW	TGTAACCCAGGACGCTGAGG	69
	RV	GAAGGTTCGAAGATGGCACC	
PPARα	FW	TTCGCAATCCATCGGCCAG	146
	RV	CCACAGGATAAGTCACCGAGG	
PPARγ	FW	ACCAAAGTGCAATCAAAGTGGA	100
	RV	ATGAGGGAGTTGGAAGGCTCT	
HM74	FW	TGACATAAAGGCAGGCACGG	103
	RV	TGCAGCTAGTGAGTCCGATG	
HM74A	FW	GACAACTATGTGAGGCGTTGG	133
	RV	CCCGGAAATACCTGTCTACCG	
HPRT-1	FW	CCTGGCGTCGTGATTAGTGA	137
	RV	CGAGCAAGACGTTCAGTCCT	
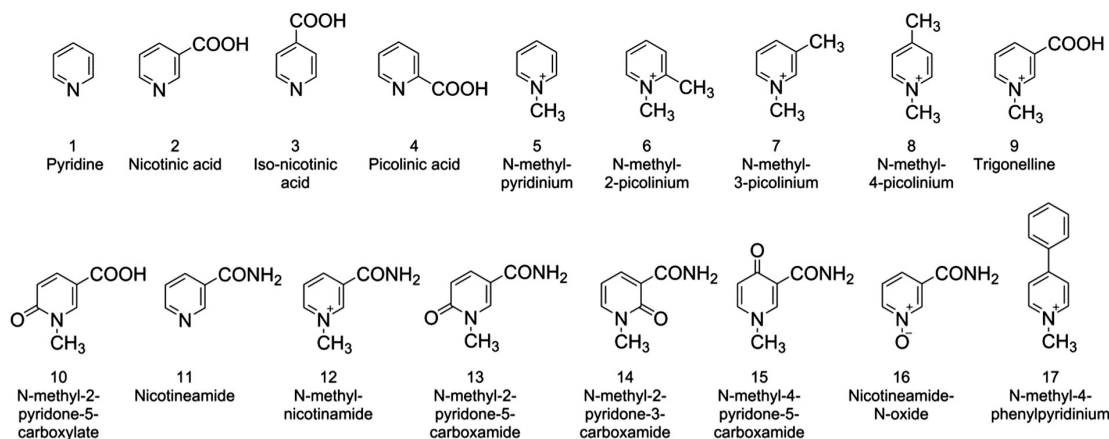
Fig. 1. Chemical structures of the pyridine derivatives tested: pyridine (**1**), NA (**2**), iso-nicotinic acid (**3**), picolinic acid (**4**), *N*-methylpyridinium (**5**), *N*-methyl-2-picolinium (**6**), *N*-methyl-3-picolinium (**7**), *N*-methyl-4-picolinium (**8**), trigonelline (**9**), *N*-methyl-2-pyridone-5-carboxylate (**10**), nicotinamide (**11**), *N*-methylnicotinamide (**12**), *N*-methyl-2-pyridone-5-carboxamide (**13**), *N*-methyl-2-pyridone-3-carboxamide (**14**), *N*-methyl-4-pyridone-5-carboxamide (**15**), nicotinamide-*N*-oxide (**16**) and MPP (**17**).

2.7. Calcium signaling

Intracellular calcium mobilization was determined in differentiated Caco-2 cells by means of the Fluo-4 Direct Calcium Assay Kit (Invitrogen, Austria). The fluo-4 dye was dissolved in the loading buffer to obtain a twice-concentrated dye solution that was further diluted with the same volume of HBSS/HEPES buffer to the final loading dye. The cell culture medium was removed and the loading dye was added. After a 30-min incubation step at 37°C in a humidified incubator, cells were kept another 90 min at room temperature to allow dye uptake before starting the experiment. NA and MPP, respectively, were diluted in HBSS/HEPES buffer and various concentrations of these compounds (0.001–1 mM) were added by direct injection applying the Tecan infinite M200 microplate reader (Tecan). Fluorescence signals after individual injections were recorded every 2 s at an emission wavelength of 520 nm after excitation at 490 nm. The AUC of fluorescence signals over the first 20 s was calculated for individual measurements and normalized to the starting fluorescence signal of each cell. Results are expressed as AUC of untreated controls (100%).

2.8. Transepithelial electrical resistance

The integrity of the epithelial barrier after treatment of differentiated Caco-2 cells with NA and MPP, respectively, was determined by means of the epithelial voltohmmeter EVOM (World Precision Instruments, Germany) connected to the EndOhm-24 chamber (World Precision Instruments) with 24-mm diameter suitable for Costar Snapwell inserts (Corning Life Sciences, Germany). Caco-2 cells were differentiated in Snapwells each filled with 450 μL culture medium in the upper compartment and 2.5 ml culture medium in the lower compartment. On the experimental day, cells were starved with serum-free medium for 1 h prior to exposure to the test compounds NA and MPP diluted in HBSS/HEPES buffer, respectively, that were added at a final concentration of 1 mM to the upper compartment only. Control cells were incubated only with medium containing 10% HBSS/HEPES buffer. TEER was measured in duplicate prior to test compound addition as well as after 30, 60 and 90 min of treatment. Therefore, Snapwells were transferred to the EndOhm chamber prefilled with 2.5 ml of serum-free medium, and the corresponding resistance was recorded with the EVOM meter. Basal background resistance was assessed in cell-free Snapwells. Results are expressed as unit area resistance (Ω*cm^2) by multiplying cell-based electrical resistance with the Snapwell membrane area.

2.9. Statistical analysis

Results are displayed as mean±S.D. of at least three individual experiments (*n*) including multiple technical replicates unless stated otherwise. The Nalimov outlier test was performed prior to the estimation of significant differences between treatments. To evaluate the impact of individual pyridine derivatives on fatty acid uptake, a one-way analysis of variance (ANOVA) with Bonferroni post hoc test versus control was applied. Significant differences to untreated controls were indicated by *P<.05, **P<.01 and ***P<.001. To extract the most important structural determinants of the tested compounds, a multiple linear regression was calculated including the percentage of fatty acid uptake as a dependent variable and the functional groups as an independent variable. The additional methyl group, the carboxamide group, the
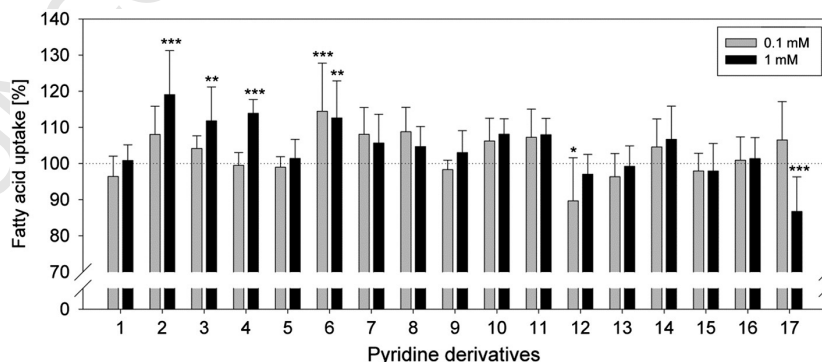
Fig. 2. Fatty acid uptake by differentiated Caco-2 cells after 30 min pretreatment with 0.1 and 1 mM of different pyridine derivatives compared to nontreated differentiated cells (=100%): pyridine (**1**), NA (**2**), iso-nicotinic acid (**3**), picolinic acid (**4**), *N*-methylpyridinium (**5**), *N*-methyl-2-picolinium (**6**), *N*-methyl-3-picolinium (**7**), *N*-methyl-4-picolinium (**8**), trigonelline (**9**), *N*-methyl-2-pyridone-5-carboxylic acid (**10**), nicotinamide (**11**), *N*-methylnicotinamide iodide (**12**), *N*-methyl-2-pyridone-5-carboxamide (**13**), *N*-methyl-2-pyridone-3-carboxamide (**14**), *N*-methyl-4-pyridone-5-carboxamide (**15**), nicotinamide-*N*-oxide (**16**) and MPP (**17**). For data analysis, the AUC after a 60-min fluorescence signal record was calculated and results were normalized to untreated controls (100%). Results are displayed as mean±S.D. of at least three individual experiments. Significant differences to untreated controls (dotted line) were determined by one-way ANOVA with Bonferroni post hoc test and are indicated as follows: *P<.05, **P<.01 and ***P<.001.

carboxyl group, the oxo-group and *N*-methylation were specified as functional characteristics and included in the regression model to characterize the structure of the pyridine derivatives applied. The presence of each functional group was given the value 1, whereas those molecules lacking a specific group were given the value 0 in a matrix-based data set. One-way ANOVA with Holm–Sidak post hoc test was applied to determine dose-dependent effects of test substances, and two-way ANOVA with Holm–Sidak post hoc test was accomplished to test for time and treatment dependency. Differences between samples were assumed at the 5% level of significance and are indicated in the figures with distinct letters. All statistical analyses were carried out using SigmaPlot software (Systat Software, Inc, San Jose, CA, USA).

3. Results

3.1. Effect of pyridine derivatives on fatty acid uptake

The ability of 17 pyridine derivatives (Fig. 1) to modify enterocyte-like Caco-2 long-chain fatty acid uptake was assessed, and results are displayed in Fig. 2. Pyridine, presenting the basic structure of the tested compounds, did not affect fatty acid uptake, neither at 0.1 mM nor at 1 mM. In contrast, treatment of the cells with the carboxylated position isomers NA (**2**), iso-nicotinic acid (**3**) and picolinic acid (**4**) increased fatty acid uptake at a concentration of 1 mM by 19.0%± 16.2%, 11.8%±9.38% and 13.9%±3.82%, respectively. *N*-methylpyridinium (**5**) had no impact on fatty acid uptake. Introduction of an additional methyl group in ortho-position stimulated fatty acid uptake at 0.1 and 1 mM (compound **6**), but did not so when present in meta- or para-position (compounds **7**, **8**). Treatment of differentiated Caco-2 cells with trigonelline (**9**) or nicotinamide (compound **11**) did not cause a significant change in fatty acid uptake. Furthermore, none of the pyridine derivatives that possess an additional oxo-group (compounds **10**, **13**, **14**, **15**) affected fatty acid uptake. Inhibition of fatty acid uptake was only observed after incubation with 0.1 mM *N*-methylnicotinamide (**12**) and 1 mM MPP (**17**), resulting in a reduction by −10.3%±11.9% and −13.3%±9.59%, respectively.

To identify the most important structural determinants of the tested pyridines with regard to their ability to modify fatty acid uptake, a multiple linear regression was performed (Table 2). Fatty acid uptake was defined as the dependent variable, whereas the functional groups were defined as independent variables. At a concentration of 0.1 mM, a weak relationship between fatty acid uptake and the presence of functional groups was observed since only 28% of the variability is explainable with the model (*P*-value of the regression=.123, R=0.710, R^2=0.505, adjusted R^2=0.280). The additional methyl group was calculated to be the only determining structural characteristic (*P*<.05). In contrast, at a concentration of 1 mM, a better prediction of the fatty acid uptake by the regression equation is provided (*P*-value of the regression=.007, R=0.853, R^2=0.728, adjusted R^2=0.640). Besides the additional methyl group (*P*<.01), the carboxylic group (*P*<.05) and the *N*-methylation (*P*<.05) presented further structural characteristics affecting the fatty acid uptake.
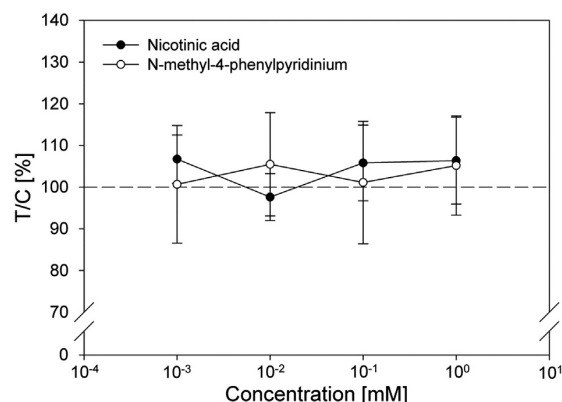

Fig. 3. Cytotoxic effects of the selected compounds NA and MPP on differentiated Caco-2 cells after 90-min incubation. Results were normalized to untreated controls (100%) and are shown as mean±S.D. of three individual experiments. One-way ANOVA was performed to exclude dose-dependent cytotoxic effects of test compounds (*P*>.05).

3.2. Cell viability after treatment with NA and MPP

Cytotoxicity was evaluated in differentiated Caco-2 cells after treatment with the selected compounds NA and MPP. No cytotoxic effects were observed after exposure of differentiated Caco-2 cells to NA and MPP for 90 min at a concentration range of 0.001–1 mM (Fig. 3).

3.3. Impact of NA and MPP on cellular glucose uptake

The uptake of 2-NBDG, a fluorescent glucose analog was determined to estimate whether NA and MPP might affect other metabolic pathways, e.g. cause a switch to glucose as energy substrate or inhibit glucose uptake to compensate increased energy supply by fatty acids. However, no changes in glucose uptake of differentiated Caco-2 cells were observed by NA (Fig. 4A) or MPP treatment (Fig. 4B).

3.4. Modulation of gene expression patters of fatty acid transporters and genes involved in fatty acid metabolism

Intestinal fatty acid absorption is mediated by transport proteins or occurs by passive diffusion [18]. Several FATPs as well as fatty acid binding proteins (FABPs) have been identified in enterocyte-like Caco-2 cells [20]. First, changes in gene expression profiles of fatty acid transporters and genes involved in fatty acid metabolism were assessed in undifferentiated and enterocyte-like differentiated Caco-2 cells. Expression of *FATP2*, *FATP4*, *CD36*, *PPARα* and *PPARγ* could be verified in undifferentiated Caco-2 cells (Table 3). However, except for *FATP2*, significantly higher expression of these genes was found in differentiated cells (Table 3). *IFABP* was below the limit of detection in undifferentiated cells since ΔcT values were above 35.

As fatty acid uptake was modified by NA and MPP, expression patters of fatty acid transporters and genes involved in fatty acid metabolism were analyzed. Treatment-dependent relative gene expressions of *CD36*, *FATP2*, *FATP4*, *IFABP*, *PPARα* and *PPARγ* are illustrated in Fig. 5. Expression of the fatty acid transporter *CD36* was promoted by incubation with NA after 30 and 60 min, resulting in a respective 1.45±0.54 fold and 1.52±0.15 fold higher gene expression in comparison to untreated controls (Fig. 5). *FATP2* and *FATP4* have also been up-regulated upon NA treatment (Fig. 5). Moreover, a slight increase in *PPARα* and *PPARγ* gene expression was found in differentiated Caco-2 cells after exposure to 1 mM NA (Fig. 5).

Table 2
Multiple linear regression analysis[a]

Functional group	0.1 mM		1 mM	
	Coefficient	*P*-value	Coefficient	*P*-value
Constant	103±3.85	<**.001**	102±3.54	<**.001**
Additional methyl group	11.3±4.43	**.027**	14.3±6.06	**.005**
Carboxamide group	−3.51±3.61	.427	3.21±3.91	.429
Carboxyl group	0.48±4.14	.909	11.6±3.80	**.011**
N-methylation	−4.51±6.26	.237	−8.94±3.32	**.021**
Oxo group	4.65±2.26	.298	4.33±3.91	.291

[a] At 0.1 mM: *P*-value of the regression=.123, R=0.710, R^2=0.505, adjusted R^2= 0.280; at 1 mM: *P*-value of the regression=.007, R=0.853, R^2=0.728, adjusted R^2= 0.640.
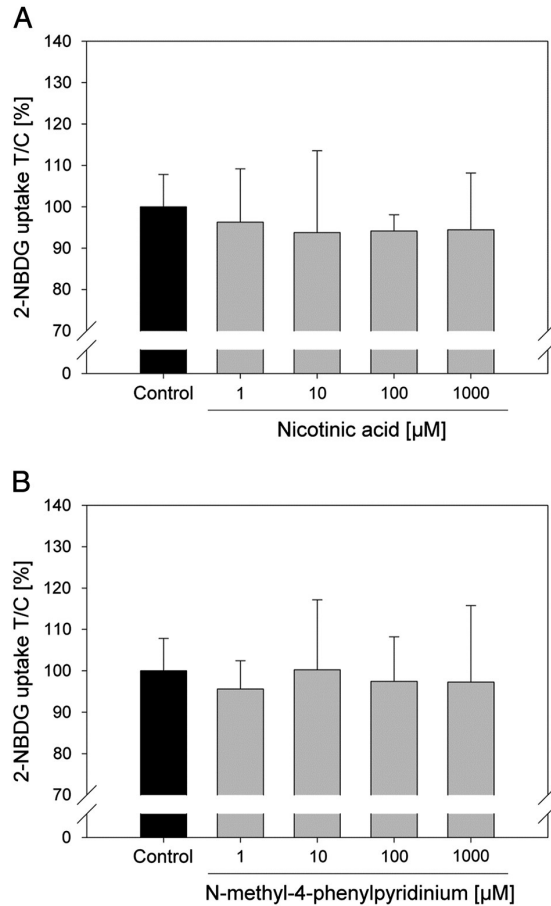
ARTICLE IN PRESS

Fig. 4. Cellular glucose uptake assessed by means of 2-NBDG uptake in differentiated Caco-2 cells after 30-min exposure to NA (A) and MPP (B). Results were normalized to untreated controls (100%) and are displayed as mean±S.D. ($n \geq 3$). One-way ANOVA was applied to test for significant differences between treatments ($P>.05$).
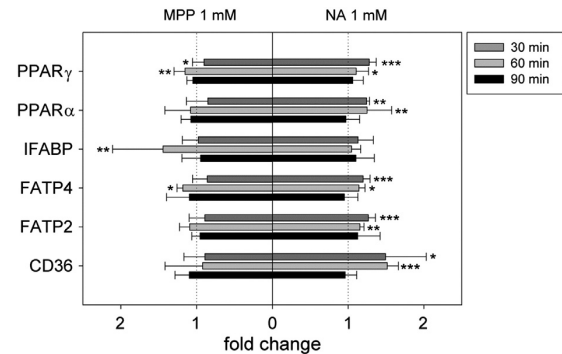

Fig. 5. Relative expression of genes involved in fatty acid uptake and regulation of cellular fatty acid metabolism determined in differentiated Caco-2 cells after treatment with 1 mM NA and 1 mM MPP. *CD36*, *FATP2*, *FATP4*, *IFABP*, *PPARα* and *PPARγ* gene expression was determined after 30-, 60- and 90-min incubation with the test compounds. Data were normalized to the reference gene *HPRT-1* and are given as fold changes of untreated controls (dotted line). Results represent mean±S.D. (n=3). A two-way ANOVA with Holm–Sidak post hoc test was performed to test for time and treatment dependency and considered as significant at $P<.05$. Significant differences to controls are indicated as follows: $^*P<.05$, $^{**}P<.01$ and $^{***}P<.001$.

Additionally, time-dependent effects of 1 mM NA on gene expression levels were evaluated. Expression of *CD36*, *FATP4*, *PPARα* and *PPARγ* showed significant differences between the time points 30 and 90 min ($P<.001$) as well as 60 and 90 min ($P<.01$), although not differing between the incubation times 30 and 60 min ($P>.05$). In contrast, *FATP2* was only affected by treatment ($P<.05$) and not by time ($P>.05$), while *IFABP* remained unaffected by NA ($P>.05$).

The incubation of Caco-2 cells with MPP also caused changes in the expression profile of the selected genes (Fig. 5). *PPARγ* was slightly down-regulated after 30 min followed by an up-regulation after 60 min. *IFABP* and *FATP4* gene expressions were only increased after 60

min of MPP treatment. Moreover, time-dependent variations in gene expression levels were calculated for *PPARγ* showing differences between all time points ($P<.05$), *IFABP* differing between 30 and 60 min ($P<.01$) as well as 60 and 90 min ($P<.01$), and *FATP4* being different between 30 and 60 min ($P<.01$) as well as 30 and 90 min ($P<.01$). However, *CD36*, *FATP2* and *PPARα* were neither affect by time or by treatment ($P>.05$).

3.5. Effect of NA and MPP on the NA receptor expression

In humans, the NA receptor, a G-protein-coupled receptor, appears in two subtypes: the HM74A or GRP109A and the HM74 or GPR109B subtype, of which HM74A lacks 24 amino acids at its C-terminus [13,21]. Undifferentiated Caco-2 cells express only marginal amounts of the NA receptor subtype *HM74* relative to the reference gene *HPRT-1* (hypoxanthine guanine phosphoribosyl transferase), that is increased upon differentiation to enterocyte-like cells (Table 3). In contrast, the *HM74A* subtype was neither detectable in undifferentiated nor in differentiated Caco-2 cells. Incubation of differentiated Caco-2 cells with 1 mM NA led to a 2.38±0.89 fold enhanced *HM74* gene expression compared to untreated controls
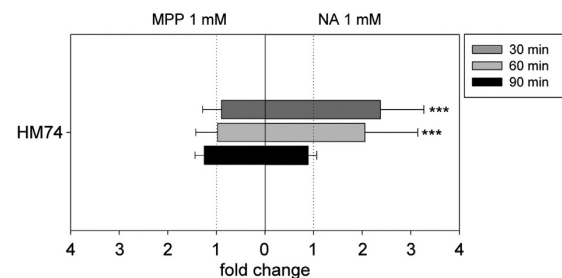
Fig. 6. Gene expression of the NA receptor *HM74* determined in differentiated Caco-2 cells after treatment with 1 mM NA and 1 mM MPP for 30, 60 and 90 min. Data were normalized to the reference gene *HPRT-1* and are given as fold changes of untreated controls (dotted line). Results represent mean±S.D. of at least three biological replicates. A two-way ANOVA with Holm–Sidak post hoc test was performed to test for time and treatment dependency and considered as significant at $P<.05$. Significant differences to controls are indicated with $^{***}P<.001$.

Table 3
Gene expression relative to HPRT-1 in undifferentiated (ud) and differentiated (d) Caco-2 cells (mean±S.D., n=3)

Gene	udCaco-2	dCaco-2	dCaco-2/udCaco-2	P-value
FATP2	0.013±0.004	0.029±0.006	2.22±0.45	**<.001**
FATP4	0.471±0.104	0.431±0.075	0.92±0.16	.365
IFABP	n.d.[a]	0.457±0.055		
CD36	0.001±0.001	0.028±0.006	27.4±6.27	**<.001**
PPARα	0.086±0.009	0.378±0.099	4.40±1.15	**<.001**
PPARγ	0.330±0.074	0.520±0.070	1.58±0.21	**<.001**
HM74	0.002±0.001	0.054±0.007	22.7±2.97	**<.001**

[a] Not detectable

(1.00±0.09) after 30 min (Fig. 6). This effect was maintained after 60 min, resulting in a 2.06±1.09 fold increased *HM74* expression in comparison to controls (1.00±0.09). After 90 min, gene expression levels reached values similar to those of control cells. Time-dependent effects of NA treatment were revealed for *HM74* gene expression between 30 and 90 min ($P<.001$) and between 60 and 90 min ($P<.001$), although not varying between the time points 30 and 60 min ($P>.05$). MPP did not affect *HM74* expression patterns (Fig. 6).

3.6. Induction of intracellular calcium mobilization

NA receptors are G_i-type G-protein-coupled receptors that, upon stimulation, inhibit intracellular cAMP accumulation but also increase intracellular Ca^{2+} mobilization by activating the G-protein α-subunit $G_{\alpha 15}$ [12]. Direct addition of NA to enterocyte-like Caco-2 cells enhanced intracellular calcium mobilization (Fig. 7). The highest tested concentration of 1 mM was applied to evaluate the expression of the NA receptor HM74-stimulated calcium mobilization, resulting in a mean increase of 186%±98.6% in comparison to untreated controls (100%±11.9%). In contrast, no effect on intracellular calcium mobilization was found after MPP treatment.
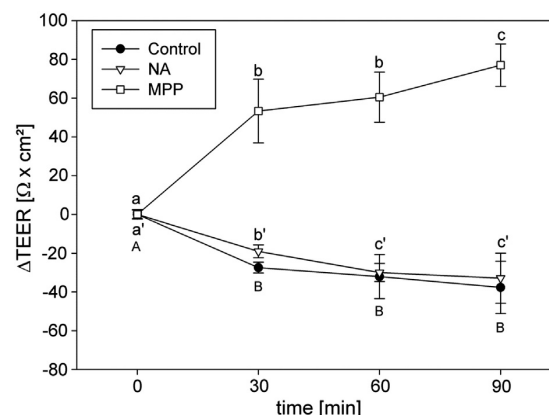
Fig. 8. TEER of Caco-2 cells after treatment with incubation medium only (control), 1 mM NA and 1 mM MPP, respectively. Measurements were carried out before as well as after 30, 60 and 90 min of incubation with NA or MPP. Results are shown as mean difference±S.D. to initial TEER ($n=3$). A two-way ANOVA with Holm–Sidak post hoc test was performed to estimate time- and treatment-dependent effects and considered as significant at $P<.05$. Significant differences ($P<.05$) between time points of each treatment are indicated with distinct letters.

3.7. Changes in TEER

Differentiated Caco-2 cells present a suitable cell model to study barrier function on intestinal epithelial cells as they form monolayers that are characterized by polarization, development of a brush border membrane and formation of intercellular tight junctions [17]. Analysis of the TEER provides evidence for the paracellular integrity of enterocyte-like Caco-2 cells.

Caco-2 cells demonstrated a mean TEER of 454±40.1 $\Omega\times cm^2$ after 21 days of differentiation, a value that is comparable to those described in the literature [22]. Addition of incubation medium containing 10% HBSS/HEPES buffer to the control cells induced a slight decrease by −27.4±2.81 $\Omega\times cm^2$ after 30 min, but remained stable throughout the following measurement time points (Fig. 8). Incubation of differentiated Caco-2 cells with 1 mM NA also reduced TEER by −19.0±3.33 $\Omega\times cm^2$ within 30 min when compared to the initial value prior to the addition of test compounds. TEER further decreased after 60 min (−30.0±4.70 $\Omega\times cm^2$), but was maintained in the same range after 90 min (−32.9±12.9 $\Omega\times cm^2$). However, monolayer integrity after NA addition was not different from controls at any time point ($P>.05$). In contrast, a strong time-dependent increase in TEER was monitored after addition of 1 mM MPP, showing the most pronounced effect with an average augmentation of 77.0±10.9 $\Omega\times cm^2$ after 90 min. Changes in TEER provoked by MPP addition significantly differed ($P<.001$) from those of controls at 30, 60 and 90 min, respectively.

4. Discussion

NA has been in use as a lipid-lowering drug for the last decades as it is effective in lowering the blood levels of low-density lipoprotein cholesterol, triglycerides and lipoprotein(a), and in increasing levels high-density lipoprotein cholesterol [7,8]. However, its effects on intestinal fatty acid uptake have been incompletely investigated. In order to elucidate the structural determinants of pyridines responsible for their impact on fatty acid uptake by enterocyte-like Caco-2 cells, NA and NA analogs were tested. Moreover, we intended to clarify the mechanisms of action by which two of the studied pyridines, NA and MPP, might modify intestinal fatty acid uptake.

Results from the multiple linear regression analysis of data obtained from the fatty acid uptake studies in differentiated
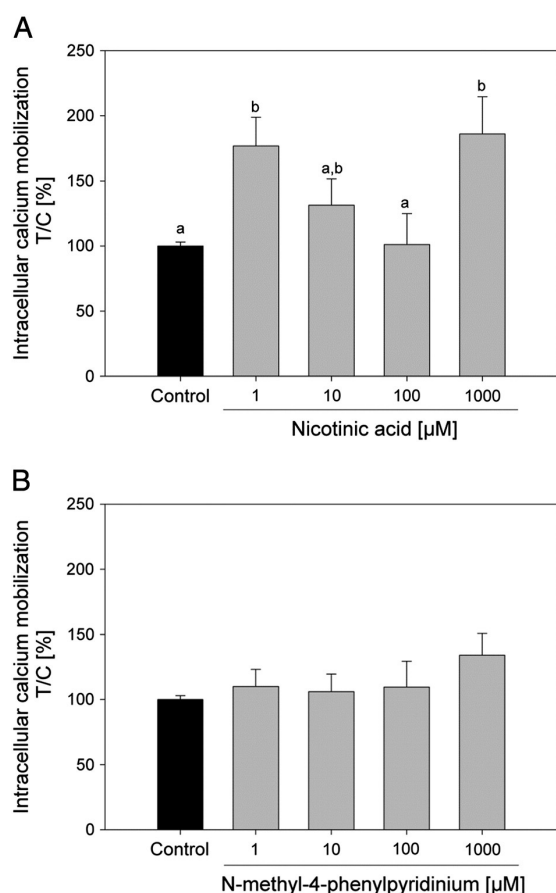

Fig. 7. Intracellular calcium mobilization after direct addition of with NA (A) and MPP (B) to differentiated Caco-2 cells. Data are shown as mean±S.E.M. ($n \geq 3$). For statistical analysis, one-way ANOVA with Holm–Sidak post hoc test was performed, and significant differences ($P<.05$) between treatments are indicated with distinct letters.

enterocyte-like Caco-2 cells revealed an additional methyl group as an important structural determinant for a compound affecting fatty acid uptake when applied at a concentration of 0.1 mM. As a result, *N*-methyl-2-picolinium presents a promising pyridine derivative that may increase intestinal fatty acid uptake. At a concentration of 1 mM, the carboxylic group was also identified as a significant structural determinant. Treatment of Caco-2 cells with the monocarboxylated pyridine derivative NA and its position isomers iso-NA and picolinic acid stimulated fatty acid uptake. In contrast, *N*-methylation was identified as an inhibitory characteristic. However, identification of the three structural determinants, the presence of (i) a methyl group, (ii) a carboxylic group and (iii) *N*-methylation, as important structural characteristics affecting fatty acid uptake in differentiated Caco-2 cells provides the first evidence for their specific mode of action.

NA, which shows the most pronounced stimulating effect on fatty acid uptake, and MPP, which inhibits fatty acid uptake, were selected for mechanistic studies.

NA is used pharmacologically to treat hyperlipidemia. Oral administration of 200 mg NA was shown to reduce plasma free fatty acids within minutes, followed by a rebound effect 1 h after administration [7]. Therefore, up to 3 g of NA per day are administered to humans to achieve a prolonged reduction of plasma lipids and total cholesterol [23–25]. However, substantial side effects, such as skin flushing, are associated with high-dose administration of NA [10]. Dietary intake of NA is far lower than that needed to obtain pharmacological effects. Lang et al. [1] estimated NA contents in several foods and found about 3.45 μg/g in breakfast cereals, 5.79 μg/g in beef liver and up to 369 μg/g in roasted coffee. However, analytical quantification of NA is challenging due to its rapid metabolism. NA has so far not been detected in generic human plasma samples [1], nor in plasma samples after administration of 350 ml freshly prepared coffee brew containing about 3.1 mg NA [2]. Plasma NA concentrations slightly above the limit of quantification (0.4 μM) were only reported in samples from a clinical pharmacokinetic study after bolus administration of 1000 mg NA [26].

In this study, no toxic effects of NA on differentiated Caco-2 cells were found in a concentration range of 0.001–1 mM for 90 min. Interfering effects of intestinal fatty acid and glucose uptake induced by NA could be excluded as glucose uptake remained unchanged after administration of NA.

Therefore, we focused on the modulation of the NA receptors involved in lipid metabolism and modifications of gene expression patterns of fatty acid transporters and genes involved in the regulation of fatty acid metabolism.

With the identification of the NA receptors, the antipolytic effect of NA in the adipose tissue could be explained [11–13]. Upon activation, these G-protein-coupled receptors inhibit the enzyme adenylyl cyclase [27] and, hence, reduce the formation of cAMP [28]. Results from tissue distribution studies point to a predominant expression of NA receptors in the adipose tissue, lung, lymphocytes and spleen [11,13]. More recently, expression of both receptor subtypes has been proven in several colon cancer cell lines but had not been investigated in Caco-2 cells [29], although HM74A has recently been verified in a subclone of Caco-2, C2BBe1 cells [30]. Here, we provide evidence that undifferentiated Caco-2 cells also express the low-affinity NA receptor HM74 and that its expression is substantially increased upon differentiation to enterocyte-like cells. In contrast, the high-affinity version HM74A was not detectable. We further demonstrated that incubation of differentiated Caco-2 cells with 1 mM NA up-regulated *HM74* expression, indicating a stimulating effect of NA on HM74 that might account for the increased fatty acid uptake. Knowles et al. [31] showed that activation of the NA receptors in macrophages promotes prostaglandin D₂ production. Both subtypes, the low-affinity version HM74 and the high-affinity version HM74A are involved in the initiation of the prostaglandin pathway [31]. Consequently, the NA-induced prostaglandin D₂ formation and subsequent PPARγ activation might explain the enhanced transcription of fatty acid translocase/CD36 monitored in monocytoid cells after a 3-h treatment with 1 mM NA [32].

In intestinal cells, several FATPs have been identified [20,33,34]. We first showed that expression of the analyzed genes was more abundant in differentiated Caco-2 cells compared to the undifferentiated cells, except for *FATP4*, thereby presenting characteristic metabolic changes of the enterocyte-like differentiated Caco-2 cells compared to undifferentiated cells.

Administration of NA up-regulated *CD36*, *FATP2* and *FATP4* gene expression in enterocyte-like Caco-2 cells. This result clearly indicates a stimulating effect on fatty acid transporters. We also monitored the short-term up-regulation of *PPARα* and *PPARγ* gene expression. PPARα is a major regulator of lipid metabolism. Activation of the transcription factor PPARα has been shown to increase CD36 expression in the liver and the intestine of mice [35]. Furthermore, PPARα is associated with enhanced fatty acid uptake, utilization and catabolism [36].

Our *in vitro* data clearly support the hypothesis that, in intestinal cells, NA is able to activate the NA receptor HM74. Its activation may lead to prostaglandin D₂ formation, subsequent PPARγ activation and stimulation of CD36 expression, resulting in an enhanced intestinal fatty acid uptake. Although an increased intestinal fatty acid uptake may lead to higher levels of circulating free fatty acids and lipoproteins, the plasma lipid-lowering effects of NAs are well established. Thus, we hypothesize that an increased intestinal fatty acid uptake in the presence of NA might be compensated by (i) repression of lipolysis in adipocytes or (ii) inhibition of hepatic diacylglycerol acyltransferase and triglyceride synthesis resulting in reduced secretion of lipoproteins from the liver [37].

We further demonstrated an inhibition of fatty acid uptake by Caco-2 cells by MPP treatment. MPP has been shown to possess toxic effects [38]. On a cellular level, treatment of neural cells with MPP caused dopaminergic neurodegeneration and bioenergetic dysfunction due to a repression of oxygen consumption as a consequence of mitochondrial respiratory complex 1 activity inhibition [39,40]. However, in this study, MPP concentrations up to 1 mM for 90 min showed no toxic effects on Caco-2 cells. No changes in glucose uptake and NA receptor *HM74* expression were monitored after MPP treatment. Fatty acid transporter and *PPARγ* gene expression were only slightly affected. These results led to the assumption that, although NA and MPP share the pyridine core and both affect fatty acid uptake in differentiated enterocyte-like Caco-2 cells, the underlying mechanisms of action differ from each other. In particular, the inhibitory effect on fatty acid uptake demonstrated for MPP is very unlikely based on inhibition of the NA receptor.

In contrast, TEER increased after the addition of MPP to differentiated Caco-2 cells. An augmented TEER was also monitored after incubation of Caco-2 cells with short-chain fatty acids [41], quercetin [42] or apple extracts [43], thus reducing paracellular permeability and enhancing the cellular barrier function. Changes in TEER have been associated with an altered membrane protein composition, contributing to a stronger conjunction of cells [42,43]. We therefore hypothesize that MPP treatment reduced fatty acid uptake by modifying the paracellular permeability and the membrane integrity, diminishing passive diffusion. Moreover, TEER increased constantly after MPP treatment. This result might be interpreted as counteraction of the cells to MPP exposure to prevent adverse effects on mitochondrial function.

In conclusion, this study elucidated the effects of pyridine derivatives on fatty acid uptake in enterocyte-like differentiated Caco-2 cells. Multiple linear regression analysis revealed a methyl group and a carboxylic group to be structural determinants for pyridines affecting the fatty acid uptake. Two of the studied

ARTICLE IN PRESS

compounds, NA and MPP, although sharing the pyridine core motif, affected fatty acid uptake in differentiated Caco-2 cells differently. Whereas the stimulating effect of high-dose NA on fatty acid uptake was very likely evoked by NA receptor activation, resulting in an enhanced expression of genes involved in lipid metabolism as well as fatty acid transporters, MPP reduced fatty acid uptake by increasing TEER and, hence, impairing passive diffusion.

References

[1] Lang R, Yagar EF, Eggers R, Hofmann T. Quantitative investigation of trigonelline, nicotinic acid, and nicotinamide in foods, urine, and plasma by means of LC-MS/MS and stable isotope dilution analysis. J Agric Food Chem 2008;56:11114–21.

[2] Lang R, Wahl A, Skurk T, Yagar EF, Schmiech L, Eggers R, et al. Development of a hydrophilic liquid interaction chromatography–high-performance liquid chromatography-tandem mass spectrometry based stable isotope dilution analysis and pharmacokinetic studies on bioactive pyridines in human plasma and urine after coffee consumption. Anal Chem 2010;82:1486–97.

[3] Somoza V, Lindenmeier M, Wenzel E, Frank O, Erbersdobler HF, Hofmann T. Activity-guided identification of a chemopreventive compound in coffee beverage using in vitro and in vivo techniques. J Agric Food Chem 2003;51:6861–9.

[4] Rubach M, Lang R, Skupin C, Hofmann T, Somoza V. Activity-guided fractionation to characterize a coffee beverage that effectively down-regulates mechanisms of gastric acid secretion as compared to regular coffee. J Agric Food Chem 2010;58:4153–61.

[5] Boettler U, Volz N, Pahlke G, Teller N, Kotyczka C, Somoza V, et al. Coffees rich in chlorogenic acid or N-methylpyridinium induce chemopreventive phase II-enzymes via the Nrf2/ARE pathway in vitro and in vivo. Mol Nutr Food Res 2011;55:798–802.

[6] Riedel A, Hochkogler CM, Lang R, Bytof G, Lantz I, Hofmann T, et al. N-methylpyridinium, a degradation product of trigonelline upon coffee roasting, stimulates respiratory activity and promotes glucose utilization in HepG2 cells. Food Funct 2014;5:454-62.

[7] Carlson LA. Nicotinic acid: the broad-spectrum lipid drug. A 50th anniversary review. J Intern Med 2005;258:94–114.

[8] Altschul R, Hoffer A, Stephen JD. Influence of nicotinic acid on serum cholesterol in man. Arch Biochem Biophys 1955;54:558–9.

[9] Carlson LA. Studies on the effect of nicotinic acid on catecholamine stimulated lipolysis in adipose tissue in vitro. Acta Med Scand 1963;173:719–22.

[10] Morrow JD, Parsons III WG, Roberts II LJ. Release of markedly increased quantities of prostaglandin D2 in vivo in humans following the administration of nicotinic acid. Prostaglandins 1989;38:263–74.

[11] Soga T, Kamohara M, Takasaki J, Matsumoto S, Saito T, Ohishi T, et al. Molecular identification of nicotinic acid receptor. Biochem Biophys Res Commun 2003;303:364–9.

[12] Tunaru S, Kero J, Schaub A, Wufka C, Blaukat A, Pfeffer K, et al. PUMA-G and HM74 are receptors for nicotinic acid and mediate its anti-lipolytic effect. Nat Med 2003;9:352–5.

[13] Wise A, Foord SM, Fraser NJ, Barnes AA, Elshourbagy N, Eilert M, et al. Molecular identification of high and low affinity receptors for nicotinic acid. J Biol Chem 2003;278:9869–74.

[14] Offermanns S, Colletti SL, Lovenberg TW, Semple G, Wise A, AP IJ. International Union of Basic and Clinical Pharmacology. LXXXII: nomenclature and classification of hydroxy-carboxylic acid receptors (GPR81, GPR109A, and GPR109B). Pharmacol Rev 2011;63:269–90.

[15] Taggart AK, Kero J, Gan X, Cai TQ, Cheng K, Ippolito M, et al. (D)-beta-hydroxybutyrate inhibits adipocyte lipolysis via the nicotinic acid receptor PUMA-G. J Biol Chem 2005;280:26649–52.

[16] Lorenzen A, Stannek C, Lang H, Andrianov V, Kalvinsh I, Schwabe U. Characterization of a G protein-coupled receptor for nicotinic acid. Mol Pharmacol 2001;59:349–57.

[17] Meunier V, Bourrie M, Berger Y, Fabre G. The human intestinal epithelial cell line Caco-2; pharmacological and pharmacokinetic applications. Cell Biol Toxicol 1995;11:187–94.

[18] Tso P, Nauli A, Lo CM. Enterocyte fatty acid uptake and intestinal fatty acid-binding protein. Biochem Soc Trans 2004;32:75–8.

[19] Boettler U, Sommerfeld K, Volz N, Pahlke G, Teller N, Somoza V, et al. Coffee constituents as modulators of Nrf2 nuclear translocation and ARE (EpRE)-dependent gene expression. J Nutr Biochem 2011;22:426–40.

[20] Sandoval A, Fraisl P, Arias-Barrau E, Dirusso CC, Singer D, Sealls W, et al. Fatty acid transport and activation and the expression patterns of genes involved in fatty acid trafficking. Arch Biochem Biophys 2008;477:363–71.

[21] Soudijn W, van Wijngaarden I, Ijzerman AP. Nicotinic acid receptor subtypes and their ligands. Med Res Rev 2007;27:417–33.

[22] Zemann N, Zemann A, Klein P, Elmadfa I, Huettinger M. Differentiation- and polarization-dependent zinc tolerance in Caco-2 cells. Eur J Nutr 2011;50:379–86.

[23] Fitzgerald O, Heffernan A, Brennan P, Mulcahy R, Fennelly JJ, McFarlane R. Effect of nicotinic acid on abnormal serum lipids. Br Med J 1964;1:157–9.

[24] Parsons Jr WB, Achor RW, Berge KG, McKenzie BF, Barker NW. Changes in concentration of blood lipids following prolonged administration of large doses of nicotinic acid to persons with hypercholesterolemia: preliminary observations. Proc Staff Meet Mayo Clin 1956;31:377–90.

[25] Shepherd J, Packard CJ, Patsch JR, Gotto Jr AM, Taunton OD. Effects of nicotinic acid therapy on plasma high density lipoprotein subfraction distribution and composition and on apolipoprotein A metabolism. J Clin Invest 1979;63:858–67.

[26] Pfuhl P, Karcher U, Haring N, Baumeister A, Tawab MA, Schubert-Zsilavecz M. Simultaneous determination of niacin, niacinamide and nicotinuric acid in human plasma. J Pharm Biomed Anal 2005;36:1045–52.

[27] Aktories K, Schultz G, Jakobs KH. Regulation of adenylate cyclase activity in hamster adipocytes. Inhibition by prostaglandins, alpha-adrenergic agonists and nicotinic acid. Naunyn Schmiedebergs Arch Pharmacol 1980;312:167–73.

[28] Butcher RW, Baird CE, Sutherland EW. Effects of lipolytic and antilipolytic substances on adenosine 3′,5′-monophosphate levels in isolated fat cells. J Biol Chem 1968;243:1705–12.

[29] Thangaraju M, Cresci GA, Liu K, Ananth S, Gnanaprakasam JP, Browning DD, et al. GPR109A is a G-protein-coupled receptor for the bacterial fermentation product butyrate and functions as a tumor suppressor in colon. Cancer Res 2009;69:2826–32.

[30] Borthakur A, Priyamvada S, Kumar A, Natarajan AA, Gill RK, Alrefai WA, et al. A novel nutrient sensing mechanism underlies substrate-induced regulation of monocarboxylate transporter-1. Am J Physiol Gastrointest Liver Physiol 2012;303:G1126–33.

[31] Knowles HJ, te Poele RH, Workman P, Harris AL. Niacin induces PPARgamma expression and transcriptional activation in macrophages via HM74 and HM74a-mediated induction of prostaglandin synthesis pathways. Biochem Pharmacol 2006;71:646–56.

[32] Rubic T, Trottmann M, Lorenz RL. Stimulation of CD36 and the key effector of reverse cholesterol transport ATP-binding cassette A1 in monocytoid cells by niacin. Biochem Pharmacol 2004;67:411–9.

[33] Nassir F, Abumrad NA. CD36 and intestinal fatty acid absorption. Immun Endoc Metab Agents Med Chem 2009;8.

[34] Wang Q, Herrera-Ruiz D, Mathis AS, Cook TJ, Bhardwaj RK, Knipp GT. Expression of PPAR, RXR isoforms and fatty acid transporting proteins in the rat and human gastrointestinal tracts. J Pharm Sci 2005;94:363–72.

[35] Motojima K, Passilly P, Peters JM, Gonzalez FJ, Latruffe N. Expression of putative fatty acid transporter genes are regulated by peroxisome proliferator-activated receptor alpha and gamma activators in a tissue- and inducer-specific manner. J Biol Chem 1998;273:16710–4.

[36] Lefebvre P, Chinetti G, Fruchart JC, Staels B. Sorting out the roles of PPAR alpha in energy metabolism and vascular homeostasis. J Clin Invest 2006;116:571–80.

[37] Ganji SH, Kamanna VS, Kashyap ML. Niacin and cholesterol: role in cardiovascular disease (review). J Nutr Biochem 2003;14:298–305.

[38] Nicotra A, Parvez SH. Cell death induced by MPTP, a substrate for monoamine oxidase B. Toxicology 2000;153:157–66.

[39] Giordano S, Lee J, Darley-Usmar VM, Zhang J. Distinct effects of rotenone, 1-methyl-4-phenylpyridinium and 6-hydroxydopamine on cellular bioenergetics and cell death. PloS one 2012;7:e44610.

[40] Nakamura K, Bindokas VP, Marks JD, Wright DA, Frim DM, Miller RJ, et al. The selective toxicity of 1-methyl-4-phenylpyridinium to dopaminergic neurons: the role of mitochondrial complex I and reactive oxygen species revisited. Mol Pharmacol 2000;58:271–8.

[41] Mariadason JM, Barkla DH, Gibson PR. Effect of short-chain fatty acids on paracellular permeability in Caco-2 intestinal epithelium model. Am J Physiol 1997;272:G705–12.

[42] Amasheh M, Schlichter S, Amasheh S, Mankertz J, Zeitz M, Fromm M, et al. Quercetin enhances epithelial barrier function and increases claudin-4 expression in Caco-2 cells. J Nutr 2008;138:1067–73.

[43] Vreeburg RA, van Wezel EE, Ocana-Calahorro F, Mes JJ. Apple extract induces increased epithelial resistance and claudin 4 expression in Caco-2 cells. J Sci Food Agric 2012;92:439–44.

2.5 "Caffeine dose-dependently induces thermogenesis but restores ATP in HepG2 cells in culture"

Riedel, A.[a], Pignitter, M.[a], Hochkogler, C. M.[a], **Rohm, B.**[a], Walker, J.[a], Bytof, G.[b], Lantz, I.[b], and Somoza, V.[a]

[a] Department of Nutritional and Physiological Chemistry, University of Vienna, Althanstrasse 14 (UZAII) Room 2B578, A-1090 Vienna, Austria. E-mail: veronika.somoza@univie.ac.at; Fax: +43 1 4277 9706; Tel: +43 1 4277 70610
[b] Tchibo GmbH, Überseering 18, 22297 Hamburg, Germany

Food & Function

PAPER

Caffeine dose-dependently induces thermogenesis but restores ATP in HepG2 cells in culture

Annett Riedel,[a] Marc Pignitter,[a] Christina M. Hochkogler,[a] Barbara Rohm,[a] Jessica Walker,[a] Gerhard Bytof,[b] Ingo Lantz[b] and Veronika Somoza[*a]

Caffeine has been hypothesised as a thermogenic agent that might help to maintain a healthy body weight. Since very little is known about its actions on cellular energy metabolism, we investigated the effect of caffeine on mitochondrial oxidative phosphorylation, cellular energy supply and thermogenesis in HepG2 cells, and studied its action on fatty acid uptake and lipid accumulation in 3T3-L1 adipocytes at concentrations ranging from 30–1500 μM. In HepG2 cells, caffeine induced a depolarisation of the inner mitochondrial membrane, a feature of mitochondrial thermogenesis, both directly and after 24 h incubation. Increased concentrations of uncoupling protein-2 (UCP-2) also indicated a thermogenic activity of caffeine. Energy generating pathways, such as mitochondrial respiration, fatty acid oxidation and anaerobic lactate production, were attenuated by caffeine treatment. Nevertheless, HepG2 cells demonstrated a higher energy charge potential after exposure to caffeine that might result from energy restoration through attenuation of energy consuming pathways, as typically found in hibernating animals. In 3T3-L1 cells, in contrast, caffeine increased fatty acid uptake, but did not affect lipid accumulation. We provide evidence that caffeine stimulates thermogenesis but concomitantly causes energy restoration that may compensate enhanced energy expenditure.

Introduction

Overweight and adiposity are among the most prevalent health problems that contribute to the development of type II diabetes mellitus and the metabolic syndrome. Maintaining a healthy body weight, therefore, is relevant to health promotion.

A reduction in body weight is the consequence of a negative energy balance whereupon energy expenditure exceeds energy intake. Food is the only energy source for the human organism to maintain its biological functions. After ingestion, nutrients are metabolized and the resulting reducing agents, $NADH/H^+$ and $FADH_2$, are used by the mitochondrial respiratory chain to produce ATP. During oxidative phosphorylation, the amounts of $NADH/H^+$, $FADH_2$ and oxygen consumed correlate directly with the synthesized amounts of ATP.[1] In contrast, during thermogenesis, mitochondrial respiration is uncoupled from oxidative phosphorylation; hence, energy is lost as heat instead of energy conservation through ATP formation.

Natural uncoupling is provoked by uncoupling proteins (UCPs) and fatty acids. Synthetic uncoupling agents like carbonylcyanide *m*-chlorophenylhydrazone (CCCP), carbonylcyanide *p*-trifluoromethoxyphenylhydrazone (FCCP) or dinitrophenol are commonly used to mimic thermogenesis *in vitro*.[2]

Several foods, such as red peppers,[3] green tea[4] or coffee,[5] are supposed to affect human energy metabolism by inducing thermogenesis and/or increasing the metabolic rate. Recent human intervention studies showed a reduction in body weight and/or body fat after long-term coffee consumption.[6,7] Acheson *et al.* presented a stimulating effect of caffeinated coffee (4 mg kg⁻¹) on the base-line metabolic rate over a time span of 150 min in normal weight and obese subjects that was stronger than that of decaffeinated coffee. The authors also postulated an increased postprandial thermogenesis for a meal when taken with caffeinated coffee.[5] *In vitro*, administration of 15 mM caffeine was demonstrated to exhibit a direct effect on the mitochondrial activity of isolated human muscle fibers by increasing the respiration rate and concomitantly decreasing the mitochondrial membrane potential.[8] Furthermore, Kogure *et al.* showed that subcutaneous caffeine injection (60 mg kg⁻¹) to obese mice upregulated UCP gene expression in skeletal muscles and brown adipose tissue and, therefore, may contribute to thermogenesis.[9] Thus, caffeine is proposed to be the active thermogenic agent of coffee in the short-term. Considering plasma peak concentrations of 54 μM in humans after consumption of about 4 cups of coffee,[10] the applied concentrations in previous *in vitro* studies

[a]Department of Nutritional and Physiological Chemistry, University of Vienna, Althanstrasse 14 (UZAII) Room 2B578, A-1090 Vienna, Austria. E-mail: veronika.somoza@univie.ac.at; Fax: +43 1 4277 9706; Tel: +43 1 4277 70610
[b]Tchibo GmbH, Überseering 18, 22297 Hamburg, Germany

are hardly transferable to humans since they are far from concentrations that can be found in plasma after coffee consumption or caffeine administration. Nevertheless, the long-term effect of caffeine on body weight regulation in humans by increase of energy expenditure remains doubtful as adaptation to caffeine occurs.[11]

In the energy deficient state, lipolysis and fatty acid oxidation in adipose tissue are stimulated to provide substrates for ATP formation through the mitochondrial respiratory chain. Induction of lipolysis and inhibition of lipid accumulation are important targets for the reduction of body fat and body weight. *In vitro* studies on caffeine already demonstrated an inhibitory effect on intracellular lipid accumulation in mouse 3T3-L1 adipocytes.[12,13]

Since caffeine has been suggested to affect energy metabolism, this study aimed to characterize the effect of moderate caffeine concentrations on mechanisms of mitochondrial energy generation, thermogenesis and substrate supplying pathways combined in HepG2 cells and 3T3-L1 cells as well as the comparison of the short-term and long-term effect in one model system to elucidate the complex mechanisms of mitochondrial energy supply by caffeine. We hypothesised that caffeine stimulates mitochondrial thermogenesis in the short-term and in the long-term, but does not necessarily increase substrate oxidation rather than induce energy restoration.

Results

Cellular oxygen consumption

Cellular respiration was assessed in HepG2 cells after direct addition and 24 h pre-treatment with caffeine. The basal respiration was significantly reduced in HepG2 cells after direct addition of caffeine, although not in a dose-dependent manner (Fig. 1A). There was no direct effect of caffeine on the non-phosphorylation respiration after inhibition of ATP-synthase by oligomycin (OM). To test for maximum respiratory capacity, the respiratory chain uncoupler FCCP was added at a final concentration of 1 μM, a concentration that was ascertained to induce maximal respiration in controls (data not shown).

FCCP-stimulation caused a 1.9-fold increase in oxygen consumption of control cells compared to basal respiration. After administration of 30 μM caffeine, no respiratory stimulation could be observed by the addition of FCCP. The respiration rate was solely $63\% \pm 13\%$ in comparison to the initial respiration prior to caffeine addition (100%) and hardly reached the value of basal respiration during caffeine addition ($73\% \pm 8\%$) (Fig. 1A). Maximum respiration was not affected by caffeine at 300 μM and 1500 μM, and reached values similar to those of control cells.

In addition to the direct effects of caffeine on mitochondrial respiration, oxygen consumption was also determined after 24 h of exposure of HepG2 cells with caffeine. A dose-dependent decrease in basal respiration was noted after treatment with caffeine (Fig. 1B). Incubation with caffeine reduced the basal oxygen consumption rate by 33% (300 μM) and 36% (1500 μM), respectively. A 24 h treatment with caffeine affected neither oxygen consumption rates during ATP-synthase inhibition by oligomycin nor FCCP-uncoupled respiration rates.

The respiratory control ratio (RCR) calculated for untreated control cells was in accordance to values previously established for HepG2 cells by Desquiret *et al.*[14] Calculation of the RCR after treatment with caffeine revealed a significant reduction of the ratio of FCCP-stimulated and ATP-synthase-inhibited respiration after direct administration of caffeine at 30 μM. Direct addition of higher caffeine concentrations as well as 24 h pre-treatment did not have an impact on the RCR of HepG2 cells (Table 1).

Mitochondrial membrane potential ($\Delta\Psi_m$)

The results displayed in Fig. 2A and Fig. 2B represent the amount of depolarised cells based on the decrease of the

Table 1 Respiratory control ratio of HepG2 cells after direct addition and 24 h incubation with caffeine[a]

	Control	30 μM	300 μM	1500 μM
Direct	4.65 ± 0.52^a	1.80 ± 0.19^b	4.24 ± 0.54^a	4.57 ± 0.55^a
24 h	4.33 ± 0.45	3.08 ± 0.37	2.82 ± 0.29	3.96 ± 0.65

[a] Results are expressed as mean $\pm$ SEM, $n \geq 5$, significant differences are indicated with the letters a and b ($p < 0.05$).
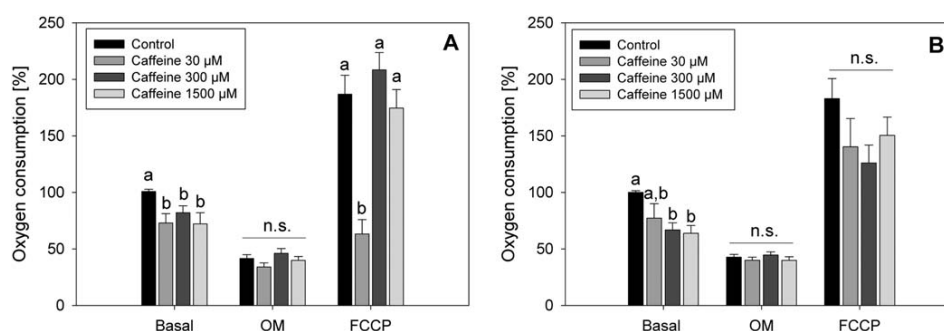
Fig. 1 Cellular oxygen consumption of HepG2 cells after direct addition of caffeine (A) and 24 h pre-treatment with caffeine (B) measured with a Clark-type electrode. The effects of caffeine on basal respiration, non-phosphorylating respiration after oligomycin (OM) addition and the maximum respiratory capacity induced by FCCP are shown for both time points. Results were normalized to basal respiration of controls (100%) (A) or initial respiration (100%) of each measurement (B), respectively. Data were expressed as mean $\pm$ SEM of at least 5 individual experiments. Significances were tested within one respiration phase by one-way ANOVA with SNK post hoc test ($p < 0.05$) and indicated with the letters a and b; n.s. = not significant.

mitochondrial membrane potential. Here, a decreased formation of JC-1 aggregates results in the reduction of yellow fluorescence.

Direct administration of caffeine led to a statistically significant increase of depolarisation induced by all tested caffeine concentrations. Although the observed effect of caffeine was not dose-dependent, an increased depolarisation up to 11% in the presence of caffeine at 300 μM could be reached, pointing to a mild uncoupling effect exhibited by caffeine directly (Fig. 2A). A more pronounced effect was observed after 24 h treatment of HepG2 cells with caffeine, leading to a significant and dose-dependent linear increase of depolarised cells. The rising amount of depolarisation induced by caffeine exposure ranged from +10% (30 μM) to +23% (1500 μM) in comparison to control cells. In contrast, treatment of cells with CCCP, a well-known respiratory chain uncoupler, led to strong induction of depolarisation of approximately 80% in total and a collapsed $\Delta\Psi_m$.

Uncoupling protein-2 (UCP-2) protein expression

The determination of UCP-2 in HepG2 cells demonstrated a dose-dependent increase in the UCP-2 content due to caffeine exposure for 24 h, as shown in Fig. 3. A treatment with caffeine at 1500 μM resulted in a significant increase ($p < 0.05$) of UCP-2 up to 40% compared to non-treated controls.

Cellular content of AMP, ADP and ATP

To establish the effect of caffeine on ATP production, cellular contents of AMP, ADP and ATP were quantified and the energy charge potential as a marker for cellular energy supply was calculated. Fig. 4A shows the energy charge potential (ECP) values after 24 h exposure of HepG2 cells in the absence or presence of caffeine. Untreated controls presented a high energy potential that surprisingly could be further increased by treatment with caffeine at 30 μM and 300 μM, respectively. The strongest effect on the ECP was achieved after incubation with caffeine at 30 μM, showing a dose-dependent reduction of the ECP with increasing caffeine concentrations, hence, obtaining values similar to controls after treatment with caffeine at 1500 μM. Quantitative data of AMP, ADP and ATP normalized to total adenosine nucleotides (TAN) demonstrated a significantly lower percentage of AMP with concomitant higher
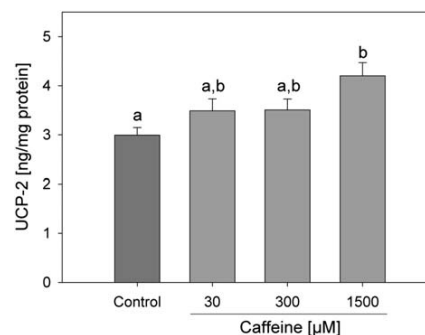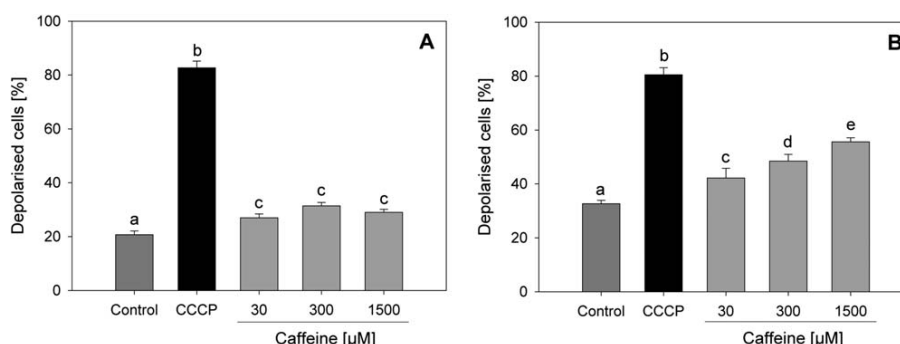

Fig. 3 UCP-2 protein expression of HepG2 cells after 24 h incubation with caffeine determined by ELISA. Significant differences ($p < 0.05$) between treatments were tested by one-way ANOVA with SNK post hoc test and are indicated with the letters a and b. Data represent mean ± SEM for four individual experiments.

percentage of ATP after 24 h treatment of HepG2 cells with 30 μM caffeine pointing to higher cellular ATP provision than in control cells (Fig. 4B). This effect could also be observed after exposure to 300 μM caffeine, although less pronounced. Data suggest a high cellular energy supply in HepG2 cells after 24 h exposure to caffeine (Fig. 4A) and an augmentation of depolarisation (Fig. 2B). The latter is associated with a decreased mitochondrial membrane potential that is typically monitored during uncoupling of the mitochondrial respiratory chain and related to reduced mitochondrial oxidative phosphorylation.

Lactate release

Glucose is the most important energy substrate that is degraded to pyruvate during glycolysis, then decarboxylated to acetyl-CoA and used for production of NADH/H⁺ through the citric acid cycle. NADH/H⁺ is a reducing agent that serves as an energy source for ATP production through mitochondrial oxidative phosphorylation.

As the mitochondrial oxygen consumption seems to be reduced in HepG2 cells due to caffeine exposure without impairment of the intracellular ATP content, lactate production as an alternative way for ATP formation was examined. Caffeine

Fig. 2 Mitochondrial membrane depolarisation of HepG2 cells induced by caffeine directly (A) and after 24 h incubation (B) measured by flow cytometry with the mitochondrial membrane potential sensitive fluorescent dye JC-1. The uncoupler CCCP (50 μM) was used as a positive control. Results are shown as mean ± SEM ($n \geq 3$) and dose-dependency was tested by one-way ANOVA with SNK post hoc test. Significant differences ($p < 0.05$) between treatments are indicated with the letters a–e.

69
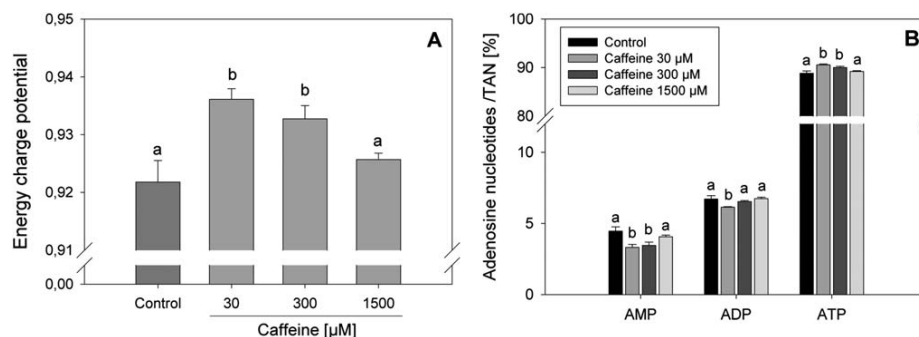
Fig. 4 Energy charge potential (ECP) (A) and cellular AMP, ADP and ATP content quantified by HPLC-DAD in HepG2 cells after 24 h treatment with caffeine. Cellular AMP, ADP and ATP content was normalized to total adenosine nucleotides (TAN). ECP = [ATP + 0.5(ADP)]/TAN was calculated according to the formula by Pradet and Raymond.[31] Results ($n = 4$) are shown as mean $\pm$ SEM (A) and percentage distribution of TAN (B). Significances were tested by one-way ANOVA with SNK post hoc test for pair-wise comparison ($p < 0.05$) and indicated with the letters a and b.

reduced lactate concentrations in the cell culture medium (Fig. 5). This decrease was statistically significant for treatment with caffeine at 1500 μM, showing a reduction of 13% in lactate production compared to control cells.

### Western blot analysis of carnitine palmitoyl transferase 1 (CPT1)

CPT1 is located in the outer mitochondrial membrane and is involved in fatty acid metabolism by regulating the transport of long-chain fatty acids into the mitochondria for β-oxidation. Western blot analyses revealed no effect of caffeine on CPT1 expression in HepG2 cells (Fig. 6A and 6B) after 24 h incubation.

Fatty acid uptake

The impact of caffeine on the uptake of long-chain fatty acids *via* fatty acid transport proteins (FATPs) was studied in 3T3-L1 adipocytes expressing FATP1 and FATP4[15] and HepG2 cells expressing FATP2 and FATP5,[16] respectively. As positive control, insulin (100 nM) was used in both cell lines.

Administration of insulin to 3T3-L1 adipocytes resulted in a significantly increased fatty acid uptake being 47% higher than in non-treated control cells (Fig. 7B), an effect that is already described in the literature.[15,17] A significant stimulating effect of insulin on fatty acid uptake could also be demonstrated in HepG2 cells (Fig. 7A), although less pronounced than in adipocytes.

Caffeine treatment of HepG2 cells caused a significant inhibition of fatty acid uptake ranging from 10% (30 μM and 300 μM) to 16% (1500 μM). In contrast, treatment of 3T3-L1 cells with caffeine enhanced fatty acid uptake (Fig. 7A). A 1.2-fold significant increase was observed by addition of caffeine at 30 μM. No effect was noticed after exposure of 3T3-L1 adipocytes to higher caffeine concentrations.
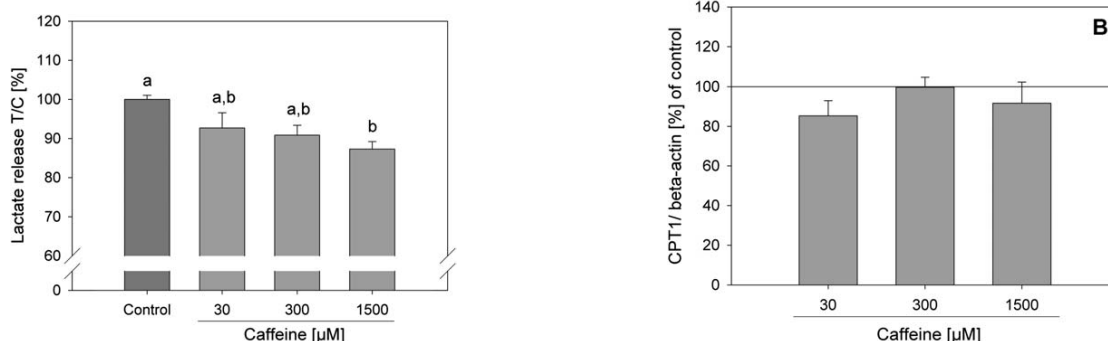
Fig. 5 Lactate release of HepG2 cells determined by LC-MS in incubation medium after 24 h exposure to caffeine. Results were normalized to untreated controls (100%) and are displayed as mean $\pm$ SEM of four individual experiments. Statistical analysis was performed by one-way ANOVA with SNK post hoc test and considered to be significant at $p < 0.05$ indicated with the letters a and b.

Fig. 6 CPT1 protein levels of HepG2 cells after exposure to caffeine (24 h) examined by Western blot analysis. A representative CPT1 blot with β-actin as internal control to ensure equal protein loading is displayed (A). CPT1/β-actin band intensity ratios after caffeine treatment were related to the corresponding ratios of untreated controls (100%) (B). Results are shown as mean $\pm$ SEM ($n = 4$).
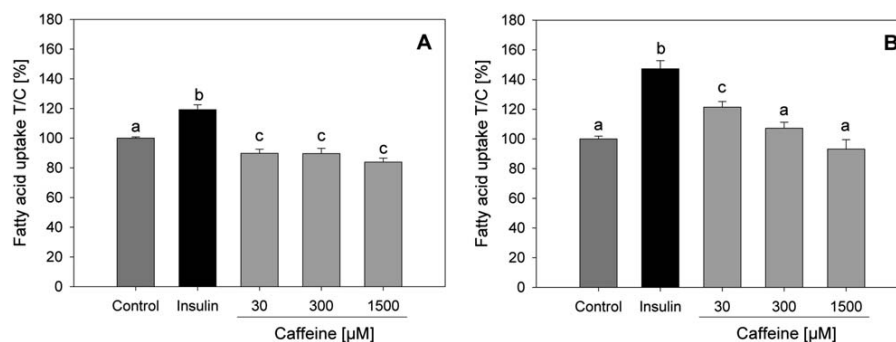
Fig. 7 Fatty acid uptake of HepG2 cells (A) and differentiated 3T3-L1 adipocytes (B) determined by addition of the BODIPY®-dodecanoic acid fluorescent fatty acid analog after 30 min pre-incubation with caffeine. Insulin (100 nM) was used as a positive control. Results represent mean $\pm$ SEM ($n = 4$) calculated from the AUC values obtained after 60 min of fluorescence measurement and normalized to untreated controls (100%). Significances between treatments were tested by one-way ANOVA with SNK post hoc test for pair-wise comparison ($p < 0.05$) and indicated with the letters a to c.

Lipid accumulation

The effect of caffeine on lipid accumulation in differentiated adipocytes was investigated by Oil Red O staining of incorporated oil droplets. However, no effect of caffeine on intracellular lipid accumulation was observed after 10 days of treatment (Fig. 8).

Discussion

This study examined the impact of caffeine on mitochondrial energy metabolism and cellular energy supply to investigate the potential effect of caffeine on cellular energy metabolism. ATP production occurs primarily in mitochondria by oxidative phosphorylation within the respiratory chain. During coupled respiration, the amount of oxygen consumed is proportional to the amount of ATP produced. We demonstrate that caffeine directly inhibited mitochondrial oxygen consumption in HepG2 cells, at a concentration of 30 μM that may be reached as peak plasma concentration after consumption of 3–4 cups of coffee.[10] In contrast, baseline plasma caffeine concentration after regular coffee intake was shown to be approximately 0.4 μM.[18] An inhibitory effect was also found by de la Cruz et al. after addition of caffeine to isolated rat liver mitochondria.[19] However, similar

Fig. 8 Lipid accumulation in differentiated 3T3-L1 adipocytes after 10 days of exposure to caffeine. Oil droplets were stained with Oil red O. A one-way ANOVA was performed to test for dose-dependency. Data are expressed as mean $\pm$ SEM for 3 individual experiments.

effects to those observed in this study were only reached after administration of at least 10 mM caffeine. Oxygen consumption studies by Dulloo et al. in interscapular brown adipose tissue from rats could not ascertain any effect of caffeine in concentrations up to 250 μM[20] and found respiratory stimulation only after treatment with concentrations higher than 2 mM.[21] A stimulating effect of respiration by direct addition of caffeine at 15 mM was also demonstrated in human muscle fibers,[22] indicating that effects of caffeine on mitochondrial respiration are partly opposed and strongly dose-dependent in various tissues.

So far, no data are available on the effects of caffeine on mitochondrial respiration after prolonged exposure. We revealed that caffeine also decreased basal respiration after 24 h incubation in a dose-dependent manner. As mitochondrial oxygen consumption is related to ATP production, these results indicate a reduced aerobic ATP production in human liver cells due to caffeine. This hypothesis is supported by the observed increase of mitochondrial membrane depolarisation. Caffeine induced a reduction of the mitochondrial membrane potential directly and more pronounced after 24 h treatment, suggesting a reduced ATP production. However, the half-life of caffeine in the plasma ranges between 2.5 and 4.5 h in healthy subjects due to rapid metabolism by the liver.[23] The observed long-term effects after exposure of HepG2 cells to caffeine, therefore, may also be mediated by endogenously generated metabolites.

Caffeine might also exhibit thermogenic effects by acting as a mild uncoupling agent that directly induces proton leaks and/or stimulates UCP-2 protein expression. We provide evidence that caffeine increases energy expenditure by inducing thermogenesis. Besides this, it was previously shown that high, non-physiological doses of caffeine (60 mg kg^{-1}) after subcutaneous injection upregulated UCP gene expression in brown adipose tissue and skeletal muscles of obese yellow KK mice.[9]

Regarding these findings, caffeine seems to alter mitochondrial energy production on the one hand by inhibiting oxygen consumption and increasing depolarisation, respectively, both resulting in a reduced ATP production, and, on the other hand, by increasing thermogenesis.

Quantification of cellular adenosine nucleotides after 24 h treatment of HepG2 cells with caffeine revealed a significantly higher ECP for caffeine at 30 μM and even an ECP value similar
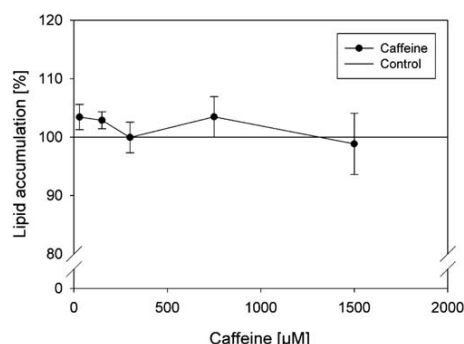
to this of controls for caffeine at 1500 μM. Since caffeine at 1500 μM reduced mitochondrial respiration, showed strong effects on mitochondrial membrane depolarisation and induced uncoupling by UCP-2, alternative pathways to supply the cellular energy or ATP demand might have been activated. An alternative way to produce ATP *via* oxidative phosphorylation is lactate production under anaerobic conditions. Oxidation of 1 mol glucose under aerobic conditions yields in 36 molecules ATP, whereas anaerobic ATP formation *via* lactate generates only 2 molecules ATP per mol of glucose. Although anaerobic ATP formation is less efficient, it represents a faster way in short-term energy supply predominantly found in muscle cells. It is known from the literature that energy production in cancer cells is shifted to lactic acid fermentation, namely known as the Warburg effect,[24] taking place even under normal oxygen conditions. Therefore, we examined lactate release of HepG2 cells after 24 h exposure to caffeine. We found that lactate release was significantly reduced after incubation with caffeine at 1500 μM, whereby lower caffeine concentrations did not show any impact on lactate release, leading to the conclusion that a shift of energy production to the lactate pathway might not contribute to the high energy supply. A further substrate used by cancer cells to produce ATP is glutamine. By "glutaminolysis", glutamine enters the citric acid cycle and (1) can be completely used for aerobic ATP production in the mitochondrial respiratory chain or (2) further converted to pyruvate, resulting in lactate production.[25] As utilisation of glutamine for ATP formation within mitochondrial oxidative phosphorylation would raise oxygen consumption and the alternative way would lead to augmented lactate production, we can exclude a shift to glutamine as substrate for the high energy supply prevalent after treatment of HepG2 cells with caffeine.

Moreover, caffeine is supposed to affect lipid metabolism *in vitro*[12,13] and *in vivo*.[13,26] A previous study by Shimoda *et al.* showed that caffeine administration resulted in a reduction of serum triglycerides in mice after olive oil-load in the short-term, but no effect of caffeine on CPT1 activity in mice liver mitochondria could be found in the long-term.[26] As CPT1 is the rate-limiting enzyme that is involved in long-chain fatty acid transport into mitochondria, we investigated the effect of caffeine on CPT1 protein levels to determine whether the increased ATP concentration presented in this study after caffeine treatment is a consequence of fatty acid oxidation. However, no effect of caffeine on CPT1 expression in HepG2 cells could be observed after 24 h incubation. Indeed, we found a direct impact of caffeine on cellular fatty acid uptake. Independent from the caffeine concentration, the fatty acid uptake of HepG2 cells was diminished, pointing to a reduced activity of fatty acid transport proteins. As energy producing pathways did not seem to be increased rather than reduced by caffeine, another possibility to maintain cellular energy potential is a depression of metabolic activity, suggesting that caffeine might cause energy restoration. Hypometabolism, as is found during hibernation, is characterized by reduction of metabolic rates and energy consuming pathways to endure harsh environmental conditions.[27] Moreover, an increase of uncoupling protein mRNA expression in various tissues, suggesting a contribution to thermogenesis during hibernation of ground squirrels, has been shown.[28] Similarly, we here ascertained the induction of UCP-2

by caffeine in HepG2 cells, a fact that is consistent with observations during hibernation.

A typical feature of hibernation is also the seasonal weight gain, primarily due to fat storage in adipocytes in preparation of hibernation.[29] Grant hypothesised that human obesity might be a preparation for hibernation that in the end does not take place.[30]

Thus, we further investigated the effect of caffeine on fatty acid uptake in differentiated 3T3-L1 adipocytes. In contrast to HepG2 cells, fatty acid uptake in 3T3-L1 cells was increased by 21% after administration of caffeine at 30 μM, whereas treatment with higher caffeine concentrations did not show differences to controls. This finding would support the hypothesis of Grant,[30] but interestingly, higher fatty acid uptake did not lead to an elevated lipid accumulation in 3T3-L1 cells after 10 day long-term exposure to caffeine, which, in contrast, disagrees with the hypothesis that caffeine may induce additional fat accumulation.

Experimental

Materials and chemicals

Unless stated otherwise, all materials, chemicals and reagents were purchased from Sigma-Aldrich, Austria.

Cell culture

HepG2 cells. The human hepatocellular carcinoma cell line HepG2 was cultured in RPMI-1640 medium (supplemented with 10% FBS, 4 mM L-glutamine and 1% penicillin/streptomycin) and maintained at 37 °C and 5% CO_2 in a humidified incubator. For studying the long-term effect of caffeine, cells were seeded one day prior 24 h treatment with caffeine (30 μM, 300 μM and 1500 μM) in incubation medium (RPMI-1640 with 4 mM L-glutamine and 1% penicillin/streptomycin). Controls were treated with incubation medium only. For determination of the direct effect, caffeine was added directly during assay performance.

3T3-L1 adipocytes. Mouse 3T3-L1 pre-adipocytes were cultured in the basal medium (high-glucose DMEM supplemented with 10% FBS, 4 mM L-glutamine and 1% penicillin/streptomycin). For differentiation, pre-adipocytes were grown two days post-confluence in basal medium and differentiation was initiated by replacing the basal medium to the differentiation medium (basal medium supplemented with 10 μg mL⁻¹ insulin, 1 μM dexamethasone and 0.5 mM isobutylmethylxanthine) for two days. Then, the medium was changed to the maturation medium (basal medium supplemented with 10 μg mL⁻¹ insulin) and cells were maintained for further two days. After additional three to five days of subsequent culture in basal medium, differentiated cells showing the typical adipocyte phenotype (accumulation of lipid droplets) were used for the measurement of direct effects of caffeine. For long-term studies, differentiated 3T3-L1 adipocytes were incubated in basal medium in the absence or presence of caffeine (30 μM, 300 μM and 1500 μM) for 10 days exchanging the incubation medium every second day.

Cell viability

HepG2 cells. Cell viability was assessed by the WST-1 assay (Roche Diagnostics, Switzerland) and performed according to the manufacture's protocol to exclude cytotoxic effects of treatments. As caffeine at 3000 μM was toxic to HepG2 cells, this concentration was excluded in further analyses (data not shown).

3T3-L1 adipocytes. Toxicity was determined by the MTT assay. After 10 days of exposure, the incubation medium was removed and MTT working solution (1 : 6 dilution of 5 mg mL^{-1} MTT stock solution in RPMI-1640 medium) was added. Cells were incubated for 4 h during which viable cells reduced the yellow MTT reagent to a purple formazan. Afterwards, the medium was removed and DMSO was added to dissolve the formazan product. Optical density was measured with a microplate reader (infinite M200, Tecan, Austria) at 550 nm using a reference wavelength of 690 nm to correct for unspecific absorbance. No toxic effects could be observed up to caffeine concentrations of 1500 μM (data not shown).

Mitochondrial oxygen consumption measurement in intact cells

Oxygen consumption measurements were carried out in intact HepG2 cells with slight modifications of the method described by Loiseau *et al.*[31] For measurement of mitochondrial oxygen consumption following 24 h treatment with caffeine, HepG2 cells were washed with PBS and harvested by trypsinization. The cell suspension was centrifuged at $110 \times g$ for 5 min. The pellet was resuspended in at 37 °C air-equilibrated RPMI-1640 medium supplemented with 4 mM L-glutamine to a final concentration of exactly 10×10^6 cells mL^{-1}. Immediately, 1 mL of cell suspension was transferred to the measurement chamber of a Clark-type oxygen electrode (Hansatech Instruments, UK) and maintained at 37 °C with constant stirring. The oxygen consumption measurement was started by recording the basal endogenous respiration rate. Then, oligomycin (8 μg mL^{-1}) was added to inhibit ATP-synthase and the non-phosphorylating respiration rate was determined. To induce the maximal respiratory activity, the uncoupler FCCP was added at a concentration of 1 μM. As FCCP acts biphasically in intact cells, a titration curve was performed to assess the optimal FCCP concentration that induced maximal uncoupled respiration (data not shown). Finally, the respiratory complexes I and III were inhibited by the addition of rotenone (1.25 μM) and antimycin A (3 μM), respectively. For measurement of the direct effect of caffeine on mitochondrial respiration, HepG2 cells were starved for 30 min prior to cell harvest and cell preparation was carried out as described above. After recording the initial basal oxygen consumption, caffeine was directly added to the cell suspension and the caffeine-induced respiration rate was assessed for 5 min. Oligomycin, FCCP, rotenone and antimycin A were subsequently added, as described above.

The linear rate of oxygen consumption during each phase of measurement was calculated. Respiration rates were related to the basal respiration rates of controls or the initial respiration rates when examining the direct effect of caffeine, respectively. Moreover, the mitochondrial respiratory control ratio (RCR) of intact cells was estimated as the ratio of oxygen consumed during uncoupling with FCCP to that during ATP-synthase inhibition after oligomycin addition.[31]

Mitochondrial membrane potential ($\Delta \Psi_m$)

Changes of the mitochondrial membrane potential were assessed using the JC-1 probe (BioVision, Inc., US) based on the method described by Cossarizza and Salvioli.[32] For determination of $\Delta \Psi_m$, 24 h pre-treated cells were washed with PBS and harvested with a detachment solution (PBS supplemented with 2 mM EDTA and 5 mM glucose). After centrifugation at $300 \times g$ for 5 min, the cell pellet was resuspended in the staining medium (MEM medium supplemented with 2 mM L-glutamine and 1% penicillin/streptomycin). The JC-1 dye dissolved in DMSO was added to a final concentration of 4 μM and samples were incubated for 15 min at 37 °C. To calibrate the method, a 5 min pre-incubation with 50 μM CCCP, an uncoupler that strongly decreases the mitochondrial membrane potential, was performed. Samples were centrifuged at $300 \times g$ for 5 min and washed once with washing buffer (PBS supplemented with 5% FBS). After another centrifugation at $300 \times g$ for 5 min, the stained cell pellets were resuspended in the washing buffer to a maximum concentration of 500 cells μL^{-1}. Yellow fluorescence, as shown by JC-1 aggregates in the mitochondrial matrix of polarised cells, as well as green fluorescence, emitted by JC-1 monomers in the cytosol of depolarised cells, were assessed with the EasyCyte 8HT flow cytometer (Millipore GesmbH, Austria). The direct effect of caffeine on the mitochondrial membrane potential was determined by adding caffeine to the cell suspension and allowing a 5 min incubation prior to staining with the JC-1 dye.

Uncoupling protein-2 (UCP-2) protein expression

The cellular UCP-2 content of HepG2 cells was determined by ELISA. After 24 h treatment with caffeine, cells were washed quickly with ice-cold PBS and harvested by scraping in lysis buffer (50 mM Tris, 25 mM NaCl, 1 mM EDTA, 1 mM NaF, 1% Igepal, pH 7.4) supplemented with 1mM PMSF, 1mM sodium *ortho*-vanadate and protease inhibitor cocktail. After homogenization and centrifugation at 16 000 × g for 10 min at 4 °C, the supernatant was used for quantification of UCP-2 by means of a commercial ELISA kit (USCN Life Sciences, China). Results were normalized for total protein content of the supernatants determined by the bicinchoninic acid assay using bovine serum albumin (BSA) as a standard (Pierce® BCA Protein Assay Kit, Thermo Scientific, Austria).

Cellular content of AMP, ADP and ATP

The cellular content of the adenosine nucleotides AMP, ADP and ATP were measured in HepG2 cell extracts by HPLC-DAD. Therefore, 24 h pre-treated cells were washed with PBS and ice-cold perchloric acid (0.3 M) was added immediately. After scraping off the cells from the plate, cell lysates were centrifuged at 16 000 × g for 10 min at 4 °C. The pH of the acid extract was adjusted to pH 6 with sodium carbonate (1 M). Prior to HPLC injection, a solid phase extraction (SPE) was performed using the strata-X-AW polymeric weak anion column (Phenomenex, Germany) according to the manufacturer's protocol (application

note CN-039) with slight modifications. After activation of the column, first with methanol, then a mixture of formic acid/methanol/water (2/25/73) and finally water, cell extracts were loaded followed by washing steps with water and a methanol/water mixture (50/50). For elution, a mobile phase of ammonium hydroxide/methanol/water (2/25/73) was used and the eluted phase was passed through a 0.22 μm nylon filter (Carl Roth, Germany). Samples were injected into a Dionex Ultimate 3000 series UHPLC system consisting of a binary pump, a degasser, an autosampler and a column compartment connected to a diode array detector (Dionex, Austria). Data was collected using the Chromeleon 6.8 software (Dionex, Austria). The separation was achieved by gradient elution with mobile phase A consisting of 10 mM tetra-butyl-ammonium bisulphate, 10 mM potassium dihydrogen phosphate in water (pH 7.0) and 10% acetonitrile filtered through 0.2 μm regenerated cellulose (Carl Roth, Germany) while mobile phase B consisted of 100% acetonitrile (HPLC grade). The gradient was as follows: 0 min 100% A, 0% B; 1 min 100% A, 0% B; 8 min 92% A, 8% B; 13.5 min 70% A, 30% B; 18 min 100% A, 0% B; 29 min 100% A, 0% B. The column was a Phenomenex Luna® C18 (5 μm, 100 Å, 250 × 3 mm) LC column running at 25 °C. The mobile phase flow rate was 0.5 mL min^{-1}. The absorbance of the adenosine nucleotides was monitored at 259 nm. For quantification, an external six-point calibration curve was recorded for each standard (AMP 0.5–50 μM, ADP 0.5–50 μM, ATP 1–100 μM). Recovery was determined by standard addition to cell extracts prior to SPE and included in the final calculation (AMP 69.8% ± 7.1, ADP 91.8% ± 8.0, ATP 95.1% ± 9.6). From the final concentrations, the total adenosine nucleotides (TAN) value was calculated by TAN = ATP + ADP + AMP as well as the energy charge potential (ECP) by ECP = [ATP + 0.5(ADP)]/TAN as described by Pradet and Raymond.[33]

Lactate release

Lactate release was determined by LC-MS after 24 h incubation of HepG2 cells with caffeine. The incubation medium was removed and centrifuged at 16 000 × g at 4 °C for 20 min. Quantification of lactate in incubation medium was performed by the external standard method. Commercially available sodium lactate was used as an external standard for a five-point calibration curve within the range 1–50 μg mL^{-1} obtaining correlation coefficients of ≥0.999. All analyses were conducted in duplicates as described by Sickmann et al.[34] on the Shimadzu Prominence HPLC system equipped with a quaternary pump and a single-quadrupole mass spectrometer with ESI as interface (Shimadzu, Austria). Data integration was performed with Shimadzu LC-MS software LabSolutions Version 5. The analyses were accomplished isocratically at 0.5 mL min^{-1} on a Luna® 5 μm C18 100 Å LC column 250 × 3 mm (Phenomenex, Germany) as stationary phase at 25 °C. The mobile phase consisted of 20% methanol and 80% ultrapure water. A volume of 5 μL was injected and the total run time was 5 min. Prior injection the samples passed through a 0.22 μm nylon filter (Carl Roth, Germany). The mass spectrometer was operated in negative-ion mode. Lactate was determined with selected ion monitoring (SIM) for specific m/z of 89. For SIM mode, a nebulizing gas (N$_2$) flow of 1.5 L min^{-1}, a drying gas (N$_2$) flow of 5.0 L min^{-1},

a desolvation line temperature of 250 °C, a heat block temperature of 200 °C and an interface voltage of 4.5 kV was selected. For reliable identification of lactate, in-source fragmentation was applied to standards and samples revealing a prominent fragment ion at m/z of 45 after a decarboxylation reaction. To achieve in-source fragmentation a desolvation line voltage of −20 V and a Qarray® DC voltage of −40 V was used.

Western blot analysis of carnitine palmitoyl transferase 1 (CPT1)

After incubation of HepG2 cells with caffeine (30 μM, 300 μM and 1500 μM) for 24 h, cell lysates were prepared as described for UCP-2 protein expression and maintained under constant agitation for 30 min at 4 °C. Then, cell lysates were centrifuged at 16 000 × g for 10 min at 4 °C and the protein content of the cleared supernatant was determined by the Bradford assay.[35] Western blot analysis of CPT1 was performed as described by Mazzarelli et al.[36] with slight modifications. Protein extracts were boiled in loading buffer for 5 min at 95 °C and a total of 40 μg protein was subjected to a 10% SDS-PAGE. After separation, proteins were transferred by semi-dry blotting for 1.5 h to PVDF membranes (PeqLab Biotechnolgy, Austria), previously activated in methanol for 2 min and ice-cold blotting buffer (48 mM Tris, 39 mM glycine, 0.08% SDS, 20% MeOH) for 5 min. The membranes were blocked with 5% skim milk for 1 h for detection of CPT1 followed by overnight incubation at 4 °C with the primary CPT1 antibody (rabbit polyclonal anti-CPT1A H95, Santa Cruz Biotechnology, Inc., Germany) 1 : 500 diluted in 5% skim milk. The membranes were washed with TBS-T buffer and incubated for 1 h at room temperature with the secondary antibody (anti-rabbit IgG-HRP, Santa Cruz Biotechnology, Inc., Germany) 1 : 4000 diluted in 5% skim milk. After another washing with TBS-T buffer, membranes were developed using the SuperSignal chemoluminescent detection kit (Thermo Scientifc, Austria) and visualized with the Fusion device (Vilber Lourmat, Germany). β-Actin was used as a loading control. Sample preparation, protein separation and protein transfer were conducted as described for CPT1 detection. Membranes were blocked with 5% BSA for 1 h and incubated with the 1 : 2000 in 5% BSA diluted primary β-actin antibody (rabbit anti-β-actin 13E5 mAb, Cell Signaling Technology®, Germany) for 1.5 h at room temperature. After washing with TBS-T buffer the secondary antibody (anti-rabbit IgG-HRP, Cell Signaling Technology®, Germany) 1 : 1000 diluted in 5% BSA was added for 1 h at room temperature. The membranes were washed with TBS-T buffer, developed and detected as described above for CPT1. Band intensities were calculated by applying the ImageJ software.

Fatty acid uptake

HepG2 cells. The fatty acid uptake was determined by the QBT™ Fatty Acid Uptake Assay Kit (Molecular Devices Corporation, Germany) employing a BODIPY®-dodecanoic acid fluorescent fatty acid analog. HepG2 cells were deprived with serum-free medium for 1 h at 37 °C followed by addition of caffeine diluted in a HBSS/Hepes buffer. For controls only HBSS/Hepes was added and cells were allowed to incubate for

30 min at 37 °C. As a positive control, insulin at a final concentration of 100 nM was used. Then, the fluorescent fatty acid analog diluted in HBSS/Hepes buffer supplemented with 0.2% fatty acid free BSA was added and fluorescence signals were recorded for 60 min at 515 nm after excitation at 485 nm with the infinite M200 microplate reader (Tecan, Austria). The area under curve (AUC) was calculated for each sample to determine the cellular fatty acid uptake and results were expressed as percentage of controls.

3T3-L1 adipocytes. Differentiated adipocytes were seeded on the experimental day and left to adhere for 4 h prior to deprivation with serum-free medium for 1 h at 37 °C. The measurement of fatty acid uptake in adipocytes was performed according to the procedure as described for HepG2 cells.

Lipid accumulation

Lipid accumulation in differentiated 3T3-L1 adipocytes was determined by Oil Red O staining after 10 days of exposure to caffeine. The incubation medium was removed and a freshly prepared 10% formalin solution was added. After 5 min, the formalin solution was renewed and cells were fixed for another hour. After washing with 60% isopropanol, the cells were stained for 30 min with the Oil Red O working solution, consisting of six parts of the 3.5% Oil Red O in isopropanol (w/v) stock solution and four parts ultrapure water. The cells were washed four times with ultrapure water, left to dry and the stained oil droplets were dissolved in 100% isopropanol. Quantification was carried out by absorbance measurement at 520 nm with a microplate reader (infinite M200, Tecan, Austria). Lipid accumulation is presented as the percentage of control cells.

Statistical analysis

Data are presented as mean ± SEM. All experiments were done in multiple replicates as stated in the figures (n = number of biological replicates). Dose-dependent effects were determined by one-way analysis of variance (ANOVA) after performing a Nalimov outlier test. The Student–Newman–Keuls (SNK) test was applied as a post hoc test for pair-wise comparison. Significant differences between treatment groups ($p < 0.05$) are indicated in the figures with distinct letters.

Conclusions

Caffeine affects mitochondrial energy production in HepG2 cells in the short-term and in the long-term by enhancing thermogenesis, probably through mitochondrial uncoupling resulting from (1) a direct induction of proton leaks and (2) enhanced expression of uncoupling proteins, *e.g.* UCP-2. The cellular energy loss due to augmented thermogenesis was not compensated by either intensified mitochondrial oxidative phosphorylation or ATP formation, or a shift to anaerobic energy production. Therefore, we conclude that caffeine provokes energy restoration that might be the result of attenuated energy consuming pathways.

Compared to HepG2 cells, adipocytes may react differently to caffeine exposure. In the presence of fatty acids, caffeine did enhance fatty acid uptake, although no effect on lipid accumulation was observed. This result provides evidence for tissue specific actions of caffeine that need further investigation to judge the overall anti-obesity effect of caffeine.

Although the results of this *in vitro* study suggest an alteration of mitochondrial energy production and energy supply by caffeine, *in vivo* studies have to be considered to demonstrate this effect.

Abbreviations

AUC	area under curve
CCCP	carbonylcyanide *m*-chlorophenylhydrazone
CPT1	carnitine palmitoyl transferase 1
ECP	energy charge potential
FATP	fatty acid transport protein
FCCP	carbonylcyanide *p*-trifluoromethoxyphenylhydrazone
HBSS	Hank's buffered salt solution
OM	oligomycin
RCR	respiratory control ratio
SNK	Student–Newman–Keul
TAN	total adenosine nucleotides
UCP	uncoupling protein

Acknowledgements

References

1 B. B. Lowell and B. M. Spiegelman, *Nature*, 2000, **404**, 652–660.
2 V. P. Skulachev, *Biochim. Biophys. Acta, Bioenerg.*, 1998, **1363**, 100–124.
3 K. Ohnuki, S. Niwa, S. Maeda, N. Inoue, S. Yazawa and T. Fushiki, *Biosci., Biotechnol., Biochem.*, 2001, **65**, 2033–2036.
4 A. G. Dulloo, C. Duret, D. Rohrer, L. Girardier, N. Mensi, M. Fathi, P. Chantre and J. Vandermander, *Am. J. Clin. Nutr.*, 1999, **70**, 1040–1045.
5 K. J. Acheson, B. Zahorska-Markiewicz, P. Pittet, K. Anantharaman and E. Jéquier, *Am. J. Clin. Nutr.*, 1980, **33**, 989–997.
6 T. Bakuradze, N. Boehm, C. Janzowski, R. Lang, T. Hofmann, J.-P. Stockis, F. W. Albert, H. Stiebitz, G. Bytof, I. Lantz, M. Baum and G. Eisenbrand, *Mol. Nutr. Food Res.*, 2011, **55**, 793–797.
7 C. Kotyczka, U. Boettler, R. Lang, H. Stiebitz, G. Bytof, I. Lantz, T. Hofmann, D. Marko and V. Somoza, *Mol. Nutr. Food Res.*, 2011, **55**, 1582–1586.
8 Z. Khuchua, Y. Belikova and A. Kuznetsov, *Biochim. Biophys. Acta, Bioenerg.*, 1994, **1188**, 373–379.
9 A. Kogure, N. Sakane, Y. Takakura, T. Umekawa, K. Yoshioka, H. Nishino, T. Yamamoto, T. Kawada, T. Yoshikawa and T. Yoshida, *Clin. Exp. Pharmacol. Physiol.*, 2002, **29**, 391–394.
10 P. Verhoef, W. J. Pasman, T. Van Vliet, R. Urgert and M. B. Katan, *Am. J. Clin. Nutr.*, 2002, **76**, 1244–1248.
11 M. S. Westerterp-Plantenga, *Physiol. Behav.*, 2010, **100**, 42–46.

12 H. Nakabayashi, T. Hashimoto, H. Ashida, S. Nishiumi and K. Kanazawa, *BioFactors*, 2008, **34**, 293–302.

13 S. Murosaki, T. R. Lee, K. Muroyama, E. S. Shin, S. Y. Cho, Y. Yamamoto and S. J. Lee, *J. Nutr.*, 2007, **137**, 2252–2257.

14 V. Desquiret, D. Loiseau, C. Jacques, O. Douay, Y. Malthièry, P. Ritz and D. Roussel, *Biochim. Biophys. Acta, Bioenerg.*, 2006, **1757**, 21–30.

15 A. Stahl, J. G. Evans, S. Pattel, D. Hirsch and H. F. Lodish, *Dev. Cell*, 2002, **2**, 477–488.

16 A. Sandoval, P. Fraisl, E. Arias-Barrau, C. C. Dirusso, D. Singer, W. Sealls and P. N. Black, *Arch. Biochem. Biophys.*, 2008, **477**, 363–371.

17 W. Zhou, P. Madrid, A. Fluitt, A. Stahl and X. S. Xie, *J. Biomol. Screening*, 2010, **15**, 488–497.

18 H. Superko, W. Bortz and P. Williams, *Am. J. Clin. Nutr.*, 1991, **54**, 599–605.

19 M. J. de la Cruz, J. Alemany, I. Roncero and P. Albert, *Comp. Biochem. Physiol., Part C: Pharmacol., Toxicol.Endocrinol.*, 1988, **91**, 443–447.

20 A. G. Dulloo, J. Seydoux, L. Girardier, P. Chantre and J. Vandermander, *Int. J. Obes.*, 2000, **24**, 252–258.

21 A. G. Dulloo, J. Seydoux and L. Girardier, *Int. J. Obes.*, 1991, **15**, 317–326.

22 W. S. Kunz, A. V. Kuznetsov and F. N. Gellerich, *FEBS Lett.*, 1993, **323**, 188–190.

23 M. J. Arnaud, *Prog. Drug Res.*, 1987, **31**, 273–313.

24 O. Warburg, *Science*, 1956, **123**, 309–314.

25 M. Yuneva, *Cell Cycle*, 2008, **7**, 2083–2089.

26 H. Shimoda, E. Seki and M. Aitani, *BMC Complementary Altern. Med.*, 2006, **6**, 9.

27 K. B. Storey, *Gerontology*, 2010, **56**, 220–230.

28 B. B. Boyer, B. M. Barnes, B. B. Lowell and D. Grujic, *Am. J. Physiol.*, 1998, **275**, R1232–1238.

29 S. L. Martin, *Diabetes Vasc. Dis. Res.*, 2008, **5**, 76–81.

30 P. J. Grant, *Diabetes Vasc. Dis. Res.*, 2004, **1**, 67.

31 D. Loiseau, D. Morvan, A. Chevrollier, A. Demidem, O. Douay, P. Reynier and G. Stepien, *Mol. Carcinog.*, 2009, **48**, 733–741.

32 A. Cossarizza and S. Salvioli, *Cytometry*, 2010, **4**, 4–8.

33 A. Pradet and P. Raymond, *Annu. Rev. Plant Physiol.*, 1983, **34**, 199–224.

34 H. M. Sickmann, A. Schousboe, K. Fosgerau and H. S. Waagepetersen, *Neurochem. Res.*, 2005, **30**, 1295–1304.

35 M. M. Bradford, *Anal. Biochem.*, 1976, **72**, 248–254.

36 P. Mazzarelli, S. Pucci, E. Bonanno, F. Sesti and L. G. Spagnoli, *Therapy*, 2007, 1606–1613.

76

3. Conclusions and Perspectives

The present thesis aimed to identify aroma compounds regulating satiety and energy metabolism and elucidate underlying mechanisms. A first screening system for the identification of food compounds regulating mechanisms food intake should be based on the potency of the compound to stimulate neurotransmitter release from neural cell models. This requires suitable cell models on the one hand, and highly sensitive assays for the unstable analytes dopamine and serotonin on the other hand.

A frequently used cell model for dopamine release are PC-12 cells. These cells are pheochromocytoma cells from the rat and well-established model for neural processes. The first presented research article *((1) Identification of coffee components that stimulate dopamine release from pheochromocytoma cells (PC-12))* demonstrates that this cell model can be used to screen food components, e.g. coffee and coffee compounds, regarding their potency to stimulate dopamine release by means of a simple luminescence assay in 96-well format. However, due to quenching effects, this assay cannot be used for colored test compounds, limiting the application area of this assay. As an alternative, stimulation of the cells in Krebs-Ringer solution with or without addition of the test compounds with subsequent quantification using a sensitive ELISA assay is presented. In addition to the option to measure also colored test compounds, this assay has the advantage that an absolute quantification instead of a simple comparison to control-treated cells is possible as well.

The second article *((2) N(epsilon)-Carboxymethyllysine (CML), a Maillard reaction product, stimulates serotonin release and activates the receptor for advanced glycation end products (RAGE) in SH-SY5Y cells)* shows the usage of another neural cell model, SH-SY5Y cells, for the measurement of dopamine release. In comparison to rat pheochromocytoma PC-12 cells, the SH-SY5Y cell model provides the advantages that the cells directly originate from human neural cells, and are able to release quantifiable amounts of serotonin. Serotonin is even more closely connected to the regulation of food intake than dopamine. SH-SY5Y cells were, thus, used for the screening of potential satiety-mediating pungent aroma compounds. In addition, the research article demonstrates the connection of the functional assay serotonin release with the gene regulation of serotonin receptors which were analyzed with a customized microarray and verified by means of RT-qPCR. The linkage between function and gene regulation is an important factor, since mRNA expression does not always correlate with protein expression or lead to changes in the function of the concerning protein. This article is also the first report of the successful application of the customized microarray,

which contains probes for the whole human genome, but with additional probes for genes involved in the regulation of food intake and obesity. A further development of the microarray synthesis is presented in the third article *((3)Simultaneous light-directed synthesis of mirror-image microarrays in a photochemical reaction cell with flare suppression)*. This technique was used for the synthesis of a miRNA microarray, which was applied to study microRNA regulation in PART II of the present thesis. However, as presented here, regulation of gene expression analyzed by microarray should be verified by using more sensitive or precise methods like quantitative Real-Time PCR or digital droplet PCR, since very small differences are unlikely to be detected by microarray.

To summarize, the first three presented research articles demonstrate the establishment of a human neural screening model on a genetic and functional level to identify food components that potentially mediate satiety and thus, reduce food and energy intake. However, validation of the test compounds should be carried out in intestinal cells and adipocytes as well. Inhibition of intestinal nutrient uptake, especially fat is one strategy to maintain a healthy body weight. The establishment of a cellular model for intestinal nutrient uptake is presented in the article (4) *"Structure-dependent effects of pyridine derivatives on mechanisms of intestinal fatty acid uptake: Regulation of nicotinic acid receptor and fatty acid transporter expression"*. This study presents the impact of pyridine derivatives on fatty acid and glucose uptake in differentiated Caco-2 cells using fluorescence-labeled analogs of fatty acids and glucose for analysis. Caco-2 cells originate from colon carcinoma cells. However, upon differentiation, the cells develop characteristics of enterocytes localized in the small intestines, like micovilli tight junctions, making Caco-2 cells a suitable model for intestinal nutrient uptake [1].

Besides regulation of satiety and intestinal nutrient uptake, regulation of fat storage, especially via an inhibition of adipogenesis, is a suitable measure to maintain a healthy body weight. A widely-distributed model to analyze differentiation of preadipocytes to mature adipocytes, the process of adipogenesis, are 3T3-L1 fibroblasts. The article (5) *"Caffeine dose-dependently induces thermogenesis but restores ATP in HepG2 cells in culture"* contains a section which describes measurement of lipid accumulation using the lipid-soluble dye Oil red O. Analysis of lipid accumulation with oil red O is a frequently used marker for

---

[1] see also I. J. Hidalgo, T. J. Raub and R. T. Borchardt, *Gastroenterology*, 1989, **96**, 736-749

the degree of adipogenesis, and was used to investigate modulation of fat storage by pungent aroma compounds in PART II of the present thesis.

In conclusion, PART I of the present thesis describes the establishment of screening models to investigate mechanisms regulating food intake, intestinal nutrient uptake and fat storage in a combined approach of functional assays and gene regulation. The human neural cell line SH-SY5Y represents a model for central control of food intake via neurotransmitter release, whereas intestinal Caco-2 cells and 3T3-L1 adipocytes are models for peripheral control of energy, especially lipid, metabolism. All three cell models were used in PART II of the thesis in order to investigate pungent aroma compounds with potential anti-obesity effects in a holistic approach.
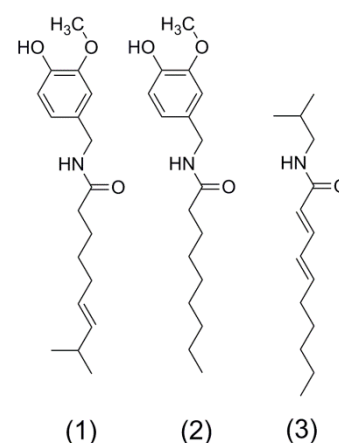
III.   PART II

Impact of the pungent aroma compounds capsaicin, nonivamide and trans-pellitorine on mechanisms regulating satiety and energy metabolism

1.   Objectives

Overweight and obesity are the result of a long-term imbalance between energy intake and consumption. The major pungent principle of red pepper, capsaicin, has been associated with increased satiety, decreased energy intake, increased thermogenesis, as well as hypolipidemic and hypocholsterolemic effects *in vivo* and *in vitro*. Mechanistic approaches reveal that the anti-obesogenic effects of capsaicin are associated with activation of the TRPV1 receptor, leading to increased intracellular Ca^{2+}, functioning as a second messenger in several signaling pathways. However, the down-side of capsaicin, being a high-affinity TRPV1 agonist is that activation of the TRPV1 receptor in the oral cavity leads to a sharp burning pain, limiting its dietary intake.

The first part of the present work was focused on the establishment of screening systems to investigate mechanisms regulating satiety and energy metabolism. However, the second part of the thesis aimed to characterize the effects of compounds, which are structurally related to capsaicin, but are not as pungent, on mechanisms regulating satiety and energy metabolism on the basis of cell culture experiments and a short-term human intervention trial. Cell culture studies were carried out in human neural SH-SY5Y cells to evaluate the effects of the target compounds on the release of the two satiety-mediating neurotransmitters serotonin and dopamine. A less pungent, direct structural analog of capsaicin, nonivamide, and the tingling

Figure 3. Chemical structures of capsaicin (1), nonivamide (2) and *trans*-pellitorine (3).

structural related compound from *Piper nigrum, trans*-pellitorine, were chosen for further mechanistic studies (**Figure 3**). The potential satiating effects of the most potent compound, nonivamide, were validated in a short-term human intervention trial that assessed plasma concentrations of the gastrointestinal satiety hormones PYY, GLP-1 and CCK as well as

glucose, insulin and serotonin after administration of a glucose solution with or without 0.15 mg nonivamide. In addition, energy intake from a standardized breakfast was recorded. In addition, further cell culture studies in Caco-2 cells compared the effects of nonivamide and another structural related compound, *trans*-pellitorine, on mechanisms of intestinal lipid metabolism to those of capsaicin. In 3T3-L1 adipocytes, the impact of nonivamide compared to capsaicin on adipogenesis and underlying mechanisms was evaluated.

2. Results

The second part of this cummulative dissertation is based on the following research articles and manuscripts:

(1) Nonivamide, a capsaicin analog, increases dopamine and serotonin release in SH-SY5Y cells via a TRPV1-independent pathway

Rohm, B.; Holik, A. K.; Somoza, M. M.; Pignitter, M.; Zaunschirm, M; Ley, J. P.;Krammer, G. E.; Somoza, V.

Molecular Nutrition and Food Research (2013), 57, 2008-18

In this manuscript, the impact of capsaicin and its less pungent structural analog, nonivamide, on TRPV1-dependent serotonin and dopamine release in the human neural cell line SH-SY5Y was assessed.

I participated in the experimental design and analyzed serotonin and dopamine release after stimulation with capsaicin and nonivamide in the presence or absence of the two different TRPV1 inhibitors capsazepine and *trans-tert*-butylcyclohexanol. Furthermore, I determined capsaicin and nonivamide-evoked intracellular calcium mobilization and gene expression levels of selected dopamine and serotonin receptors after incubation with nonivamide using qPCR and a customized microarray. For this purpose, I participated in microarray design and synthesis. In addition, I performed a subcellular fractionation of the cells for quantification of intracellular nonivamide uptake. Terminally, I performed the statistical analysis and prepared most of the manuscript.

Moreover, these data were the basis for the patent application "N-Nonanoylvanillylamin as a compound, as compound mixtures, as an orally consumable product and related technologies to reduce appetite, induce satiation, and improve mood" (Publication No. EP2,614,727,2013) J. Ley, G. Krammer, V. Somoza, **B. Rohm**

(2) Neurotransmitter-releasing potency of structural capsaicin-analogs in SH-SY5Y cells.

Rohm, B.,Zaunschirm, M.,Widder, S.,Ley, J. P.,Krammer, G.E.,Somoza,V.

In: Proceedings of the 10th Wartburg Symposium Eisenach (T. Hofmann, W. Meyerhof, P. Schieberle eds.) Verlag Deutsche Forschungsanstalt für Lebensmittelchemie.(2014). in press.

This study compared the potencency of nonivamide and *trans*-pellitroine, which are structurally related to capsaicin, to stimulate dopamine and serotonin relase in SH-SY5Y cells.

I participated in the experimental design and analyzed the effects of nonivamide on serotonin and dopamine release, and the effects of *trans*-pellitorine on serotonin release. In did the statistical analysis of the data and wrote the manuscript.

Moreover, these data were the basis for the patent application "Alkamides as means to reduce appetite" (application No. EP 13 155556.7) G. Krammer, J. Ley, S. Widder, M. Zaunschirm, **B. Rohm**, V. Somoza.

(3) The pungent capsaicin analog nonivamide decreases total energy intake and enhances plasma serotonin levels in men when administered in an OGTT: a randomized, crossover intervention

Hochkogler, C. M.; **Rohm, B**.; Hojdar, K.; Pignitter, M.;Widder, S.; Ley, J.P.; Krammer, G.E.; Somoza,V

Molecular Nutrition and Food Research (2014), epub ahead of print, DOI: 10.1002/mnfr.201300821

The impact of a bolus administration of 0.15 mg nonivamide to healthy volunteers in an oral glucose tolerance test on energy intake and plasma levels of satiety-mediating hormones was assessed.

I provided scientific input to the study design, and did the blood sample preparations on the intervention days. Furthermore, I was involved in the discussion of the data and supported writing of the manuscript.

(4) Capsaicin, nonivamide and *trans*-pellitorine decrease free fatty acid uptake without TRPV1 activation and increase acetyl-coenzyme A synthetase activity in Caco-2 cells

Rohm, B.; Riedel, A.; Widder, S.; Ley, J. P.; Krammer, G. E.; Somoza,V.

Food and Function (2014), submitted

The impact of capsaicin, nonivamide and *trans*-pellitorine on mechanisms regulating intestinal fatty uptake in Caco-2 cells were compared.

I participated in the experimental design and analyzed fatty acid uptake after pre-incubation with capsaicin, nonivamide and *trans*-pellitorine in the presence or absence of TRPV1 and ENaC inhibitors in differentiated Caco-2 cells. In addition, I performed cytotoxicity tests, 2-NBDG uptake, gene expression analysis and analyzed the trans-epithelial electrical resistance. In addition, I calculated IC_{50} concentrations and did the statistical analysis of the data. Finally, I also prepared the manuscript.

(5) Nonivamide, a capsaicin analog, decreases via TRPV1 activation adipogenesis and peroxisome proliferator-activated receptor gamma expression, and enhances miRNA let-7d expression in 3T3-L1 cells

Rohm, B.; Holik, A.-K.; Kretschy, N.; Somoza, M.M.; Widder, S.; Ley, J.P.; Krammer, G.E.; Somoza, V.

Journal of Biological Chemistry (2014), submitted

The impact of nonivamide, compared to capsaicin, on adipogenesis of 3T3-L1 pre-adipocytes and underling mechanisms, was determined.

I participated in the experimental design and assessed lipid accumulation as a marker for adipogenesis with or without addition of TRPV1-inhibitor *trans-tert*-butylcyclohexanol in 3T3-L1 cells. In addition, I analyzed PPARγ content on genetic and protein level and performed miRNA analysis using a microarray and digital droplet PCR. Therefore, I participated in the microarray design and hybridization. I performed the statistical analysis of the data and prepared the manuscript.

2.1 "**Nonivamide, a capsaicin analog, increases dopamine and serotonin release in SH-SY5Y cells via a TRPV1-independent pathway**"

Rohm, B.[a]; Holik, A. K.[b]; Somoza, M. M.[c]; Pignitter, M.[b]; Zaunschirm, M. [b]; Ley, J. P.[d]; Krammer, G. E.[d]; Somoza, V.[a,b]

a Christian Doppler Laboratory for Bioactive Aroma Compounds, University of Vienna, Vienna, Austria

b Department of Nutritional and Physiological Chemistry, University of Vienna, Vienna, Austria

c Department of Inorganic Chemistry, University of Vienna, Vienna, Austria

d Symrise AG, Holzminden, Germany

RESEARCH ARTICLE

Nonivamide, a capsaicin analog, increases dopamine and serotonin release in SH-SY5Y cells via a TRPV1-independent pathway

Barbara Rohm[1], Ann-Katrin Holik[2], Mark M. Somoza[3], Marc Pignitter[2], Mathias Zaunschirm[2], Jakob P. Ley[4], Gerhard E. Krammer[4] and Veronika Somoza[1,2]

[1] Christian Doppler Laboratory for Bioactive Aroma Compounds, University of Vienna, Vienna, Austria
[2] Department of Nutritional and Physiological Chemistry, University of Vienna, Vienna, Austria
[3] Department of Inorganic Chemistry, University of Vienna, Vienna, Austria
[4] Symrise AG, Holzminden, Germany

Scope: Dietary intake of capsaicin has been shown to reduce body weight by increasing energy expenditure, and to enhance alertness and mood by stimulating the brain's reward system. Binding of capsaicin to the vanilloid receptor 1 (transient receptor potential cation channel subfamily V member 1 (TRPV1)) is one of the major cellular mechanisms responsible for these effects. However, strong TRPV1 agonists like capsaicin elicit a sharp, burning pain that limits their dietary intake. The present study aimed to investigate the effect of the less pungent capsaicin-analog nonivamide on dopamine and serotonin release in neural SH-SY5Y cells.

Methods and results: Nonivamide (1 μM) stimulated the Ca^{2+}-dependent release of serotonin ($272 \pm 115\%$) and dopamine ($646 \pm 48\%$) in SH-SY5Y cells compared to nontreated cells (100%) to a similar extent as capsaicin. qRT-PCR analysis of 1 μM nonivamide-treated SH-SY5Y cells revealed gene regulation of the receptors dopamine D1 and D2, serotonin HTR1A, 1B and 2A, cannabinoid 1, and TRPV1. Co-incubation experiments of SH-SY5Y cells with the TRPV1 inhibitors *trans-tert*-butylcyclohexanol and capsazepine demonstrated that capsaicin, but not nonivamide, induces serotonin and dopamine release through TRPV1 activation.

Conclusion: The results indicate a TRPV1-independent signaling pathway for nonivamide that might allow dietary administration of higher doses of nonivamide compared to capsaicin.

1 Introduction

Dietary intake of the major pungent compound of *Capsicum annuum*, capsaicin, and its derivative capsiate, have been shown to benefit weight management through increased energy expenditure induced by activation of the transient receptor potential cation channel subfamily V member 1 (TRPV1), also known as the capsaicin receptor or the vanilloid recep-

Correspondence: Professor Veronika Somoza, Department of Nutritional and Physiological Chemistry, University of Vienna, Althanstraße 14, 1090 Vienna, Austria
E-mail: Veronika.Somoza@univie.ac.at
Fax: +43-1-4277-9706

Abbreviations: 5-HT, serotonin; **BCH**, *trans-tert*-butylcyclohexanol; **CZE**, capsazepine; **qRT-PCR**, quantitative real-time PCR; **T/C**, treated/control (fold change); **TRPV1**, transient receptor potential cation channel subfamily V member 1
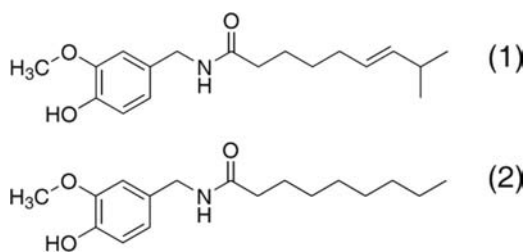
tor 1 [1–3]. Activation of the TRPV1 receptor not only affects mechanisms of energy metabolism, there is also a link to the brain's reward system, since the TRPV1 receptor interacts with the dopamine and the cannabinoid receptor systems [4, 5]. Capsaicin, a TRPV1 agonist that derives from the amino acid phenylalanine [6], is known to stimulate the firing rate of dopaminergic neurons in the ventral tegmental area of the brain [7] and to increase the expression of the serotonin receptor gene HTR2A [8]. Both mechanisms are part of the brain's reward system and are involved in the regulation of mood and food intake through release of the neurotransmitters dopamine and serotonin. Inhibition of the TRPV1 receptor demonstrated that release of these neurotransmitters is mediated by a nonselective TRPV1 cation channel [7], which is permeable to Ca^{2+} ions and responsible for triggering dopamine and serotonin release in neural cells [9, 10]. Capsaicin promotes Ca^{2+} influx via the TRPV1 cation channel and promotes phosphorylation of the downstream

Figure 1. Chemical structures of capsaicin (1) and nonivamide (2).

signaling factor Ca^{2+}/calmodulin-dependent protein kinase II [11], which might be a mechanism of capsaicin-induced TRPV1 activation. Moreover, capsaicin also stimulates Ca^{2+}-release from a ryanodine-sensitive intracellular calcium store [12].

The downside of capsaicin, being a high-affinity agonist of the TRPV1 receptor, is that its dietary intake evokes a sharp, burning pain in mammals. Therefore, less pungent structural analogs of capsaicin are sought to counteract the limited intake while still exhibiting positive effects on energy metabolism and the brain's reward system. Another TRPV1 agonist that affects mechanisms of energy homeostasis and the brain's reward system is the cannabinoid anandamide, also known as *N*-arachidonoylethanolamine [13]. Anandamide is less pungent than capsaicin, but its rapid degradation by the enzyme fatty acid amide hydrolase limits the metabolic efficacy of this compound.

The structural capsaicin analog, nonivamide, which differs from capsaicin in one double bound and one methyl group on the carbon chain (Fig. 1), is another known agonist of the TRPV1 receptor, although with lower TRPV1 binding affinity and, thus, a reduced pungency (9 200 000 scoville heat units) compared to capsaicin (16 000 000 scoville heat units) [14]. Since both compounds, capsaicin and nonivamide, have been detected in blood, lung, and liver after aerosol administration [15], systemic effects seem likely, although data on the effects of nonivamide on neurotransmitter release associated with the brain's reward system and food intake are yet not available.

Here, we studied the effect of nonivamide on dopamine and serotonin release in neural SH-SY5Y cells and investigated whether nonivamide evokes a Ca^{2+}-dependent neurotransmitter release mediated by TRPV1 receptor activation like capsaicin.

2 Materials and methods

2.1 Materials

SH-SY5Y cells (ATCC CLR-2266) were obtained from the American Type Culture Collection (USA). All chemicals and reagents were obtained from Sigma Aldrich, Austria unless indicated otherwise.

2.2 Cell culture

The human neuroblastoma cell line SH-SY5Y was cultured in a 1:1 mixture of Eagle's Minimum Essential Medium and F12 Ham medium, supplemented with 10% FBS (Life Technologies Corporation, Carlsbad, CA, USA), 4 mM L-glutamine and 1% penicillin/streptomycin, and maintained at 37°C and 5% CO_2 in a humidified incubator. Cells were seeded 24–48 h prior to the experiments in 35 or 100 mm cell culture dishes (Becton, Dickinson and Company, Heidelberg, Germany).

2.3 Cell viability assay

Cytotoxic effects of nonivamide were excluded via Trypan blue staining. After incubation with 0.1 to 10 μM nonivamide for 48 h, the cells were harvested and stained with Trypan blue in a dilution of 1:10. Stained (dead) and nonstained (vital) were counted separately using a hemocytometer. The vitality of the cells in percent was calculated according to the following formula: vitality (%) = (dead cell number/total cell number) × 100.

2.4 Cellular recovery of nonivamide

2.4.1 Subcellular fractionation

A total of 17.5×10^6 SH-SY5Y cells were incubated with 100 μM nonivamide in Krebs-Ringer HEPES buffer (KRHB, 128 mM NaCl, 1.9 mM KCl, 1.2 mM KH_2PO_4, 2.4 mM $CaCl_2$, 1.3 mM $MgSO_4$, 10 mM glucose, 10 mM HEPES) with 0.1% ethanol, or KRHB with 0.1% ethanol (control) for 5 min at 37°C. Cells were subsequently washed twice with ice-cold PBS and harvested with 0.9% NaCl solution using a cell scraper and washed again twice with 0.9% NaCl solution. The cell pellet was resuspended in mitochondrial isolation buffer (210 mM mannitol, 70 mM saccharose, 10 mM Tris/HCl pH 7.5, 1 mM EDTA). A homogenate was prepared by lysing the cells in one freeze-thaw cycle and using a dounce-type homogenizer. Intact cells and larger cell constituents were removed via centrifugation at 1000 × *g*. For mitochondria enrichment, the homogenate was centrifuged at 12 000 × *g*. The postnuclear supernatant thus obtained was removed and the pellet containing mitochondria was resuspended in mitochondrial isolation buffer. The incubation solutions, the supernatants after incubation, the homogenate, the postnuclear supernatant as well as the mitochondrial fraction were analyzed using LC-MS as described below.

2.4.2 LC-MS analysis of nonivamide

LC-MS analyses were performed using an HPLC system (Shimadzu Prominence, Austria) equipped with a single quadrupole mass spectrometer (Shimadzu LCMS-2020,

Austria). The samples passed through a 0.45 μm polyvinylidene difluouride syringe filter, and 5 or 50 μL were loaded on a Phenomenex Luna 5 μm C18 100 Å column with dimensions of 250 × 3 mm. All samples were analyzed in duplicate. HPLC measurements were performed according to Reilly et al. [16] at 40°C with a mobile phase consisting of 60% methanol and 40% water acidified with 0.1% formic acid. Nonivamide eluted after 17 min at a flow rate of 0.6 mL/min. The mass spectrometer was operated with an ESI source in positive mode. Nonivamide was quantified using selected ion monitoring at m/z of 294. The nebulizing gas flow (nitrogen) was set at 1.5 L/min, the drying gas (nitrogen) flow at 6 L/min, the desolvation line temperature at 250°C, the heat block temperature at 200°C, and the interface voltage at 4.5 kV. For quantification, external calibration was conducted using nonivamide concentrations in the range of 0.1–100 μM. The limit of nonivamide detection was 0.7 pmol, the limit of quantification was 2.3 pmol. Recovery of nonivamide (84.4 ± 13.6%) was determined by addition of standards to the incubation buffer prior to sample clean-up. These results are in agreement with previously reported data [15]. Since Reilly et al. [15] demonstrated a major loss in the compounds' stability when stored at room temperature for 24 h, the incubation time of 5 min applied in our study was not expected to result in a significant degradation of nonivamide. Furthermore, Reilly et al. [15] reported no reduction in stability for repeated thawing/freezing cycles.

The mean recovery of 84.4% determined in this study was taken into account for final data calculation. Data processing was performed with the Shimadzu LCMS software LabSolutions Version 5.

2.5 Customized DNA microarray

Custom oligonucleotide 60 mer gene expression microarrays were synthesized containing 145 genes known or expected to be involved in mechanisms of satiety. Four to 15 probes per target gene were designed using OligoWiz v2.2. Four replicates per probe were included on each array. Microarrays were synthesized on glass slides using the technique of maskless array synthesis [17]. Detailed synthesis procedures can be found in [18].

After incubation with 1 or 100 μM nonivamide respectively, for 3 h, the RNA was extracted using the RNeasy Mini Kit (Qiagen, Hilden, Germany) and its quality controlled with agarose gel electrophoresis and a NanoQuant Plate on an infinite plate reader (Tecan, Menningen, Switzerland). Labeling was carried out using Cy3-labeled random nonamers (Tebu Bio, Offenbach, Germany) as primers during reverse transcription reaction as described by Ouellet et al. [19]. The Cy3-labeled cDNA was hybridized to the microarrays for 24 h. The microarrays were scanned using an Axon GenePix 4100A microarray scanner (Molecular Devices, Sunnyvale, CA, USA). Intensity data from the scanned images were extracted using NimbleScan 2.1 software (NimbleGen, Madison, USA).

Microarray experiments were performed in triplicate and normalized using the robust multichip analysis (RMA). Differences in labeling efficiencies were excluded by normalization to the expression values of five nonregulated genes (HPRT, NM_000194; UBC, NM_021009; MRPL, NM_006428; TBP, NM_003194; NSE, NM_001975) and the fold change (T/C) calculated using Excel (2007). Statistical analysis was carried out with ArrayStar 3.0 (DNASTAR, Madison, USA).

2.6 Quantitative real-time PCR (qRT-PCR)

After incubation of 2.5 × 10⁶ SH-SY5Y cells with 1 μM nonivamide for 0.25, 0.5, 1, 3, 6, 12, 24, and 48 h, mRNA was extracted with RNeasy mini kit (Qiagen) and reverse transcribed to cDNA using the high-capacity cDNA Kit (Life Technologies Corporation). Real-Time PCR was carried out in triplicate on a StepOnePlus Real-Time PCR device with SYBR Green MasterMix (Life Technologies Corporation). The starting concentrations of the respective inserted mRNA (N_0 value) were calculated with LinRegPCR v.12.8 [20, 21] and normalized with TBP (TATA-Box binding protein) as an internal standard, which was previously shown to be a stable reference gene for qRT-PCR in brain tissues [22, 23]. Effect of nonivamide treatment on gene expression of different genes is presented in comparison to nontreated control cells (N_0 control cells = 1). Sequences of the primers used during PCR reactions are provided in Table 1. All primers were designed using Primer3Plus software [24] and synthesized by VBC Biotech, Vienna, Austria.

2.7 Intracellular Ca²⁺ mobilization

Intracellular Ca^{2+} mobilization was analyzed in a 96-well format using the fluorescent dye fluo-4 (Invitrogen, Life technologies, Carlsbad, USA) as described previously [25]. Briefly, fluorescent intensity after stimulation with Hank's Balanced Salt solution (buffer control with or without 0.1% ethanol), 50 mM KCl (positive control) or different concentrations of nonivamide (0.01–10 μM) were measured at 490 nm excitation and 520 nm emission for 1.5 min every 2 s using Tecan infinite plate reader with injectors (Tecan). The corresponding areas under the curve were calculated with SigmaPlot 11.0.

2.8 Serotonin release

A total of 1.25 × 10⁶ SH-SY5Y cells were stimulated with either KRHB (pH 6.2), KRHB containing 0.1% ethanol or nonivamide/capsaicin in a concentration range of 0.1–10 μM for 5 min. Incubation conditions (buffer pH, incubation time) were optimized in preliminary experiments (data not shown). Serotonin concentrations in the supernatant were determined using an ELISA (Serotonin ELISA sensitive, DLD Diagnostika, Hamburg). The intraassay variation

Table 1. Oligonucleotides (5′-3′) used as primers in the PCR reactions

Gene name	Forward primer	Reverse primer	Product length (bp)
HTR1A	TCATCGTGGCTCTTGTTCTG	CGGGGGTTAAGCAGAGAGTTG	108
HTR1B	CTGGTGTGGGTCTTCTCCAT	AGAGGATGTGGTCGGTGTTC	109
HTR2A	GTTGCTTACTCGCCGATGATA	TGCCAAGATCACTTACACACAAA	144
CNR1	GCTGCCTAAATCCACTCTGC	TGGACATGAAATGGCAGAAA	115
DRD1	CCATCACACAAAACGGTCAG	GTGTGTTGGAAAGCAGCAGA	166
DRD2	CCACTACAACTACTATGCCACAC	GAATTTCCACTCACCTACCACC	211
TBP	CCCGAAACGCCGAATATAATCC	GACTGTTCTTCACTCTTGGCTC	130
TRPV1	CCGGTGGTGCTTCAGGGTGG	GCGCTTGACGCCCTCACAGT	100

of this kit is 7–9% and the lower limit of detection is 0.39 pg/sample. Serotonin levels were normalized to the DNA content of each sample. Prior to analysis, the cells were lysed with a sodium lauryl sarcosinate containing buffer and the DNA content was determined using a NanoQuant plate on an infinite 2000 plate reader (Tecan).

2.9 Dopamine release

Dopamine release was measured as described previously [25]. In brief, a total of 1.25×10^6 SH-SY5Y cells were stimulated for 3.5 min with either KRHB (pH 5), KRHB containing 0.1% ethanol, or nonivamide/ capsaicin in a concentration range of 0.1 to 10 μM for 3.5 min. Incubation conditions (buffer pH, incubation time) were optimized in preliminary experiments (data not shown). Dopamine concentrations in the supernatant were determined using an enzyme-linked immunosorbent assay (Dopamine ELISA, DLD Diagnostika, Hamburg). The intra-assay variation of this kit is 8–12% and the lower limit of detection is 29 pg/mL. Dopamine levels were normalized to the DNA content of each sample. Prior to analysis, the cells were lysed with a sodium lauryl sarcosinate-containing buffer and the DNA content was determined using a NanoQuant plate on an infinite 2000 plate reader (Tecan).

2.10 Statistical analysis

Data are presented as means $\pm$ SD or fold change (T/C) unless indicated otherwise. All experiments were carried out in multiple replicates as indicated in the figures and tables (n = number of biological replicates with at least two technical replicates). Outliers were excluded using the Nalimov outlier test. Significant effects versus nontreated control cells were determined with one-way ANOVA versus control with Bonferroni posthoc test. Dose- and time-dependent effects were assessed by one- or two-way ANOVA, respectively, performing Holm–Sidak posthoc test. Statistical analysis of the microarray data was carried out using ArrayStar 3.0 (DNASTAR) software. Significant differences are indicated in the figures and tables using the following code: $*p < 0.05$; $**p < 0.01$; $***p < 0.001$ versus control or indicated with the letters a, b, and c for dose-dependent effects, at which the same letter indicates no significant difference.

3 Results

3.1 Cell viability

To exclude cytotoxic effects of the nonivamide treatment, cells were stained with Trypan blue. The viability of the control cells incubated with media was 98.3 $\pm$ 2.00%. Treatment of the cells with 0.1% ethanol as solvent control (97.7 $\pm$ 2.19%), 0.1, 1.0, or 10 μM nonivamide dissolved in 0.1% ethanol did not change the vitality compared to controls (95.7 $\pm$ 6.27%; 98.3 $\pm$ 3.33%; 97.6 $\pm$ 1.76%, resp.; one-way ANOVA: $p = 0.825$). For capsaicin in a concentration of 10 μM, cytotoxic effects on wild-type SH-SY5Y cells were excluded previously [9].

3.2 Cellular uptake of nonivamide by SH-SY5Y cells

To show that nonivamide is taken up into the cell and may affect intracellular Ca^{2+} mobilization that is involved in neurotransmitter release, a subcellular fraction of SH-SY5Y cells was isolated after incubation with 100 μM nonivamide, corresponding to a concentration of 200 nmol nonivamide in 2 mL of the cell culture medium, and subjected to LC-MS analysis. Of the initial amount of 200 nmol nonivamide added to the cell culture medium, an amount of 223.9 $\pm$ 94.2 nmol was quantified in the cellular supernatant. In the lysed cell homogenate and in the postnuclear supernatant, 1.65 $\pm$ 0.71 nmol and 0.95 $\pm$ 0.43 nmol nonivamide were quantified, whereas no nonivamide could be detected in the mitochondria and endoplasmatic reticulum fraction (Table 2). Nontreated control cells demonstrated nonivamide concentrations below the limit of detection of 0.7 pmol.

3.3 Effect of nonivamide on dopamine and serotonin receptor gene expression in SH-SY5Y cells

The influence of nonivamide on gene expression levels of the receptors dopamine D1 and D2, serotonin HTR1A, HTR1B, and HTR2A and cannabinoid CNR1 was examined with customized microarrays (1 and 100 μM nonivamide, 3 h incubation) and qRT-PCR (1 μM nonivamide, time-course experiment).

Table 2. Absolute (in nmol) and relative (in percent, incubation media = 100%) cellular recovery of nonivamide in different steps of the subcellular fractionation

Step	Recovery nonivamide (nmol)	Recovery nonivamide (%)
Incubation media	200	100
Cellular supernatant	223 ± 94.2	94.5
Homogenate	1.65 ± 0.71	0.7
Postnuclear supernatant	0.95 ± 0.43	0.4
Mitochondrial fraction	nd	0

Results are expressed as mean ± SD; $n = 3$; nd = not detected.

Table 3. Gene expression levels after incubation with 1 or 100 µM nonivamide using a customized microarray

Gene name	1 µM nonivamide (mean fold change)	100 µM nonivamide (mean fold change)
HTR1A	1.08 ± 0.21	1.02 ± 0.16
HTR1B	0.96 ± 0.15	1.04 ± 0.16
HTR2A	1.05 ± 0.16	1.07 ± 0.23
CNR1	0.99 ± 0.24	1.00 ± 0.18
DRD1	0.98 ± 0.16	1.02 ± 0.17
DRD2	1.01 ± 0.17	1.05 ± 0.17
TRPV1	0.85 ± 0.03	1.04 ± 0.10

Fold changes (T/C) in receptor expression after treatment with 1 or 100 µM nonivamide, control = 1; $n = 3$.

No effect on gene expression levels of the dopamine receptors D1 and D2, the serotonin receptors HTR1A, HTR1B, and HTR2A, the cannabinoid receptor CNR1 receptor and the TRPV1 receptor was detected after incubation with 1 µM nonivamide using the microarrays (Table 3). Also, increasing the nonivamide concentration to 100 µM did not result in changes in gene expression of any of the satiety-related genes studied (Table 3).

However, time-course experiments using qRT-PCR revealed that gene expression levels of satiety and reward mediating receptors D1 and D2, HTR1A, HTR1B, HTR2A, and the cannabinoid receptor CNR1 as well as the TRPV1 receptor were significantly regulated in a time-dependent manner after treatment with 1 µM nonivamide (Table 4, 5). Maximum gene expression of 1.90 ± 0.36 (control = 1) for the serotonin auto-receptor HTR1A in SH-SY5Y cells was achieved after a 48 h exposure, whereas minimum levels were found after treatment for 6 h (0.44 ± 0.19). The satiety-mediating receptors HTR1B and HTR2A were maximally upregulated after 1 and 48 h, respectively, with fold changes of 2.80 ± 0.98 and 2.40 ± 2.09 versus control. Serotonin receptor HTR1B expression reached its minimum after 0.5 h (0.33 ± 0.03 versus control). mRNA levels encoding for the adenylate cyclase inhibiting dopamine receptor D1 was maximally increased (1.74 ± 0.46 versus control) after 48 h of incubation with nonivamide, and maximally decreased (0.53 ± 0.20 versus control) after 0.5 h. In contrast, gene expression of the adenylate cyclase activating dopamine receptor D2 was upregulated up to 1.49 ± 0.48 after 0.5 h of incubation and downregulated after 1 h to 0.74 ± 0.15 compared to nontreated control cells. Gene expression analysis of cannabinoid receptor CNR1 after treatment with 1 µM nonivamide showed a downregulation to 0.36 ± 0.02 after 0.5 h, whereas no upregulation was detected at any of the time points tested. For TRPV1 receptor gene expression, a maximum increase of 1.39 ± 0.80 was analyzed after 3 h of exposure, whereas a 6 h treatment resulted in the most pronounced downregulation of 0.55 ± 0.04 compared to nontreated control cells (Table 4, 5).

Table 4. Gene expression levels for serotonin receptors HTR1A, 1B, and 2A after incubation with 1 µM nonivamide after different time points using qRT-PCR

Gene name	HTR1A		HTR1B		HTR2A	
Incubation time (h)	Control	Nonivamide	Control	Nonivamide	Control	Nonivamide
0.25	1.00 ± 0.05	0.45 ± 0.23[***]	1.00 ± 0.03	0.52 ± 0.16[***]	1.00 ± 0.04	0.55 ± 0.30
0.5	1.00 ± 0.07	0.46 ± 0.13[***]	1.00 ± 0.05	0.33 ± 0.03[***]	1.00 ± 0.09	0.58 ± 0.28
1	1.00 ± 0.05	0.64 ± 0.20[**]	1.00 ± 0.04	2.80 ± 0.98[***]	1.00 ± 0.07	0.74 ± 0.13
3	1.00 ± 0.03	0.75 ± 0.40[*]	1.00 ± 0.06	0.53 ± 0.19[***]	1.00 ± 0.10	0.56 ± 0.14
6	1.00 ± 0.07	0.44 ± 0.19[***]	1.00 ± 0.05	0.38 ± 0.04[***]	1.00 ± 0.11	0.81 ± 0.55
12	1.00 ± 0.05	1.09 ± 0.54	1.00 ± 0.09	0.95 ± 0.34	1.00 ± 0.05	0.64 ± 0.10
24	1.00 ± 0.03	0.91 ± 0.07	1.00 ± 0.06	0.68 ± 0.26[*]	1.00 ± 0.18	1.36 ± 0.83
48	1.00 ± 0.14	1.90 ± 0.36[***]	1.00 ± 0.06	1.52 ± 0.40[***]	1.00 ± 0.26	2.40 ± 2.09[***]
p-Value factor time	<0.001		<0.001		<0.001	

Fold changes (T/C) in receptor expression after treatment with 1 µM nonivamide versus control; $n = 3–4$; Time-dependent effects are tested with two-way ANOVA and pairwise multiple comparison between treatments using the Holm–Sidak posthoc test ([*]$p < 0.05$; [**]$p < 0.01$; [***]$p < 0.001$ versus nontreated cells).

Table 5. Gene expression levels for cannabinoid receptor (CNR1) dopamine receptors D1 and D2, TRPV1 after incubation with 1 μM nonivamide after different time points using qRT-PCR

Gene name	CNR1		DRD1		DRD2		TRPV1	
Incubation time (h)	Control	Nonivamide	Control	Nonivamide	Control	Nonivamide	Control	Nonivamide
0.25	1.00 ± 0.10	0.51 ± 0.27[***]	1.00 ± 0.07	0.70 ± 0.31	1.00 ± 0.02	1.09 ± 0.11	1.00 ± 0.07	0.90 ± 0.52
0.5	1.00 ± 0.11	0.36 ± 0.02[***]	1.00 ± 0.13	0.53 ± 0.20[***]	1.00 ± 0.05	1.49 ± 0.48[***]	1.00 ± 0.06	0.81 ± 0.37
1	1.00 ± 0.06	0.90 ± 0.24	1.00 ± 0.06	1.68 ± 1.11[*]	1.00 ± 0.04	0.83 ± 0.13[**]	1.00 ± 0.05	1.19 ± 0.34
3	1.00 ± 0.07	0.62 ± 0.26[***]	1.00 ± 0.09	0.78 ± 0.36	1.00 ± 0.05	0.84 ± 0.13	1.00 ± 0.08	1.39 ± 0.80[**]
6	1.00 ± 0.05	0.41 ± 0.05[***]	1.00 ± 0.07	0.81 ± 0.44	1.00 ± 0.04	1.02 ± 0.14	1.00 ± 0.10	0.55 ± 0.04[**]
12	1.00 ± 0.08	0.84 ± 0.34	1.00 ± 0.07	0.96 ± 0.30	1.00 ± 0.08	0.94 ± 0.17	1.00 ± 0.05	0.94 ± 0.23
24	1.00 ± 0.06	0.97 ± 0.22	1.00 ± 0.14	1.29 ± 0.32	1.00 ± 0.06	0.94 ± 0.16	1.00 ± 0.05	1.04 ± 0.18
48	1.00 ± 0.12	1.33 ± 0.67	1.00 ± 0.07	1.74 ± 0.46[***]	1.00 ± 0.06	0.84 ± 0.21	1.00 ± 0.08	0.69 ± 0.14
p-Value factor time	0.002		<0.001		0.035		0.002	

Fold changes (T/C) in receptor expression after treatment with 1 μM nonivamide versus control; $n = 3$–4; Time-dependent effects are tested with two-way ANOVA and pairwise multiple comparison between treatments using the Holm–Sidak posthoc test (*$p < 0.05$; **$p < 0.01$; ***$p < 0.001$ versus nontreated cells).

## 3.4 Effect of capsaicin and nonivamide on Ca^{2+} mobilization and neurotransmitter release in SH-SY5Y cells

Neurotransmitter release is known to be mediated by increased intracellular Ca^{2+} levels. To get an insight of the effects of nonivamide and capsaicin on neurotransmitter release and its mechanism, intracellular Ca^{2+} mobilization was measured fluorimetrically.

Treatment of SH-SY5Y cells with capsaicin increased intracellular Ca^{2+} mobilization in a concentration range of 0.01–10 μM, Fig. 2A.

Treatment with nonivamide also significantly increased intracellular Ca^{2+} mobilization in SH-SY5Y cells in a con-

centration range of 0.01–10 μM. Even the lowest tested concentration (0.01 μM) showed comparable effects ($177 \pm 61\%$, $p < 0.001$ versus control) to the positive control (50 mM KCl, $180 \pm 53\%$, $p < 0.001$ versus control), whereas Ca^{2+} mobilization was most pronounced at the highest tested concentration of 10 μM ($268 \pm 105\%$, $p < 0.001$ versus control, Fig. 2B).

Treatment of SH-SY5Y cells with capsaicin significantly increased dopamine release in a concentration-dependent manner: A concentration of 1 μM increased dopamine release to $594 \pm 215\%$ ($p < 0.001$ versus control), whereas treatment with 10 μM increased the dopamine release by $1295 \pm 534\%$ ($p < 0.001$ versus control) in comparison to the buffer control (Fig. 3A). Serotonin release was also increased in cells treated
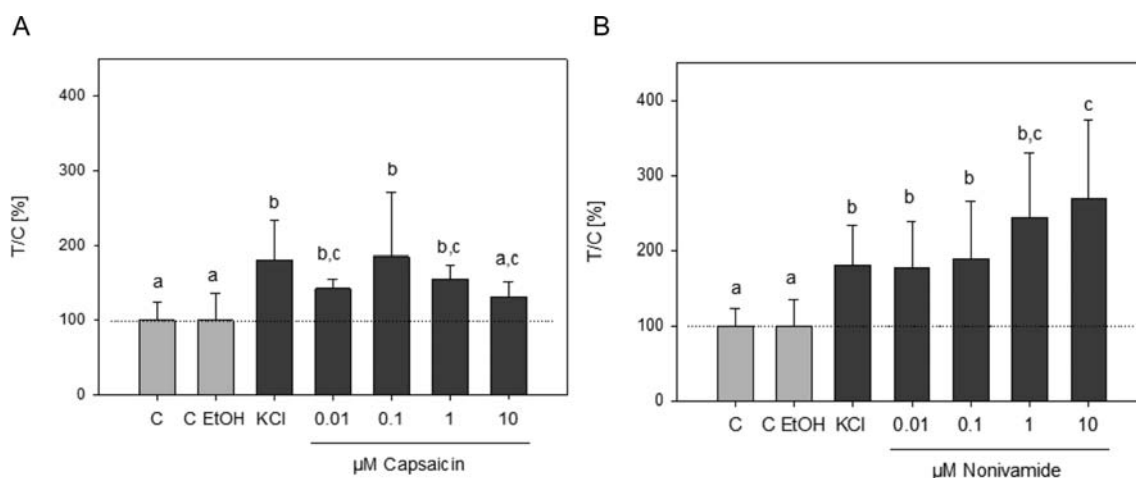
Figure 2. Intracellular Ca^{2+} mobilization after stimulation with 50 mM KCl (positive control) or different concentrations of capsaicin (A) nonivamide (B). Results are displayed as area under the curve in percent compared to control (buffer/buffer 0.1% EtOH). $n = 3$–4 (tr = 3–12) Significant differences between treatments are tested with one-way ANOVA followed by Holm–Sidak posthoc test and marked with the letters a, b, and c.
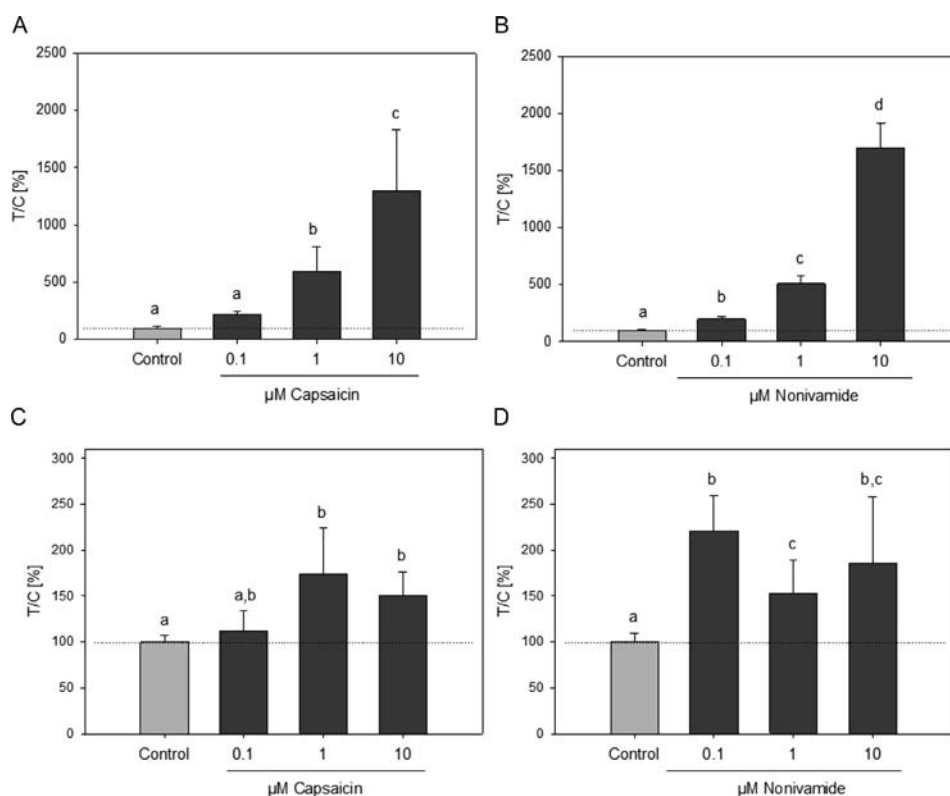
Figure 3. Dopamine (A and B) and serotonin (C and D) release after stimulation with different concentrations of capsaicin (A and C) or nonivamide (B and D). Results are displayed as T/C in percent compared to control (buffer with 0.1% ethanol, set to 100%). $n = 3$–8 (tr = 2). Significant differences between treatments are tested with one-way ANOVA followed by Holm–Sidak posthoc test and marked with the letters a, b, and c.

with capsaicin: Application of 1 or 10 μM induced a serotonin release of 174 $\pm$ 51% ($p < 0.001$ versus control) and 151 $\pm$ 26% ($p = 0.002$ versus control), respectively (Fig. 3C).

Incubation of the SH-SY5Y cells with nonivamide leads to an induction of neurotransmitter release as well. Dopamine release increased in a concentration-dependent manner. An incubation with nonivamide at concentrations of 0.1, 1, and 10 μM resulted in an increase of dopamine of 196 $\pm$ 22, ($p < 0.001$ versus control), 507 $\pm$ 71 ($p < 0.001$ versus control), and 1699 $\pm$ 212% ($p < 0.001$ versus control) compared to the buffer control, respectively (Fig. 3B). Serotonin levels were increased by 221 $\pm$ 38% ($p < 0.001$ versus control) and 152 $\pm$ 36% ($p < 0.001$ versus control) after stimulation with nonivamide in concentrations of 0.1 and 1 μM, respectively (Fig. 3D).

3.5 Effect of nonivamide on induced neurotransmitter release in the presence of a TRPV1 inhibitor in SH-SY5Y cells

In order to demonstrate whether the nonivamide-induced neurotransmitter release depends on TRPV1 receptor activation, SH-SY5Y cells were co-incubated with nonivamide and different concentrations of the selective TRPV1-inhibitor *trans-tert*-butylcyclohexanol (BCH, IC$_{50}$ = 34 $\pm$ 5 μM) [26] or the well-investigated TRPV1-inhibitor capsazepine (CZE, IC$_{50}$ = 5.4 nM) [27]. Incubation of SH-SY5Y cells with 1 μM

capsaicin led to an increase in dopamine and serotonin release of 594 $\pm$ 215% and 174 $\pm$ 51%, respectively. Co-incubation of capsaicin and 25, 50, or 80 μM BCH decreased dopamine (315 $\pm$ 44% ($p = 0.022$); 322 $\pm$ 142% ($p = 0.008$); 278 $\pm$ 39% ($p < 0.001$)) and serotonin release (120 $\pm$ 6% ($p = 0.014$); 101 $\pm$ 14% ($p > 0.001$); 107 $\pm$ 22% ($p = 0.005$)) in comparison with the treatment with 1 μM capsaicin only (Fig. 4A and C). Co-incubation of 1 μM capsaicin and 0.1, 1, and 10 μM of TRPV1-inhibitor CZE also decreased dopamine (411 $\pm$ 68% ($p = 0.038$); 363 $\pm$ 105% ($p = 0.002$); 410 $\pm$ 73% ($p = 0.037$)) release in comparison with the treatment with 1 μM capsaicin only (Fig. 5A). Serotonin release was decreased after co-incubation with 1 and 10 μM of CZE (124 $\pm$ 14% ($p = 0.016$); 116 $\pm$ 15% ($p = 0.003$), a concentration of 0.1 μM CZE did not decrease serotonin release (155 $\pm$ 20% ($p = 0.775$)) in comparison to the effect of 1 μM capsaicin only (Fig. 5C). Incubation with 1 μM nonivamide also increased dopamine (507 $\pm$ 71%) and serotonin release (152 $\pm$ 36%) in a comparable manner to capsaicin. However, co-incubation of nonivamide and BCH did not affect dopamine ($p = 0.066$) or serotonin ($p = 0.510$) release in comparison to treatment with 1 μM nonivamide only (Fig. 4B and D). Co-incubation of 1 μM nonivamide and 0.1, 1, and 10 μM CZE did also not change dopamine ($p = 0.172$) or serotonin ($p = 0.224$) release (Fig. 5B and D). A treatment of the cells with BCH or CZE alone did not affect serotonin release ($p = 0.067$ or 0.144). However, dopamine release was decreased after treatment with BCH in concentration of 25
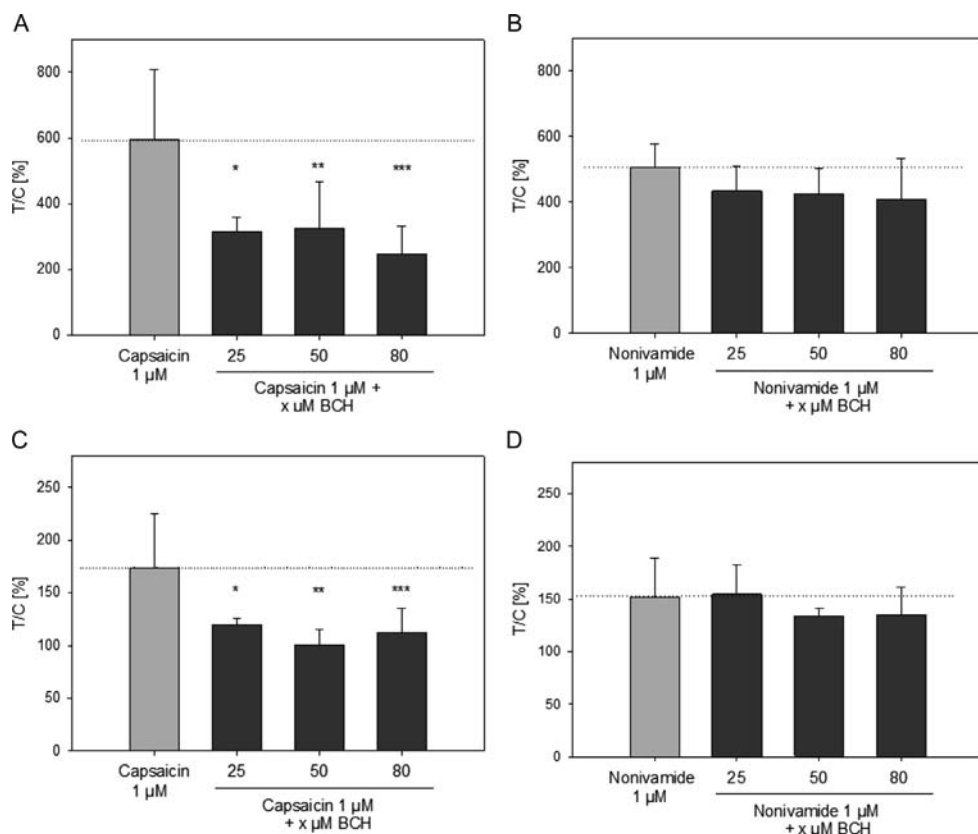
Figure 4. Dopamine (A and B) and serotonin (C and D) release after stimulation with 1 μM capsaicin (A and C) or nonivamide (B and D) or 1 μM capsaicin/nonivamide and different concentrations of the selective TRPV1-inhibitor *trans-t*-butylcyclohexanol (BCH). Results are displayed as T/C in percent compared to control (buffer with 0.1% ethanol, set to 100%). *n* = 3–8 (tr = 2). Significant differences between treated cells (capsaicin/nonivamide plus BCH) in comparison to their corresponding control (capsaicin/nonivamide) are tested with one-way ANOVA followed by Bonferroni posthoc test and marked with *$p < 0.05$; **$p < 0.01$; or ***$p < 0.001$.
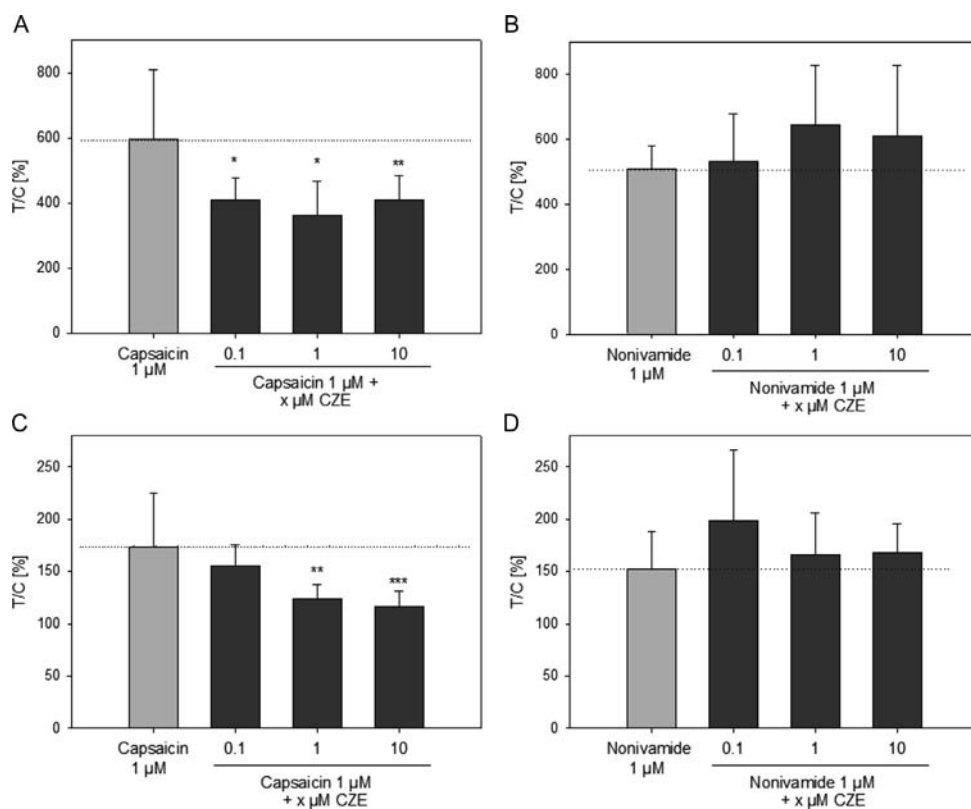
Figure 5. Dopamine (A and B) and serotonin (C and D) release after stimulation with 1 μM capsaicin (A and C) or nonivamide (B and D) or 1 μM capsaicin/nonivamide and different concentrations of the TRPV1-inhibitor capsazepine (CZE). Results are displayed as T/C in percent compared to control (buffer with 0.1% ethanol, set to 100%). *n* = 3–8 (tr = 2). Significant differences between treated cells (capsaicin/nonivamide plus CZE) in comparison to their corresponding control (capsaicin/nonivamide) are tested with one-way ANOVA followed by Bonferroni posthoc test and marked with *$p < 0.05$; **$p < 0.01$; or ***$p < 0.001$.

and 50 μM (49 ± 21% ($p < 0.001$); 74 ± 28% ($p = 0.032$)), but significantly increased after treatment with 1 or 10 μM of CZE (265 ± 136% ($p < 0.001$); 226 ± 136% ($p < 0.001$), data not shown).

4 Discussion

The pungent compound of *C. annuum*, capsaicin, increases the firing rate of dopaminergic neurons via a TRPV1-dependent pathway [7]. The capsaicin analog nonivamide is also a known agonist of the TRPV1 receptor, although less pungent due to its lower TRPV1 binding affinity compared to capsaicin [14]. For capsaicin, an EC_{50} value of 0.7 μM has been determined [28], whereas as for nonivamide an EC_{50} value of 1.4 μM has been published [29]. In order to examine whether the structural difference also leads to different effects in neurotransmitter release, we investigated the effects of capsaicin and nonivamide on dopamine and serotonin release in the presence/absence of the selective TRPV1 inhibitor BCH and the well-investigated TRPV1 inhibitor CZE.

Exposure of neural SH-SY5Y cells to nonivamide and capsaicin in concentrations ranging from 0.1 to 10 μM significantly stimulated intracellular Ca^{2+} mobilization, pointing to an effect of the capsaicinoides on neurotransmitter release. Intracellular Ca^{2+} mobilization after stimulation with capsaicin reached 185 ± 43% at a concentration of 0.1 μM. A comparable effect was achieved after stimulation with the same concentration of nonivamide (189 ± 77%). Treatment of the SH-SY5Y cells with a concentration of 1 μM capsaicin resulted in an increased Ca^{2+} release of + 55 ± 17%. These findings confirm the results of Eun et al. [12], who reported a similar Ca^{2+} release (166 ± 6.2%) after treatment with 1 μM capsaicin in dorsal root ganglion cells of adult rats. Treatment with capsaicin also stimulated the Ca^{2+}-dependent dopamine and serotonin release compared to nontreated control cells, confirming, in the human neuroblastoma cell line SH-SY5Y, results reported for rat brain slices containing the nucleus accumbens [7]. The capsaicin-evoked neurotransmitter release demonstrated in this study was markedly reduced by co-incubation with the two TRPV1 inhibitors BCH and CZE. Since nonivamide is, like capsaicin, a TRPV1 agonist [30], we hypothesized that nonivamide elicits the same mechanism of action. In contrast to this hypothesis, there was no significant change in dopamine or serotonin release when cells were treated with nonivamide in the presence of the TRPV1 inhibitors BCH and CZE compared to treatment with nonivamide alone, indicating different signaling pathways for the two capsaicinoides. Thus, the present study demonstrates that the Ca^{2+}-stimulated neurotransmitter release in the presence of nonivamide does not seem to be dependent on binding to the extracellular surface receptor TRPV1. Instead, a TRPV1-independent intracellular Ca^{2+} mobilization might contribute to the nonivamide-induced neurotransmitter release. This hypothesis is supported by results from Eun

et al. [12] who demonstrated that capsaicin also stimulates Ca^{2+} release from intracellular, ryanodine-sensitive calcium stores.

Since exposure of SH-SY5Y cells to nonivamide resulted in quantifiable amounts of this compound in the postnuclear supernatant, which is lacking larger cell components like the nucleus and membranes, this study shows that nonivamide is taken up by SH-SY5Y cells and, therefore, may unfold its effects not only via membrane-standing receptors, but also intracellularly. An intracellular Ca^{2+} increase, which mediates neurotransmitter release, may not only be stimulated via membrane stitded TRPV1 activation, but also, similar to capsaicin, by mobilization of Ca^{2+} from of intracellular ryanodine-sensitive Ca^{2+} stores.

The present study also demonstrates that treatment with nonivamide influences expression levels of selected genes involved in the regulation of the brain's reward system and food intake.

The two hypothalamic neurotransmitters serotonin and dopamine are both involved in mechanisms regulating mood and satiety via the brain's reward system [31]. Downstream signaling is mediated by the corresponding target receptors which are for dopamine, among others, the D1 and the D2 receptor, and for serotonin, among others, the HTR1A, 2A, and 1B receptor [32, 33]. A close interaction between the capsaicin receptor TRPV1 and dopamine and serotonin receptors as well as the cannabinoid receptor CNR1 has been shown in several previous studies [4, 5, 34]. It also has been demonstrated before that capsaicin influences expression of the serotonin receptor HTR2A and leads to changes in expression of dopamine receptors D1 and D2, and the cannabinoid receptor CNR1 [8].

In this study, customized cDNA microarray analysis after treatment with 1 and 100 μM of nonivamide and a qRT-PCR time-course experiment after treatment with 1 μM of nonivamide for 0.25, 0.5, 1, 3, 6, 12, 24, 48 h were carried out to analyze gene expression of related genes. A concentration of 1 μM for qRT-PCR and microarray experiments was chosen since 1 μM of capsaicin was shown to modify Ca^{2+} signaling and neurotransmitter release in neural cells [7, 12]. As a result, changes in gene expression levels of D1, D2 HTR1A, HTR1B, HTR2A, CNR1, and TRPV1 receptors could only be demonstrated by qRT-PCR, which is known to be more sensitive than cDNA microarray techniques [35, 36]. Pronounced effects were found after 48 h of treatment for the three serotonin receptors HTR1A, 1B, and 2A, and the dopamine receptor D1. These gene expression data indicate that nonivamide may influence the hypothalamic dopamine and serotonin system on a regulatory level. Since about 80% of dietary capsaicin and capsaicin derivatives are absorbed in the gastrointestinal tract [37], resulting in plasma concentrations in the nmolar range, and since these compounds are known to pass the blood–brain barrier [38], similar absorption and transport mechanisms of dietary nonivamide may result in comparable neurotransmitter release from the

brain. However, to date, in vivo data on the effect of dietary nonivamide on the brain's reward system are lacking. Future studies may address these questions since animal data obtained from aerosol administration suggest that capsaicin, as well as nonivamide, are absorbed into circulation [15], thereby supporting the general hypothesis of systemic effects of nonivamide.

In conclusion, capsaicin and nonivamide have been demonstrated to induce a calcium-dependent release of the neurotransmitters dopamine and serotonin. Capsaicin evokes these calcium-dependent signals through activation of TRPV1, which results in pain sensation after dietary intake. Since the less pungent nonivamide does not stimulate TRPV1 activation as potently as capsaicin, but still provokes similar neurotransmitter release, it may be applied at higher concentrations to regulate mechanisms of mood and satiety. Additionally, the use of TRPV1 inhibitors would reduce not only the pain sensation but also the effects on neurotransmitter release from capsaicin, but not from nonivamide. However, further verification of the reported effects of nonivamide in vivo is needed.

Potential conflict of interest statement: the authors J. P. Ley and G. E. Krammer are employees at Symrise AG, Holzminden, Germany.

5   References

[1] Ludy, M. J., Mattes, R. D., The effects of hedonically acceptable red pepper doses on thermogenesis and appetite. *Physiol. Behav.* 2011, *102*, 251–258.

[2] Ludy, M. J., Moore, G. E., Mattes, R. D., The effects of capsaicin and capsiate on energy balance: critical review and meta-analyses of studies in humans. *Chem. Senses* 2012, *37*, 103–121.

[3] Kawabata, F., Inoue, N., Masamoto, Y., Matsumura, S. et al., Non-pungent capsaicin analogs (capsinoids) increase metabolic rate and enhance thermogenesis via gastrointestinal TRPV1 in mice. *Biosci. Biotechnol. Biochem.* 2009, *73*, 2690–2697.

[4] Tzavara, E. T., Li, D. L., Moutsimilli, L., Bisogno, T. et al., Endocannabinoids activate transient receptor potential vanilloid 1 receptors to reduce hyperdopaminergia-related hyperactivity: therapeutic implications. *Biol. Psychiat.* 2006, *59*, 508–515.

[5] Micale, V., Cristino, L., Tamburella, A., Petrosino, S. et al., Anxiolytic effects in mice of a dual blocker of fatty acid amide hydrolase and transient receptor potential vanilloid type-1 channels. *Neuropsychopharmacology* 2009, *34*, 593–606.

[6] Koleva, II, van Beek, T. A., Soffers, A. E., Dusemund, B. et al., Alkaloids in the human food chain–natural occurrence and possible adverse effects. *Mol. Nutr. Food Res.* 2012, *56*, 30–52.

[7] Marinelli, S., Pascucci, T., Bernardi, G., Puglisi-Allegra, S. et al., Activation of TRPV1 in the VTA excites dopaminergic neurons and increases chemical- and noxious-induced dopamine release in the nucleus accumbens. *Neuropsychopharmacology* 2005, *30*, 864–870.

[8] Zavitsanou, K., Dalton, V. S., Wang, H., Newson, P. et al., Receptor changes in brain tissue of rats treated as neonates with capsaicin. *J. Chem. Neuroanat.* 2010, *39*, 248–255.

[9] Lam, P. M., Hainsworth, A. H., Smith, G. D., Owen, D. E. et al., Activation of recombinant human TRPV1 receptors expressed in SH-SY5Y human neuroblastoma cells increases [Ca(2+)](i), initiates neurotransmitter release and promotes delayed cell death. *J. Neurochem.* 2007, *102*, 801–811.

[10] Nagy, I., Santha, P., Jancso, G., Urban, L., The role of the vanilloid (capsaicin) receptor (TRPV1) in physiology and pathology. *Eur. J. Pharmacol.* 2004, *500*, 351–369.

[11] Han, E. H., Kim, H. G., Choi, J. H., Jang, Y. J. et al., Capsaicin induces CYP3A4 expression via pregnane X receptor and CCAAT/enhancer-binding protein beta activation. *Mol. Nutr. Food Res.* 2012, *56*, 797–809.

[12] Eun, S. Y., Jung, S. J., Park, Y. K., Kwak, J. et al., Effects of capsaicin on Ca(2+) release from the intracellular Ca(2+) stores in the dorsal root ganglion cells of adult rats. *Biochem. Biophys. Res. Commun.* 2001, *285*, 1114–1120.

[13] Banni, S., Di Marzo, V., Effect of dietary fat on endocannabinoids and related mediators: consequences on energy homeostasis, inflammation and mood. *Mol. Nutr. Food Res.* 2010, *54*, 82–92.

[14] Haas, J. S., Whipple, R. E., Grant, P. M., Andresen, B. D. et al., Chemical and elemental comparison of two formulations of oleoresin capsicum. *Sci. Justice* 1997, *37*, 15–24.

[15] Reilly, C. A., Crouch, D. J., Yost, G. S., Fatah, A. A., Determination of capsaicin, nonivamide, and dihydrocapsaicin in blood and tissue by liquid chromatography-tandem mass spectrometry. *J. Anal. Toxicol.* 2002, *26*, 313–319.

[16] Reilly, C. A., Ehlhardt, W. J., Jackson, D. A., Kulanthaivel, P. et al., Metabolism of capsaicin by cytochrome P450 produces novel dehydrogenated metabolites and decreases cytotoxicity to lung and liver cells. *Chem. Res. Toxicol.* 2003, *16*, 336–349.

[17] Singh-Gasson, S., Green, R. D., Yue, Y., Nelson, C. et al., Maskless fabrication of light-directed oligonucleotide microarrays using a digital micromirror array. *Nat. Biotechnol.* 1999, *17*, 974–978.

[18] Agbavwe, C., Kim, C., Hong, D., Heinrich, K. et al., Efficiency, error and yield in light-directed maskless synthesis of DNA microarrays. *J. Nanobiotechnol.* 2011, *9*, 57.

[19] Ouellet, M., Adams, P. D., Keasling, J. D., Mukhopadhyay, A., A rapid and inexpensive labeling method for microarray gene expression analysis. *BMC Biotechnol.* 2009, *9*, 97.

[20] Ruijter, J. M., Ramakers, C., Hoogaars, W. M., Karlen, Y. et al., Amplification efficiency: linking baseline and bias in the

analysis of quantitative PCR data. *Nucleic Acids Res.* 2009, *37*, e45.

[21] Tuomi, J. M., Voorbraak, F., Jones, D. L., Ruijter, J. M., Bias in the Cq value observed with hydrolysis probe based quantitative PCR can be corrected with the estimated PCR efficiency value. *Methods* 2010, *50*, 313–322.

[22] Valente, V., Teixeira, S. A., Neder, L., Okamoto, O. K. et al., Selection of suitable housekeeping genes for expression analysis in glioblastoma using quantitative RT-PCR. *BMC Mol. Biol.* 2009, *10*, 17.

[23] Wierschke, S., Gigout, S., Horn, P., Lehmann, T. N. et al., Evaluating reference genes to normalize gene expression in human epileptogenic brain tissues. *Biochem. Biophys. Res. Commun.* 2010, *403*, 385–390.

[24] Untergasser, A., Nijveen, H., Rao, X., Bisseling, T. et al., Primer3Plus, an enhanced web interface to Primer3. *Nucleic Acids Res.* 2007, *35*, W71–W74.

[25] Walker, J., Rohm, B., Lang, R., Pariza, M. W. et al., Identification of coffee components that stimulate dopamine release from pheochromocytoma cells (PC-12). *Food Chem. Toxicol.* 2012, *50*, 390–398.

[26] Kueper, T., Krohn, M., Haustedt, L. O., Hatt, H. et al., Inhibition of TRPV1 for the treatment of sensitive skin. *Exp. Dermatol.* 2010, *19*, 980–986.

[27] Seabrook, G. R., Sutton, K. G., Jarolimek, W., Hollingworth, G. J. et al., Functional properties of the high-affinity TRPV1 (VR1) vanilloid receptor antagonist (4-hydroxy-5-iodo-3-methoxyphenylacetate ester) iodo-resiniferatoxin. *J. Pharmacol. Exp. Ther.* 2002, *303*, 1052–1060.

[28] Caterina, M. J., Schumacher, M. A., Tominaga, M., Rosen, T. A. et al., The capsaicin receptor: a heat-activated ion channel in the pain pathway. *Nature* 1997, *389*, 816–824.

[29] Thomas, K. C., Ethirajan, M., Shahrokh, K., Sun, H. et al., Structure-activity relationship of capsaicin analogs and transient receptor potential vanilloid 1-mediated human lung

epithelial cell toxicity. *J. Pharmacol. Exp. Ther.* 2011, *337*, 400–410.

[30] Constant, H. L., Cordell, G. A., West, D. P., Nonivamide, a constituent of capsicum oleoresin. *J. Nat. Prod.* 1996, *59*, 425–426.

[31] Meguid, M. M., Fetissov, S. O., Varma, M., Sato, T. et al., Hypothalamic dopamine and serotonin in the regulation of food intake. *Nutrition* 2000, *16*, 843–857.

[32] Terry, P., Gilbert, D. B., Cooper, S. J., Dopamine receptor subtype agonists and feeding behavior. *Obes. Res.* 1995, *3*(Suppl 4), 515S–523S.

[33] Curzon, G., Gibson, E. L., Oluyomi, A. O., Appetite suppression by commonly used drugs depends on 5-HT receptors but not on 5-HT availability. *Trends Pharmacol. Sci.* 1997, *18*, 21–25.

[34] Van Steenwinckel, J., Noghero, A., Thibault, K., Brisorgueil, M. J. et al., The 5-HT2A receptor is mainly expressed in nociceptive sensory neurons in rat lumbar dorsal root ganglia. *Neuroscience* 2009, *161*, 838–846.

[35] Rajeevan, M. S., Vernon, S. D., Taysavang, N., Unger, E. R., Validation of array-based gene expression profiles by real-time (kinetic) RT-PCR. *J. Mol. Diagn.* 2001, *3*, 26–31.

[36] Li, H., Shao, J., Lu, X., Gao, Z., Yu, Y., Identification of early responsive genes in human amnion epithelial FL cells induced by *N*-methyl-*N'*-nitro-*N*-nitrosoguanidine using oligonucleotide microarray and quantitative real-time RT-PCR approaches. *Mutat. Res.* 2008, *644*, 1–10.

[37] Chaiyasit, K., Khovidhunkit, W., Wittayalertpanya, S., Pharmacokinetic and the effect of capsaicin in *Capsicum frutescens* on decreasing plasma glucose level. *J. Med. Assoc. Thai.* 2009, *92*, 108–113.

[38] Kang, Y. S., Kim, J. M., Permeability of a capsaicin derivative, [14C]DA-5018 to blood-brain barrier corrected with HPLC method. *Arch. Pharm. Res.* 1999, *22*, 165–172.

2.2 "Neurotransmitter-releasing potency of structural capsaicin-analogs in SH-SY5Y cells."

Rohm, B.[a], Zaunschirm, M.[b], Widder, S.[c], Ley, J. P.[c], Krammer, G.E.[c], Somoza, V.[a,b]

[a] Christian Doppler Laboratory for Bioactive Aroma Compounds, University of Vienna, Althanstraße 14, Vienna, Austria

[b] Department of Nutritional and Physiological Chemistry, University of Vienna, Althanstraße 14, Vienna, Austria

[c] Symrise AG, Mühlenfeldstraße 1, Holzminden, Germany

Neurotransmitter-releasing potency of structural capsaicin-analogs in SH-SY5Y cells

Barbara Rohm [1], Mathias Zaunschirm [2], Sabine Widder [3], Jakob P.Ley[3], Gerhard E. Krammer[3], VERONIKA SOMOZA,[2*]

[1] *Christian Doppler Laboratory for Bioactive Aroma Compounds,*
University of Vienna, Althanstraße 14, Vienna, Austria
[2] *Department of Nutritional and Physiological Chemistry,*
University of Vienna, Althanstraße 14, Vienna, Austria
[3] *Symrise AG, Mühlenfeldstraße 1, Holzminden, Germany*
[*]*Correspondence: Veronika Somoza, Althanstraße 14, 1090 Vienna, Austria.*
*Tel: +43 1 4227 70601, Fax: +43 1 4277 9706, e-mail:*
Veronika.Somoza@univie.ac.at

Abstract

The major pungent principle of *Capsicum annuum*, capsaicin, is known to stimulate dopamine release and the serotonin system via TRPV1 activation. However, the downside of capsaicin binding to the TRPV1 receptor is that its dietary intake results in a sharp, burning pain. Therefore, less pungent structural analogs of capsaicin that still exhibit positive effects on neurotransmitter release of the reward system are of interest. Recently, we identified the less pungent capsaicin-analog nonivamide as a promising candidate. The work presented here compares the effects of the structurally-related alkamide *trans*-pellitorine on neurotransmitter release in SH-SY5Y cells to those of nonivamide and capsaicin. *trans*-Pellitorine induced serotonin and dopamine release in SH-SY5Y cells, accompanied by an intracellular Ca^{2+}-mobilization. However, the potency of *trans*-pellitorine to stimulate neurotransmitter release is weaker compared to that of the capsaicin-analog nonivamide.

Introduction

Capsaicin, the major pungent component of *Capsicum anuum*, is a well-investigated agonist of the transient receptor potential cation channel subfamily V member 1 (TRPV1). Binding of capsaicin to the TRPV1 is known to affect the dopamine and cannabinoid systems, linking capsaicin with the brain's reward mechanisms [1, 2]. Marinnelli et al. (155) demonstrated that capsaicin stimulates the firing rate of dopaminergic neurons in rat brain slices at concentrations ranging from 1 to 10 µM. Inhibition of the TRPV1 receptor with 300 nM NG+5'-iodo-resiniferatoxin (IRTX) prevented a capsaicin-induced dopamine release. From a mechanistic point of view, the TRPV1 receptor is a non-selective cation channel and permeable to Ca^{2+} ions [6]. Capsaicin promotes Ca^{2+} influx into the cell via activation of the TRPV1 ion channel, which is one of the proposed pathways for capsaicin-induced neurotransmitter release [4]. On the other hand, capsaicin was also shown to stimulate Ca^{2+} release from a ryanodine-sensitive calcium store [5] (Figure 1).
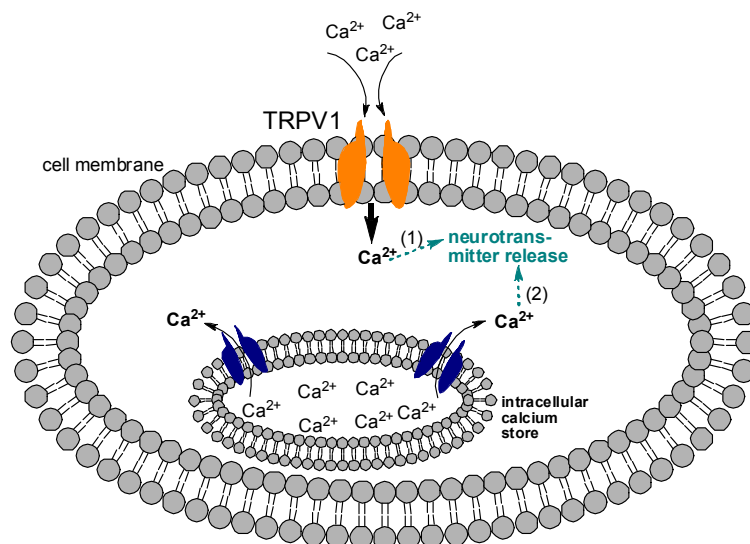
Figure 4.*Proposed pathways for capsaicin-induced, Ca^{2+}-mediated neurotransmitter release. (1) Activation of TRPV1 ion channels leads to Ca^{2+} influx [4]; (2) Ca^{2+} release from intracellular calcium stores (e.g. ryanodine sensitive calcium store) [5]*

Next to its effects on dopamine release, capsaicin is well-known to stimulate serotonin release and the expression of various serotonin receptors in neural cells. Capsaicin was, for instance, shown to increase the expression of the serotonin receptor HTR2A [7] and to release serotonin from the lumbar spinal cord after intradermal application in cats [8].

However, the downside of capsaicin being a high-affinity agonist of the TRPV1 receptor is that TRPV1 receptor activation also evokes a pungent sensation, limiting the dietary intake of high-affinity ligands. Therefore, less pungent structural analogs of capsaicin are sought that may still exhibit positive effects on the neurotransmitter release and the reward system. Recently, we demonstrated that nonivamide, a structural analog of capsaicin, differing from capsaicin only in one double bond and one methyl group (Figure 2), has similar effects on dopamine and serotonin release as capsaicin in neural SH-SY5Y cells [9]. Nonivamide has a lower binding affinity to the TRPV1 receptor in comparison to capsaicin, resulting in a major decrease in pungency [10]. However, inhibition of the TRPV1 receptor using two different TRPV1-inhibitors, *trans*-butylcyclohexanol and capsazepine, demonstrated the TRPV1 receptor being an important factor for capsaicin-induced neurotransmitter release, but is not crucial for the nonivamide-evoked dopamine and serotonin release in SH-SY5Y cells. Mechanistically, it is hypothesised that nonivamide stimulates Ca^{2+} from intracellular stores such as ryanodine-sensitive calcium stores as a major pathway [9].

The alkamide *trans*-pellitorine may also be a potential agonist of ion channels such as TRPV1 and TRPA1 receptors [11].

The present study compares the effects of the alkamide *trans*-pellitorine, a non-pungent structural analog of capsaicin (Figure 2), on Ca^{2+}-mediated serotonin and dopamine release to those of the less pungent capsaicin analog nonivamide in the human neural cell line SH-SY5Y.

(1)   (2)   (3)
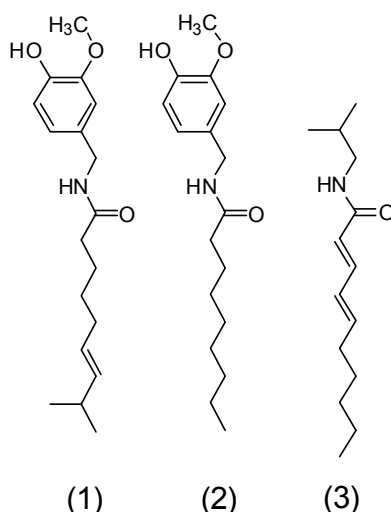
Figure 2. *Chemical structures of capsaicin (1), nonivamide (2) and trans-pellitorine (3)*

Experimental

Materials

All chemicals and reagents were purchased from Sigma Aldrich Austria unless stated otherwise.

Cell culture

SH-SY5Y cells (ATCC, CLR-2266) were maintained as described previously [9]. Toxicity of the test compounds was excluded by trypan blue staining [9] or MTT assay [12].

Serotonin and dopamine release

Serotonin and dopamine release was measured using a sensitive ELISA (DLD Diagnostika, Hamburg, Germany) as described before [9].

Intracellular calcium mobilization

Intracellular calcium mobilization was measured fluorimetrically (fluo-4, life technologies, Carlsbad, USA). A detailed experimental procedure is described at [13].

Quantitative real-time PCR

Real-time PCR experiments were carried out in technical triplicates on a StepOnePlus Real-Time PCR device (life technologies, Carlsbad, USA) using SYBR green fast MasterMix for detection (life technologies, Carlsbad, USA) with cDNA as starting material. For this purpose, mRNA was extracted by means of the PeqGold RNA isolation Kit (Peqlab Biotechnologie GmbH, Erlangen, Germany). cDNA was generated from the isolated mRNA using the high capacity cDNA Kit (life technologies, Carlsbad, USA). Details regarding data analysis and primer sequences

for TRPV1 receptor and the reference gene TBP can be found in [9]. Table 1 provides details on the primers used for TRPA1 receptor gene expression measurement.

Table 1. *Oligonucleotides (5'-3') used as primers in the PCR reaction*

| Gene name	sequence	
	Forward primer	*Reverse primer*
TRPA1	GCAGCCAGTTATGGGCGTAT	TTTGCTGCCAGATGGAGAGG

Statistics

Data are presented as means ± SD or fold change (treated / control). The number of biological replicates (n), each with at least two technical replicates, is indicated in the figures. Outliers were identified using the Nalimov outlier test and excluded from data analysis. Significant effects versus non-treated control cells were tested using one-way ANOVA with Holm-Sidak post hoc test, significant effects between different treatments and/or concentrations were tested using two-way ANOVA respectively, performing a Holm-Sidak post hoc test.

Results

As demonstrated previously, capsaicin increased dopamine release in SH-SY5Y cells in a dose-dependent manner [9]. A concentration of 1 µM increased dopamine release by 494 ± 215%, whereas treatment with 10 µM resulted in an increase of 1295 ± 534% in comparison to non-treated control cells (Figure 3A). In the same concentrations, serotonin release was increased significantly as well. A concentration of 1 µM induced serotonin release by 74 ± 51% and a concentration of 10 µM by 51± 26% (Figure 3B) [9].

These results confirmed the results from Marinelli et al. (155), who demonstrated a significant increase in the dopamine firing rate in rat brain slices after stimulation with 1 to 10 µM capsaicin. Our previous results [9] are, thus, well in line with literature evidence that shows an influence of capsaicin as a TRPV1 agonist on the serotonin system [7-9].
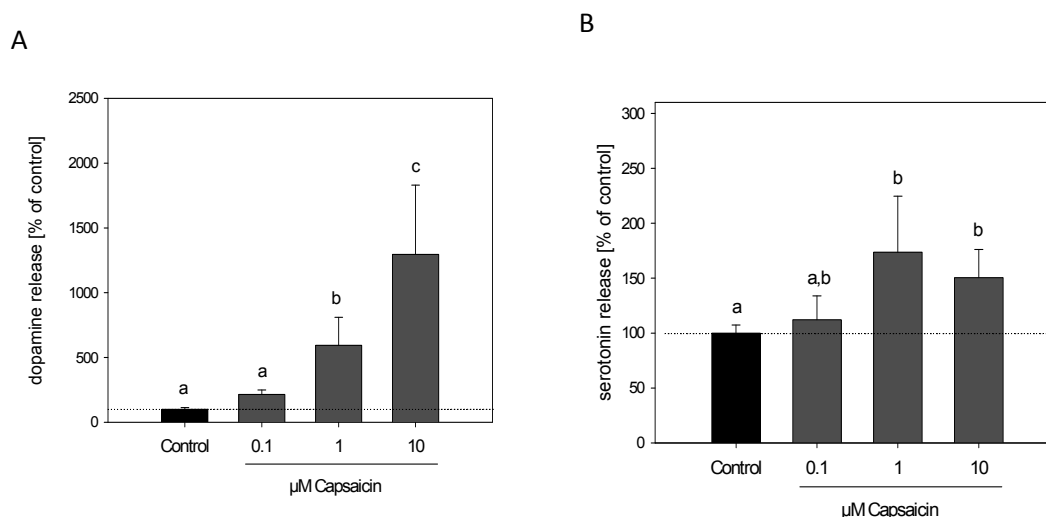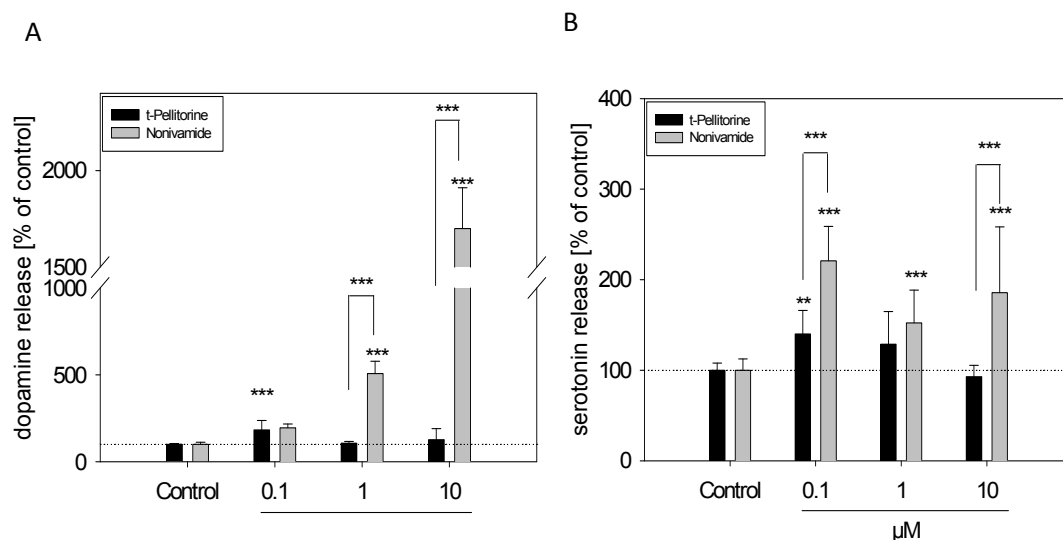
Figure 3. *Dopamine (A) and serotonin (B) release after stimulation with 0.1 to 10 µM capsaicin. Results are displayed as T/C compared to buffer control in %. n=3-4. Statistics: One-Way ANOVA with Holm-Sidak post hoc test*

The capsaicinoide nonivamide and the alkamide *trans*-pellitorine have structural similarities to capsaicin (Figure 2), but are not as pungent, and were, hence, compared in this work for their potency to stimulate dopamine and serotonin release in SH-SY5Y cells. Figure 4A displays the dopamine release after stimulation with *trans*-pellitorine and nonivamide. Dopamine release was increased in a concentration-dependent manner by 95.6 ± 22%, 407 ± 71.% and 1599 ± 212% after stimulation with 0.1, 1 or 10 µM nonivamide, respectively (Figure 4A) [9]. At a concentration of 0.1 µM, *trans*-pellitorine stimulated dopamine release up to 182 ± 42%, which was not different to the result obtained after stimulation with 0.1 µM nonivamide. However, *trans*-pellitorine did not stimulate dopamine release at any of the higher concentrations of 1 and 10 µM, whereas nonivamide did. Similar results were obtained regarding the serotonin release after stimulation with the two capsaicin-analogs (Figure 4B). Serotonin release was stimulated after treatment with 0.1 to 10 µM nonivamide up to 221 ± 38 % and 152 ± 36%, respectively, in comparison to the buffer control (Figure 4B) [9]. *trans*-Pellitorine increased serotonin release at a concentration of 0.1 µM by 40.2 ± 25.9%, but not at any of the higher concentrations tested. Except for a concentration of 1 µM, nonivamide more potently induced the serotonin release.

An increase in intracellular calcium levels has been described earlier as key factor in neurotransmitter release [14]. For capsaicin [4, 5] and nonivamide [9], a calcium-dependent pathway has already been demonstrated. In order to examine whether the neurotransmitter release induced by *trans*-pellitorine is Ca^{2+}-dependent as well, intracellular calcium mobilization was analyzed. *trans*-Pellitorine significantly induced intracellular calcium mobilization at concentrations between 0.01 and 10 µM in comparison to non-treated control cells. A maximum increase up to 173±32% in comparison to the buffer control was shown after stimulation with 0.1 µM *trans*-pellitorine.

However, at this concentration, the effect of *trans*-pellitorine on intracellular calcium mobilization was not different from those seen for nonivamide and capsaicin. At concentrations of 1 and 10 µM, nonivamide was the most potent compound in stimulating intra-cellular calcium mobilization (Figure 5).

Figure 4. *Dopamine (A) and serotonin (B) release after stimulation with 0.1 to 10 µM nonivamide or trans-pellitorine. Results are displayed as T/C compared to buffer control in %. n=4-6. Statistics: One-Way ANOVA vs control with Holm-Sidak post hoc test for effects vs control and two-way ANOVA for comparison of multiple treatments. * p<0.05, ** p<0.01, ***p<0.001*
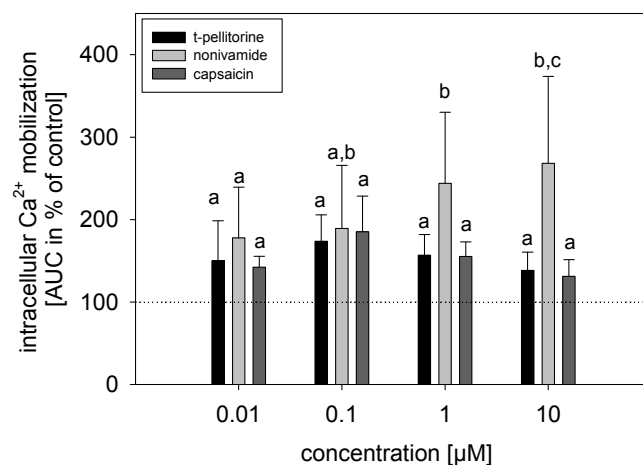
Figure 5. *Intracellular calcium mobilization after stimulation with 0.01 to 10 µM trans-pellitorine, nonivamide or capsaicin. Results are displayed as area under the curve (AUC) compared to buffer control in %. n=3-4. Statistics: Two-way ANOVA with Holm-Sidak post hoc test*
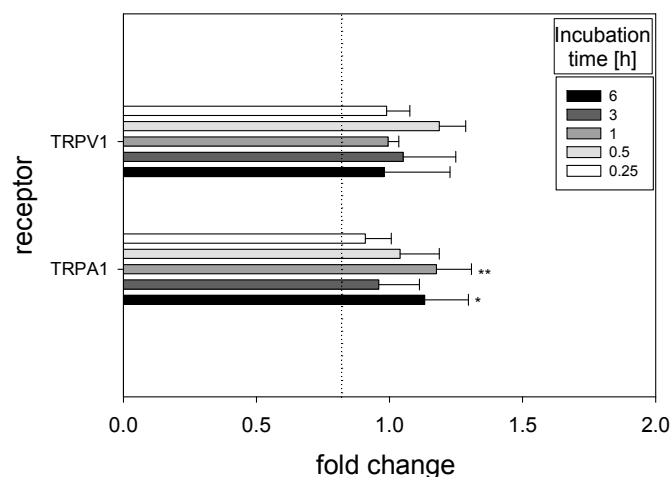
Figure 6. *Fold changes in receptor expression after treatment with 0.1 µM trans-pellitorine. Results are displayed as fold change vs. control. n=3-4. Statistics: Two-Way ANOVA with Holm-Sidak post hoc test. * p<0.05, ** p<0.01, ***p<0.001 vs. non-treated control cells*

trans-Pellitorine is structurally related to capsaicin and nonivamide and also discussed as an agonist of the TRPV1 receptor. However, also TRPA1 is a possible target receptor for the alkamide [11]. A time-dependent gene-expression analysis of two potential target receptors for *trans*-pellitorine, TRPV1 and TRPA1 was carried out to get first insights into which of these receptor(s) might play a pivotal role in signal transduction for *trans*-pellitorine-evoked neurotransmitter release in SH-SY5Y cells. Figure 6 displays the mean fold change in gene expression after incubation with 0.1 µM *trans*-pellitorine for 0.25, 0.5, 1, 3 and 6 h. There was no effect on expression of TRPV1 receptor at any timepoint. Gene expression of the TRPA1 receptor was slightly up-regulated ($p < 0.05$ vs. non-treated controls) after 1 and 6 h and reached a fold change of 1.18 ± 0.13 or 1.13 ± 0.16, respectively. This gene expression analysis points to an impact of *trans*-pellitorine on the ion channel TRPA1, but not on TRPV1. Further studies are needed to elucidate the receptors involved in the mechanisms underlying *trans*-pellitorine-induced neurotransmitter release.

Conclusion

This study demonstrates that the alkamide *trans*-pellitorine induces serotonin and dopamine release in SH-SY5Y cells, accompanied by an intracellular Ca^{2+}-mobilization. However, the potency of *trans*-pellitorine to stimulate neurotransmitter release is significantly weaker compared to that of capsaicin and its analog nonivamide.

Abbreviations

AUC	area under curve
BCH	*trans-tert*-butylcyclohexanol
qPCR	quantitative Real-Time PCR
T/C	treated / control (fold change)
TRPV1	transient receptor potential cation channel subfamily V member 1
TRPA1	transient receptor potential cation channel subfamily A member 1

References

1. Tzavara ET, Li DL, Moutsimilli L, Bisogno T, Di Marzo V, Phebus LA, Nomikos GG, Giros B (2006) Biol Psychiatry 59:508-515
2. Micale V, Cristino L, Tamburella A, Petrosino S, Leggio GM, Drago F, Di Marzo V(2009) Neuropsychopharmacology 34:593-606
3. Marinelli S, Pascucci T, Bernardi G, Puglisi-Allegra S, Mercuri NB (2005) Neuropsychopharmacology 30:864-870
4. Bleakman D, Brorson JR, Miller RJ (1990) Br J Pharmacol 101:423-431
5. Eun SY, Jung SJ, Park YK, Kwak J, Kim SJ, Kim, J(2001) Biochem Biophys Res Commun 285:1114-1120
6. Nagy I, Santha P, Jancso G, Urban L (2004) Eur J Pharmacol 500:351-369
7. Zavitsanou K, Dalton VS, Wang H, Newson P, Chahl LA (2010) J Chem Neuroanat 39:248-255
8. Sorkin LS, McAdoo DJ (1993) Brain Res 607:89-98
9. Rohm B, Holik A.-K, Somoza MM, Pignitter M, Ley JP, Krammer GE, Somoza V (2013) Mol Nutr Food Res, accepted
10. Haas JS, Whipple RE, Grant PM, Andresen BD, Volpe AM, Pelkey GE (1997) Sci Justice 37:15-24
11. Sharma V, Boonen J, Chauhan NS, Thakur M, De Spiegeleer B, Dixit VK (2011) Phytomedicine 18:1161-1169
12. Riedel A, Pignitter M, Hochkogler CM, Rohm B, Walker J, Bytof G, Lantz I, Somoza V (2012) Food Funct 3:955-964
13. Walker J, Rohm B, Lang R, Pariza MW, Hofmann T, Somoza V (2012) Food Chem Toxicol 50:390-398
14. Thanawala MS, Regehr WG (2013) J Neurosci 33:4625-4633

2.3 "The pungent capsaicin analog nonivamide decreases total energy intake and enhances plasma serotonin levels in men when administered in an OGTT: a randomized, crossover intervention"

Hochkogler, C. M.[a]; **Rohm, B**.[a]; Hojdar, K.[a]; Pignitter, M.[b] Widder, S.,[c]; Ley, J.P.[c]; Krammer, G.E.[c]; Somoza,V. [a,b]

[a] Christian Doppler Laboratory for Bioactive Aroma Compounds, University of Vienna, Vienna, Austria

[b] Department of Nutritional and Physiological Chemistry, University of Vienna, Vienna, Austria

[c] Symrise AG, Holzminden, Germany

RESEARCH ARTICLE

The capsaicin analog nonivamide decreases total energy intake from a standardized breakfast and enhances plasma serotonin levels in moderately overweight men after administered in an oral glucose tolerance test: A randomized, crossover trial

Christina M. Hochkogler[1], Barbara Rohm[1], Karin Hojdar[1], Marc Pignitter[2], Sabine Widder[3], Jakob P. Ley[3], Gerhard E. Krammer[3] and Veronika Somoza[1,2]

[1] Christian Doppler Laboratory for Bioactive Aroma Compounds, University of Vienna, Vienna, Austria
[2] Department of Nutritional and Physiological Chemistry, University of Vienna, Vienna, Austria
[3] Symrise AG, Holzminden, Germany

Scope: Since bolus administration of capsaicin has been shown to reduce appetite and ad libitum energy intake, this study elucidated the satiating effect of the less pungent capsaicin analog, nonivamide, on subjective feelings of hunger, ad libitum food intake, and satiating hormones in moderately overweight male subjects.

Methods and results: Following a randomized, crossover design, 24 male subjects (BMI 27.5 ± 1.53 kg/m^2) received either 75 g glucose in 300 mL water (control treatment, CT) or the same glucose solution supplemented with 0.15 mg nonivamide (nonivamide treatment, NT). Ratings of hunger were assessed before and 2 h after each intervention by means of visual analog scales. Ad libitum energy and macronutrient intakes from a standardized breakfast 2 h postintervention were calculated. Plasma glucose, insulin, peptide YY (3–36), glucagon-like peptide 1, and serotonin were quantified in blood samples drawn before and 15, 30, 60, 90, and 120 min after each intervention. NT reduced subjective feelings of hunger and ad libitum energy and carbohydrate intakes from a standardized breakfast compared to CT. Plasma analysis revealed higher mean plasma glucagon-like peptide 1 and serotonin concentrations after NT versus CT.

Conclusion: Addition of 0.15 mg nonivamide to a glucose solution reduced ad libitum energy intake from a standardized breakfast in moderately overweight men.

1 Introduction

Overweight and obesity have become one of the most severe health problems worldwide and are associated with co-

Correspondence: Professor Veronika Somoza, Department of Nutritional and Physiological Chemistry, University of Vienna, Althanstraße 14, 1090 Vienna, Austria
E-mail: Veronika.Somoza@univie.ac.at
Fax: +43-1-4277-9706

Abbreviations: 5-HT, serotonin; **AUC**, area under curve; **CNS**, central nervous system; **GLP-1**, glucagon-like peptide 1; **oGTT**, oral glucose tolerance test; **PYY**, peptide YY (3–36); **SHU**, scoville heat units; **TRPV1**, transient receptor potential cation channel subfamily V member 1; **VAS**, visual analog scale

morbidities such as diabetes mellitus type II, cardiovascular diseases, and several types of cancer [1]. Losing weight and maintaining a healthy body weight has been demonstrated to effectively lower the risk for obesity-associated morbidities and resulting mortalities [2–4]. The main approach for body weight management is to decrease energy intake and/or to increase energy expenditure. Although dietary strategies to consume fewer calories such as limiting portion sizes, certain food groups or macronutrients, such as carbohydrates or fats, can help to moderate calorie intake, particularly during the short term, they are difficult to implement long term. One barrier that prevents individuals from reducing energy intake is that these approaches may compromise diet quality or cause feelings of hunger and dissatisfaction, which can limit their acceptability, sustainability, and long-term

Figure 1. Structure of capsaicin (A), nonivamide (B), and capsiate (C).

effectiveness. In this context, there is increasing interest in enhancing the satiating capacity of foods, for example by the addition of satiating compounds [5].

Capsaicin (Fig. 1), the major pungent principle of red pepper, has been shown to increase satiety and to reduce appetite in healthy volunteers [6, 7]. The downside of capsaicin is that its strong pungency evoked by activation of the transient receptor potential cation channel subfamily V member 1 (TRPV1), also known as the capsaicin receptor or the vanilloid receptor 1 [8] limits its dietary intake. Whether the pungent sensation of capsaicin is mandatory for its satiating activity has not been elucidated so far. Since satiating effects have not only been shown for hot chili peppers containing high amounts of capsaicin [9] but also for CH-19 sweet pepper rich in nonpungent capsinoids such as capsiate (Fig. 1) [9], activation of the TRPV1 receptor and a resulting pungent sensation might not be the only mechanism for promoting satiation.

The present study investigated the satiating effect of *N*-nonanoyl 4-hydroxy-3-methoxybenzylamide, "nonivamide," a less pungent structural analog of capsaicin, which is also known as "synthetic capsaicin" (Fig. 1). The chemical structure of nonivamide differs from capsaicin only in one double bond and one methyl group. It was first synthesized in 1919 by Nelson [10] and demonstrated to be significantly less pungent (9,200,000 scoville heat units, SHU) than capsaicin (16,100,000 SHU) [11]. Like capsaicin, nonivamide also occurs naturally in fresh chili peppers from capsicum oleoresin [12, 13], and is used as food additive and in pharmaceutical products in the United States and Europe (FEMA 2787 and FL no. 16.006) to replace capsaicin. In a recent study of our own group, nonivamide was shown to increase serotonin release from human neuroblastoma cells in culture, independent of TRPV1 activation, which points to potential satiating effects of nonivamide [14].

The regulation of satiation, which occurs during an eating episode and brings it to an end, and satiety, which starts after the end of eating and prevents further eating before the return of hunger [15], is a complex system involving the central nervous system (CNS), the gastrointestinal tract, and

metabolic signals. The hypothalamic neurotransmitter serotonin (5-HT), produced in the intestine and the CNS, plays an important role in the control of food intake and is associated with satiation [16, 17]. The intestinal peptides, peptide YY (3–36) (PYY) and glucagon-like peptide 1 (GLP-1), secreted from endocrine L-cells in the ileum, unfold anorexigenic effects and, thus, also promote satiation in humans [18].

The aim of this human intervention trial was to investigate the short-term effects of the capsaicinoide nonivamide on self-reported desire to eat and total food intake and ad libitum energy intake from a standardized breakfast following an oral glucose tolerance test (oGTT) with and without supplementation with nonivamide. In addition, concentrations of the gastrointestinal hormones PYY and GLP-1, the neurotransmitter serotonin as well as glucose and insulin were analyzed in plasma samples of moderately overweight volunteers before and after the oGTT.

2   Materials and methods

2.1   Characteristics of the subjects

A total of 24 male volunteers were recruited between September and October 2012 by notices in web forums and advertisements on billboards at University of Vienna. Women were excluded due to their menstrual cycle as estrogen has been shown to interfere with serotonin levels [19]. Inclusion criteria were (i) nonsmoking, (ii) moderate overweight (BMI) between 25 and 32 kg/m^2), (iii) age between 20 and 40 years, (iv) no abnormal eating behavior, (v) no alcohol abuse, (vi) no medication, (vii) metabolically healthy, (viii) sensorially untrained, and (ix) fasting blood glucose <120 mg/dL. All subjects underwent a medical screening (hemogram, serum-glutamate-oxalacetate-transaminase, serum-glutamate-pyruvate-transferase, alkaline phosphatase, and gamma glutamyl transferase as well as the blood lipids triglycerides, total, high-density lipoprotein and low-density lipoprotein cholesterol, creatinine, glomerular filtration rate, and fasting blood glucose) prior to the intervention. The presence of eating disorders was excluded by performing a SCOFF questionnaire [20]. Based on the results of the medical screening, 15 eligible subjects were included in the intervention. Baseline characteristics of the volunteers are shown in Table 1. Body weight was assessed by a digital scale (Seca Bella 840, Germany) to the nearest of 100 g and body height was measured by a stadiometer with a precision of 0.1% (Seca 213, Germany). The experimental protocol was approved by the ethics committee of the city of Vienna (registration no. EK 12–084–0812). All volunteers gave their written consent after detailed information.

2.2   Study design

The crossover study was designed as follows (Fig. 2): after randomization in two groups and an overnight fast, each

3

Table 1. Study participants characteristics

		Value
Age (year)	Median (range)	25.0 (20.0–39.0)
Height (m)	Mean ± SD	1.83 ± 0.07
Weight (kg)	Mean ± SD	92.1 ± 8.06
BMI (kg/m^2)	Mean ± SD	27.5 ± 1.53
Fasting blood glucose (mg/dL)	Mean ± SD	87.4 ± 6.40
SGOT[a)] (U/L)	Mean ± SD	26.0 ± 5.99
SGPT[b)] (U/L)	Median (range)	28.0 (19.0–75.0)
ALP[c)] (U/L)	Mean ± SD	69.3 ± 5.33
GGT[d)] (U/L)	Median (range)	12.0 (12.0–109)
Cholesterol (mg/dL)	Median (range)	165 (132–242)
HDL[e)] (mg/dL)	Mean ± SD	50.9 ± 10.4
LDL[f)] (mg/dL)	Median (range)	93.0 (63.0–172)
Triglycerides (mg/dL)	Median (range)	90.0 (55.0–242)
Creatinine (mg/dL)	Mean ± SD	0.97 ± 0.04
GFR[g)] (mL/min/ 1.73 m^2)	Mean ± SD	103 ± 21.7

a) SGOT, serum-glutamate-oxalacetate-transaminase.
b) SGPT, serum-glutamate-pyruvate-transferase.
c) ALP, alkaline phosphatase.
d) GGT, gamma-glutamyl transferase.
e) HDL, high-density lipoprotein.
f) LDL, low-density lipoprotein.
g) GFR, glomerular filtration rate.

volunteer participated in an oGTT (75 g glucose + 15 μL ethanol: control treatment) and an oGTT supplemented with nonivamide (75 g glucose + 15 μL ethanol + 0.15 mg nonivamide: nonivamide treatment) at two study visits between 8 and 9 a.m. The two visits were carried out 1 wk apart. Before and after each oGTT, subjects were asked to give a rating of their momentary feeling of hunger on a 100-mm visual analog scale (VAS). The standardized breakfast served on a tray 2 h after the oGTTs consisted of four rolls, three slices of bread, 100 g strawberry jam, 60 g honey, four slices of ham, four slices of cheese, 180 g yogurt, 80 g creamery butter, 20 g sugar, 40 g coffee creamer, 200 mL water, and 200 mL coffee or tea. The breakfast provided had a total energy content of

12.1 MJ and a total of 355 g carbohydrates, 126 g fat, and 80 g proteins. Participants were asked to eat until satiated. The remaining food on each subjects' tray was weighed and the net ad libitum energy and macronutrient intakes were calculated by means of the German Food Code and nutrient database BLS II (Bundeslebensmittelschlüssel).

2.3 Blood sample collection

Venous blood samples for determination of plasma concentrations of GLP-1 and serotonin were collected in EDTA-coated tubes (Sarstedt, Nümbrecht, Germany) before and 15, 30, 60, 90, and 120 min after the oGTTs. In order to obtain plasma, blood was centrifuged immediately after drawing at 1800 × g at 4°C for 15 min. Plasma samples for glucose and insulin analyses were obtained by centrifugation (1800 × g for 15 min at 4°C) of blood samples collected in EDTA- and fluoride-coated or heparin-coated tubes (Sarstedt), respectively. For determination of PYY concentrations, the dipeptidyl peptidase (DPP-IV) protease inhibitor (Merck Millipore, Darmstadt, Germany) was added to the blood immediately after drawing before centrifugation at 1800 × g at 4°C for 15 min. All plasma samples were stored in aliquots at −80°C until analysis.

2.4 Glucose, insulin, PYY, GLP-1, and serotonin assays

Plasma glucose concentrations were assessed colorimetrically (Cayman Europe, Tallinn, Estonia). For determination of plasma insulin concentrations, an ELISA kit purchased from IASON, Graz, Austria was used. Plasma PYY and GLP-1 concentrations were measured by means of ELISA kits (Merck Millipore). Serotonin levels were either assessed by an ELISA kit, purchased from DLD Diagnostika, Hamburg, Germany. All assays were carried out following the instructions provided by the manufacturer's protocols.
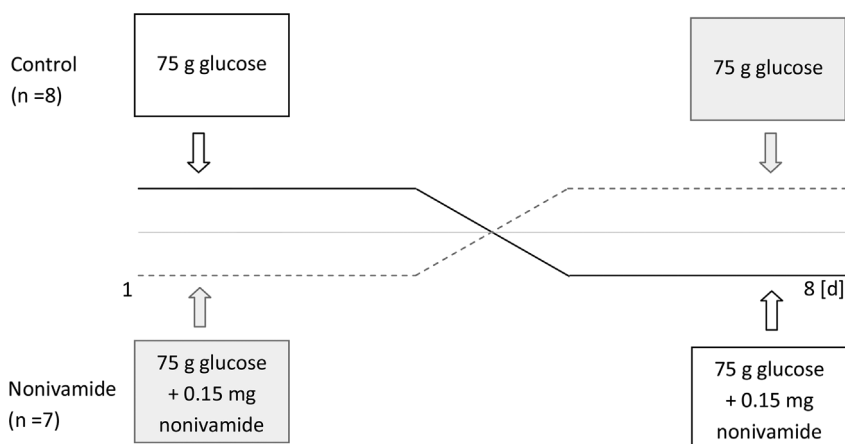
Figure 2. Schematic illustration of the crossover study design.

2.5   LC–MS analysis of plasma concentrations of nonivamide

Nonivamide was analyzed in plasma at fasting and after administration of nonivamide with slight modifications according to Rohm et al. [14] A total of 150 μL plasma samples were mixed with 450 μL cold acetonitrile. The mixture was stored at −20°C for 1 h. The samples were vortexed and centrifuged at 13,000 × *g* for 10 min. After the supernatant was vacuum-dried, the samples were reconstituted using 300 μL water/acetonitrile (8/2, v/v). Prior to LC–MS analysis, the samples were passed through a 0.45 μm polyvinylidene fluoride (PVDF) filter. The samples were loaded on a C18 trap column (NanoACQ 2G-V/M SymC18 5 μm, 180 μm × 20 mm, Waters, Vienna, Austria) and separated on a C18 nanocapillary (XBridge BEH130, 3.5 μm, 75 μm × 150 mm NanoEase, Waters, Vienna, Austria). A gradient was used, starting with 15% solvent B, consisting of 0.1% formic acid in acetonitrile, and 85% solvent A, consisting of 0.1% formic acid in water. The acetonitrile gradient was increased to 70% B within 70 min to finally reach 100% B after 73 min, which was held constant for 7 min. After injection of 5 μL sample, nonivamide eluted after 43.4 min at a flow rate of 0.3 μL/min at 35°C. The nano-LC system (Dionex Ultimate 3000 RSLC, Thermo Fisher Scientific, Vienna, Austria) was equipped with an LTQ Velos Orbitrap (Thermo Fisher Scientific, Vienna, Austria), which was operated in the nano-ESI(+) mode scanning in the range of 100–1000 *m/z*. The capillary temperature was set to 300°C and a capillary voltage of 3.0 kV was applied. Higher energy collisional dissociation with a normalized collision energy of 30% was applied for fragmentation of the precursor ion 294.21 *m/z* to yield the specific product ion 137.06 *m/z*, corresponding to the vanillyl residue, as described elsewhere [21]. The limit of detection for nonivamide was 5 fmol. The recovery was determined to be 45.1%.

2.6   Statistical analyses

Statistical analyses were conducted using the statistical software SigmaPlot 11.0. A power analysis based on energy intake from the study by Westerterp-Plantenga et al. [7] was performed for determination of sample size, with total energy intake as the main outcome measure.

A Shapiro–Wilk test was carried out to test for normal distribution. Normally distributed data are presented as means ± SEM unless stated otherwise. In case of absent normal distribution, data are shown as median (range).

For mean plasma PYY, glucose and insulin concentrations statistical difference ($p < 0.05$) between control and nonivamide was tested using a two-way repeated measures ANOVA for time and treatment.

Incremental area under curve (iAUC) was calculated over time for plasma GLP-1 levels and then tested for statistical significance ($p < 0.05$) between control and nonivamide by

applying one-sample Student's *t*-test. Total AUC was computed for plasma serotonin levels over time. To test the statistical difference ($p < 0.05$) between control and nonivamide treatment, one-sample Student's *t*-test was performed.

Differences in the feeling of satiety after control versus nonivamide treatment, determined by means of a VAS before and after each oGTT, were tested using one-sample Student's *t*-test. For energy and macronutrient intake, statistical difference ($p < 0.05$) between control and nonivamide treatment was calculated performing one-sample Student's *t*-test. Spearman correlation coefficient was computed for changes of energy intake and plasma serotonin levels from baseline.

3   Results

3.1   Plasma concentrations of nonivamide

Plasma concentrations of nonivamide were measured at fasting and 15, 30, 60, 90, and 120 min after administration of 0.15 mg nonivamide using LC–MS analysis but were all analyzed below the limit of detection (5 fmol nonivamide).

3.2   Total energy and macronutrient intakes from breakfast and ratings of hunger

Administration of a glucose solution (75 g/300 mL) supplemented with 0.15 mg nonivamide compared to administration of the unsupplemented glucose solution (control) resulted in a reduction of total ad libitum energy intake from a standardized breakfast 2 h after the intervention: mean total energy intake after control treatment was 4.75 ± 0.45 MJ compared to 4.26 ± 0.33 MJ ($p < 0.05$) after the nonivamide intervention, accounting for a mean difference of 7.8 ± 4.0% (Fig. 3). This reduced food intake was associated with a
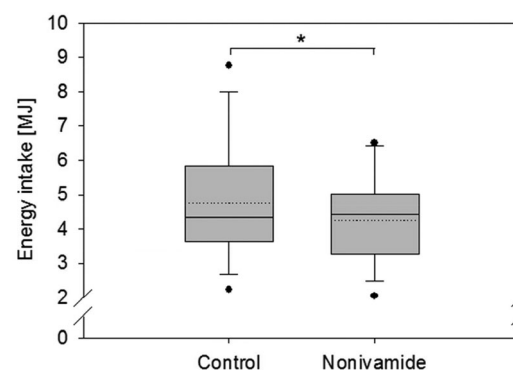
Figure 3. Total ad libitum energy intake from a standardized breakfast 2 h after administration of 75 g glucose without (control) and with supplementation with 0.15 mg nonivamide (nonivamide) in 15 healthy male volunteers. Statistical difference ($p < 0.05$) was assessed by one-sample Student's *t*-test and indicated by "*". Means are shown as dotted lines.

Table 2. Mean macronutrient intake of healthy male volunteers from a standardized breakfast 2 h after administration of 75 g glucose without (control) or with supplementation of 0.15 mg nonivamide (nonivamide)
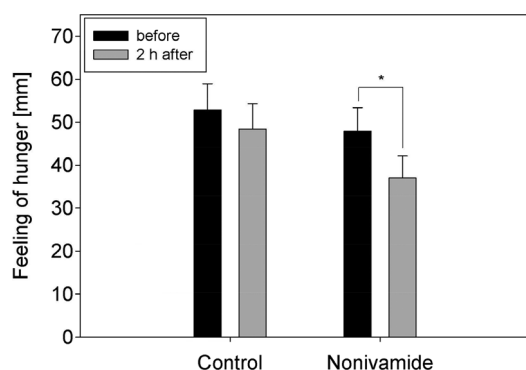
	Control (*n* = 15)	Nonivamide (*n* = 15)	*p*-value
Fat (g)	49.1 ± 20.0	44.2 ± 16.6	0.13
Proteins (g)	41.8 ± 15.9	39.3 ± 12.8	0.52
Carbohydrates (g)	129 ± 54.5	113 ± 41.5	0.03

Values are shown as mean ± SD. Statistical difference ($p < 0.05$) between control and nonivamide group was assessed by paired Student's *t*-test.
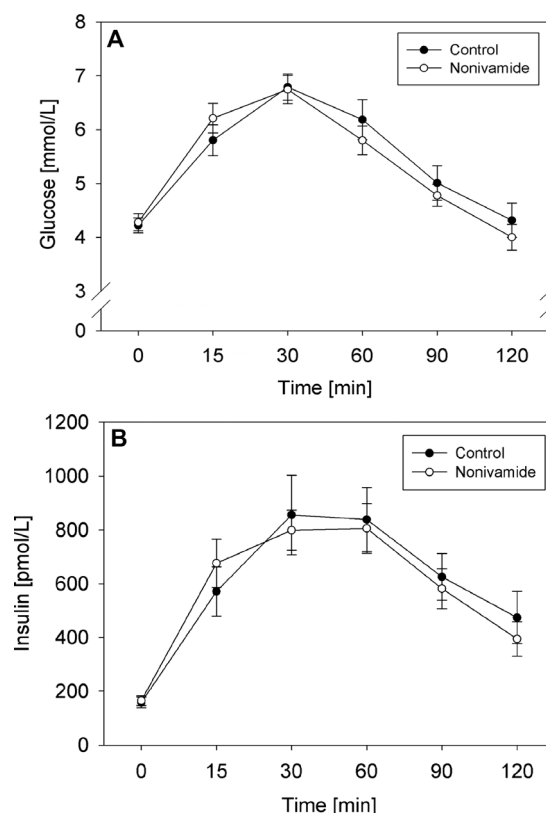

Figure 4. Mean values of the feeling of hunger determined by a 100-mm VAS before and 2 h after administration of 75 g glucose without (control) and with supplementation with 0.15 mg nonivamide (nonivamide). Values are shown as mean ± SEM. Statistical difference ($p < 0.05$) between control and nonivamide treatment was assessed by paired Student's *t*-test and indicated by "*".

significant reduction in carbohydrate intake by 11.6 ± 7.2 g after control (125 ± 13.6 g) versus nonivamide (114 ± 10.0 g) treatment. Fat or protein intake did not differ between control and nonivamide treatments (Table 2).

Feeling of hunger was assessed before and 2 h after control/nonivamide intervention by subjects' ratings on a continuous 100-mm VAS. A significant difference in the feeling of hunger after administration of glucose solution containing nonivamide ($p < 0.05$) was reported, whereas administration of the glucose solution alone did not change subjective hunger feelings (Fig. 4).

3.3 Plasma glucose and insulin concentrations

Administration of nonivamide did not affect mean plasma glucose levels after oral glucose challenge, as the mean plasma glucose concentrations over time did not differ between the treatments and neither did the AUC (672.3 ± 26.96 control vs. 654.7 ± 19.10 nonivamide, $p < 0.05$). Moreover, there was no difference in the mean plasma insulin response at any of the time points after control versus nonivamide

Figure 5. Mean plasma glucose (A) and insulin (B) concentrations before and 15, 30, 60, 90, and 120 min after administration of 75 g glucose without (control) and with supplementation with 0.15 mg nonivamide (nonivamide) in 15 healthy male volunteers. Values are shown as mean ± SEM. Statistical difference ($p < 0.05$) was determined by two-way repeated measures ANOVA for time and treatment.

treatment (AUC: 80,043 ± 9,234 control vs. 76,884 ± 6,740; Fig. 5).

3.4 Plasma PYY and GLP-1 concentrations

Mean plasma PYY and GLP-1 concentrations (Fig. 6 and 7) did not differ between control and nonivamide treatment at any of the time points. However, the incremental AUC for plasma GLP-1 concentrations was increased (20.31 ± 116.3 control, 228.0 ± 125.8 nonivamide, $p < 0.05$) after administration of the glucose solution supplemented with nonivamide compared to administration of the glucose solution (control treatment). The maximum difference between control and nonivamide treatment was observed 15 min postload, at which treatment with nonivamide increased GLP-1 levels by 8.2% from baseline control levels (16.9 ± 2.47 pmol/L vs. 18.5 ± 2.44 pmol/L). GLP-1 levels at 30, 60, 90, and 120 min did not differ between the two treatments (Fig. 7).
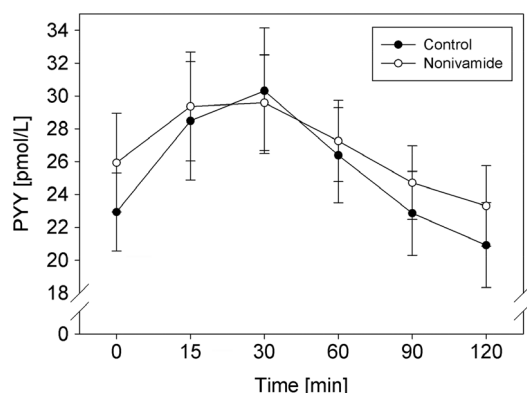
6   C. M. Hochkogler et al.

Mol. Nutr. Food Res. 2014, *00*, 1–9

Figure 6. Mean plasma PYY concentrations before and 15, 30, 60, 90, and 120 min after administration of 75 g glucose without (control) and with supplementation with 0.15 mg nonivamide (nonivamide) in 15 healthy male volunteers. Values are shown as mean ± SEM. Statistical difference ($p < 0.05$) was determined by two-way repeated measures ANOVA for time and treatment.
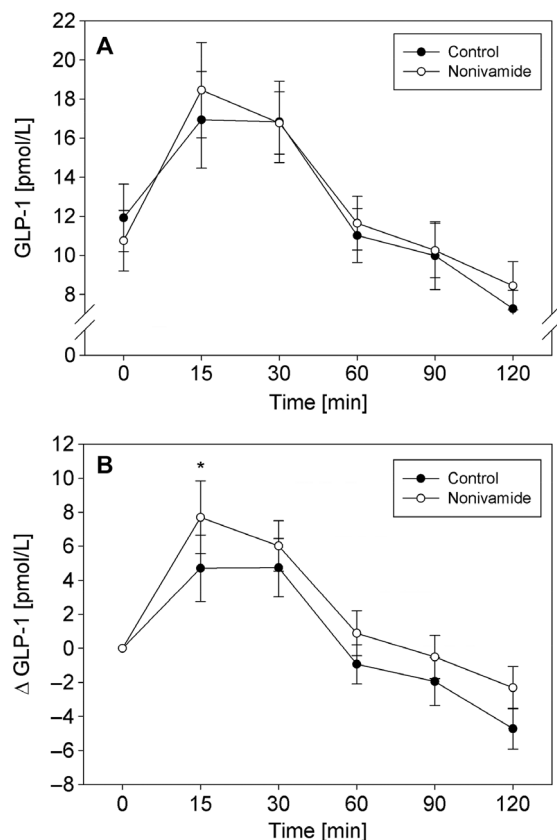
Figure 7. Mean plasma GLP-1 (A) concentrations and mean delta values from baseline levels (B) before and 15, 30, 60, 90, and 120 min after administration of 75 g glucose without (control) and with supplementation with 0.15 mg nonivamide (nonivamide) in 15 healthy male volunteers. Values are shown as mean ± SEM. Statistical difference ($p < 0.05$) was determined by two-way repeated measures ANOVA for time and treatment followed by Student–Newman Keuls test as post hoc test and differences between the two treatments are indicated by "*".
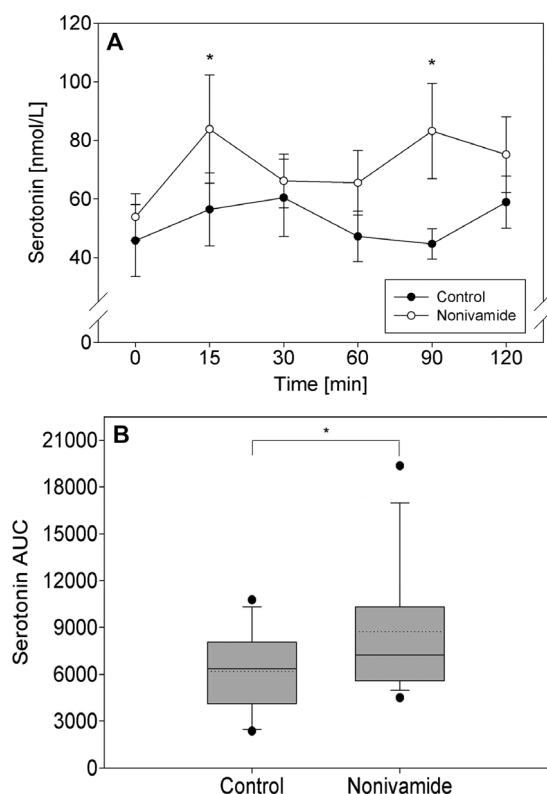
3.5 Plasma serotonin levels

Mean plasma serotonin concentrations were not different between control and nonivamide treatment at baseline. One participant was excluded from statistical analysis due to baseline plasma serotonin levels outside the reference range (536.8 nmol/L, reference range 0.6–179 nmol/L [22]). However, reference plasma serotonin concentrations are controversially discussed [22] since preanalytical contamination by serotonin released from activated platelets might contribute to plasma concentrations >3 nmol/L. Although this bias cannot be excluded in the present study, the effect observed for nonivamide should not be biased by preanalytical treatment since the same work up protocol was applied to all samples of the crossover study.

AUC for plasma serotonin was higher ($p < 0.05$) by 28.9% after nonivamide treatment (8738 ± 1098) in comparison to control (6190 ± 688.2). At 15 and 90 min after the intervention, plasma serotonin concentrations exceeded those after control treatment (Fig. 8).

A Spearman correlation coefficient was calculated for energy intake and plasma serotonin concentrations. Here, a trend for an inverse correlation was assessed between changes in total energy intake from breakfast and changes of plasma serotonin levels at 15 min from baseline ($r = -0.50$, $p = 0.06$).

4   Discussion

The aim of this randomized, crossover trial was to address the effects of a single administration of nonivamide, a capsaicin analog, on ad libitum energy intake and markers of satiation in moderately overweight men. Administration of a breakfast containing 10 g of red pepper has been shown to decrease the desire to eat and reduce ad libitum food intake [6]. Capsaicin has been hypothesized to be the active principle in red pepper. Capsaicin administration to healthy volunteers in amounts ranging from 0.375 to 1003 mg reduced the self-reported hunger [7], and the desire to eat fatty, sweet, and salty foods [23]. Despite this convincing evidence for the satiating effect of capsaicin, its use as a satiating compound in foods is limited due to its pungency. Less pungent capsaicinoids exhibiting appetite-reducing effects may offer an alternative. The capsaicinoide nonivamide, for which the pungency is evaluated with only 9,200,000 SHU compared to 16,100,000 SHU for capsaicin, has recently been shown to stimulate dopamine and serotonin released from human neuroblastoma cells in culture, independent of TRPV1 activation [14]. These results point to a possible effect of nonivamide on mechanisms regulating food intake. In this study, the effects of a bolus administration of nonivamide on ad libitum food and energy intake, and markers of satiation were investigated in a randomized, crossover intervention trial. The subjective feeling of hunger was assessed by a 100-mm VAS. The use of a VAS is a simple, but reliable way to

7

Figure 8. Plasma serotonin concentrations (A) and AUC values (B) before and 15, 30, 60, 90, and 120 min after administration of 75 g glucose without (control) and with supplementation with 0.15 mg nonivamide (nonivamide) in 14 healthy male volunteers. Values are shown as mean ± SEM. For plasma serotonin concentrations, statistical difference ($p < 0.05$) between treatments was determined by two-way repeated measures ANOVA for time and treatment followed by Student–Newman Keuls test as post hoc test; differences between the two treatments for each time point are indicated by "*". No time-dependent effect was found. Statistical difference in AUC values ($p < 0.05$) was assessed by one sample Student's *t*-test and indicated by "*." Means are shown as dotted lines.

satiating effect of capsaicinoids. Moreover, the reduction of the ad libitum energy intake, evoked by administration of only 0.15 mg nonivamide, could help to improve the satiating capacity of foods and, thus, may support body weight management. Epidemiological data from the United States show that decreasing daily total energy by 0.42 MJ would be sufficient to maintain a healthy subject's body weight [25].

Short-term regulation of food intake is influenced by numerous gastrointestinal hormones, and the majority among them unfolds anorexigenic effects [18]. For example, enhanced secretion of the intestinal hormones GLP-1 and PYY into circulation has been shown to reduce food intake and increase satiation in humans [18, 26]. GLP-1, which is produced by intestinal L-cells and secreted after intake of macronutrients, reduces gastric motility and secretion, stimulates satiation, and influences glucose metabolism by stimulating insulin [27]. Another peptide that is mainly produced by intestinal L-cells is PYY, which is thought to reduce appetite via slowing down gastric motility [26]. In this study, secretion of GLP-1, PYY, and serotonin as well as glucose and insulin as major outcome measures of satiation and satiety [28] was induced by applying a standard oGTT, administrating 75 g glucose dissolved in 300 mL water.

GLP-1 concentrations were increased 15 min after ingestion of the nonivamide containing glucose solution in comparison to glucose administration solely. This result is consistent with findings reported by Smeets and Westerterp-Plantenga [29], who demonstrated an increase in GLP-1 after administration of a lunch meal supplemented with 1.03 g of red pepper. The authors proposed that the satiating effect of capsaicin on the gut-derived hormone might be due to increased gastric emptying [29]. However, this hypothesis is not entirely supported by results from this study since nonivamide treatment had no effect on PYY response, which is also involved in the regulation of gastric emptying.

According to the "glucostatic theory," which was proposed from Jean Mayer about 60 years ago, enhanced blood glucose concentrations result in increased feelings of satiation and satiety [30]. However, plasma and glucose and insulin responses were not influenced by nonivamide treatment in this study, indicating that plasma glucose homeostasis is not affected by this capsaicin analog.

The hypothalamic neurotransmitter serotonin, produced in the CNS and intestines, is implicated in a large number of functions such as sleep, mood, and general behavior. It has also been shown to be strongly involved in the regulation of food intake and satiety [16, 31], and to generate satiety signals in the brain [32]. At least 14 different serotonin receptor subtypes are known to mediate the mechanisms of action of serotonin [33], but only a few of them are provably associated with an altered food intake. In animal studies, signaling stimulation and protein expression of the receptors 5-HT$_{1A}$, 5-HT$_{1B}$, 5-HT$_{2A}$, 5-HT$_{2C}$ reduced food intake [34, 35]. These results are in agreement with recent findings from our own group, demonstrating that treatment of SH-SY5Y cells in culture with 1 µM nonivamide enhances the expression of

measure feelings of hunger and satiety. VAS results correlate well with subsequent food intakes, even under controlled dietary conditions and repeated measures designs, which are both given in the current study [24].

Two hours after administration of the glucose solution supplemented with 0.15 mg nonivamide, subjects' hunger was less distinct in comparison to administration of the glucose solution alone. This decreased subjective feeling of hunger was reflected by a reduced energy intake, confirming the reliability of the VAS measurement. Nonivamide treatment also reduced total ad libitum energy intake from a standardized breakfast by 7.8% in comparison to control treatment (administration of 300 mL glucose solution solely). Notably, participants did not report any difference in pungency between the two glucose solutions. These results clearly demonstrate that a pungent sensation is not crucial for the

serotonin receptor genes (5-HT$_{1A,}$ $_{1B,}$ and $_{2A}$) in a time-dependent manner [14].

Notably, approximately 95% of total endogenous serotonin is secreted from enterochromaffin cells in the intestines [36]. Beside the regulation of digestive functions, there is strong evidence that intestinal 5-HT is involved in the control of food intake as well. Furthermore, results from recent studies indicate that the 5-HT$_{1A}$ receptor is also expressed by mast cells in the human intestines [37], and by human Caco-2 cells in culture [38].

In rodents, peripheral 5-HT has been shown to stimulate vagal jejunal afferents [39]. This stimulation was demonstrated to result in an activation of areas in the brain that are involved in mechanism regulating satiety [40]. Moreover, animal experiments with obese mice showed an impairment in afferent sensitivity to the satiety mediator 5-HT. Thus, a decreased signaling from the intestine through vagal jejunal afferents is suggested to result in enhanced food intake and promoting weight gain [41]. We hypothesize that peripheral serotonin might be involved in the regulation of food intake through stimulation of vagal afferents.

Although absorption of nonivamide from the intestine has to be clarified in further studies, we suppose that intestinal absorption is similar to its structural analog capsaicin, for which a percent absorption of 80% has been reported [42]. We here hypothesize that plasma concentrations of nonivamide were below the limit of detection of 5 fmol because of the very small amount of 0.15 mg nonivamide administered. In a previous study, we demonstrated a 0.4% percent uptake of nonivamide by human neural cells in culture [14]. However, intestinal uptake experiments for nonivamide are warranted.

In this study, oral administration of 0.15 mg nonivamide increased plasma serotonin concentrations in moderately overweight men, which may have contributed to the decreased feeling of hunger and reduction of ad libitum energy intake. Moreover, Spearman correlation coefficient for energy intake and plasma serotonin levels point to a trend toward an inverse correlation. Analyses of the macronutrient intakes revealed further that the reduced energy intake was primarily based on a reduction of carbohydrate intake. In contrast, low blood levels of serotonin have been hypothesized to promote craving for carbohydrates [17].

In conclusion, this study demonstrated that bolus administration of 0.15 mg nonivamide, dissolved in a 300 mL glucose solution (250 g/L) decreased subjective feelings of hunger and reduced total ad libitum energy intake from a standardized breakfast in comparison to administration of a nonsupplemented glucose solution. The reported reduction in energy intake was reflected by a decrease in carbohydrate intake. Furthermore, increased plasma serotonin and GLP-1 levels might be at least partly responsible for this satiating effect of nonivamide shown for the moderately overweight male volunteers studied. Future studies are warranted to prove the effect of nonivamide on long-term food intake and its potential to help to maintain a healthy body weight.

5   References

[1] Louie, S. M., Roberts, L. S., Nomura, D. K., Mechanisms linking obesity and cancer. *Biochim. Biophys. Acta* 2013, *1831*, 1499–1508.

[2] Penn, L., White, M., Lindstrom, J., den Boer, A. T. et al., Importance of weight loss maintenance and risk prediction in the prevention of type 2 diabetes: analysis of European Diabetes Prevention Study RCT. *PloS One* 2013, *8*, e57143.

[3] Sierra-Johnson, J., Romero-Corral, A., Somers, V. K., Lopez-Jimenez, F. et al., Prognostic importance of weight loss in patients with coronary heart disease regardless of initial body mass index. *Eur. J. Cardiovasc. Prev. Rehabil.* 2008, *15*, 336–340.

[4] Neter, J. E., Stam, B. E., Kok, F. J., Grobbee, D. E. et al., Influence of weight reduction on blood pressure: a meta-analysis of randomized controlled trials. *Hypertension* 2003, *42*, 878–884.

[5] Van Kleef, E., Van Trijp, J. C., Van Den Borne, J. J., Zondervan, C., Successful development of satiety enhancing food products: towards a multidisciplinary agenda of research challenges. *Crit. Rev. Food Sci. Nutr.* 2012, *52*, 611–628.

[6] Yoshioka, M., St-Pierre, S., Drapeau, V., Dionne, I. et al., Effects of red pepper on appetite and energy intake. *Br. J. Nutr.* 1999, *82*, 115–123.

[7] Westerterp-Plantenga, M. S., Smeets, A., Lejeune, M. P., Sensory and gastrointestinal satiety effects of capsaicin on food intake. *Int. J. Obes.* 2005, *29*, 682–688.

[8] Tzavara, E. T., Li, D. L., Moutsimilli, L., Bisogno, T. et al., Endocannabinoids activate transient receptor potential vanilloid 1 receptors to reduce hyperdopaminergia-related hyperactivity: therapeutic implications. *Biol. Psychiatry* 2006, *59*, 508–515.

[9] Reinbach, H. C., Smeets, A., Martinussen, T., Moller, P. et al., Effects of capsaicin, green tea and CH-19 sweet pepper on appetite and energy intake in humans in negative and positive energy balance. *Clin. Nutr.* 2009, *28*, 260–265.

[10] Nelson, E. K., Vanillyl-acyl amides. *J. Am. Chem. Soc.* 1919, *41*, 2121–2130.

[11] Haas, J. S., Whipple, R. E., Grant, P. M., Andresen, B. D. et al., Chemical and elemental comparison of two formulations of oleoresin capsicum. *Sci. Justice* 1997, *37*, 15–24.

[12] Reilly, C. A., Crouch, D. J., Yost, G. S., Quantitative analysis of capsaicinoids in fresh peppers, oleoresin capsicum and pepper spray products. *J. Forensic Sci.* 2001, *46*, 502–509.

[13] Constant, H. L., Cordell, G. A., West, D. P., Nonivamide, a constituent of capsicum oleoresin. *J. Nat. Prod.* 1996, *59*, 425–426.

[14] Rohm, B., Holik, A. K., Somoza, M. M., Pignitter, M. et al., Nonivamide, a capsaicin analog, increases dopamine and serotonin release in SH-SY5Y cells via a TRPV1-independent pathway. *Mol. Nutr. Food Res.* 2013, *57*, 2008–2018.

[15] Bellisle, F., Drewnowski, A., Anderson, G. H., Westerterp-Plantenga, M. et al., Sweetness, satiation, and satiety. *J. Nutr.* 2012, *142*, 1149S–1154S.

[16] Halford, J. C., Harrold, J. A., Lawton, C. L., Blundell, J. E., Serotonin (5-HT) drugs: effects on appetite expression and use for the treatment of obesity. *Curr. Drug Targets* 2005, *6*, 201–213.

[17] Erlanson-Albertsson, C., How palatable food disrupts appetite regulation. *Basic. Clin. Pharmacol. Toxicol.* 2005, *97*, 61–73.

[18] Naslund, E., Hellstrom, P. M., Appetite signaling: from gut peptides and enteric nerves to brain. *Physiol. Behav.* 2007, *92*, 256–262.

[19] DeSoto, M. C., Geary, D. C., Hoard, M. K., Sheldon, M. S. et al., Estrogen fluctuations, oral contraceptives and borderline personality. *Psychoneuroendocrino.* 2003, *28*, 751–766.

[20] Morgan, J. F., Reid, F., Lacey, J. H., The SCOFF questionnaire: assessment of a new screening tool for eating disorders. *BMJ* 1999, *319*, 1467–1468.

[21] Reilly, C. A., Ehlhardt, W. J., Jackson, D. A., Kulanthaivel, P. et al., Metabolism of capsaicin by cytochrome P450 produces novel dehydrogenated metabolites and decreases cytotoxicity to lung and liver cells. *Chem. Res. Toxicol.* 2003, *16*, 336–349.

[22] Brand, T., Anderson, G. M., The measurement of platelet-poor plasma serotonin: a systematic review of prior reports and recommendations for improved analysis. *Clin. Chem.* 2011, *57*, 1376–1386.

[23] Ludy, M. J., Mattes, R. D., The effects of hedonically acceptable red pepper doses on thermogenesis and appetite. *Physiol. Behav.* 2011, *102*, 251–258.

[24] Stubbs, R. J., Hughes, D. A., Johnstone, A. M., Rowley, E. et al., The use of visual analogue scales to assess motivation to eat in human subjects: a review of their reliability and validity with an evaluation of new hand-held computerized systems for temporal tracking of appetite ratings. *Br. J. Nutr.* 2000, *84*, 405–415.

[25] Rodearmel, S. J., Wyatt, H. R., Barry, M. J., Dong, F. et al., A family-based approach to preventing excessive weight gain. *Obesity* 2006, *14*, 1392–1401.

[26] Degen, L., Oesch, S., Casanova, M., Graf, S. et al., Effect of peptide YY3–36 on food intake in humans. *Gastroenterology* 2005, *129*, 1430–1436.

[27] Naslund, E., Barkeling, B., King, N., Gutniak, M. et al., Energy intake and appetite are suppressed by glucagon-like peptide-1 (GLP-1) in obese men. *Int. J. Obes. Relat. Metab. Disord.* 1999, *23*, 304–311.

[28] EFSA, Guidance on the scientific requirements for health claims related to appetite ratings, weight management, and blood glucose concentrations. *EFSA J.* 2012, *10*, 2604(1–11).

[29] Smeets, A. J., Westerterp-Plantenga, M. S., The acute effects of a lunch containing capsaicin on energy and substrate utilisation, hormones, and satiety. *Eur. J. Nutr.* 2009, *48*, 229–234.

[30] Mayer, J., Regulation of energy intake and the body weight: the glucostatic theory and the lipostatic hypothesis. *Ann. N.Y. Acad. Sci.* 1955, *63*, 15–43.

[31] Meguid, M. M., Fetissov, S. O., Varma, M., Sato, T. et al., Hypothalamic dopamine and serotonin in the regulation of food intake. *Nutrition* 2000, *16*, 843–857.

[32] Lam, D. D., Heisler, L. K., Serotonin and energy balance: molecular mechanisms and implications for type 2 diabetes. *Expert. Rev. Mol. Med.* 2007, *9*, 1–24.

[33] Hoyer, D., Hannon, J. P., Martin, G. R., Molecular, pharmacological and functional diversity of 5-HT receptors. *Pharmacol. Biochem. Behav.* 2002, *71*, 533–554.

[34] Heal, D. J., Gosden, J., Smith, S. L., A review of late-stage CNS drug candidates for the treatment of obesity. *Int. J. Obes.* 2013, *37*, 107–117.

[35] Lam, D. D., Garfield, A. S., Marston, O. J., Shaw, J. et al., Brain serotonin system in the coordination of food intake and body weight. *Pharmacol. Biochem. Behav.* 2010, *97*, 84–91.

[36] Berger, M., Gray, J. A., Roth, B. L., The expanded biology of serotonin. *Annu. Rev. Med.* 2009, *60*, 355–366.

[37] Wang, G. D., Wang, X. Y., Zou, F., Qu, M. et al., Mast cell expression of the serotonin1A receptor in guinea pig and human intestine. *Am. J. Physiol. Gastrointest. Liver Physiol.* 2013, *304*, G855–G863.

[38] Iceta, R., Mesonero, J. E., Aramayona, J. J., Alcalde, A. I., Expression of 5-HT1A and 5-HT7 receptors in Caco-2 cells and their role in the regulation of serotonin transporter activity. *J. Physiol. Pharmacol.* 2009, *60*, 157–164.

[39] Hillsley, K., Grundy, D., Serotonin and cholecystokinin activate different populations of rat mesenteric vagal afferents. *Neurosci. Lett.* 1998, *255*, 63–66.

[40] Mazda, T., Yamamoto, H., Fujimura, M., Fujimiya, M., Gastric distension-induced release of 5-HT stimulates c-fos expression in specific brain nuclei via 5-HT3 receptors in conscious rats. *Am. J. Physiol. Gastrointest. Liver Physiol.* 2004, *287*, G228–G235.

[41] Daly, D. M., Park, S. J., Valinsky, W. C., Beyak, M. J., Impaired intestinal afferent nerve satiety signalling and vagal afferent excitability in diet induced obesity in the mouse. *J. Physiol.* 2011, *589*, 2857–2870.

[42] Chaiyasit, K., Khovidhunkit, W., Wittayalertpanya, S., Pharmacokinetic and the effect of capsaicin in capsicum frutescens on decreasing plasma glucose level. *J. Med. Assoc. Thai.* 2009, *92*, 108–113.

2.4 "Capsaicin, nonivamide and *trans*-pellitorine decrease free fatty acid uptake without TRPV1 activation and increase acetyl-coenzyme A synthetase activity in Caco-2 cells"

[5]   **Rohm, B**.[a]; Riedel, A.[b]; Widder, S.[c]; Ley, J. P.[c]; Krammer, G. E.[c]; Somoza,V.[a,b]

[a] Christian Doppler Laboratory for Bioactive Aroma Compounds, Althanstraße 14, 1090 Vienna

[b] Department for Nutritional and Physiological Chemistry, Althanstraße 14, 1090 Vienna

[c] Symrise AG, Mühlenfeldstraße, Holzminden, Germany

Capsaicin, nonivamide and trans-pellitorine decrease free fatty acid uptake without TRPV1 activation and increase acetyl-coenzyme A synthetase activity in Caco-2 cells

5 **Barbara Rohm,**[a,b] **Annett Riedel**[b] **, Jakob P. Ley**[c]**, Sabine Widder**[c]**, Gerhard E. Krammer**[c]**, and Veronika Somoza**[a,b]*

Red pepper and its major pungent component, capsaicin, have been associated with hypolipidemic effects in rats, although mechanistic
10 studies regarding the effects of capsaicin and/or structurally related compounds on lipid metabolism are scarce. Here, the effects of capsaicin and its structural analog nonivamide, the aliphatic alkamide trans-pellitorine and vanillin as basic structural element of all vanilloids on mechanisms of intestinal fatty acid uptake in differentiated intestinal Caco-2 cells were studied. Capsaicin and nonivamide were found to reduce fatty acid uptake, with IC_{50} values of 0.49 μM and 1.08 μM, respectively. trans-Pellitorine was shown to reduce fatty acid uptake by 14.0 ± 2.14 % at 100 μM, whereas vanillin was not effective, indicating a pivotal role of the alkyl chain with the acid
15 amide group in fatty acid uptake by Caco-2 cells. This effect was neither associated with activation of the transient receptor potential cation channel subfamily V member 1 (TRPV1) or the epithelial sodium channel (ENaC), nor with effects on paracellular transport or glucose uptake. However, acetyl coenzyme A synthetase activity increased ($p<0.05$) in the presence of 10 μM capsaicin, nonivamide or trans-pellitorine, pointing to an increased fatty acid biosynthesis that might counteract a decreased fatty acid uptake.

Introduction

Dietary fats are essential for normal body function, since they not only provide energy, but also essential fatty acids and facilitate the uptake of fat-soluble vitamins. However, the recommended total fat intake of 20 – 35% of total calories for adults is exceeded
25 by large proportions of Western populations, despite longstanding dietary recommendations (156). An excessive energy (including fat) intake over energy expenditure has been demonstrated to be a major risk factor for various cancers, osteoporosis, dementia, and chronic diseases, such as obesity, diabetes, hyperlipidemia or
30 hypercholesterolemia associated with macrovascular disease (96,156). Dietary measures to reduce total energy or total fat uptake not only include reduced food intake, but also administration of satiating compounds or compounds that limit intestinal lipid digestion. Lipase inhibitors prevent the enzymatic
35 cleavage of triacylglycerols which results in a reduced intestinal fatty acid uptake. However, inhibition of lipase activity in the gut has been associated with side effects, e.g. an impaired availability of lipid soluble vitamins. Compounds specifically targeting mechanisms of fatty acid uptake might allow intestinal digestion
40 of lipids, maintaining lipid soluble nutrient availability (10). In addition, dietary compounds increasing the total energy demand via thermogenesis, or compounds promoting the utilization of lipids as primary substrates for cellular energy formation may help to prevent body weight gain in a sedentary lifestyle (10).In

45 this context, red pepper and its major pungent compound capsaicin are often considered as anti-obesity agents, since their administration to animals and humans has been associated with decreased food intake, increased energy metabolism, and with hypolipidemic effects (142,157). Although red pepper and
50 capsaicin have been shown to be effective in reducing body fat, yet when used clinically (158), it requires a strong compliance to a certain dosage, that has not been shown to be feasible yet due to their intense pungency. In a recent pre-clinical trial, we could demonstrate that nonivamide, a capsaicinoid about half the
55 pungency than capsaicin, reduced ad libitum food and energy intake from a standardized breakfast in healthy overweight male subjects (159). However, the mechanisms of action for the hypolipidemic effects have not yet been elucidated for capsaicinoids. The present study aimed to investigate whether
60 capsaicin and the less pungent structural analog nonivamide, the aliphatic relative trans-pellitorine and vanillin as the parent structural motif of vanilloids affect intestinal fatty acid uptake to help to combat hyperlipidemia and body weight gain.
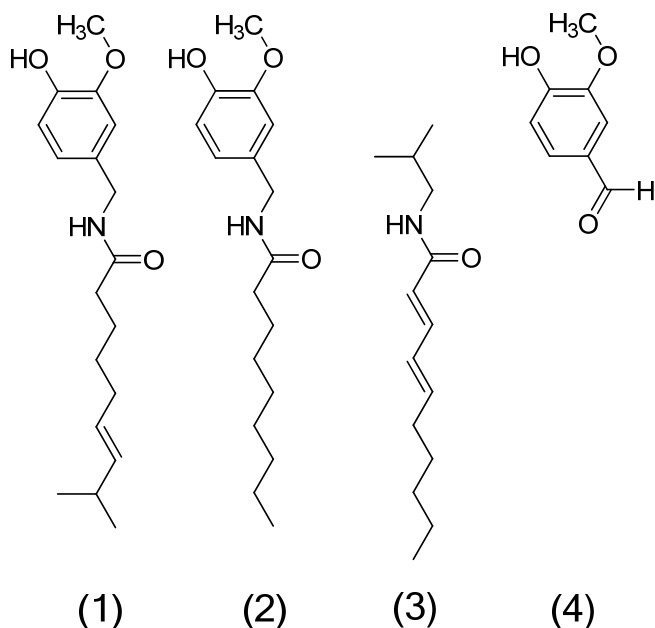
Fig.1 Chemical structures of capsaicin (1), nonivamide (2), t-pellitorine (3), and vanillin (4).

The pungent sensation of capsaicin is caused by depolarization of mechano-heat sensitive afferent trigeminal or dorsal neurons by lowering the temperature threshold through binding to the transient receptor potential cation channel subfamily V member 1 (TRPV1), also known as the capsaicin receptor or the vanilloid receptor 1 (2). As a consequence, the calcium ion influx via the TRPV1 is increased at body temperature causing a pain signal. Nonivamide is another TRPV1-agonist that differs from capsaicin in one double bond and one methyl group in the carbon chain only (Figure 1), and may exhibit similar effects on lipid metabolism as capsaicin. The aliphatic alkamide trans-pellitorine is structurally related to capsaicin as well, but is lacking the vanillyl-group (Figure 1). Because of its tingling effect on the tongue, trans-pellitorine is also discussed as agonist of TRPV1 and TRPA1 (160-161). The widely-used aroma compound vanillin is, like capsaicin and nonivamide, a vanilloid, but is not an amide and lacking the alkyl chain (Figure 1). Since it is not clear whether the vanillyl-amide part of capsaicin is a necessary structural component for its effect on intestinal fatty acid uptake, vanillin was also included as a target compound in this study. Mechanistically, activation of the TRPV1 leads to an increased Ca^{2+}-influx into the cell. An increased intracellular Ca^{2+} concentration has been shown to affect membrane permeability in human intestinal Caco-2 cells in culture (162). Caco-2 cells are widely used for studying lipid metabolism as they exhibit many characteristics of mature villus epithelial cells of the small intestine upon differentiation, including the formation of a brush border membrane and intracellular tight junctions, and the expression of fatty acid binding proteins (163-164). Since capsaicin and nonivamide have not only been demonstrated to act as TRPV1 ligands but also to increase Ca^{2+} mobilization in

neural SH-SY5Y cells (165), we hypothesize that the selected compounds
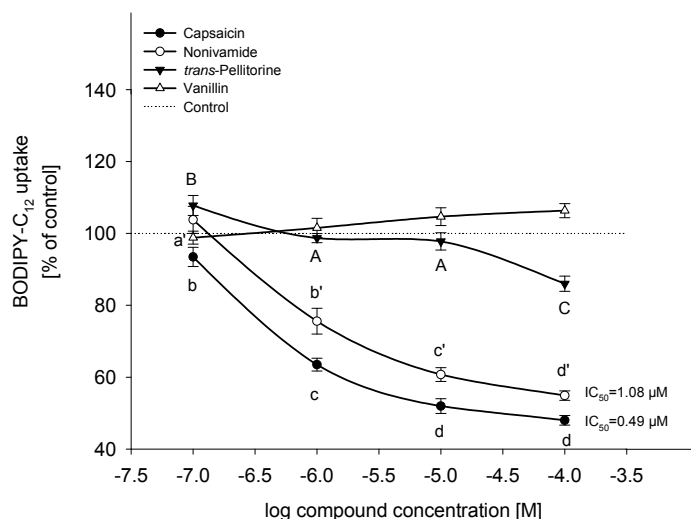
Fig.2 Bodiypy-C12 uptake by differentiated Caco-2 cells after 30 min of pre-treatment with 0.1-100 µM capsaicin, nonivamide and trans-pellitorine compared to non-treated control cells (=100%, dotted line). IC_{50} values for capsaicin and nonivamide were calculated using one site competition (max =100) curve fitting in SigmaPlot 11.0. Values are presented are means ± SEM for three to four experiments assayed in triplicates. Significant differences between test concentrations within were tested using one-Way ANOVA with Holm-Sidak post-hoc test and are marked with distinct letters (control=a).

affect fatty acid uptake in differentiated Caco-2 cells via paracellular diffusion induced by TRPV1 activation. To test whether a compound-induced effect on cellular fatty acid uptake was associated with functional changes of the cell membrane and related proteins, activation of the TRPV1 receptor or the epithelial Na+ channel (ENaC), specific inhibitors were used. In addition, we further studied parameters of membrane function, including barrier function via trans epithelial electrical resistance (TEER) and changes in the activity of glucose transporters via glucose uptake, as well as gene expression of fatty acid transport- and binding-proteins after incubation with the target compounds in the presence and absence of fatty acid uptake inhibitors. Target compounds for which the results revealed a decrease of fatty acid uptake in differentiated Caco-2 cells were studied for their effects on the enzymatic activity of acetyl-coenzyme A synthetase as an indicator of intracellular fatty acid biosynthesis.

Results

Cell viability

Cell viability was assessed using MTT assay after treatment of differentiated Caco-2 cells with the test compounds capsaicin, nonivamide, trans-pellitorine, and vanillin in a concentration range of 0.1-100 µM, as well as the inhibitors capsazepine (1-100 µM), BCH (25-100 µM) and benzamil (1-100 µM) or a combination thereof. No significant difference (p>0.05) between treatment for 90 min with the test compounds/ inhibitors and non-treated control was detected (one-Way ANOVA vs. control, Holm-Sidak post-hoc test; data not shown).

Bodipy-C12-uptake after capsaicin, nonivamide, *trans*-pellitorine and vanillin treatment

The effects of capsaicin, nonivamide, *trans*-pellitorine and vanillin on Bodipy-C12-uptake are displayed in Figure 2. Since stock solutions of the four test compounds were prepared in ethanol, cells treated with the respective ethanol concentrations were also studied. As a result, there was no difference between treatment with buffer (HBSS/HEPES) solely or buffer supplemented with 0.1 % ethanol (p=0.552, Student's t-test). Treatment with capsaicin reduced fatty acid uptake to 93.5 ± 2.68% (p<0.05 vs. control) at 0.1 μM and to 63.5 ± 1.77%, 51.9 ± 2.06% and 48.0 ± 1.35% (each p<0.001 vs. control) at 1 μM, 10 μM and 100 μM, respectively. Addition of 0.1 μM of nonivamide had no effect on fatty acid uptake, whereas addition of 1 to 100 μM of nonivamide reduced fatty acid uptake in a dose-dependent manner as well (75.6±3.59 at 1 μM to

54.9±1.32% at 100 μM), although to a weaker extent than capsaicin (p<0.05 vs. capsaicin). In contrast, incubation with trans-pellitorine stimulated fatty acid uptake by 7.77 ± 2.77% (p<0.05 vs. control) at the lowest test concentration of 0.1 μM, but showed a decreasing effect at the highest test concentration of 100 μM by 14.0 ± 2.14% (p<0.001 vs. control). This decrease was significantly weaker compared to the decrease after incubation with 100 μM nonivamide (p<0.001) or capsaicin (p<0.001). Incubation with 0.1 to 100 μM of vanillin did not change fatty acid uptake (p=0.075) and was therefore, not further investigated.

TRPV1-dependency of fatty acid uptake in Caco-2 cells

To investigate whether the reduction in fatty acid uptake induced by capsaicin, nonivamide and *trans*-pellitorine depends on TRPV1 activation, the effect of two different TRPV1 antagonists, capsazepine and BCH with/without the presence of the test
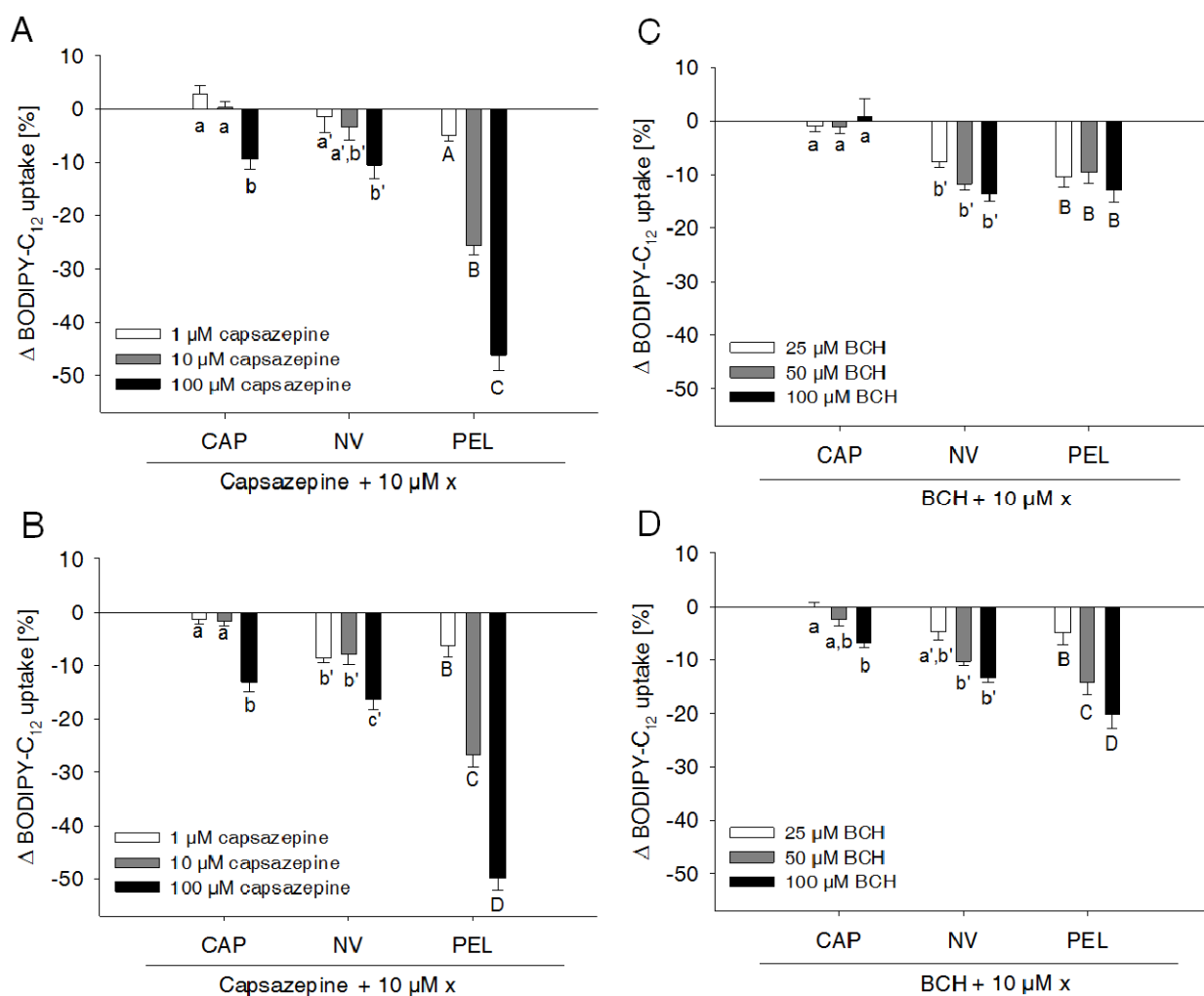
Fig. 3 ΔBodiypy-C12 uptake by differentiated Caco-2 cells after treatment with the TRPV1 inhibitors capsazepine (CZE) (A, B) or *trans-tert*-butycyclohexanol (BCH) (C, D). Inhibitors were added concomitantly (A, C) or 30 min prior to (B, D) to the addition of 10 μM capsaicin (CAP), nonivamide (NV) and *trans*-pellitorine (PEL). Data are presented as Δ means compared to cells treated with CAP, NV or PEL solely ± SEM from three different experiments with three technical replicates each. Significant differences between the treatments with CAP/ NV / PEL and different concentrations of the inhibitors were tested using two-Way ANOVA with Holm-Sidak post-hoc test and are marked with distinct letters (control = a).
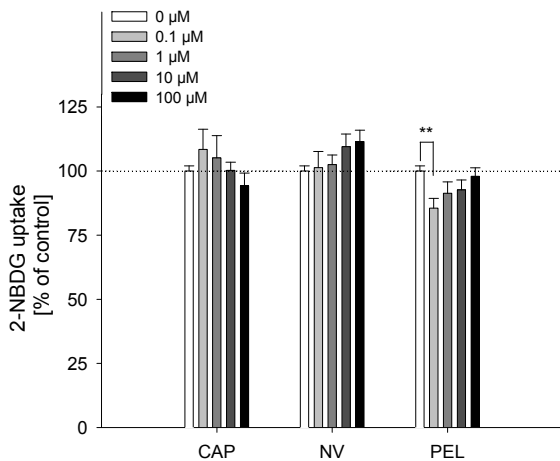
compounds on Bodipy-C12-uptake was assessed (Figure 3).

Fig.4 2-NBDG uptake by differentiated Caco-2 cells after 30 min of pretreatment with 0.1-100 µM capsaicin, nonivamide and *trans*-pellitorine compared to non-treated control cells (=100%). Values are presented are means ± SEM for three to four experiments assayed in triplicates. Significant differences between test concentrations were tested using one-Way ANOVA with Holm-Sidak post-hoc test. ** p<0.01 vs. control.
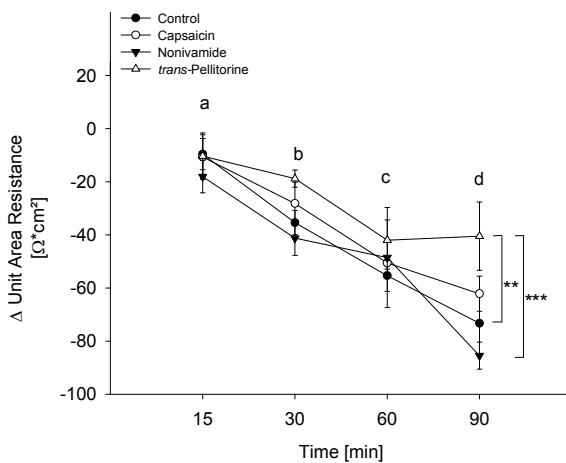
Fig. 5 Evaluation of the trans epithelial electrical resistance (TEER) of differentiated Caco-2 cells after treatment with 10 µM capsaicin, nonivamide or *trans*-pellitorine for 15, 30, 60 and 90 min or non-treated control cells. Values are presented are means ± SEM for three to four experiments assayed in duplicates. Significant differences were analyzed with Two-Way ANOVA followed by Holm-Sidak post hoc test. Time-dependent effects marked with distinct letters and differences between treatments using the following code: **:p<0.01, **:p<0.001.

Treatment of the cells with the TRPV1 antagonist capsazepine reduced free fatty acid uptake in a dose dependent manner to $92.5 \pm 2.42\%$ (p<0.05 vs. control = 100%) at 1 µM down to $49.1 \pm 2.59\%$ (p<0.001 vs. control) at a concentration of 100 µM (data not shown in figures).

Concomitant addition of 1 µM capsazepine to the incubation media containing 10 µM of capsaicin, nonivamide or *trans*-pellitorine did not alter fatty acid uptake in comparison to a treatment with capsaicin, nonivamide or *trans*-pellitorine alone (Figure 3A). Also, co-incubation with 10 µM capsazepine did not significantly change the reduction of fatty acid uptake induced by capsaicin and nonivamide, but reduced fatty acid uptake in combination with *trans*-pellitorine by $25.7 \pm 1.68\%$ (p<0.001) in comparison to treatment with *trans*-pellitorine alone. Co-incubation with the highest test concentration of 100 µM capsazepine and capsaicin, nonivamide and *trans*-pellitorine further decreased fatty acid uptake by $9.39 \pm 1.91\%$ (capsaicin, p<0.01), $10.5 \pm 2.63\%$ (nonivamide, p<0.001) and $47.2 \pm 2.99\%$ (*trans*-pellitorine, p<0.001), respectively. In further experiments, capsazepine was added to the incubation media 30 min before addition of one of the other test substances (Figure 3 B). Pre-incubation with capsazepine alone for 30 min did not alter fatty acid uptake at 1 µM, but reduced fatty acid uptake by $26.5 \pm 1.01\%$ (p<0.001) at 10 µM and by $44.4 \pm 2.47\%$ (p<0.001) at 100 µM (data not shown in figure). The effect of 10 µM capsaicin (-48.0 ± 2.06%) was not reduced by pretreatment with 1 and 10 µM, but with 100 µM of capsazepine (-61.1 ± 1.96%, p<0.001 vs. capsaicin). However, the effects of nonivamide and *trans*-pellitorine were significantly amplified by pre-treatment with capsazepine at all test concentrations (1-100 µM) (Figure 3B). The selective TRPV1 antagonist BCH was applied at 25, 50 and 100 µM, with no effect on fatty acid uptake at concentrations of 25 µM and 50 µM (data not shown in figure). Application of 100 µM BCH reduced the fatty acid uptake by $13.7 \pm 2.19\%$ (p<0.001 vs. control, data not shown). However, co-incubation of 25-100 µM BCH with capsaicin did not affect fatty acid uptake compared to treatment with capsaicin alone, but led to a reduced fatty acid uptake when co-incubated with nonivamide by up to $13.6 \pm 1.37\%$ at 100 µM and *trans*-pellitorine by up to $13.0 \pm 2.18\%$ compared to a treatment with nonivamide and *trans*-pellitorine alone (Figure 3 C). Pre-incubation with BCH for 30 min led to a decrease of fatty acid uptake not only at 100 µM (-14.9 ± 1.67%, p<0.001), but also at the lower test concentrations of 50 µM (-12.4 ± 1.14%, p<0.001) and 25 µM (-7.78 ± 1.47%, p<0.01, data not shown). Addition of 25-100 µM BCH 30 min prior to the application of 10 µM capsaicin led to further reduction of fatty acid uptake at 100 µM (-6.74 ± 0.81%), but not at 25 and 50 µM, compared to the application of capsaicin solely (Figure 3D). The effect of nonivamide on fatty acid uptake was increased by pretreatment with 50 µM (-11.5 ± 1.04%, p<0.001) and 100 µM (-13.59 ± 1.37%, p<0.001) BCH, and the effect of *trans*-pellitorine by up to -13.0 ± 2.18% (100 µM BCH, p<0.001) at all test concentrations.

Glucose uptake after capsaicin, nonivamide, *trans*-pellitorine treatment

In order to investigate whether a reduced fatty acid uptake is accompanied by an altered glucose uptake, 2-NBDG uptake after 30 min pretreatment with capsaicin, nonivamide and *trans*-pellitorine was measured (Figure 4). Insulin independent 2-NBDG uptake in Caco-2 cells was not affected by treatment with 0.1 to 100 µM of capsaicin (p=0.503) or nonivamide (p=0.277). Incubation with *trans*-pellitorine reduced glucose uptake by

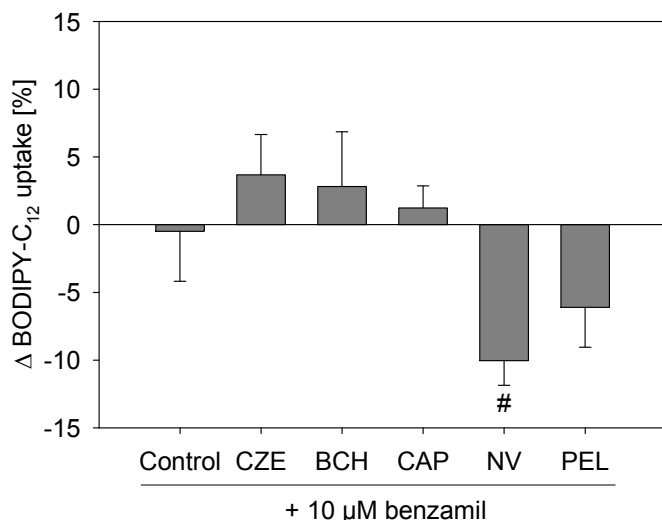14.4 ± 3.77% (p=0.004) at a concentration of 0.1 µM, but did not affect glucose uptake in higher concentrations (p>0.05).

Fig. 6 ∆Bodiypy-C12 uptake by differentiated Caco-2 cells after treatment with 10 µM of the endothelial sodium channel (ENaC) inhibitor benzamil. Benzamil was added 30 min in advance to the addition of 10 µM capsaicin (CAP), nonivamide (NV) and *trans*-pellitorine (PEL), capsazepine (CZE) and 100 µM *trans-tert*-butylcyclohexanol (BCH). Data are presented as relative means compared to capsaicin, nonivamide or *trans*-pellitorine treatment ± SEM from three different experiments with three technical replicates each. Significant differences (# p<0.05) between treatment solely with the test compounds (CAP/NV/PEL/CZE/BCH) and addition of benzamil to test compound were tested with Student's t-test .

Trans epithelial electrical resistance (TEER)

TEER was determined after 0, 15, 30, 60 and 90 min of incubation with 10 µM capsaicin, nonivamide and *trans*-pellitorine in order to exclude a reduction of fatty acid uptake by modified paracellular transport (Figure 5). Untreated, differentiated Caco-2 cells demonstrated a mean TEER of 514 ± 12.9 $\Omega*cm^2$ (n=23) after 60 min of starving. △TEER of control cells (treated with HBSS/HEPES buffer) remained stable after 15 min, but was decreased after 30, 60 and 90 min of incubation by 40.1 ± 7.89, 63.1 ± 4.35 and 72.4±8.12 $\Omega*cm^2$ (p<0.001 for all timepoints) in comparison to the initial TEER value (t=0). Addition of 0.1% ethanol to the incubation media did not change △TEER at any time point in comparison to treatment with HBSS/HEPES solely. Also, incubation media supplemented with 10 µM capsaicin or nonivamide did not change △TEER in the time course experiment in comparison to control cells. However, after 90 min, △TEER was significantly higher (p<0.01) after treatment with 10 µM *trans*-pellitorine (-40.51 ± 12.8 $\Omega*cm^2$) in comparison to untreated control cells (-72.4 ± 8.12 $\Omega*cm^2$), treatment with 0.1% ethanol (-73.3 ±11.9 $\Omega*cm^2$) or 10 µM nonivamide (-85.5 ± 5.09 $\Omega*cm^2$), but not compared to capsaicin (-62.2±6.60 $\Omega*cm^2$,Figure 5).

Effect of epithelial Na^+- channel (ENaC) inhibition on fatty acid uptake reduction by capsaicin, nonivamide, *trans*-pellitorine, capsazepine and BCH

Sodium homeostasis of the cells is mediated by different sodium-selective channels and transporters, like the ENaC or SLC5A8, whose sodium transport is coupled to short chain fatty acids (166). Activation of ENaC leads to an increased sodium resorption (167), which may reduce activity of sodium transporters like SLC5A8, thereby affecting fatty acid uptake.

Since long chain fatty acids like arachidonic acid (168), but also capsazepine (169), influence ENaC activity, the effect of the specific ENaC inhibitor benzamil on fatty acid uptake reduction caused by capsaicin, nonivamide, *trans*-pellitorine, capsazepine and *trans-tert*-butylcyclohexanol was examined. Treatment with 10 µM benzamil alone, which was added 30 min prior to the addition of other test substances, did not alter fatty acid uptake in Caco-2 cells (Figure 6). Treatment with 10 µM benzamil had no impact on reduced fatty acid uptake evoked by capsazepine, BCH, capsaicin or *trans*-pellitorine treatment. However, pretreatment with benzamil followed by incubation with nonivamide reduced fatty acid uptake by 10.4 ± 1.82% (p<0.01, Student's t-test), compared to an incubation with nonivamide solely.

Gene expression analysis of modulators of fatty acid uptake in Caco-2 cells

To address whether fatty acid uptake modulation by capsaicin, nonivamide or *trans*-pellitorine is accompanied by changes in gene expression of fatty acid transport proteins and other factors involved in fatty acid metabolism, time-dependent gene expression of genes encoding for fatty acid transport proteins 2 and 4 (FATP2 & FATP4), intestinal fatty acid binding protein (IFABP), fatty acid translocase (CD36), peroxisome proliferator-activated receptor γ and α (PPARγ and PPARα) were determined after treatment with 10 µM capsaicin, nonivamide or *trans*-pellitorine for 15, 30, 60 and 90 min (Table 1).

FATP2 gene expression significantly peaked after 60 min of treatment with capsaicin (1.47 ± 0.11, p<0.001), nonivamide (1.51 ± 0.14, p<0.001) or *trans*-pellitorine (1.33 ± 0.06, p=0.004) in comparison to control cells (1.00 ± 0.02). However, there was no difference between the three different treatments. Likewise, FATP4 expression peaked after 60 min of treatment with capsaicin (1.29 ± 0.09, p=0.003) or nonivamide (1.32 ± 0.08, p=0.001), but not after *trans*-pellitorine treatment. Furthermore, treatment with capsaicin increased IFABP expression after 30 min by 1.37 ± 0.04 (p<0.001), whereas treatment with nonivamide led to increased gene expression after 60 min (1.32 ± 0.08, p<0.01). Furthermore, treatment with nonivamide for 30 min and 60 min promoted CD36 gene expression in comparison to control cells to 1.82 ± 0.23 (p<0.01) or 3.97 ± 0.59 (p<0.001), respectively. This effect was more pronounced (p<0.001) compared to the effect of capsaicin (1.89 ± 0.14, p<0.01 vs. control) and *trans*-pellitorine-treatment (1.71 ± 0.16, p<0.05 vs. control), which demonstrated increased CD36 gene expression after 60 min in comparison to control cells as well. PPARα and PPARγ gene expressions were most pronounced

after 60 min incubation time with capsaicin, nonivamide and *trans*-pellitorine compared to control cells (each p<0.001) as well. Treatment with capsaicin increased PPARα expression to 1.29 ± 0.08 and PPARγ by 1.29 ± 0.07, whereas nonivamide
5 promoted PPARα expression to 1.28 ± 0.08 and PPARγ to 1.50 ± 0.05. *trans*-Pellitorine led to an increase of PPARα gene expression up to 1.31 ± 0.05 and PPARγ gene expression up to 1.40 ± 0.03 (Table 1).

The time course experiment revealed the most pronounced effects
10 on gene expression of modulators of fatty acid uptake after 60 min. Therefore, further gene expression experiments were carried out after 60 min incubation, while exactly mimicking incubation conditions during the fatty acid uptake experiments. Cells were incubated after 60 min of starving, using a mixture of
15 serum-free DMEM and test substance dissolved in HBSS/HEPES (9:1) with or without addition of 5 µM lauric acid to also investigate effects of substrate addition on gene expression of modulators of fatty acid uptake (Table 2).

Comparison of control, capsaicin, nonivamide and
20 *trans*-pellitorine treatment with or without 5 µM lauric acid demonstrated no impact of substrate addition on FATP2, PPARγ, IFABP gene expression. However, the addition of lauric acid to capsaicin-containing incubation media significantly decreased PPARα expression from 1.19 ± 0.04 to 0.96 ± 0.02 (p<0.05) and
25 CD36 gene expression from 1.68 ± 0.18 to 1.21 ± 0.06 (p<0.05). Furthermore, FATP4 gene expression of control cells was slightly upregulated by 0.18 ± 0.06 (p<0.05) when adding lauric acid to the buffer control (Table 2).

30 **Changes in acteyl-coenzyme A synthetase activity after capsaicin, nonivamide and *trans*-pellitorine incubation**

As demonstrated above, incubation with capsaicin, nonivamide and *trans*-pellitorine in the µM range decreased fatty acid uptake without compensating for this lack of energy by altering glucose
35 uptake. In order to investigate whether Caco-2 cells compensate a possible intracellular lack of fatty acids by an increased fatty acid de-novo synthesis, acetyl coenzyme A synthetase activity was assessed using an enzymatic assay. This enzyme catalyses the activation of acetate by conversion into acetyl-coenzyme A ,
40 which is used for de novo fatty acid synthesis (170). Acetyl CoA synthetase activity in differentiated Caco-2 cells in comparison to non-treated control cells was significantly increased after 90 min incubation with 10 µM of capsaicin (+3.00 ± 1.10 mU/mg protein, p<0.05), nonivamide (+3.96 ± 0.72, p<0.05) and *trans*-
45 pellitorine (+3.90 ± 0.70, p<0.05) to the same extent (Figure 7).
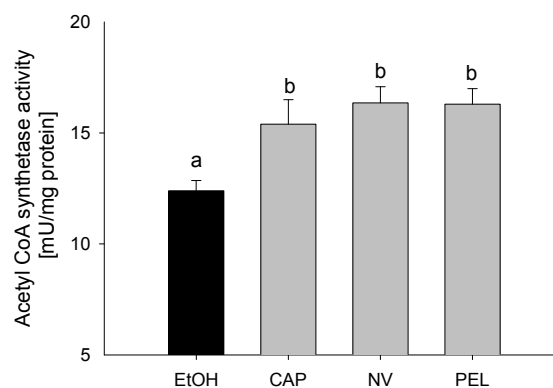
Table 1. Relative gene expression levels for *FATP2*, *FATP4*, *IFABP*, *CD36*, *PPARα* and *PPARγ* after incubation with 10 µM capsaicin, nonivamide or *trans*-pellitorine for 15, 30, 60 and 90 min using qRT-PCR.

Gene	time (min)	Control	Capsaicin	Nonivamide	*trans*-Pellitorine
FATP2	15	1.00±0.02	0.99±0.08	0.86±0.11	1.09±0.05
	30	1.00±0.02	1.08±0.03	1.04±0.06	0.98±0.08
	60	1.00±0.02	1.47±0.11***	1.51±0.14***	1.33±0.06**
	90	1.00±0.02	1.03±0.10	1.15±0.10	1.09±0.12
FATP4	15	1.00±0.01	0.91±0.04	1.17±0.06	0.98±0.07
	30	1.00±0.01	1.05±0.04	0.99±0.03	0.92±0.01
	60	1.00±0.02	1.29±0.09**	1.32±0.08**	1.22±0.10
	90	1.00±0.01	1.01±0.09	1.10±0.11	1.15±0.13
IFABP	15	1.00±0.01	1.18±0.11	0.94±0.03	1.12±0.05
	30	1.00±0.03	1.37±0.04***	1.12±0.09	1.06±0.07
	60	1.00±0.03	1.19±0.13	1.32±0.08**	1.08±0.04
	90	1.00±0.03	1.03±0.11	1.08±0.08	0.90±0.05
CD36	15	1.00±0.03	1.17±0.12	1.38±0.13	1.31±0.11
	30	1.00±0.02	1.46±0.25	1.82±0.23**	1.17±0.09
	60	1.00±0.02	1.89±0.14***	3.97±0.59***	1.71±0.16***
	90	1.00±0.02	1.26±0.16	1.72±0.04	1.51±0.05
PPARα	15	1.00±0.03	0.80±0.03	1.04±0.07	0.95±0.05
	30	1.00±0.01	1.07±0.07	1.02±0.05	0.96±0.02
	60	1.00±0.03	1.29±0.08***	1.28±0.08***	1.31±0.05***
	90	1.00±0.02	1.04±0.07	0.94±0.04	1.15±0.10
PPARγ	15	1.00±0.03	1.00±0.11	1.04±0.07	0.95±0.05
	30	1.00±0.02	1.16±0.08	1.05±0.04	1.01±0.04
	60	1.00±0.02	1.29±0.07***	1.50±0.05***	1.40±0.03***
	90	1.00±0.03	0.99±0.08	1.00±0.08	1.15±0.10

Relative gene expression after treatment with 10 µM capsaicin, nonivamide or *trans*-pellitorine compared to non-treated control cells. Gene expression was normalized to *HPRT* expression levels. Data are shown as mean fold change ± SEM from 3-4 experiments assayed in triplicates. Significant differences between treatments are tested with two-way ANOVA and pairwise multiple comparison between treatments using the Holm-Sidak post hoc test (p<0.05:*, p<0.01: **, p<0.001:*** vs. non-treated cells)

Table 2. Relative gene expression levels for *FATP2*, *FATP4*, *IFABP*, *CD36*, *PPARα* and *PPARγ* after 60 min starving followed by incubation with 10 µM capsaicin, nonivamide or *t*-pellitorine for 60 min with or without addition of 10 µM lauric acid using qRT-PCR

	FATP2		*FATP4*		*IFABP*		*CD36*		*PPARα*		*PPARγ*	
	wo LA	with LA	wo LA	with LA	wo LA	with LA	wo LA	with LA	wo LA	with LA	wo LA	with LA
Control	1.00±0.03	1.15±0.07	**1.00±0.01**	**1.18±0.06***	1.00±0.03	1.17±0.02	1.00±0.04	1.21±0.12	1.00±0.02	1.17±0.03	1.00±0.02	1.06±0.06
Capsaicin	1.12±0.05	0.89±0.03	1.19±0.04	1.05±0.07	1.31±0.02	1.42±0.02	**1.68±0.18**	**1.21±0.06***	**1.19±0.04**	**0.96±0.02***	1.04±0.03	0.94±0.05
Nonivamide	1.29±0.16	1.20±0.18	1.10±0.05	1.26±0.08	1.30±0.07	1.50±0.16	1.67±0.20	2.06±0.29	1.22±0.06	1.32±0.10	0.94±0.05	1.01±0.03
***trans*-Pellitorine**	1.56±0.15	1.60±0.18	1.24±0.06	1.30±0.10	1.38±0.06	1.59±0.18	1.63±0.07	1.99±0.17	1.24±0.07	1.33±0.14	1.00±0.05	1.01±0.08

Relative gene expression after treatment compared to non-treated control cells after 1 h starving followed by 1 h incubation with 10 µM capsaicin, nonivamide or *trans*-pellitorine with or without addition of 5 µM lauric acid (LA) to the incubation media. Gene expression was normalized to *HPRT* expression levels and is displayed as fold change of non-treated control cells ± SEM from 3-4 experiments assayed in triplicates. Significant differences between treatments are tested with two-way ANOVA and pairwise multiple comparison between treatments using the Holm-Sidak post hoc test (*p<0.05 vs. treatment without lauric acid,(LA))

Discussion

Red pepper and its major pungent compound capsaicin have been associated with hypocholesterolemic and hypotriglyceridemic effects in rats (139-142) and humans (124). Although a decreased cholesterol absorption combined with an increased expression of hepatic LDL receptors and enhanced fecal excretion of bile acids is discussed to account for hypocholsterolemic effects of capsaicin (143), the effect of capsaicin on intestinal fatty acid uptake has not been studied so far. The present study aimed to investigate whether capsaicin, nonivamide, *trans*-pellitorine or vanillin affect intestinal fatty acid uptake via activation of TRPV1 *in vitro*. Differentiated Caco-2 cells were chosen as a cell model for epithelial cells of the small intestine.

The results demonstrate that capsaicin and nonivamide reduce fatty acid uptake in differentiated Caco-2 cells. Nonivamide differs from capsaicin only in one double bond and one methyl group. This slight structural difference led to a major decrease in the potency to reduce fatty acid uptake, with IC_{50} values of 0.49 µM and 1.08 µM calculated for capsaicin and nonivamide, respectively. Statistical comparison confirmed that capsaicin decreased fatty acid uptake more potently than nonivamide at concentrations of 0.1 to 10 µM. Incubation with the alkamide *trans*-pellitorine, which bears a carbon chain with an amide group like capsaicin and nonivamide but is lacking the vanillyl group, increased fatty acid uptake in the lowest tested concentration of 0.1 µM, but also reduced fatty acid uptake at 100 µM by 14% (p<0.001). Vanillin, which was tested to exploit the function of the vanillyl group, did not alter fatty acid uptake. These data give rise to the conclusion that the carbon chain or the amide group or the combination thereof - as opposed to the vanilly-group – might play a pivotal role in the reduction of fatty acid uptake by Caco-2 cells in culture.

Molecular mechanisms underlying intestinal fatty acid absorption are not fully understood yet. However, diffusion seems to coexist with protein-mediated mechanisms (171). Paracellular diffusion relies on membrane permeability, which is associated with tight junction permeability (172). In addition, increased intracellular Ca^{2+} levels have been associated with changes in membrane permeability, possibly via protein kinase C activation (173). Since activation of the TRPV1 receptor leads to an increased Ca^{2+}-influx (174), a modulation of paracellular fatty acid uptake via a TRPV1 dependent pathway seemed likely. Capsaicin, nonivamide and *trans*-pellitorine have been shown to stimulate intracellular Ca^{2+} mobilization in SH-SY5Y cells (165,175), and a capsaicin-induced increase in intracellular Ca^{2+} levels has also been reported in Caco-2 cells (176). To investigate whether TRPV1 receptor activation plays a role in the capsaicinoid-induced decrease in fatty acid uptake, the effect of two different TRPV-1 antagonists, capsazepine and *trans-tert*-butycyclohexanol (BCH) on Bodipy-C12 uptake was assessed. Hence, capsazepine and BCH were applied in different concentrations concomitantly or 30 min prior to

treatments with capsaicin, nonivamide or *trans*-pellitorine. Concomitant application of capsazepine and BCH led to a further reduction of fatty acid uptake. When Caco-2 cells were pre-incubated with capsazepine and BCH for 30 min at concentrations that did not affect fatty acid uptake, the reducing effect on fatty acid uptake demonstrated for nonivamide and *trans*-pellitorine was amplified. These results indicate that one or more other receptors than TRPV1 mediate the reduction of fatty acid uptake induced by capsaicin, nonivamide and *trans*-pellitorine, while TRPV1 activation might not be mandatory. However, an increased fatty acid uptake is also facilitated by modulation of membrane permeability and paracellular diffusion. In order to investigate whether reduction of fatty acid uptake is accompanied by an altered glucose uptake, possibly through changes in the activity of glucose transporters or membrane permeability as well, 2-NBDG uptake after 30 min pretreatment with capsaicin, nonivamide and *trans*-pellitorine was assessed. However, there was no change in glucose uptake after treatment with capsaicin and nonivamide. In contrast, glucose uptake was decreased after treatment with 0.1 µM *trans*-pellitorine. This concentration led to an increased fatty acid uptake, a result that could argue for a compensatory mechanism rather than disruption of membrane-specific processes like changes in permeability or modulation of glucose transporters. However, a slight decrease in tight junction pore size would reduce the permeability for larger molecules like fatty acids, but not necessarily affect the transport of small molecules like glucose (162). Modulation of paracellular diffusion can, thus, not be excluded and needs further investigation. A good measure for paracellular diffusion is the trans-epithelial electrical resistance (TEER). A decrease in TEER is associated with an increased paracellular membrane permeability as a parameter for tight-junction permeability (172). Tsukara et al. (177) found that treatment with 100 µM of capsaicin for 2 h caused a significant decrease in TEER without effects on cell viability. To exclude that fatty acid uptake inhibition by 0.1 to 100 µM capsaicin, nonivamide and *trans*-pellitorine is caused by an increase in TEER, which would point to a decrease in paracellular transport, TEER was monitored in differentiated Caco-2 cells after 15, 30, 60 and 90 min of treatment. Untreated, differentiated Caco-2 cells showed a mean TEER of 585 Ω*cm², which is comparable to those described in other studies (94). Although the TEER decreased over time, the values measured never decreased below ~330 Ω*cm², a value which indicates an intact monolayer (178-179). Since there was no difference between control and capsaicin or nonivamide treatment, effects of capsaicin and nonivamide on barrier function and paracellular fatty acid transport can be excluded. In contrast, after 90 min of treatment with *trans*-pellitorine, TEER was significantly increased compared to control cells, which could partly account for fatty acid uptake inhibition after *trans*-pellitorine treatment.

As a further measure of membrane function, a possible involvement of the epithelial sodium channel in the

126

regulation of fatty acid uptake in Caco-2 cells was excluded. The sodium transport of some sodium transporters like SLC5A8 is coupled to short chain fatty acids (166). Caco-2 cells were previously shown to express delta, alpha, beta and gamma subunits of the epithelial sodium channel (ENaC) (180), whose activation leads to an increased sodium resorption (181). Recently, Yamamura et al. (169) demonstrated that capsazepine modulates ENaC activity. But also long chain fatty acids like arachidonic acid lead to an altered ENac activity (168), which could, in return, possibly affect the activity of sodium transporters like SLC5A8 and, thereby, also fatty acid uptake. Thus, the impact of a specific ENaC inhibitor, benzamil (167), to which Caco-2 cells were shown to be sensitive (182), on fatty acid uptake reduction caused by capsaicin, nonivamide and *trans*-pellitorine was investigated. There was no impact on fatty acid uptake reduction caused by capsazepine, BCH, capsaicin and *trans*-pellitorine. Co-incubation of benzamil with nonivamide further decreased fatty acid uptake compared to a treatment with nonivamide alone. Hence, an influence of the ENaC activity on fatty acid reduction by the test substances in Caco-2 cells can be excluded.

Besides diffusion, protein-mediated mechanisms account for fatty acid uptake. Intracellular fatty acid concentrations are two- or three-fold higher than external unbound fatty acid concentrations (183), therefore fatty acid uptake into cells against a concentration gradient requires effective transport systems. Members of the fatty acid receptor family include fatty acid translocase (CD36), plasma membrane associated fatty acid binding proteins (FABP), fatty acid transport proteins (FATPs) and long chain Acyl-CoA synthetase (ACSl) (84). In the present study, the influence of capsaicin, nonivamide and *trans*-pellitorine on genes encoding for fatty acid transport mechanisms were examined using qPCR. In detail, gene expression of *CD36*, *IFABP*, *FATP2*, *FATP4* and *PPARα* and *PPARγ* was determined in a time course experiment. FATP2 and FATP4, which both have ACSl activity and transport long chain fatty acids (84), were shown to be the predominant FATPs in Caco-2 cells (184). In addition, gene expression of the intestinal fatty acid binding protein (IFABP, also called gut FABP) was determined, since FABPs are thought to mediate intracellular binding and transport of fatty acids. A pivotal role in fat absorption but also in fat perception is discussed for CD36 (171), whose gene expression was previously shown in Caco-2 cells (185). Additionally, gene expression of *PPARα* and *PPARγ* was assessed as representatives for modulators of fatty acid metabolism. The time course experiment revealed most pronounced effects after 60 min of treatment with the three compounds with the tendency to an up-regulation. Given that capsaicin and its analogs reduced fatty acid uptake without markedly changing glucose uptake, the up-regulating effect of the compounds might be a counteraction of the cell towards a lack of energy. In order to exactly mimic the conditions during fatty acid uptake experiments with Bodipy-C12 and to investigate the effect of substrate addition, further gene expression

experiments were carried out, with or without the addition of 5 μM lauric acid. No effect was demonstrated for lauric acid addition on *FATP2*, *PPARγ* and *IFABP* gene expression and only partial effects on the expression of the other genes. Overall, treatment with capsaicin, nonivamide and *trans*-pellitorine resulted in a slight up-regulation of *CD36*, *IFABP*, *FATP2*, *FATP4* and *PPARα* and *PPARγ* gene expression, which was not markedly influenced by substrate (lauric acid) addition, pointing to a counteraction towards fatty acid uptake reduction.

The strong decrease of fatty acid uptake after incubation with capsaicin and the related compounds presumably led to a major lack of fatty acids, which is, in the experiments shown here, energetically not compensated by an increase in glucose uptake. However, after 90 min of incubation with capsaicin, nonivamide and *trans*-pellitorine, the enzymatic activity of the acetyl CoA synthetase was increased compared to non-treated control cells. Acetyl CoA synthetase catalyzes the conversion of acetate into acetyl-CoA, which is used, amongst others, for the de novo fatty acid synthesis (170). It is therefore likely, that Caco-2 cells compensate the reduced fatty acid uptake by an increase in endogenous fatty acid biosynthesis.

To summarize, the present study demonstrates that capsaicin, nonivamide and *trans*-pellitorine reduce fatty acid uptake in differentiated Caco-2 cells, with the capsaicinoids being the most potent compounds. In contrast to our hypothesis, there is no change in membrane permeability caused by TRPV1 activation or disruption of other membrane specific processes, like glucose uptake and tight junction permeability. In addition, this fatty acid uptake reduction does not depend on ENaC activation. Therefore, it can be assumed that capsaicin, nonivamide and *trans*-pellitorine induce a decrease in activity of one or more fatty acid transporters, which is accompanied by a counter-regulation on a genetic level and an increase in acetyl CoA synthetase activity, pointing to increased endogenous fatty acid biosynthesis.

Capsaicin is often referred to as an anti-obesity compound, not only because of its hypolipidemic effect, but also because its potential to reduce energy intake (157). However, due to its high affinity to the TRPV1 receptor resulting in a pungent sensation, oral intake of capsaicin is limited and demands less pungent alternatives. It was recently demonstrated that dietary administration of 0.15 mg of the less pungent capsaicinoid nonivamide in an oral glucose tolerance test reduced ad libitum energy intake from a standardized breakfast in slightly overweight male subjects (159). The here presented results demonstrate that nonivamide, and even the alkylamide *trans*-pellitorine, although less pronounced, reduce intestinal fatty acid uptake by intestinal Caco-2 cells. This mechanism might contribute to the hypolipidemic effects described for capsaicin (124,142), whereas activation of the TRPV1 receptor does not seem to be mandatory. Since the IC_{50} values of capsaicin and the less pungent nonivamide were in the same order of magnitude, nonivamide might be a promising capsaicinoid to be tested for is hypolipidemic

effects in healthy volunteers to elucidate its clinical relevance. In addition, the present study could help to explain the hypolipidemic effects of red pepper and capsaicin on a mechanistic level.

Materials & Methods

Materials

trans-tert-Butylcyclohexanol (BCH), nonivamide (NV) and *trans*-pellitorine (PEL) were provided by Symrise AG (Germany). All other chemicals were purchased from Sigma Aldrich (Austria), unless stated otherwise. The human colon carcinoma cell line Caco-2 was obtained from ATCC.

Cell culture

Caco-2 cells were maintained at 37°C and 5% CO_2 in Dulbecco's modified Eagle Medium (DMEM) supplemented with 10% fetal bovine serum, 2% L-glutamine and 1% penicillin/streptomycin at humidified atmosphere. Cells were passaged at 80-90 % confluence and used until passage 20. For differentiation into an enterocyte cell model, cells were seeded in the desired format reaching confluence after two days. Media was changed every second to third day and the differentiated cells were used for the different assays on day 21.

Stock solutions (1000x) in ethanol (0.1-100 mM) of the test compounds capsaicin (CAP), nonivamide, *trans*-pellitorine, vanillin (VAN), capsazepine (CZE) and butylcylohexanol were prepared freshly each time. Final ethanol concentration on the cells during the assays never exceeded 0.2%.

Cell Viability

Negative effect on cell viability of any of the test compounds capsaicin, nonivamide, *trans*-pellitorine, vanillin, capsazepine, BCH, and benzyl-amiloride (benzamil) were excluded using MTT assay in a 96-well format. This assay is based on the reduction of the yellow tetrazolium salt MTT (3-(4,5-Dimethylthiazol-2-yl)-2,5-diphenyltetrazolium bromide) to a purple formazan by mitochondrial and ER enzymes (186). For this purpose, cells were starved in serum free media for one hour, followed by addition of the different test compounds or a combination of those, respectively, diluted in Hank's Balanced salt solution supplemented with 20 mM HEPES (HBSS/HEPES). After 90 min of treatment, media was replaced by MTT working solution, which contained a final concentration of 0.83 mg/mL MTT diluted in PBS/ serum-free media (1:5). The reaction was stopped after 10 to 20 min by removal of the MTT working solution. The purple formazan formed during incubation was solved in 150 μL DMSO per well and the absorbance was measured at 550 nm with 690 nm as reference wavelength using multiwell plate reader (Tecan infinite M200, Tecan Austria). Cell viability was assessed relative to untreated control cells (100%).

Fatty Acid Uptake

Free fatty acid uptake in differentiated Caco-2 cells was measured in 96-well plates using the QBT ^{TM} fatty acid uptake kit (Molecular Devices Germany GmbH, Germany), according to manufacturers' protocol. This assay measures the transport of the fluorescent fatty acid analog BODIPY-C12 into the cells, leading to an increase in fluorescence, while extracellular fluorescence is quenched. Differentiated, one-hour serum-deprived Caco-2 cells were pretreated with the test compounds diluted in HBSS/HEPES for 30 min at 37 °C. The inhibitors capsazepine, BCH and benzamil were added 30 min prior or simultaneously to the addition of the test compounds. After addition of the loading dye, containing BODIPY-C12 and 0.2% essentially fatty acid free BSA diluted in HBSS/HEPES, fluorescence was recorded every 20 s at 515 nm emission and 485 nm excitation for 60 min. The area under the curves (AUC) from corresponding signal/time plots for each test compound were calculated using SigmaPlot 11.0 and the data are calculated relative to control cells (100%).

Glucose uptake

Glucose uptake in the absence of insulin was assessed using 2-(N-(7-nitrobenz-2-oxa-1,3-diazol-4-yl)amino)-2-deoxyglucose (2-NBDG) as described before (185). Briefly, differentiated Caco-2 cells were starved in DMEM w/o serum, glucose, L-glutamine and phenolred for one hour at 37 °C, before incubation with the test compounds diluted in HBSS/HEPES for further 30 min. 2-NBDG was added to the cells at a final concentration of 200 μM and incubated at 37°C for 30 min. Cells were washed three times with ice-cold PBS and fluorescence was measured at 550 nm emission and 480 nm excitation. Data are calculated relative to non-treated control cells (100%).

Trans epithelial electrical resistance (TEER)

TEER of differentiated Caco-2 cells was assessed using the EVOM resistance meter (World Precision Instruments, Germany) in combination with the EndOhm-24SNAP chamber (World Precision Instruments, Germany). Caco-2 cells were grown in Snapwell^{TM} culture cups (Corning Costar, Austria) and, after differentiation, starved for one hour in serum-free DMEM. Capsaicin, nonivamide and *trans*-pellitorine dissolved in HBSS/HEPES were added to the upper compartment at a final concentration of 10 μM and resistance was measured in duplicates after 15, 30, 60 and 90 min of incubation at 37 °C. Resistance was normalized to the initial resistance prior to test compound addition and the corresponding unit area resistance ($\Omega*cm^2$) was calculated by multiplication with the surface area of the Snapwell membrane.

qPCR

Gene expressions of fatty acid transport protein 2 (*FATP2*) and 4 (*FATP4*), fatty acid translocase (*CD36*), intestinal fatty acid binding protein (*IFABP*), peroxisome proliferated activated receptor alpha (*PPARα*) or gamma (*PPARγ*) were measured using a two-step quantitative real-time polymerase chain reaction (qPCR). Therefore, differentiated Caco-2 were incubated with 10 μM capsaicin, nonivamide or *trans*-pellitorine in serum

free DMEM for 15, 30, 60 and 90 min. Alternatively, cells were starved for one hour in serum-free DMEM and the test compound, diluted in HBSS/HEPES, to a final concentration of 10 µM, was added for further 60 min with or without addition of 5 µM lauric acid as substrate. After washing with ice-cold PBS, total RNA was isolated using the PeqGold Total RNA Isolation Kit (Peqlab, Germany). RNA concentration and quality was measured using the NanoQuant Plate on an infinite M200 Tecan reader before reverse transcription using the high capacity cDNA Kit (Life Technologies, Austria) following manufactures' protocol. Real-time PCR was subsequently carried out in triplicates on a Step-One Plus device (Life technologies) using Fast SYBR Green Master Mix (Life technologies) and primers as described before (185). Starting concentrations of the respective mRNA used for reverse transcription were calculated using LinRegPCR v.12.8 (187-188) and compared to those of non-treated control cells (=1) after normalization to hypoxanthine guanine phosphoribosyl transferase (HPRT1) as a reference gene.

Acetyl-CoA Synthethase (ACS) Activity

ACS activity was assessed as first described by Brown et al. (189) using the following enzymatic net reaction:

acetate + ATP+ L-malate + NAD^+ $\rightarrow$ citrate + AMP + $NADH/H^+$
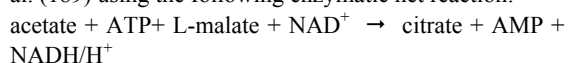
Differentiated Caco-2 cells in 6 cm-cell culture dishes were starved for one hour in serum-free DMEM, before addition of the test compounds at a final concentration of 10 µM diluted in HBSS/HEPES for further 90 min. Residual test compounds were removed by washing cells two-times with ice-cold PBS and the cells were harvested in 65mM KH_2PO_4 buffer using a cell scraper. Protein extracts for ACS determination were obtained by ultrasonic cell dissociation (4x 10 s, 60 % power), followed by centrifugation at 15,000 x g, 4°C for 15 min. Protein content of the cell lysate was determined using Bradford test (190). A total of 40 µL of the cell-free supernatant was added to 140 µL reaction mix containing 7 parts 100 mM Tris/HCl (pH 7.8) and one part each of 50 mM L-malate, 20 mM ATP, 50 mM $MgCl_2$, 2 mM coenzyme A trilithium salt, 60 mM NAD^+, 50 U/mL malate dehydrogenase, 25 U/mL citrate synthase. The reaction was started by the addition of 20 µL 1 M sodium acetate and increase in absorbance at 340 nm was recorded immediately every 10 s for 5 min using a Tecan M200 multiwell plate reader equipped with injectors (Tecan, Austria). The maximum slope in △absorbance/time plot was used for calculation of ACS activity. Data are expressed in mU/mg protein.

Statistical analysis

Data are presented as means ± SEM or fold change (T/C, treated / control) ± SEM from multiple replicates as indicated in the text or figure and table legends, where n refers to the number of biological replicates with at least two technical replicates each. Outliers determined with the Nalimov outlier test were excluded from calculation. Significant effects versus non-treated control cells were determined using Student's t-test or one-way ANOVA vs. control followed by Holm-Sidak post hoc test. Significant differences between multiple treatments (time and dose-dependent effects) were assessed by one-or two-Way ANOVA with Holm-Sidak post hoc test or Student-Newman-Keuls post hoc test as noted in the figure and table legends. Significant differences versus control cells are marked in the figures and tables with * p<0.05; ** p<0.01; ***p<0.001. Time –and dose dependent effects are indicated with distinct letters, at which no common letter indicates significance. IC_{50} values were calculated using one site competition (max =100) curve fitting in SigmaPlot 11.0.

Abbreviations

BCH   trans-tert-butycyclohexanol
CAP   capsaicin
CoA   coenzyme A
CZE   capsazepine
ENaC   epithelial sodium channel
FAU   fatty acid uptake
NV   nonivamide
PEL   *trans*-pellitorine
TRPV1   transient receptor potential cation channel subfamily V member 1

Acknowledgements

Conflict of interest

The authors S. Widder, J.P. Ley and G.E. Krammer are employees at Symrise AG, Holzminden, Germany.

Notes and references

1. L. B. Dixon and N. D. Ernst, *J. Nutr.*, 2001, **131**, 510S-526S.
2. M. L. Wahlqvist, *Asia Pac J Clin Nutr*, 2005, **14**, 313-318.
3. G. A. Bray and L. A. Tartaglia, *Nature*, 2000, **404**, 672-677.
4. K. Diepvens, K. R. Westerterp and M. S. Westerterp-Plantenga, *Am. J. Physiol. Regul. Integr. Comp. Physiol.*, 2007, **292**, R77-85.
5. R. K. Kempaiah and K. Srinivasan, *J. Nutr. Biochem.*, 2006, **17**, 471-478.
6. D. Tsi, A. K. Nah, Y. Kiso, T. Moritani and H. Ono, *J Nutr Sci Vitaminol (Tokyo)*, 2003, **49**, 437-441.
7. C. M. Hochkogler, B. Rohm, K. Hojdar, M. Pignitter, S. Widder, J. P. Ley, G. E. Krammer and V. Somoza, *Mol Nutr Food Res*, 2014, **accepted**.
8. V. Sharma, J. Boonen, N. S. Chauhan, M. Thakur, B. De Spiegeleer and V. K. Dixit, *Phytomedicine*, 2011, **18**, 1161-1169.
9. J. Boonen, A. Bronselaer, J. Nielandt, L. Veryser, G. De Tre and B. De Spiegeleer, *J. Ethnopharmacol.*, 2012, **142**, 563-590.
10. T. Lindmark, Y. Kimura and P. Artursson, *J Pharmacol Exp Ther*, 1998, **284**, 362-369.

11. E. Grasset, M. Pinto, E. Dussaulx, A. Zweibaum and J. F. Desjeux, *Am. J. Physiol.*, 1984, **247**, C260-267.
12. I. J. Hidalgo, T. J. Raub and R. T. Borchardt, *Gastroenterology*, 1989, **96**, 736-749.
13. B. Rohm, A. K. Holik, M. M. Somoza, M. Pignitter, M. Zaunschirm, J. P. Ley, G. E. Krammer and V. Somoza, *Mol. Nutr. Food Res.*, 2013, **57**, 2008-2018.
14. M. V. Berridge, P. M. Herst and A. S. Tan, *Biotechnol. Annu. Rev.*, 2005, **11**, 127-152.
15. A. Riedel, R. Lang, B. Rohm, M. Rubach, T. Hofmann and V. Somoza, *J. Nutr. Biochem.*, 2014, doi:10.1016/j.jnutbio.2014.03.002
16. J. M. Ruijter, C. Ramakers, W. M. Hoogaars, Y. Karlen, O. Bakker, M. J. van den Hoff and A. F. Moorman, *Nucleic Acids Res*, 2009, **37**, e45.
17. J. M. Tuomi, F. Voorbraak, D. L. Jones and J. M. Ruijter, *Methods*, 2010, **50**, 313-322.
18. T. D. Brown, M. C. Jones-Mortimer and H. L. Kornberg, *J. Ethnopharmacol.*, 1977, **102**, 327-336.
19. M. M. Bradford, *Anal. Biochem.*, 1976, **72**, 248-254.
20. S. Miyauchi, E. Gopal, Y.-J. Fei and V. Ganapathy, *J. Biol. Chem.*, 2004, **279**, 13293-13296.
21. M. L. Chalfant, K. Peterson-Yantorno, T. G. O'Brien and M. M. Civan, *Am. J. Physiol.*, 1996, **271**, F861-870.
22. Y. Wei, D.-H. Lin, R. Kemp, G. S. Yaddanapudi, A. Nasjletti, J. R. Falck and W.-H. Wang, *J. Gen. Physiol.*, 2004, **124**, 719-727.
23. H. Yamamura, S. Ugawa, T. Ueda, M. Nagao and S. Shimada, *J. Biol. Chem.*, 2004, **279**, 44483-44489.
24. V. Starai and J. Escalante-Semerena, *Cell. Mol. Life Sci.*, 2004, **61**, 2020-2030.
25. K. Sambaiah and M. N. Satyanarayana, *Indian J. Exp. Biol.*, 1980, **18**, 898-899.
26. M. R. Srinivasan, K. Sambaiah, M. N. Satyanarayana and M. V. L. Rao, *Nutr. Rep. Int.*, 1980, **21**, 455-467.
27. M. R. Srinivasan and M. N. Satyanarayana, *J Bioscience*, 1987, **12**, 143-152.
28. M. P. Lejeune, E. M. Kovacs and M. S. Westerterp-Plantenga, *Br J Nutr*, 2003, **90**, 651-659.
29. J. A. Negulesco, S. A. Noel, H. A. Newman, E. C. Naber, H. B. Bhat and D. T. Witiak, *Atherosclerosis*, 1987, **64**, 85-90.
30. F. Nassir and N. A. Abumrad, *Immunol. Endocr. Metab. Agents Med. Chem.*, 2009, **9**, 3-10.
31. M. Shimizu, A. Mori, Y. Mine and F. Shahidi, eds., *Tight-junction-modulatory factors in food*, CRC Press LLC, 2006.
32. M. van der Stelt, M. Trevisani, V. Vellani, L. De Petrocellis, A. S. Moriello, B. Campi, P. McNaughton, P. Geppetti and V. Di Marzo, *The EMBO journal*, 2005, **24**, 3026-3037.
33. B. Rohm, M. Zaunschirm, S. Widder, J. P. Ley, G. E. Krammer and V. Somoza, in *Proceedings of the 9th Wartburg Symposium Eisenach „Advances and Challenges in Flavor Chemistry & Biology*, ed. T. Hofmann, W. Meyerhof and P. Schieberle, Verlag Deutsche Forschungsanstalt für Lebensmittelchemie, 2014, vol. in press.
34. H. Isoda, J. Han, M. Tominaga and T. Maekawa, *Cytotechnology*, 2001, **36**, 155-161.
35. Y. Tsukura, M. Mori, Y. Hirotani, K. Ikeda, F. Amano, R. Kato, Y. Ijiri and K. Tanaka, *Biol. Pharm. Bull.*, 2007, **30**, 1982-1986.
36. A. Sandoval, A. Chokshi, E. D. Jesch, P. N. Black and C. C. DiRusso, *Biochem. Pharm.*, 2010, **79**, 990-999.
37. M. Traber, H. Kayden and M. Rindler, *J. Lipid. Res.*, 1987, **28**, 1350-1363.
38. P. J. Trotter and J. Storch, *J. Lipid. Res.*, 1991, **32**, 293-304.
39. H.-L. Ji, X.-F. Su, S. Kedar, J. Li, P. Barbry, P. R. Smith, S. Matalon and D. J. Benos, *J Biol Chem*, 2006, **281**, 8233-8241.
40. B. Rossier, *News Physiol. Sci.*, 1996, **11**, 102-102.
41. M. Fukuda, A. Ohara, T. Bamba and Y. Saeki, *Jpn J Physiol*, 2000, **50**, 215-225.
42. J. P. Kampf and A. M. Kleinfeld, *J Biol Chem*, 2004, **279**, 35775-35780.
43. P. N. Black, A. Sandoval, E. Arias-Barrau and C. C. DiRusso, *Immunol. Endocr. Metab. Agents Med. Chem.*, 2009, **9**, 11-17.
44. A. Sandoval, P. Fraisl, E. Arias-Barrau, C. C. DiRusso, D. Singer, W. Sealls and P. N. Black, *Arch. Biochem. Biophys.*, 2008, **477**, 363-371.

a Christian Doppler Laboratory for Bioactive Aroma Compounds, Althanstraße 14, 1090 Vienna, E-mail: Veronika.Somoza@univie.ac.at; Fax:+43 1 4277 9706; Tel: +43 1 4227 70601
b Department for Nutritional and Physiological Chemistry, Althanstraße 14, 1090 Vienna
c Symrise AG, Mühlenfeldstraße, Holzminden, Germany

2.5 Nonivamide, a capsaicin analog, decreases via TRPV1 activation adipogenesis and peroxisome proliferator-activated receptor gamma expression, and enhances miRNA let-7d expression in 3T3-L1 cells

Rohm, B. [a]; Holik, A.-K.[b]; Kretschy, N.[c]; Somoza, M.M.[c]; Widder, S.[d]; Ley, J.P.[d]; Krammer, G.E.[d]; Somoza, V.[a,b]

[a] Christian Doppler Laboratory for Bioactive Aroma Compounds, Althanstraße 14, 1090 Vienna

[b] Department for Nutritional and Physiological Chemistry, Althanstraße 14, 1090 Vienna

[c] Department of Inorganic Chemistry, University of Vienna, Währinger Straße 42, Vienna, Austria

[d] Symrise AG, Mühlenfeldstraße, Holzminden, Germany

Nonivamide, a capsaicin analog, decreases via TRPV1 activation adipogenesis and peroxisome proliferator-activated receptor gamma expression, and enhances miRNA let-7d expression in 3T3-L1 cells *

Barbara Rohm[1], Ann-Katrin Holik[2], Nicole Kretschy[3], Mark M. Somoza[3], Sabine Widder[4], Jakob P. Ley[4], Gerhard E. Krammer[4], Veronika Somoza[1,2]

[1] Christian Doppler Laboratory for Bioactive Aroma Compounds, Althanstraße 14, 1090 Vienna

[2] Department for Nutritional and Physiological Chemistry, Althanstraße 14, 1090 Vienna

[3] Department of Inorganic Chemistry,
University of Vienna, Währinger Straße 42, Vienna, Austria

[4] Symrise AG, Mühlenfeldstraße, Holzminden, Germany

*Running titel: *Nonivamide decreases adipogenesis in 3T3-L1 cells*

To whom correspondence should be addressed: Veronika Somoza, Department of Nutritional and Physiological Chemistry, Christian DopplerLaboratory for Bioactive Aroma Compounds, University of Vienna, Althanstraße 14, 1090 Vienna, Austria. Tel: +43 1 4227 70601, Fax: +43 1 4277 9706, e-mail: Veronika.Somoza@univie.ac.at

Keywords: *trans-tert*-butylcyclohexanol, lipid accumulation, 3T3-L1, adipogenesis, Cell differentiation, MicroRNA, Obesity, Peroxisome proliferator-activated receptor (PPAR)

Background: Regulation of total body fat mass as affected by adipogenesis
Results: The natural pungent aroma compound nonivamide reduces lipid accumulation when added during differentiation of 3T3-L1 preadipocytes to a similar extent as capsaicin
Conclusion: Nonivamide has similar anti-adipogenic effects as capsaicin
Significance: Nonivamide is less pungent than capsaicin, thus can be administered in higher concentrations for enhanced anti-obesity effects

ABSTRACT

Red pepper and its major pungent principle, capsaicin, have been shown to be effective anti-obesity agents by reducing energy intake, enhancing energy metabolism, decreasing serum triacylglycerol content, and inhibiting adipogenesis via activation of the transient receptor potential cation channel subfamily V member 1 (TRPV1). However, the binding of capsaicin to the TRPV1 receptor is also responsible for its pungent sensation, strongly limiting its dietary intake. Here, the effects of a less pungent structural capsaicin-analog, nonivamide, on adipogenesis and underlying mechanisms in 3T3-L1 cells were studied. Nonivamide was found to reduce mean lipid accumulation, a marker of adipogenesis, to a similar extent as capsaicin, up to 10.4% (p<0.001). Blockage of the TRPV1 receptor with the specific inhibitor *trans-tert*-butylcyclohexanol revealed that the anti-adipogenic activity of nonivamide depends, as with capsaicin, on TRPV1 receptor activation. In addition, in cells treated with nonivamide during adipogenesis, protein levels of the pro-adipogenic transcription factor peroxisome-proliferator activated receptor γ (PPAR γ) decreased. Results from miRNA microarrays and digital droplet PCR analysis demonstrated an increase in the expression of the miRNA mmu-let-7d-5p, which has been associated with decreased PPAR γ levels.

Adipose tissue plays a key role in metabolic homeostasis via secretion of adipokines, which interact with central and peripheral organs (95). Pathophysiological overgrowth of adipose tissue is associated with overweight, obesity and subsequent diseases like diabetes type II, chronic inflammation, dementia, and macrovascular diseases (96,191). One possible mean to regulate total fat mass is to reduce adipogenesis (10), the differentiation of preadipocytes to mature adipocytes (98), which determines the total number of adipocytes. This process starts during embryonic development, and white adipose tissue largely expands postnatal (192). However, adults are also capable of adipogenesis (98); about 10% of adipocytes are renewed per year, (193) making

the regulation of adipogenesis an interesting target in body weight maintenance.

Capsaicin, the most abundant capsaicinoid in red pepper, has been shown to be an effective anti-obesity agent. Capsaicin reduces energy intake (122), enhances energy metabolism , and decreases serum triacylglycerol content (194). Administration of 0.014% (w/w) capsaicin with a 30% lard diet has been shown to reduce perirenal adipose tissue weight in rats (194). *In vitro*, capsaicin has been demonstrated to inhibit adipogenesis in 3T3-L1 cells (195), a widely studied *in vitro* model for the differentiation of preadipocytes to adipocytes. The anti-adipogenic activity in 3T3-L1 cells is accompanied by decreased PPAR γ, C/EPBα and leptin expression (195). Using TRPV1 deficient 3T3-L1 cells and knock-out mice, Zhang et al. demonstrated that prevention of adipogenesis depends on the activation of the transient receptor potential vanilloid type-1 (TRPV1) (151). However, binding of capsaicin to the TRPV1 receptor is also responsible for the pungency of capsaicin, limiting its dietary intake. This study focuses on the adipogenesis effects of the less pungent capsaicin-analog, nonivamide.

Nonivamide, which naturally occurs in *Capsicum oleoresin* as a minor component (196), is a direct structural analog of capsaicin (Fig. 1). It differs from capsaicin by one methyl group and one double bond on the carbon chain, and exhibits a markedly reduced TRPV1 binding affinity. An EC_{50} value of 0.7 μM for pure capsaicin has been calculated (154), whereas twice as much of nonivamide is needed for the same effect (EC_{50}= 1.4 μM) (155). The decrease in TRPV1 binding affinity is accompanied by a major decrease in pungency; pure capsaicin is rated with 16,000,000 Scoville Heat Units (SHU), whereas nonivamide is rated at 9,200,000 SHUs (197). To investigate the hypothesis, that the less pungent capsaicinoid nonivamide may produce anti-adipogenic activities similar to those of capsaicin, lipid accumulation after treatment with capsaicin and nonivamide was assessed in well-defined pre-adipocytes, 3T3-L1 cells, as a model (198). The process of adipogenesis in 3T3-L1 cells is well-investigated. After reaching confluence, contact inhibition leads to a growth arrest in 3T3-L1 preadipocytes. A standard hormone cocktail containing insulin, cAMP analogs, and glucocorticoides starts mitotic clonal expansion,

involving replication of preadipocytes before terminal differentiation to adipocytes (199). This process is regulated by a transcriptional cascade, which involves, but is not limited to PPAR γ, CCAAT-enhancer binding protein (C/EBP) α, β and δ and the transcription factors E2F1 and 4 (200-201). However the involvement of several miRNAs has also been demonstrated (111).
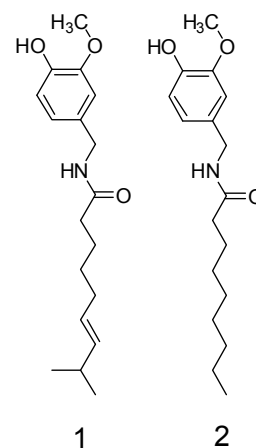
FIGURE 1. Chemical structures of capsaicin (1) and its analog nonivamide (2).

In order to elucidate mechanisms by which the capsaicin analog nonivamide may regulate adipogenesis in 3T3-L1 cells, the dependency of the anti-adipogenic effects by capsaicin and nonivamide on TRPV1-receptor activation was examined using the specific TRPV1-inhibitor *trans-tert*-butylcyclohexanol (BCH) (202). In addition, PPAR γ expression, which has previously been described as a target of capsaicin (195), was determined at both the levels of gene expression regulation and protein abundance. To elucidate miRNA involvement in the effect of nonivamide, a genome-wide micro-RNA (miRNA) expression analysis was performed by means of a custom-made microarray. Effects for selected members of the mmu-let-7 group were validated using digital droplet PCR.

EXPERIMENTAL PROCEDURES

Materials-Nonivamide and *trans-tert*-butylcyclohexanol (BCH) were kindly provided by Symrise AG. Unless stated otherwise, all other chemicals were obtained from Sigma-Aldrich (Austria). Mouse fibroblasts (3T3-L1) were purchased from ATCC.

Cell culture-3T3-L1 pre-adipocytes cells were maintained in DMEM supplemented with 10% fetal bovine serum, 4% L-glutamine and 1% penicillin/streptomycin at 37°C and 5% CO_2 in a humidified atmosphere. Cells were passaged at ~75-80% confluence and used between passage 6 and 20.

133

Differentiation into adipocytes was carried out as described before (203). Briefly, differentiation was initiated two days post-confluence (day 0) via the addition of differentiation media, consisting of growth medium supplemented with 0.5 mM 3-isobutyl-1-methylxanthine, 1 µM dexamethasone and 10 µg/mL insulin. After 48 h, differentiation media was replaced by maturation media (DMEM supplemented with 10 µg/mL insulin) on which cells were maintained for a further 48 h. Cells were kept in normal growth media for an additional five days. Mature adipocytes were used for experiments on day 9 after initiation of differentiation. Only monolayers with a differentiation grade of ~90% or higher were used for the experiments.

The test compounds capsaicin (CAP), nonivamide and BCH stock were dissolved in ethanol to 1000 x stock solutions freshly each time and final ethanol concentration during the assays never exceeded 0.2%.

Cell Viability-Cell viability after treatment with the test compounds was measured using the MTT assay in 96-well format. In the MTT assay, the reduction of yellow tetrazolium salt MTT (3-(4,5-dimethylthiazol-2-yl)-2,5-diphenyltetrazolium bromide) to a purple formazan by mitochondrial and ER enzymes is used as a measure for cell viability (204).

Cells were seeded in 96-well plates and treated with 1 nM – 10 µM capsaicin or nonivamide with or without addition of 25-100 µM BCH for 12 d after initiation of differentiation. Cell culture media was exchanged every second day. On day 12, 100 µL of the MTT working reagent (0.83 mg/mL MTT diluted in PBS/ serum-free media (1:5)), was added to each well, and cells were incubated at 37°C for approximately 15 min. The MTT working solution was removed and the purple formazan formed during incubation was dissolved in 150 µL DMSO per well. Absorbance was measured at 550 nm with

690 nm as reference wavelength using multiwell plate reader (Tecan infinite M200, Tecan Austria). Cell viability was calculated relative to untreated control cells (100%).

Oil red O staining-Accumulation of lipids was assessed by oil red O staining as described previously (203). Briefly, 3T3-L1 pre-adipocytes were seeded in 24-well plates at a density of 2×10^4 cells/ml. Cells underwent differentiation as described above, but were maintained in maturation media for 10 d. Substance addition was started at day 0 or 2 after induction of differentiation. On day 12, cells were fixated in 10% (v/v) formalin in PBS for 1 h. Cells were subsequently stained for 10 min with 200 µL oil red O working solution, which contained 21 mg/mL oil red O dye in 60% isopropanol. Residual oil red O dye was removed by washing four times with double distilled water. Quantification of the staining was carried out by reading the 520 nm absorbance of the oil red dye from the lipid droplets of the cell monolayer, dissolved in 750 µL isopropanol, on a Tecan infinite M200 multiwell plate reader. Lipid accumulation was calculated as % of untreated control cells.

qRT-PCR-Quantitative Real-Time PCR was carried out for determination of gene expression levels of PPAR γ, C/EBPα, FABP4 and CPT1α. The RNA of 3T3-L1 cells was extracted on day 0 (undifferentiated control) and day 9 after initiation of differentiation with or without compound treatment using the RNeasy Lipid Tissue Mini Kit (Qiagen) according to manufacturer's protocol. Quality and concentration of the RNA was analyzed using the NanoQuant Plate on an infinite M200 Tecan reader. Reverse transcription was carried out using the high capacity cDNA Kit (Life technologies, Austria). Increasing fluorescence signals during qRT-PCR reaction were measured in triplicate on a Step-One Plus device using the Fast SYBR green master mix (Life technologies, Austria). Specific primers for each target gene

TABLE 1. Oligonucleotides used during PCR reaction

target	Forward primer	Reverse primer	Product length [bp]
HPRT	GAGAGCGTTGGGCTTACCTC	ATCGCTAATCACGACGCTGG	136
PPARγ	GTGCCAGTTTCGATCCGTAGA	GGCCAGCATCGTGTAGATGA	142
C/EBPα	GCCCCGTGAGAAAAATGAAGG	ATCCCCAACACCTAAGTCCC	129
FABP4	TTTGGTCACCATCCGGTCAG	TGATGCTCTTCACCTTCCTGTC	110

were designed using NCBI Primer-BLAST and synthesized by Sigma-Aldrich Austria (Table 1). Gene expression is given as fold change compared to undifferentiated control cells (=1), calculated from the respective starting mRNA levels, which were determined using LinRegPCR v.12.8 and normalized to hypoxanthine guanine phosphoribosyl transferase (HPRT1) as a reference gene.

PPAR γ ELISA-Quantification of PPAR γ was carried out using a specific ELISA Kit (mouse PPAR γ, Cloud-Clone Corp., USA) with a sensitivity of 0.66 ng/mL. 3T3-L1 cells were washed twice with ice-cold PBS and harvested in lysis buffer (50 mM Tris, 25 mM NaCl, 1 mM EDTA, 1 mM NaF, 1% of the non-denaturing detergent Igepal, pH 7.4) supplemented with 1mM PMSF, 1mM sodium ortho-vanadate and protease inhibitor cocktail. Samples were homogenized by passing the lysate several time through a 20-gauge needle (Sterican, B.Braun Melsungen AG, Germany) and subsequent agitation for 30-45 min at 4°C. The lysate was centrifuged at 16,900xg for 15 min at 4°C and the PPAR γ content in the supernatant quantified by means of the ELISA as recommend by manufacturer's protocol.

Customized miRNA array

miRNA extraction and labeling-miRNA was extracted using the RNeasy Lipid Tissue Mini Kit (Qiagen) according to the manufacturers protocol, but exchanging wash buffer RW1 with wash buffer RWT (Qiagen) to preserve RNA pieces < 200 bp during washing. RNA quality and concentration was determined with a NanoQuant Plate on an infinite M200 Tecan reader. miRNA was labeled with synthetic 5'-phosphate-cytidyl-uridyl-DY547-3' RNA dinucelotides (Thermo Fisher Scientific) using T4 ligase (New England Biolabs). 300 ng of total RNA (plus synthetic spike-in controls) were added to the reaction mix containing 1 mM ATP, 50 mM Tris-HCl (pH 7.8), 10 mM MgCl$_2$, 1 mM DTT, 10 µg/mL BSA, 25% DMSO, 50 µM labeled dinucleotide, and 20 U T4 ligase. The reaction was allowed to take place for 2 h at 4°C and the labeled RNA was purified using a MicroBioSpin 6 column (Bio-Rad)(205).

miRNA microarray design and synthesis- Four identical customized micorarrays were synthesized *in situ* on a glass substrate using a light-directed maskless array synthesizer

as described before (206). The usage of a novel photochemical reaction cell allowed the simultaneous synthesis on two glass substrates, creating eight independently hybridizable microarrays at once (207).

Probes were designed for all mature mouse miRNA sequences in the Sanger microRNA database (MiRBase release 19). To equalize melting temperatures of the miRNA probes, microarray probes with very high melting temperatures were shortened at the 3' side. Since sequences homology among miRNA tends to be near the 5' end, this shortening has only little effect on sequence specificity; second, microarray probes corresponding to miRNA with very low melting temperatures were extended at the 5' end by the addition of G or 5'-AG-3'to allow pairing with one or two bases of the ligated dinucleotide (205).

Hybridization and data analysis- Each microarray was hybridized using a custom design adhesive hybridization chamber (SecureSeal, Grace Biolabs) with a separate compartment for each of the microarrays. The purified, labeled miRNA was applied to the microarray chamber in a hybridization solution containing 100 mM MES, 1 M Na$^+$, 20 mM EDTA, 0.01% Tween20, and 0.06% BSA. Hybridization was carried out at 42°C with constant rotation. Microarrays were scanned with a GenePix 4400 microarray scanner (Molecular Devices, USA) and intensity data for each feature were extracted using NimbleScan software. Each hybridization was performed in duplicates and miRNA levels are presented as mean fold change of the two technical replicates compared to those of undifferentiated control cells.

Digital droplet PCR- Absolute concentrations (copies/µL) of mmu-let-7a-5p, mmu-let-7b-3p, mmu-let-7d-5p, mmu-miR-143-3p and mmu-miR-103-1-5p were determined using the Bio-Rad QX200 Droplet Digital PCR System. For this purpose, miRNA was extracted as described under the microarray section. Extracted miRNA from undifferentiated control cells or mature adipocytes treated with the compounds of interest for 9 d, was subsequently reversely transcribed using the TaqMan MicroRNA Reverse Transcription Kit with specific primers for the target miRNA (Life technologies, Austria). PCR reaction was carried out on a C1000 thermocycler (Bio-Rad) using

droplet PCR supermix (Bio-Rad) and TaqMan miRNA Assays (Life technologies, Austria) for each target miRNA after partition of the sample into 20,000 single droplets by means of the droplet generator. Per assay and treatment, between 11,300 and 17,800 droplets were analyzed and the absolute concentrations computed with the QuantaSoft software.

Statistical analysis- Data are presented as means ± SEM or fold change compared to control cells (± SEM). Except for the microarray experiments, data are calculated from multiple experiments with at least two technical replicates as indicated in the figure or table legends, at which n refers to the number of biological replicates. Outliers were excluded from calculations after performing Nalimov outlier test. Significant differences between multiple treatments (compound and/ or concentration) were determined using One- or Two-Way ANOVA with Holm-Sidak post hoc test. Significant differences between two groups were analyzed with Student's t-test and considered to be different at $p<0.05$. Differences between groups are marked in figures and tables with * $p<0.05$, **$p<0.01$, and ***$p<0.001$.

RESULTS

Cell viability- Negative effects of long-term treatment with any of the test substances (capsaicin, nonivamide, BCH) or a combination thereof, on cell viability, were excluded using the MTT assay. There was no reduction in cell viability after a treatment with 0.01 to 10 µM capsaicin or nonivamide with or without the addition of 25-100 µM BCH for 12 d compared to control cells (One-Way ANOVA vs. control, $p>0.05$, data not shown).

Treatment with capsaicin and nonivamide reduces lipid accumulation in
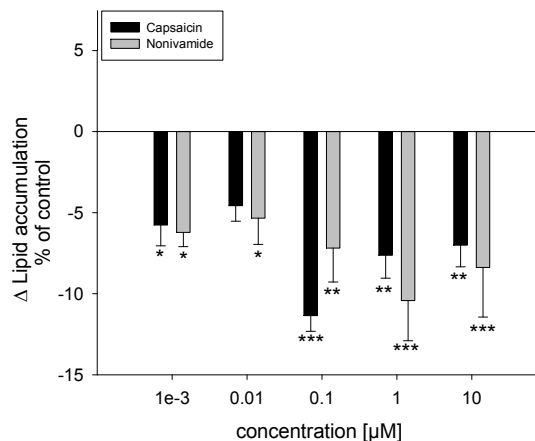
FIGURE 2. Difference in lipid accumulation in % of control (0.1% EtOH) ± SEM after addition of 0.01-10 µM capsaicin or nonivamide during differentiation and maturation of 3T3-L1 cells. Lipids in fully mature adipocytes were stained 12 d after initiation of differentiation with oil red O and data are shown as means of control treated cells from 3-4 independent experiments with at least 3 technical replicates each. *:$p<0.05$, **$p<0.01$,***$p<0.001$ vs. control treated cells.

3T3-L1 adipocytes- Accumulation of lipids during the differentiation process, assessed via oil red O staining, is a frequently used functional marker for the degree of adipogenesis in 3T3-L1 cells (151,195,208-209). In the present study, the effect of the addition of 0.01-10 µM capsaicin or nonivamide during differentiation and maturation (12 d) of 3T3-L1 cells on lipid accumulation was assessed (Fig. 2). First, an effect of addition of 0.1% ethanol as a solvent control to the media was excluded ($p>0.05$, data not shown). The effects of nonivamide and capsaicin are thus presented compared to cells treated with the solvent control. Capsaicin reduced lipid accumulation by 5.76 ± 1.03% ($p<0.05$) at 0.01 µM up to 10.1 ± 1.50% ($p<0.001$) at 0.1 µM in comparison to control cells. Treatment with nonivamide reduced lipid accumulation to a similar extent as capsaicin; the

TABLE 2. Results of the gene expression analysis of *C/EBPα* and *FABP4*. Data are shown as fold changes compared to undifferentiated control cells (=1) from three independent experiments with at least two technical replicates. mRNA for the experiments was extracted on day 0 (undifferentiated control) and day 9 after initiation of differentiation, during which cells were either treated with 0.1% EtOH or 10 µM capsaicin or nonivamide.

Target gene	solvent control	Capsaicin	Nonivamide
C/EBPα	7.51±0.43	7.69±0.59	6.28±0.33
FABP4	153±10.2	155±21.3	144±9.78

Fold changes in gene expression after treatment with 0.1% EtOH (solvent control) or 10 µM capsaicin or nonivamide compared to undifferentiated control cells (=1). n=3 with three technical replicates.

effects were not different from the effects after capsaicin treatment at any of the tested concentrations. Compared to untreated control cells, treatment with nonivamide decreased lipid accumulation by 5.34±1.03% (p<0.05) at 0.01 μM up to 10.4 ± 2.47% (p<0.001) at 1 μM.

Reduction in lipid accumulation by capsaicin and nonivamide can be blocked by the addition of a TRPV1 inhibitor- Activation of the TRPV1 receptor has been shown to be responsible for the anti-adipogenic effects of capsaicin *in vitro* and *in vivo* (151). In order to examine whether the effects of nonivamide on lipid accumulation also depend on TRPV1 activation, 3T3-L1 cells were co-incubated with 1 μM nonivamide and 25-100 μM of the specific TRPV1-inhibitor *trans-tert*-butylcyclohexanol (BCH) during differentiation and maturation for a total of 12 d (Fig. 3). A concentration of 1 μM nonivamide was chosen for co-incubation studies, since this concentration demonstrated the greatest effect. As a positive control for TRPV1 inhibition by BCH, the effect of concomitant incubation of the TRPV1 inhibitor BCH and capsaicin was determined. Addition of BCH to capsaicin-containing media prevented reduction in lipid accumulation by capsaicin, leading to no difference between control treatment and a treatment with 1 μM capsaicin plus 25 μM (-4.71 ± 1.45%), 50 μM (-3.62 ± 2.49%) and 100 μM BCH (+1.06 ± 1.73%, p<0.05 vs. control), whereas treatment with 1 μM capsaicin alone reduced lipid accumulation by 7.63 ± 1.41% (p<0.001, Fig. 3). Likewise, addition of 25, 50, and 100 μM BCH to media containing 1 μM nonivamide prevented reduction in lipid accumulation caused by 1 μM nonivamide (-10.4 ± 2.47%,p<0.001 vs. control, Fig. 3) as well. There was, similarly to the results obtained for capsaicin, no difference between control-treated cells and cells treated with 25 μM (-1.83 ± 2.00%), 50 (+2.15 ± 1.25%), and 100 μM BCH (+1.0 ± 2.18%) in combination with nonivamide (p>0.05 for each treatment vs. control, Fig. 3). Incubation of 3T3-L1 cells for 12 d during differentiation and maturation with 25-100 μM BCH did not affect lipid accumulation compared to control cells (p>0.05) and was between 2.07 ± 1.35% and -0.96 ± 1.93% (data not shown in Fig.).

Treatment with nonivamide decreases expression of PPAR γ - PPAR γ and C/EBPα are major factors regulating adipogenesis and have been demonstrated as a target of capsaicin (195).
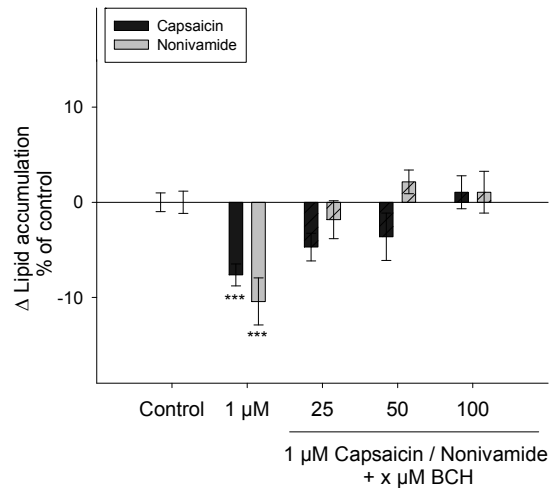
FIGURE 3. Difference in lipid accumulation in % of control (0.1% EtOH) ± SEM after treatment with 1 μM capsaicin or nonivamide with or without the addition of 25-100 μM of the selective TRPV1 inhibitor trans-tert-butylcyclohexanol (BCH) during differentiation and maturation (12 d) of 3T3-L1 cells. Lipids in fully mature adipocytes were stained 12 d after initiation of differentiation with oil red O and data are shown as means compared to control treated cells from 3-4 independent experiments with at least 3 technical replicates each. *** p< 0.001 vs. control.

Thus, gene expression levels of PPAR γ, C/EBPα and FABP4 after treatment with 10 μM nonivamide or capsaicin for 9 d or of control treated cells were determined using qPCR. Compared to undifferentiated control cells, gene expression of PPAR γ, C/EBPα and FABP4 increased to 4.26 ± 0.25, 7.51 ± 0.43 and 153 ± 10.2 in control treated cells (Fig. 4, Table 2). However, there was no significant impact of capsaicin or nonivamide treatment on gene expression of C/EBPα and FABP4 and PPAR γ, although there was a trend (p=0.056) towards a down-regulation of PPARγ mRNA levels after treatment with nonivamide (3.55 ± 0.06, Fig. 4, left side).

In order to investigate whether PPAR γ - levels are down-regulated at the protein level, the PPAR γ content per mg protein of 3T3-L1 cell lysates 9 d after initiation of differentiation with or without treatment with capsaicin or nonivamide was determined. Undifferentiated control cells had an average PPAR γ content of 59 ± 16.7 ng/mg protein. Upon differentiation, PPAR γ levels increased by a factor of 132, to 5894 ± 416.6 ng/mg protein (p<0.001) in control

treated cells. Treatment with capsaicin did not change PPAR γ levels (7882 ± 3654 ng/mg protein) compared to those of control treated cells, whereas treatment with nonivamide led to a decrease of PPAR γ to 4016 ± 116 ng/mg protein compared to control treated cells (p<0.05, Fig. 4, right side).

Treatment with nonivamide regulates expression of mmu-let-7d-5p- Since several miRNAs have been associated with the regulation of adipogenesis and obesity (see review: (111)), a genome-wide miRNA array was performed. By means of this customized array, miRNA levels of undifferentiated 3T3-L1 cells, control treated cells (0.1% EtOH) and cells treated with 10 µM nonivamide during adipogenesis for 9 d were compared. Fold changes of control and nonivamide-treated cells compared to undifferentiated cells of selected miRNAs, which have been associated with the regulation of adipogenesis before, are displayed in Table 3. On day 9 after initiation of adipogenesis, expression levels of mmu-miR-103-3p (4.35), mmu-miR-210-3p (1.73), as well as mmu-let-7a-5p (2.04) and mmu-let-7d-5p (1.82) were increased compared to undifferentiated control cells (=1), using an absolute fold change of 1.5 as cut-off criteria (210). In contrast, there was neither an effect on other isoforms of the upregulated miRNAs, nor on further adipogenesis-regulating miRNAs like mmu-miR-143, mmu-miR-193, mmu-miR-27 or mmu-miR-448. However, treatment with nonivamide for 9 d increased expression of mmu-let-7a-5p from 2.04 (control treatment/undifferentiated control) to 3.38 (nonivamide treatment/undifferentiated control), corresponding to an absolute fold change of 1.66. Also other members of the let-7 group were up-regulated after nonivamide treatment, leading to an increased expression of mmu-let-7b-3p from 1.10 to 3.77, corresponding to an absolute fold change of 1.66, and mmu-let-7d-5p from 1.82 to 2.73, corresponding to an absolute fold change of 1.5. In contrast, mmu-miR-103-1-

5p and mmu-miR-103-2-5p were down-regulated after nonivamide treatment to 0.06 and 0.25 compared to 1.16 and 0.93 after control treatment. Nonivamide-treatment also reduced expression of mmu-miR-143-3p (0.06), mmu-miR-210-3p (0.14), mmu-miR-27a-3p and -5p to 0.17 or 0.09, respectively and mmu-miR-27b-5p to 0.19 (table 3).

TABLE 3. Results of the customized miRNA microarray using an absolute fold change (compared to undifferentiated control cells) of 0.5 or 1.5 respectively, as cut-off criteria. Data are shown as fold changes compared to undifferentiated control cells (=1) of selected miRNAs, that were shown to regulate adipogenesis in 3T3-1 cells. miRNA for the experiments was extracted on day 0 (undifferentiated control) and day 9 after initiation of differentiation, during which cells were either treated with 0.1% EtOH or 10 µM nonivamide.

mature miRNA	solvent control	Nonivamide
mmu-let-7a-5p	2.04	3.38
mmu-let-7b-3p	1.10	3.77
mmu-let-7d-5p	1.82	2.73
mmu-miR-103-3p	4.35	6.37
mmu-miR-103-1-5p	1.16	0.06
mmu-miR-103-2-5p	0.93	0.25
mmu-miR-143-3p	1.29	0.06
mmu-miR-193a-3p	1.00	0.09
mmu-miR-193a-5p	0.94	0.01
mmu-miR-193b-5p	0.88	0.26
mmu-miR-27a-3p	1.03	0.17
mmu-miR-27a-5p	1.04	0.09
mmu-miR-27b-5p	0.79	0.19
mmu-miR-210-3p	1.73	0.14
mmu-miR-448-3p	0.79	0.02
mmu-miR-448-5p	0.81	0.10

Fold changes in miRNA expression after treatment with 0.1% EtOH (solvent control) or 10 µM nonivamide compared to undifferentiated control cells (=1). n=1 with two technical replicates.
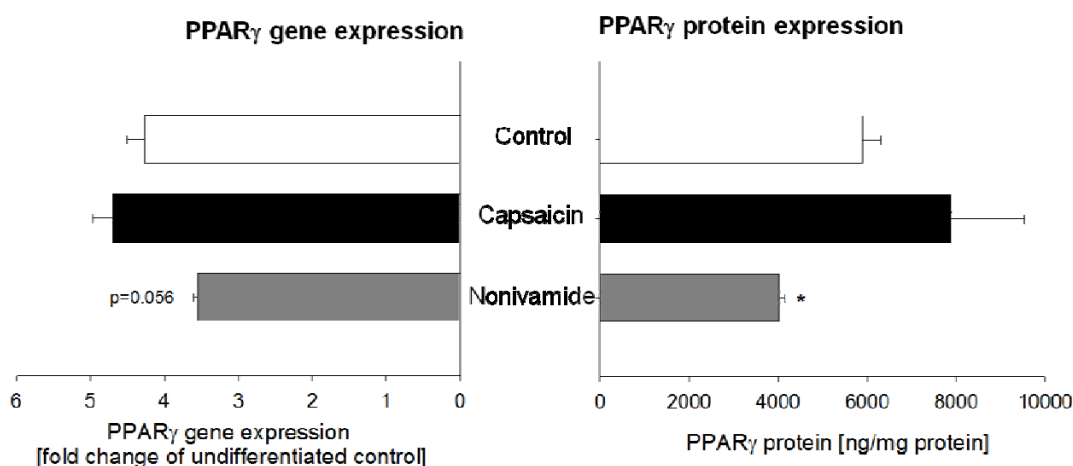
FIGURE 4. PPARγ expression on genetic level (as mean fold change ± SEM compared to undifferentiated control cells, left side) and protein (in ng/mg protein ± SEM, right side) level in 3T3-L1 adipocytes. mRNA or protein was extracted on day 9 after initiation of differentiation. During differentiation and maturation, 3T3-L1 cells were treated with either 0.1% EtOH, 10 μM capsaicin or nonivamide. Data are shown as mean from three independent experiments. *: $p < 0.05$ vs. control

Since the present study detected a similar expression pattern after nonivamide treatment for several members of mmu-let-7, the expression of selected isoforms was validated using highly sensitive digital droplet PCR. This methods allows an absolute quantification of the target gene copy number per μL by partition of the 20 μL test sample into 20,000 single droplets that are separately analyzed for a positive or negative fluorescence signal (Fig. 5) Compared to undifferentiated control cells, expression of mmu-let-7a-5p, mmu-let-7b-3p and mmu-let-7d-5p was increased to a fold change of 1.44 ± 0.07, 5.91 ± 0.83 or 2.22 ± 0.19, respectively within 9 d after initiation of differentiation in control cells. Treatment with the solvent control 0.1% EtOH during differentiation led to similar fold changes compared to undifferentiated cells with 1.47 ± 0.30 for mmu-let-7a-5p, 5.86 ± 0.43 for mmu-let-7b-3p and 2.47 ± 0.28 for mmu-let-7d-5p ($p > 0.05$). In contrast to the miRNA array results, mmu-let-7a-5p expression was not affected by treatment with capsaicin or nonivamide with fold changes to the solvent control of 1.11 ± 0.26 or 1.18 ± 0.08, respectively (Fig. 6). However, expression of mmu-let-7b-3p increased to 8.05 ± 0.64 in capsaicin-treated cells compared to the solvent control (5.86 ± 0.43, $p < 0.05$), corresponding to a fold change of 1.38 ± 0.11 (Fig. 6). Treatment with nonivamide increased mmu-let-7b-3p expression to a comparably mean fold change of 8.32±2.46 (1.42 ± 0.42 compared to the solvent control), without reaching the level of significance ($p > 0.05$). Expression of mmu-let-7d-5p increased (2.95 ± 0.0.13) in nonivamide-treated cells compared to control cells (2.22 ± 0.19, $p < 0.01$), but not compared to the solvent control (corresponding fold change 1.20 ± 0.05, $p > 0.05$). Treatment with capsaicin led to a similar fold change of undifferentiated control cells of 3.25 ± 0.17, corresponding to a fold change of 1.32 ± 0.28 of the solvent control, without reaching the level of significance ($p > 0.05$). No difference in mmu-let-7 expression in response to capsaicin and nonivamide-treatment was found (Fig. 6).
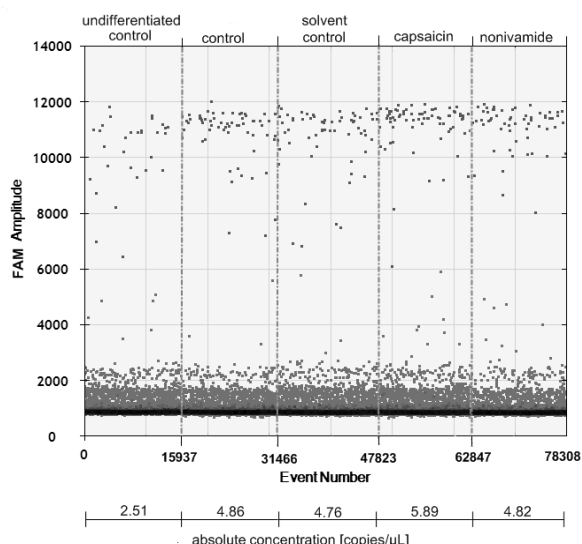
FIGURE 5. Visual representation of one example measurement of the weakly expressed mmu-let-7b-3p using ddPCR. The x-axis shows the accumulating number of counted droplets. Per treatment, between 15,024 (capsaicin) and 16,357 (solvent control) droplets were accepted for analysis of a negative or positive FAM signal. FAM signal intensity is displayed on the y-axis. The lower cluster represents negative droplets, whereas the upper cluster represents droplets with a positive signal, allowing calculation of absolute copy numbers (copies/ µL) using QuantaSoft software.

DISCUSSION

Red pepper and its major pungent principle, capsaicin are often discussed as anti-obesity agents. Beside reducing energy intake (122), increasing energy metabolism and lowering serum triacylglycerol content (194), administration of 0.01% (w/w) capsaicin has been shown to reduce visceral adipose tissue and subcutaneous fat in mice fed a high fat diet (151). In addition, capsaicin has been shown to reduce adipogenesis in 3T3-L1 pre-adipocytes (151,195). Knock out experiments in *in vitro* and *in vivo* model systems have shown that anti-adipogenic activity of capsaicin is mediated by activation of the TRPV1 cation channel (151). However, the downside of capsaicin, being a highly potential TRPV1 agonist, is that its contact with mucous membranes, for example in the oral cavity, leads to a sharp burning pain in mammals. This pungency strongly limits dietary intake of capsaicin, especially in European countries. In the present study, we investigated whether the less pungent capsaicinoid, nonivamide, may exhibit similar effects on

adipogenesis in 3T3-L1 cells as capsaicin. Nonivamide is a direct structural analog of capsaicin, although the slight structural difference reduces its TRPV1 binding affinity and hence, also its pungency by half. In the present study, we analyzed lipid accumulation by oil red O staining, as an indicator for adipogenesis. Oil red O staining is a frequently used marker for differentiation of pre-adipocytes to adipocytes in 3T3-L1 cells (209,211-212). Beside the visible accumulation of lipid droplets, the strong increase compared to undifferentiated control cells in PPARγ gene and protein expression as well as C/EBPα and FABP4 gene expression further confirmed the differentiation of 3T3-L1 pre-adipoyctes to mature adipocytes upon addition of the hormone cocktail two days post-confluence.

The results demonstrate that addition of 0.01-10 µM nonivamide reduces lipid accumulation in 3T3-L1 cells up to 10.4 ± 2.47% when added at a final concentration of 1 µM during differentiation and maturation for 12 d, which is comparable to the results obtained for capsaicin. Treatment with capsaicin reduced lipid accumulation up to 10.1 ±1 .50%at 0.1 µM, confirming the results of Zhang et al. (151,195), who showed reduced oil red O staining of
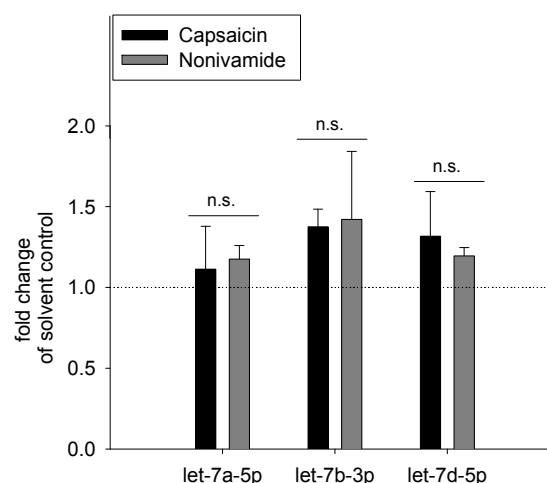
FIGURE 6. Mean fold changes of mmu-let-7a-5p, mmu-let-7b-3p, mmu-let-7d-5p expression analyzed using digital droplet PCR. miRNA from 3T3-L1 cells was extracted on day 0 (undifferentiated control) and day 9 after control treatment, treatment with 0.1% ethanol (solvent control) or 10 µM capsaicin or nonivamide during differentiation and maturation. Data are as mean fold change compared to the solvent control (=1, dotted line) of three independent experiments compared to undifferentiated control cells.

3T3-L1 cells after treatment with 1 μM of capsaicin during adipogenesis. In order to investigate whether the nonivamide-induced reduction in lipid accumulation is mediated via TRPV1 activation, the effect of concomitant addition of the selective TRPV1 inhibitor *trans-tert*-butylcyclohexanol (BCH) and nonivamide on lipid accumulation was analyzed. BCH has been successfully used as a TRPV1-inhibitor in previous studies (165,213). Since the anti-adipogenic effect of capsaicin depends on TRPV1 receptor activation (151,195), the effect of BCH on the reduction of lipid accumulation by capsaicin was used as a positive control for TRPV1 blockage by BCH. In the presence of 25-100 μM BCH, addition of 1 μM capsaicin did not reduce lipid accumulation, proving the effectiveness of BCH and confirming previous results (151,195). However, addition of 25-100 μM BCH to nonivamide-containing media prevented the anti-adipogenic activity of nonivamide, leading to no reduction in lipid accumulation compared to control treated cells. This result demonstrates that activation of the TRPV1 receptor by both capsaicin and nonivamide inhibits adipogenesis in 3T3-L1 cells. However, since ethanol has also been discussed to activate the TRPV1 receptor (214-215), an effect of low doses of ethanol as solvent (0.1-0.2%) for the test substances on lipid accumulution was excluded in preliminary experiments.

As a signaling pathway for TRPV1-mediated inhibition of adipogenesis, increased calcium entry from the extracellular space via the TRPV1 channel with intracellular calcium accumulation targets adjacent calcineurin (152). Activation of calcineurin is thought to inhibit the pro-adipogenic factors PPARγ and C/EBPα, thus repressing adipogenesis (152). This suggested pathway is supported by a study from Hsu et al. (195), who demonstrated that treatment of mature 3T3-L1 adipocytes with high concentrations (25-100 μM) capsaicin for 12-24 h down-regulated expression of PPARγ and C/EBPα. Thus, we investigated the effect of capsaicin and nonivamide treatment during adipogenesis on gene expression of *C/EBPα* and *PPARγ*, and, as a further marker for adipogenesis, *FABP4*. Gene expression of the three markers increased during adipogenesis, although there was no effect of capsaicin and nonivamide treatment compared to control treated cells. Since there was a trend (p=0.056)

towards a *PPARγ* down-regulation after nonivamide treatment, PPARγ protein expression was analyzed as well. In contrast to capsaicin exposure, nonivamide-treatment reduced PPARγ expression compared to control-treated cells. This down-regulation of PPARγ could at least partly account for inhibition of adipogenesis by nonivamide. Although the comparable anti-adipogenic activities of capsaicin and nonivamide both depend on TRPV1 activation, treatment with capsaicin did not affect PPARγ treatment, contrary to the hypothesis and existing evidence from the literature. However, down-regulation of PPARγ after capsaicin treatment in the study by Hsu et al. was observed after treatment with far higher concentrations of capsaicin (25-100 μM). In addition, in the study by Hsu et al. (195), mature 3T3-L1 adipocytes were treated, whereas in the present study, 3T3-L cells were treated during differentiation process. Also, a counter-regulation of other genes cannot be excluded. However, the differences in PPARγ expression between capsaicin and nonivamide treatment are unexpected, and point to possible differences in signaling pathways. Differences in signaling after capsaicin and nonivamide treatment have been shown before in neural SH-SY5Y cells (165), and can hence not be excluded for the present study as well.

The pro-adipogenic transcription factor PPARγ has been shown to be a target of some miRNAs, which have been recently identified as a novel group of adipogenic regulators. For instance, the ectopic expression of pro-adipogenic miR-103 revealed an up-regulation of PPARγ_2, which probably mediates the pro-adipogenic effects of miR-103 (216). On the other hand, miR-27b was shown to directly target PPARγ, whose decreased expression led to an impaired adipogenesis (112). However, also miR-143 and let-7a have been associated with an increased or decreased, respectively, of PPARγ expression (217-218). To investigate, whether the anti-adipogenic activity of nonivamide involves, beside TRPV1 activation and PPARγ down-regulation, also a regulation of miRNAs, a customized miRNA microarray was carried out for a first screening. During adipogenesis, miRNA-103-3p, miR-210-3p and let-7a-5p, let-7b-3p and let-7d-5p expression increased compared to undifferentiated control cells. This is in accordance with previous studies (216-

217,219), although other isoforms of the presented miRNAs were not regulated.

Treatment with nonivamide led to a down-regulation of miR-27a-3p/ -5p and miR-27b-5p compared to control treatment, which would rather argue for a PPAR γ up-regulation than the analyzed PPAR γ down-regulation after nonivamide treatment (112). In contrast, the detected down-regulation of miR-143-3p after nonivamide treatment compared to control treatment could at least partly explain inhibition of PPAR γ expression (218). Also expression levels of the anti-adipogenic mmu-let-7a-5p, mmu-let-7b-3p and mmu-let-7d-5p increased after nonivamide treatment compared to control treatment, which has been associated with an decreased PPAR γ expression before (217). Changes in expression of mmu-let-7a-5p, mmu-let-7b-3p and mmu-let-7d-5p were validated using ddPCR, which allows a much more precise, absolute quantification of the target gene/miRNA than qPCR or microarray (220-221). Absolute quantification of these selected members of the let-7 group in undifferentiated control cells (day 0) and 9 d after initiation of differentiation confirmed the results of the microarray by demonstrating an up-regulation of all three representatives of the let-7 group during adipogenesis. However, using ddPCR, there was no impact of capsaicin or nonivamide treatment on mmu-let-7a-5p expression. Capsaicin-treated cells showed an increased let-7b-3p expression compared to solvent control-treated cells, whereas treatment with nonivamide led to an increased expression of mmu-let-7d-5p compared to the control. An increased expression of mmu-let-7d-5p after nonivamide-treatment compared to solvent control treated cells was also detected using the customized microarray, validating the stimulating impact of nonivamide treatment on mmu-let-7d-5p expression. Increased expression of let-7 has been shown to be accompanied by decreased PPARγ expression (217). Thus, increased mmu-let-7d-5p may be responsible for the decreased PPARγ in nonivamide-treated cells and hence be involved in the anti-adipogenic activity of nonivamide in 3T3-L1 cells . It is also remarkably that, although treatment with capsaicin did not reduce PPAR γ expression, there was no difference in the expression of the investigated let-7 representatives between nonivamide and capsaicin treated cells.

In conclusion, the present study demonstrates for the first time that the less pungent capsaicin-analog nonivamide impairs adipogenesis to a similar extent as capsaicin. Using a specific inhibitor, it was demonstrated that the anti-adipogenic activity of nonivamide depends, like the anti-adipogenic activity of capsaicin, on the activation of the TRPV1 receptor. Nonivamide has a lower binding affinity than capsaicin to the TRPV1 receptor, however, in the tested range of concentrations, effects of nonivamide and capsaicin on adipogenesis were equal. The effects of lower test concentrations would be needed to clearly identify the activity threshold for both compounds, and to determine whether the threshold can be correlated with TRPV1 binding affinity, and thus, pungency. However, a different downstream-signaling pathway after TRPV1 activation is conceivable, since contrary to capsaicin, treatment with nonivamide decreased PPAR γ -levels. This could, at least partly, be explained by an increased expression of the miRNA mmu-let-7d. Since the capsaicinoide nonivamide is rated to almost half as pungent as capsaicin (197), an oral application of higher doses compared to capsaicin is possible and reveals nonivamide as a less pungent, but still potent novel anti-obesity compound from nature.

Although data from long-term human intervention studies with nonivamide are lacking, nonivamide seems to be a promising candidate to target different medicinal strategies in the treatment of obesity. Beside the here demonstrated inhibition of adipogenesis, nonivamide has also been shown to decrease fatty acid uptake in Caco-2 cells (213), which may support the prevention of hyperlipidemia. In addition, administration of 0.15 mg nonivamide in an oral glucose tolerance test reduced total energy intake from a standardized breakfast in slightly overweight male subjects (222), supporting the effectiveness of the less pungent capsaicin-analog.

REFERENCES

1.   Harwood, H. J., Jr. (2012) The adipocyte as an endocrine organ in the regulation of metabolic homeostasis. *Neuropharmacol.* **63**, 57-75
2.   Wahlqvist, M. L. (2005) Dietary fat and the prevention of chronic disease. *Asia Pac. J. Clin. Nutr.* **14**, 313-318
3.   Kivipelto, M., Ngandu, T., Fratiglioni, L., Viitanen, M., Kåreholt, I., Winblad, B., Helkala, E.-L., Tuomilehto, J., Soininen, H., and Nissinen, A. (2005) Obesity and vascular risk factors at midlife and the risk of dementia and Alzheimer disease. *Arch. Neurol.* **62**, 1556-1560
4.   Bray, G. A., and Tartaglia, L. A. (2000) Medicinal strategies in the treatment of obesity. *Nature* **404**, 672-677
5.   Hausman, D. B., DiGirolamo, M., Bartness, T. J., Hausman, G. J., and Martin, R. J. (2001) The biology of white adipocyte proliferation. *Obes. Rev.* **2**, 239-254
6.   Poissonnet, C. M., Burdi, A. R., and Garn, S. M. (1984) The chronology of adipose tissue appearance and distribution in the human fetus. *Early Hum. Dev.* **10**, 1-11
7.   Spalding, K. L., Arner, E., Westermark, P. O., Bernard, S., Buchholz, B. A., Bergmann, O., Blomqvist, L., Hoffstedt, J., Naslund, E., Britton, T., Concha, H., Hassan, M., Ryden, M., Frisen, J., and Arner, P. (2008) Dynamics of fat cell turnover in humans. *Nature* **453**, 783-787
8.   Yoshioka, M., St-Pierre, S., Drapeau, V., Dionne, I., Doucet, E., Suzuki, M., and Tremblay, A. (1999) Effects of red pepper on appetite and energy intake. *Br. J. Nutr.* **82**, 115-123
9.   Kawada, T., Hagihara, K., and Iwai, K. (1986) Effects of capsaicin on lipid metabolism in rats fed a high fat diet. *J. Nutr.* **116**, 1272-1278
10.   Hsu, C. L., and Yen, G. C. (2007) Effects of capsaicin on induction of apoptosis and inhibition of adipogenesis in 3T3-L1 cells. *J. Agric. Food Chem.* **55**, 1730-1736
11.   Zhang, L. L., Yan Liu, D., Ma, L. Q., Luo, Z. D., Cao, T. B., Zhong, J., Yan, Z. C., Wang, L. J., Zhao, Z. G., Zhu, S. J., Schrader, M., Thilo, F., Zhu, Z. M., and Tepel, M. (2007) Activation of transient receptor potential vanilloid type-1 channel prevents adipogenesis and obesity. *Circ. Res.* **100**, 1063-1070
12.   Constant, H. L., Cordell G.A., and West, D. P. (1996) Nonivamide, a Constituent of Capsicum oleoresin. *J. Nat. Prod* **59**, 425-426
13.   Caterina, M. J., Schumacher, M. A., Tominaga, M., Rosen, T. A., Levine, J. D., and Julius, D. (1997) The capsaicin receptor: a heat-activated ion channel in the pain pathway. *Nature* **389**, 816-824
14.   Thomas, K. C., Ethirajan, M., Shahrokh, K., Sun, H., Lee, J., Cheatham, T. E., 3rd, Yost, G. S., and Reilly, C. A. (2011) Structure-activity relationship of capsaicin analogs and transient receptor potential vanilloid 1-mediated human lung epithelial cell toxicity. *J. Pharmacol. Exp. Ther.* **337**, 400-410
15.   Haas, J. S., Whipple, R. E., Grant, P. M., Andresen, B. D., Volpe, A. M., and Pelkey, G. E. (1997) Chemical and elemental comparison of two formulations of oleoresin capsicum. *Sci. Justice* **37**, 15-24
16.   Green, H., and Kehinde, O. (1975) An established preadipose cell line and its differentiation in culture. II. Factors affecting the adipose conversion. *Cell* **5**, 19-27
17.   Gregoire, F. M., Smas, C. M., and Sul, H. S. (1998) Understanding adipocyte differentiation. *Physiol. Rev.* **78**, 783-809
18.   Farmer, S. R. (2006) Transcriptional control of adipocyte formation. *Cell Metab.* **4**, 263-273
19.   Rosen, E. D., and Spiegelman, B. M. (2000) Molecular regulation of adipogenesis. *Annu. Rev. Cell Dev. Biol.* **16**, 145-171
20.   McGregor, R. A., and Choi, M. S. (2011) microRNAs in the regulation of adipogenesis and obesity. *Curr. Mol. Med.* **11**, 304-316
21.   Kueper, T., Krohn, M., Haustedt, L. O., Hatt, H., Schmaus, G., and Vielhaber, G. (2010) Inhibition of TRPV1 for the treatment of sensitive skin. *Exp. Dermatol.* **19**, 980-986
22.   Riedel, A., Pignitter, M., Hochkogler, C. M., Rohm, B., Walker, J., Bytof, G., Lantz, I., and Somoza, V. (2012) Caffeine dose-dependently induces thermogenesis but restores ATP in HepG2 cells in culture. *Food Funct.* **3**, 955-964
23.   Berridge, M. V., Herst, P. M., and Tan, A. S. (2005) Tetrazolium dyes as tools in cell biology: new insights into their cellular reduction. *Biotechnol. Annu. Rev.* **11**, 127-152

24. Wang, H., Ach, R. A., and Curry, B. (2007) Direct and sensitive miRNA profiling from low-input total RNA. *Rna* **13**, 151-159

25. Agbavwe, C., Kim, C., Hong, D., Heinrich, K., Wang, T., and Somoza, M. M. (2011) Efficiency, error and yield in light-directed maskless synthesis of DNA microarrays. *J. Nanobiotechnology* **9**, 1-17

26. Sack, M., Kretschy, N., Rohm, B., Somoza, V., and Somoza, M. M. (2013) Simultaneous light-directed synthesis of mirror-image microarrays in a photochemical reaction cell with flare suppression. *Anal. Chem.* **85**, 8513-8517

27. Hwang, J. T., Park, I. J., Shin, J. I., Lee, Y. K., Lee, S. K., Baik, H. W., Ha, J., and Park, O. J. (2005) Genistein, EGCG, and capsaicin inhibit adipocyte differentiation process via activating AMP-activated protein kinase. *Biochem. Biophys. Res. Commun.* **338**, 694-699

28. Arumugam, M., Vijayan, P., Raghu, C., Ashok, G., Dhanaraj, S. A., and Kumarappan, C. T. (2008) Anti-adipogenic activity of Capsicum annum (Solanaceae) in 3T3 L1. *J. Compl. Integr. Med.* **5**, 1-9

29. Li, Y., Li, J., Belisle, S., Baskin, C. R., Tumpey, T. M., and Katze, M. G. (2011) Differential microRNA expression and virulence of avian, 1918 reassortant, and reconstructed 1918 influenza A viruses. *Virology* **421**, 105-113

30. Zhang, K., Guo, W., Yang, Y., and Wu, J. (2011) JAK2/STAT3 pathway is involved in the early stage of adipogenesis through regulating C/EBPbeta transcription. *J. Cell Biochem.* **112**, 488-497

31. Yoshitomia, H., Qinb, L., Liub, T., and Gaoa, M. (2012) Guava Leaf Extracts Inhibit 3T3-L1 Adipocyte Differentiation Via Activating AMPK. *J. Nutr. Ther.* **1**, 107-113

32. Rohm, B., Holik, A. K., Somoza, M. M., Pignitter, M., Zaunschirm, M., Ley, J. P., Krammer, G. E., and Somoza, V. (2013) Nonivamide, a capsaicin analog, increases dopamine and serotonin release in SH-SY5Y cells via a TRPV1-independent pathway. *Mol. Nutr. Food Res.* **57**, 2008-2018

33. Rohm, B., Riedel, A., Widder, S., Ley, J. P., Krammer, G. E., and Somoza, V. (2014) Capsaicin, nonivamide and trans-pellitorine decrease free fatty acid uptake without TRPV1 activation and increase acetyl-coenzyme A synthetase activity in Caco-2 cells. *Food Funct.* **submitted**

34. Trevisani, M., Smart, D., Gunthorpe, M. J., Tognetto, M., Barbieri, M., Campi, B., Amadesi, S., Gray, J., Jerman, J. C., Brough, S. J., Owen, D., Smith, G. D., Randall, A. D., Harrison, S., Bianchi, A., Davis, J. B., and Geppetti, P. (2002) Ethanol elicits and potentiates nociceptor responses via the vanilloid receptor-1. *Nat. Neurosci.* **5**, 546-551

35. Blednov, Y., and Harris, R. (2009) Deletion of vanilloid receptor (TRPV1) in mice alters behavioral effects of ethanol. *Neuropharmacol.* **56**, 814-820

36. Cioffi, D. L. (2007) The skinny on TRPV1. *Circ. Res.* **100**, 934-936

37. Xie, H., Lim, B., and Lodish, H. F. (2009) MicroRNAs induced during adipogenesis that accelerate fat cell development are downregulated in obesity. *Diabetes* **58**, 1050-1057

38. Karbiener, M., Fischer, C., Nowitsch, S., Opriessnig, P., Papak, C., Ailhaud, G., Dani, C., Amri, E. Z., and Scheideler, M. (2009) microRNA miR-27b impairs human adipocyte differentiation and targets PPARgamma. *Biochem. Biophys. Res. Commun.* **390**, 247-251

39. Sun, T., Fu, M., Bookout, A. L., Kliewer, S. A., and Mangelsdorf, D. J. (2009) MicroRNA let-7 regulates 3T3-L1 adipogenesis. *Mol. Endocrinol.* **23**, 925-931

40. Esau, C., Kang, X., Peralta, E., Hanson, E., Marcusson, E. G., Ravichandran, L. V., Sun, Y., Koo, S., Perera, R. J., Jain, R., Dean, N. M., Freier, S. M., Bennett, C. F., Lollo, B., and Griffey, R. (2004) MicroRNA-143 regulates adipocyte differentiation. *J. Biol. Chem.* **279**, 52361-52365

41. Liang, W. C., Wang, Y., Wan, D. C., Yeung, V. S., and Waye, M. M. (2013) Characterization of miR-210 in 3T3-L1 adipogenesis. *J. Cell Biochem.* **114**, 2699-2707

42. Hindson, B. J., Ness, K. D., Masquelier, D. A., Belgrader, P., Heredia, N. J., Makarewicz, A. J., Bright, I. J., Lucero, M. Y., Hiddessen, A. L., and Legler, T. C. (2011) High-throughput droplet digital PCR system for absolute quantitation of DNA copy number. *Anal. Chem.* **83**, 8604-8610

43.   Hindson, C. M., Chevillet, J. R., Briggs, H. A., Gallichotte, E. N., Ruf, I. K., Hindson, B. J., Vessella, R. L., and Tewari, M. (2013) Absolute quantification by droplet digital PCR versus analog real-time PCR. *Nat. Methods* **10**, 1003-1005

44.   Hochkogler, C. M., Rohm, B., Hojdar, K., Widder, S., Ley, J. P., Krammer, G. E., and Somoza, V. (2014) The pungent capsaicin analog nonivamide decreases total energy intake and enhances plasma serotonin levels in men when administered in an OGTT: a randomized, crossover intervention. *Mol. Nutr. Food Res.* **DOI: 10.1002/mnfr.201300821**

*Conflict of interest-*The authors S. Widder, J.P. Ley and G.E. Krammer are employees at Symrise AG, Holzminden, Germany.

FOOTNOTES

To whom correspondence should be addressed: Veronika Somoza, Department of Nutritional and Physiological Chemistry, Christian DopplerLaboratory for Bioactive Aroma Compounds, University of Vienna, Althanstraße 14, 1090 Vienna, Austria. Tel: +43 1 4227 70601, Fax: +43 1 4277 9706, e-mail: Veronika.Somoza@univie.ac.at

The abbreviations used are*:* BCH, *trans-tert*-butycyclohexanol; TRPV1, transient receptor potential cation channel subfamily V member 1; miRNA, microRNA

3. Conclusions and Perspectives

Overweight and obesity, with its comorbitites like diabetes mellitus type 2, chronic microinflammation, coronary heart diseases and hyperlipdemia, have reached the extent of an epidemic and are one of the greatest health problems of the 21st century. Measures to reduce body weight include reduction of food intake, modulation of intestinal fat uptake and modulation of fat storage, e.g. via regulation of adipogenesis.

In this context, fruits of the genus *Capsicum* and its ingredients capsaicin and capsiate are often considered as anti-obesity agents, since their administration to animals and humans has been associated with enhanced energy metabolism, reduced food intake, and decreased serum triacylglycerol contents. Although both compounds have been shown to be effective in several human intervention trials, it requires compliance to a certain pungent sensation in the gastrointestinal tract, including the oral cavity in the case of capsaicin. The pungent sensation results from activation of the TRPV1 receptor by capsaicinoides as well as capsinoids. Thus, the aim of the present thesis was 1) to identify compounds that are structurally related to capsaicin and unfold similar anti-obesity effects, but are not as pungent and 2) elucidate the underlying mechanisms. A first screening of the compounds was based on their potency to stimulate the release of the satiety-mediating neurotransmitters serotonin and dopamine from neural cells. In PART I of the present thesis, stimulation of SH-SY5Y cells combined with ELISA technique for quantification of the neurotransmitters was shown to be a suitable model for this purpose. Using this test system, a direct structural analog of capsaicin, nonivamide, was shown to stimulate dopamine and serotonin release from SH-SY5Y cells in a comparable manner to capsaicin *((1)"Nonivamide, a capsaicin analog, increases dopamine and serotonin release in SH-SY5Y cells via a TRPV1-independent pathway")*. Mechanistic studies revealed that stimulation of SH-SY5Y cells with both capsaicinoids is accompanied by increased intracellular Ca^{2+} levels. However, using the two specific TRPV1-antagonists capsazepine and *trans-tert*-butylcyclohexanol, it was shown that, in contrast to capsaicin, neurotransmitter release evoked by nonivamide does not depended on TRPV1 receptor activation. After a sub-cellular fractionation, nonivamide was detected in the post-nuclear supernatant, which did not contain larger cell compartments as the nucleus and cell membrane. It was therefore concluded that nonivamide is able to enter the cell und may, thus, unfold its effects not only via binding to membrane-standed receptors like the TRPV1 receptor, but also unfold its effects intracellularly. This is consistent with time-dependent changes in gene regulation of

dopamine and serotonin receptors after incubation with nonivamide in SH-SY5Y cells. As a mechanism, it is proposed that nonivamide is able to affect intracellular calcium stores, such as ryanodine-sensitive stores, that have been shown to be sensitive to capsaicin before. Independence of TRPV1-receptor activation of nonivamide-evoked neurotransmitter release allows oral administration of higher amounts to unfold satiating effects, since a concomitant administration of TRPV1 inhibitor is possible. This would allow reduction of pungent sensations throughout the gastrointestinal tract, including the oral cavity, without loss of its neurotransmitter-releasing activity.

In a second study (*"Neurotransmitter-releasing potency of structural capsaicin-analogs in SH-SY5Y cells"*), the effects of the alkamide *trans*-pellitorine on serotonin and dopamine release in comparison to those of nonivamide are presented. *trans*-Pellitorine is, like capsaicin and nonivamide, an amide, but is lacking the vanillyl-group, and is also a discussed agonist for the TRPV1 receptor. *trans*-Pellitorine was shown to stimulate serotonin and dopamine release in SH-SY5Y cells as well, with a maximum efficacy at 0.1 µM. At this concentration, *trans*-pellitorine stimulated serotonin and dopamine release to a similar extent as nonivamide. At the higher test concentrations of 1-10 µM, effects of nonivamide were more pronounced compared to the effects of *trans*-pellitorine. However, it has to considered for both cell culture studies, that plasma concentrations for *trans*-pellitorine and nonivamide after oral consumption of an agreeable dose are not known yet and can only be estimated by comparison of pharmacokinetic studies with a structural related compounds such as capsaicin or plant extracts containing pellitorine. For capsaicin plasma concentrations in a nanomolar range were described after application of 5 g red pepper, containing 26.6 mg capsaicin to rats [2]. For *trans*-pellitorine, plasma concentrations in the nanomolar range have been reported as well, after application of 500 mg/kg body weight of an extract of *Piper sarmentosum*, containing 52.10 mg/g *trans*-pellitorine to rats [3]. In addition, *trans*-pellitorine, but also nonivamide are lipophilic compounds and their molecular weight is <500 g/mol, thus, crossing of the blood brain barrier to reach neural cells after oral intake is likely.

Since nonivamide more potently stimulated serotonin and dopamine release from SH-SY5Y neural cells compared to *trans*-pellitorine, the effects of nonivamide on satiety and

---

[2] See also Chaiyasit K, Khovidhunkit W, Wittayalertpanya S. *J Med Assoc Thai*, 2009, **92**, 108-113

[3] See also Hussain K, Ismail Z, Sadikun A, Ibrahim P., *Evid Based Complement Alternat Med.* 2011, **2011**:1-7

energy intake were validated in a short-term human intervention trial with 15 slightly overweight male subjects (*"The pungent capsaicin analog nonivamide decreases total energy intake and enhances plasma serotonin levels in men when administered in an OGTT: a randomized, crossover intervention"*). The cross-over intervention demonstrated that the application of 0.15 mg nonivamide during an oral glucose tolerance test (2 h) as nutritive stimulus increased self-reported satiety, which was determined by a 100-mm visual analog scale. Increased feeling of satiety was reflected in a reduced total energy intake and carbohydrate intake from a subsequent standardized breakfast. Since the very low dose of nonivamide of 0.15 mg in 300 ml glucose solution did not evoke a significant pungent sensation in the test subjects, an effect of pungency on satiety and energy intake during this study can be mostly excluded. Glucose and insulin response during the oral glucose tolerance test was not affected by nonivamide application, nor were as plasma concentrations of the satiety-mediating gastro-intestinal hormones PPY and CCK. In contrast, GLP-1 levels increased 15 min after application of nonivamide in comparison to control. In addition, the total area under the curve (AUC) of serotonin plasma levels was increased after application of 0.15 mg nonivamide, which confirms the *in vitro* findings from SH-SY5Y cells. However, so far, there is no clear evidence that peripheral serotonin, produced by enterochromaffin cells in the intestines, unfolds the same satiety-effects as central serotonin. However, in this study, Spearmen correlation coefficient showed a trend towards an inverse correlation between plasma serotonin levels and energy intake. Therefore, it is hypothesized that a decreased signaling after nonivamide application from the intestine via vagal jejunal afferents may contribute to increased satiety and reduced food intake, allowing also peripheral serotonin to influence food intake. Further studies with more subjects are needed to investigate this hypothesis. Also, data from a long-term human intervention and effects of nonivamide in a food matrix are lacking so far.

Beside regulation of food intake, also modulation of intestinal nutrient uptake, especially fat, is thought to support maintenance of a healthy body weight. Since capsaicin is associated with hypolipidemia and hypocholesterolemia, part of this dissertation was focused on modulation of *in vitro* intestinal fatty acid uptake by nonivamide and trans-pellitorine compared to capsaicin (*"Capsaicin, nonivamide and trans-pellitorine decrease free fatty acid uptake without TRPV1 activation and increase acetyl-coenzyme A synthetase activity in Caco-2 cells"*). Both compounds were chosen on the basis of their potency to stimulate neurotransmitter release and, as a cellular model, enterocyte-like Caco-2 cells were used as

described in PART I of this dissertation. Results indicated that capsaicin very potently reduced intestinal fatty acid uptake in a dose-dependent manner with an IC_{50} value of 0.49 µM. Slight structural changes in the carbon chain already led to a minor loss of activity, as approximately twice as much of the direct structural capsaicin-analog nonivamide was needed to reach similar inhibition of fatty acid uptake (IC_{50}=1.08 µM). The alkamide *trans*-pellitorine reduced fatty acid acid uptake at the highest test concentration of 100 µM, whereas vanillin did not affect fatty acid uptake in a range of concentrations of 0.1-100 µM. According to these findings, the amide group with the carbon chain rather than the vanillyl-group, or a combination thereof, seems to be an important structural motif for inhibition of fatty aid uptake. Mechanistic studies using specific inhibitors demonstrated, that reduction of fatty acid uptake depends neither on activation of the TRPV1 receptor, nor of the epithelial sodium channel (ENaC). Also, treatment with capsaicin, nonivamide and *trans*-pellitorine did not change paracellular transport compared to control-treated cells, which was assessed via trans-epithelial electrical resistance and glucose uptake. A direct modulation of fatty acid transporters or fatty acid binding proteins is not excluded. However, acetyl coenzyme A synthetase activity increased after 90 min of incubation with capsaicin, nonivamide and *trans*-pellitorine, pointing to an increased fatty acid biosynthesis to counteract reduced fatty acid uptake. Future studies are needed to address the question whether short-term reduction of intestinal fatty acid uptake also leads to long-term changes in cellular composition or whether it may even explain the hypolipidemic effects of capsaicin.

Earlier studies described that Ca^{2+}-influx via activation of the TRPV1 cation channel leads to an activation of calcineurin, which in turn inhibits the pro-adipogenic transcription factors PPARγ and C/EBPα, and results in an impaired adipogenesis. Reduction of adipogenesis leads to decreased total fat mass by determining the total number of adipocytes, which may be a supporting factor to maintain a healthy body weight. The last part of the present thesis comprises mechanistic studies comparing the effects of the TRPV1-agonists capsaicin and nonivamide on adipogenesis in 3T3-L1 cells as a model *("Nonivamide, a capsaicin analog, inhibits TRPV1-dependently adipogenesis accompanied by decreased PPARgamma expression and enhanced miRNA let-7d expression in 3T3-L1 cells")*. Treatment of 3T3-L1 cells during differentiation with nonivamide reduced lipid accumulation, which was analyzed as a biomarker for adipogenesis, to a similar extent as treatment with capsaicin. Co-incubation experiments with the selective TRPV1-antagonists *trans-tert*-butylcyclohexanol revealed that the anti-adipogenic activity of nonivamide depended on

149

TRPV1-receptor activation likewise to the effects of capsaicin. The decreased lipid accumulation after nonivamide treatment, but not after capsaicin treatment was accompanied by a down-regulation of pro-adipogenic PPARγ protein levels. Results from a genome-wide miRNA microarray analysis indicated a regulation of several miRNAs during the differentiation process, which were partly influenced by nonivamide treatment. Regulation of selected members of the anti-adipogenic let-7 group was validated using digital droplet PCR, revealing that treatment with nonivamide let to an up-regulation of mmu-let-7d-5p. Since members of the let-7 group have been associated with regulation of PPARγ before, it is assumed that treatment with nonivamide down-regulates PPARγ levels via increased mmu-let-7d expression. Unexpected, similar to the neurotransmitter-releasing potency of capsaicin and nonivamide, signaling pathways for both compounds regarding their anti-adipogenic activity seem to differ, although both compounds share structural core motifs.

However, it has to be considered, that these data originate from *in vitro* studies solely, and require careful *in vivo* validation.

In summary, the present thesis describes the successful identification of the less pungent, but structural capsaicin-relatives nonivamide and *trans*-pellitorine as means to maintain a healthy body weight. Nonivamide has been demonstrated to be a promising candidate to target different medicinal strategies in the treatment of obesity. On the one hand, it was shown that application of nonivamide elevated serotonin levels, both *in vitro* and *in vivo*, and this effect was accompanied with increased self-reported satiety a reduced energy intake in the short-term human intervention study. Besides, nonivamide effectively reduced intestinal fatty acid uptake in Caco-2 cells, and prevented adipogenesis in 3T3-L1 pre-adipocytes, demonstrating that nonivamide may also act on energy, especially lipid metabolism, as well. The pungent sensation following oral application of nonivamide is reduced by half compared to capsaicin. Thus, nonivamide may be applied in higher concentrations compared to capsaicin to unfold combined effects on different targets of body weight maintenance.

Future studies should address the effectiveness of a long-term nonivamide application on food intake and lipid metabolism, especially when administered with complex food matrices.

IV.   *Abstract*

Overweight and obesity are the result of a long-term imbalance between energy intake and consumption. The major pungent principle of red pepper, capsaicin, has been shown to promote body weight maintenance in humans. The first part of the present work was focused on the establishment of screening models to investigate mechanisms regulating satiety and energy metabolism. The second part of the thesis summarizes research regarding the effects of aroma compounds, which are structural related to capsaicin, but are not as pungent, on mechanisms regulating satiety, uptake of glucose and fat and adipogenesis. The pungency of a compound is determined by its potency to activate the transient receptor potential cation channel 1 (TRPV1), whose activation increases intracellular Ca^{2+} influx. The capsaicin analog nonivamide, also being a TRPV1 agonist, was shown to stimulate the release of the satiety-mediating neurotransmitters dopamine and serotonin from human neural SH-SY5Y cells. However, in contrast to capsaicin, the nonivamide-evoked neurotransmitter release did not solely depend on TRPV1 receptor activation. Another structurally related compound, also discussed as to act through binding to TRPV1, is *trans*-pellitorine, which was shown to stimulate dopamine and serotonin release from human neural SH-SY5Y cells through intracellular Ca^{2+} mobilization as well, although not as potent as nonivamide or capsaicin. The satiety-mediating effect of the potent serotonin-stimulating nonivamide was validated in a short-term human intervention study. Administration of 0.15 mg nonivamide in an oral glucose tolerance test reduced energy intake from a standardized breakfast and increased serotonin plasma levels in moderately overweight male subjects. In addition, capsaicin, nonivamide and *trans*-pellitorine were shown to inhibit free fatty acid uptake in intestinal Caco-2 cells. Although the compounds' potency to reduce the uptake of fatty acids increased with TRPV1 binding affinity, it was shown that the effect did not depend on TRPV1 receptor activation. Moreover, studies using 3T3-L1 preadipocytes revealed that nonivamide inhibits adipogenesis to a similar extent as capsaicin, via binding to TRPV1. This effect was accompanied by an up-regulation of the miRNA let-7d-5p and a down-regulation of PPARγ protein, explaining the anti-adipogenic activity of nonivamide on a mechanistic level. In conclusion, the here presented work demonstrates that also less pungent compounds like nonivamide are promising compounds that may help to maintain a healthy body weight by targeting different tissues and mechanisms regulating energy metabolism and satiety.

V. Zusammenfassung

Übergewicht und Adipositas sind die Folge eines langfristigen Ungleichgewichts zwischen Energieaufnahme- und Energieverbauch. Die Aufnahme des mengenmäßig bedeutsamsten Scharfstoffs aus Chili, Capsaicin, wird mit der Erhaltung eines gesunden Körpergewichts assoziiert. Der erste Teil der vorliegenden Arbeit zeigt die Etablierung verschiedener Screening-Systeme zur Untersuchung von Mechanismen der Sättigungsregulation. Der zweite Teile dieser Arbeit beschreibt den Einfluss von Aromastoffen, die strukturell verwandt mit Capsaicin sind, aber nicht so scharf schmecken, auf Mechanismen der Sättigung, der Nährstoffaufnahme und der Adipogenese. Die Schärfe einer Substanz wird durch ihre Bindungsaffinität an den TRPV1-Rezptor bestimmt, dessen Aktivierung zu einem intrazellulären Ca^{2+}-Einstrom führt. Es konnte gezeigt werden, dass Nonivamid, ein strukturelles Analog zu Capsaicin und ein bekannter TRPV1-Agonist, die Ausschüttung der Sättigungs-vermittelnden Neurotransmitter Serotonin und Dopamin in neuronalen SH-SY5Y Zellen stimulierte. Im Gegensatz zu Capsaicin basierte dieser Effekt jedoch nicht maßgeblich auf einer Aktivierung des TRPV1-Rezptors. Ein weitere, strukturell ähnliche Substanz und potentieller TRPV1-Agonist ist *trans*-Pellitorin, das ebenfalls Ca^{2+}-abhängig die Serotonin und Dopamin-Ausschüttung von SH-SY5Y Zellen stimulierte, jedoch weniger potent als Capsaicin oder Nonivamid wirkte. Eine anschließende humane Intervention bestätigte den sättigenden Effekt von Nonivamid. So reduzierte die Gabe Nonivamid in einem oralen Glukosetoleranztest die Energieaufnahme von einem standardisierten Frühstück und erhöhte die Plasma-Serotoninkonzentration in leicht übergewichtigen Männern. Zudem wurde eine Verminderung der Fettsäureaufnahme in intestinalen Caco-2-Zellen durch Capsaicin, Nonivamid und *trans*-Pellitorin gezeigt. Obwohl die Stärke der Inhibierung mit der TRPV1-Bindungsaffinität zunahm, war der Effekt nicht an eine Aktivierung des TRPV1-Rezptors geknüpft. Darüber hinaus zeigten Studien mit 3T3-L1 Preadipozyten, dass Nonivamid, in einem vergleichbaren Ausmaß wie Capsaicin, TRPV1-abhängig die Adipogenese hemmt. Dieser Effekt ging mit einer Erhöhung der miRNA let-7d-5p und einer Verringerung der PPARγ-Expression einher. Zusammenfassend zeigt die vorliegende Arbeit, dass auch die Aufnahme von weniger scharf schmeckenden Verbindungen, wie Nonivamid, zur Erhaltung eines gesunden Körpergewichtes beitragen könnten, in dem sie in verschiedenen Zielgeweben in Mechanismen der Regulation des Energiestoffwechsels und der Sättigungsregulation eingreifen.

VI. Curriculum vitae

Education

2009- 2014   PhD research at the Department of Nutritional and Physiological Chemistry, University of Vienna

Research interest: Impact of aroma compounds on mechanisms regulating satiety and energy metabolism

Supervisor: Prof. Veronika Somoza

2008-2009   Master's research at the Leibniz Institute for Natural Product Research and Infection Biology - Hans-Knöll-Institute, Jena, Germany

Title: Toxin-production of food-relevant *Burkholderia*

Supervisor: Prof. Christian Hertweck

2004-2009   Academic studies of Nutritional Sciences at the Friedrich Schiller University Jena, Germany (completed with high honours)

Scientific Expertise and research interest

Diploma thesis (Hans-Knöll-Institut, Jena, Germany)

Application of standard biomolecular (cloning, PCR) and analytical techniques (HPLC, mass spectrometry, NMR) to investigate the presence and biosynthesis *Burkholderia* toxins in foods

PhD thesis (Department of Nutritional and Physiological Chemistry, Vienna, Austria)

Elucidation of the impact of aroma compounds on mechanisms regulating food intake and energy metabolism in different *in vitro* and *in vivo* test systems (neural and intestinal cells, adipocytes, human intervention trials) using various analytical techniques , e.g. ELISA, Western Blot, qPCR, ddPCR, microarrays, flow cytometry and liquid scintillation counting of radio-labeled markers.

Publications

Manuscripts in preparation

(1) Missbach, B., **Rohm, B**., König, J., Somoza, V. (2014) *The role of food appearance and composition in controlling psychological, sensory and metabolic factors of food intake*. Mol Nutr Food Res, *in preparation*.

Submitted manuscripts

2014

(2) **Rohm, B.,**Riedel, A.,Widder, S.,Ley, J. P., Krammer, G.E., Somoza,V. (2014) *Capsaicin, nonivamide and trans-pellitorine decrease free fatty acid uptake without TRPV1 activation and increase acetyl-coenzyme A synthetase activity in Caco-2 cells*.Food and Function**, submitted**.

(3) **Rohm, B.,**Holik, A. K.,Kretschy, N.,Somoza, M. M., Widder, S.,Ley, J. P., Krammer, G.E., Somoza,V. (2014) *Nonivamide, a capsaicin analog, decreases via TRPV1 activation adipogenesis and peroxisome proliferator-activated receptor gamma expression, and enhances miRNA let-7d expression in 3T3-L1 cells* . J Biol Chem**, submitted**.

Original contributions

2014

(4) Riedel, A., Lang, R., **Rohm, B.**, Rubach, M., Hofmann, T., Somoza,V., (2014) *Structure-dependent effects of pyridine derivatives on mechanisms of intestinal fatty acid uptake: Regulation of nicotinic acid receptor and fatty acid transporter expression, and modification of trans-epithelial electrical resistance in enterocyte-like Caco-2 cells*. Journal of Nutritional Biochemistry**,** *epub ahead of print, DOI:10.1016/j.jnutbio.2014.03.002*.

(5) Hochkogler, C. M., **Rohm, B.**, Hojdar, K., Pignitter, M., Widder, S., Ley, J. P., Krammer, G.E., Somoza,V., (2014) *The pungent capsaicin analog nonivamide decreases total energy intake and enhances plasma serotonin levels in men when administered in an OGTT: a randomized, crossover intervention*. Mol Nutr Food Res**,** *epub ahead of print, DOI:10.1002/mnfr.201300821*.

(6) **Rohm, B.**, Zaunschirm, M., Widder, S., Ley, J. P., Krammer, G.E., Somoza,V. (2014) *Neurotransmitter-releasing potency of structural capsaicin-analogs in SH-SY5Y cells*. In: Proceedings of the 10th Wartburg Symposium Eisenach (T. Hofmann, W. Meyerhof, P. Schieberle eds.) Verlag Deutsche Forschungsanstalt für Lebensmittelchemie. *in press*.

2013

(7) **Rohm, B.**, Holik, A. K., Somoza, M. M.,Pignitter, M.*,* Ley, J. P.,Krammer, G.E.,Somoza,V. (2013) *Nonivamide, a capsaicin analog, increases dopamine and serotonin release in SH-SY5Y cells via a TRPV1-independent pathway.* Mol Nutr Food Res *57,* 2008-18.

(8) Sack, M., Kretschy, N., **Rohm, B.**, Somoza, V., Somoza, M. M., (2013) *Simultaneous light-directed synthesis of mirror-image microarrays in a photochemical reaction cell with flare suppression.* Anal Chem *85,* 8513-7.

(9) Holik, A. K., **Rohm, B.**, Somoza, M. M., and Somoza, V. (2013) *N(epsilon)-Carboxymethyllysine (CML), a Maillard reaction product, stimulates serotonin release and activates the receptor for advanced glycation end products (RAGE) in SH-SY5Y cells*, Food Funct 4, 1111-1120.

2012

(10) Moebius, N., Ross, C., Scherlach, K., **Rohm, B**., Roth, M., and Hertweck, C. (2012) *Biosynthesis of the respiratory toxin bongkrekic acid in the pathogenic bacterium Burkholderia gladioli*, Chem Biol *19*, 1164-1174.

(11) Riedel, A., Pignitter, M., Hochkogler, C. M., **Rohm, B**., Walker, J., Bytof, G., Lantz, I., and Somoza, V. (2012) *Caffeine dose-dependently induces thermogenesis but restores ATP in HepG2 cells in culture*, Food Funct 3, 955-964.

(12) Walker, J., **Rohm, B**., Lang, R., Pariza, M. W., Hofmann, T., and Somoza, V. (2012) *Identification of coffee components that stimulate dopamine release from pheochromocytoma cells (PC-12)*, Food Chem Toxicol 50, 390-398.

2010

(13) **Rohm, B.**, Scherlach, K., and Hertweck, C. (2010) *Biosynthesis of the mitochondrial adenine nucleotide translocase (ATPase) inhibitor bongkrekic acid in Burkholderia gladioli*, Org Biomol Chem 8, 1520-1522.

(14) **Rohm, B.**, Scherlach, K., Mobius, N., Partida-Martinez, L. P., and Hertweck, C. (2010) *Toxin production by bacterial endosymbionts of a Rhizopus microsporus strain used for tempe/sufu processing*, Int J Food Microbiol 136, 368-371.

Patent applications

(1) Alkamides as means to reduce appetite (application No. EP 13 155556.7) G. Krammer, J. Ley, S. Widder, M. Zaunschirm, **B. Rohm**, V. Somoza

(2) N-Nonanoylvanillylamin as a compound, as compound mixtures, as an orally consumable product and related technologies to reduce appetite, induce satiation, and improve mood) (publication number EP2, 614, 727, 20B) J. Ley, G. Krammer, V. Somoza, **B. Rohm**

International Conferences

08/2013	Poster presentation: ECRO meeting 2013, Leuven, Belgium
05/2013	Poster presentation: 33rd Blankenese Conference 2013, Hamburg, Germany
04/2013	Poster presentation: 10th Wartburg Symposium, Eisenach, Germany
04/2013	Poster presentation: DIfE Symposium, Potsdam, Germany
08/2012	Oral presentation: 244th American Chemical Society National Meeting & Exposition, Philadelphia, USA
03/2012	Oral and poster presentation: 49th scientific congress of the German Nutrition Society, Freising, Germany
07/2011	Attendance: "Advances in microarray technology" in Hamburg, Germany
03/2011	Oral and poster presentation: 48th scientific congress of the German Nutrition Society, Potsdam, Germany

Reviewing Activities

Journal of Agriculture and Food Chemistry